The Role of Apobec2 During Zebrafish Retina and Optic Nerve Regeneration

by

Curtis Rich Powell

A dissertation submitted in partial fulfillment
of the requirements for the degree of
Doctor of Philosophy
(Biological Chemistry)
in the University of Michigan
2014

Doctoral Committee:

Professor Daniel J. Goldman, Chair
Professor Robert Denver
Assistant Professor Aaron C. Goldstrohm
Professor Audrey F. Seasholtz
Associate Professor David L. Turner

Dedication

To my wife, Siri Cooper Powell.

Acknowledgements

While I am the primary author to this thesis, I can by no means claim full credit for its contents. It is my desire in this section to express thanks and to give warranted acknowledgment to individuals who have directly or indirectly influenced this work. Upon commencing this endeavor, I realized that to include all those who have molded my character and engendered my love of science is unrealistic. Thus, this is not an exhaustive list. Here I attempt to provide special acknowledgment to those who have provided noteworthy contribution, specifically during my time as a graduate student.

Much thanks goes to Dan Goldman, my mentor, who believed enough in my capabilities to take me on in his lab. Dan dedicated significant time to my development as a scientist, writer, and presenter. I really appreciate that while Dan allowed me to work independently, his office door was always open, and he was always willing to discuss the design of my experiments and help in troubleshooting. His excitement about the work was contagious! Dan was very good at stretching my comfort zone and inspiring me to tackle difficult questions by any means necessary. For this I am particularly grateful, for I now know that I am capable of things I did not know I was previously.

Many people have contributed to performing the experiments described in this dissertation. First, I would like to thank the contributing authors to the papers I have published: Dan Goldman, Eli Cornblath, Ana Rodrigues Grant, and Rose Elsaeidi. A special thanks goes to Eli who has performed experiments with me for a number of years and was always willing to work late at night and on weekends and holidays. In addition, I would like to thank current and former members of the Goldman lab including Peter Macpherson, Rajesh Ramachandran, Xiaofeng Zhao, Jin Wan, and Aaron Reifler. These are the individuals who most impacted my training in molecular biology and research involving zebrafish, of which I am grateful. Aaron Reifler in particular became a close friend and a great source of advice in many aspects of graduate life. I thank Mike Bemben, Pershang

Farshi, Tom Jurkiw, Hui Xu, and Remu Gangji who are also current or past members of the Goldman lab. A special thanks goes to Tori Melendez, Randy Karr, and Josh Kirk, current and past managers of the fish facility, who were responsible for the health and maintenance of the zebrafish used in my studies. Randy has become a good friend and has helped me enjoy the Michigan outdoors. These gifted people of the Goldman lab established a great atmosphere for science and collegiality.

I would like to thank the members of my dissertation committee: Dave Turner, Audrey Seasholtz, Aaron Goldstrohm, and Bob Denver. Thank you for your mentorship during the bulk of my dissertation research and your willingness to provide recommendation letters. I would like to thank the members of my preliminary exam committee: Dave Turner, Mike Uhler, Tom Kerppola, and Roland Kwok. Thank you for your early advice that set the stage for my dissertation research. Other faculty members that merit mentioning included Anne Vojtek who provided academic and scientific advice, Miriam Meisler and Peter Hitchcock who directed training programs that I participated in, and Stephen Ragsdale and Ursula Jakob in whose labs I rotated. I would also like to thank Beth Goodwin who has been an outstanding resource to me as a graduate student.

Outside of the support network of the Biological Chemistry Department and the University of Michigan, I have been blessed with two additional sources of support: my family and The Church of Jesus Christ of Latter-day Saints. First and foremost, I thank my family. Siri has continually been a tremendous support. I draw on this support daily. With her, my greatest accomplishment during my tenure as a graduate student was achieved, becoming a father. My family is my favorite pastime. I thank my mom who was always my greatest fan and who provided me with inspiration to do hard things. I thank my dad who has been my greatest example and role model and one of my truest friends. Thank you Dad, Kris, Gary, Paula, Jason, Taylor, Erica, Aubri, Josh, Michelle, Shalie, and Sean for traveling to see us here in Michigan! I thank all other members of my and Siri's family.

My membership in The Church of Jesus Christ of Latter-day Saints has introduced me to a large number of new friends in the Ann Arbor area who were a source of healthy distraction during my graduate life. Through a number of church sponsored activities including basketball, softball, volleyball, and scouting, I was able to unwind and contribute

to the community. In particular I thank the Beck family, Mark Johnson, and Mark Livingston.

Finally, I thank God for an eternal perspective and the life that I have.

Preface

The exact events that instilled within me the desire to pursue a PhD, even to me, are unclear. In fact, growing up in a small town in Idaho, I cannot recall having an acquaintance that held a PhD until enrolling in my first year of college. If such an acquaintance existed, I was unaware of it. What is clear to me is that even at an early age I had an intrinsic drive to explore, observe, and learn. I spent a considerable amount of time collecting insects and exploring nature with my father and family. Through these experiences, I acquired a deep appreciation for life in its many forms. These intrinsic desires and my appreciation for nature are likely the most contributing factors that led me to pursue a PhD in a life science. These, in combination with my upbringing focused on personal character and hard work, have been great assets during my graduate education.

Connecting the dots between my deciding to pursue a PhD and my performing research on zebrafish retina regeneration is no less enigmatic, though a report I prepared as an undergraduate at Brigham Young University-Idaho likely initiated the process. At this time the technology of induced pluripotent stem cells was just surfacing, and my report covered some of the early findings showing that by introducing certain combinations of pluripotency factors into cells, they could acquire stem cell characteristics. This is similar to the events occurring as cells reprogram during regeneration. In fact, the first time I spoke with Professor Daniel Goldman I was interested to find that some of the key factors found to be involved in zebrafish retina regeneration are shared with those involved in the generation of induced pluripotent stem cells.

At the completion of my first year of graduate school I joined Dan's lab at which time we discussed possible projects that I could develop. Dan mentioned the topic of DNA methylation, which plays a critical role in cellular identity. This field was interesting to me, particularly the topic of DNA demethylation, which was at the time, and continues to be, a topic of high interest to the scientific community. With this in mind, I searched the scientific

literature to identify any gene that was in any way correlated with DNA demethylation, and I performed preliminary survey experiments to determine if their mRNA levels were regulated during zebrafish retina regeneration. The first evidence that *apobec2b* mRNA was regulated during regeneration was found in a gel I ran on June 30, 2009. I still remember going into Dan's office to show him an image of that gel. Soon after that we found the regulation of *apobec2b* mRNA during optic nerve regeneration.

This thesis reports my work focused on determining the role that these Apobec2 proteins play during zebrafish retina and optic nerve regeneration and is composed of six chapters. Chapter 1 provides an introduction to the fields of retina regeneration, DNA methylation, and Apobec proteins. Chapter 2 describes the initial characterization of Apobec2 proteins in retina and optic nerve regeneration, demonstrating their necessity for these events and placing them within the context of a previously characterized signaling cascade. Chapters 3 and 4 describe experiments designed with the goal of determining the biochemical function of Apobec2 proteins, including the regulation of DNA methylation, the editing of mRNA, and the identification and characterization of interacting proteins. Chapter 5 is divided into two parts and describes my research that remains incomplete. Chapter 6 includes the conclusion of this work and potential directions for future work.

This thesis is submitted in partial fulfillment of the requirements for the degree of Doctor of Philosophy in Biological Chemistry in the University of Michigan. It contains research carried out from April 2009 to March 2014. All of the work presented henceforth was conducted at the University of Michigan under the supervision of Professor Daniel Goldman. This work is to the best of my knowledge original, except where references are made to previous work. The material in this thesis has not been submitted for a degree, diploma, or any other qualification at any other university.

Chapters 2 and 3 of this work have been presented in the following publications:

Powell C, Elsaeidi F, & Goldman D (2012) Injury-dependent Müller glia and ganglion cell reprogramming during tissue regeneration requires Apobec2a and Apobec2b. *J Neurosci* 32(3):1096-1109. I was the lead investigator, responsible for all major areas of concept formation, experimental design, data collection, and data analysis, as well as the majority of the manuscript composition. Goldman D contributed to concept formation,

experimental design, data analysis, and manuscript preparation. Elsaeidi F contributed to data collection.

Powell C, Grant AR, Cornblath E, & Goldman D (2013) Analysis of DNA methylation reveals a partial reprogramming of the Müller glia genome during retina regeneration. *Proc Natl Acad Sci U S A* 110(49):19814-19819. I was the lead investigator, responsible for all major areas of concept formation, experimental design, data collection, and data analysis, as well as the majority of the manuscript composition. Goldman D contributed to concept formation, experimental design, data analysis, and manuscript preparation. Grant AR contributed to data analysis. Cornblath E contributed to data collection and analysis.

Chapter 4 is a manuscript in preparation of which I was the lead investigator, responsible for all major areas of concept formation, experimental design, data collection, and data analysis, as well as the majority of the manuscript composition. Daniel Goldman contributed to concept formation, experimental design, data analysis, and manuscript preparation. Ana Grant contributed to data analysis. Eli Cornblath contributed to experimental design, data collection, and analysis.

Chapter 5 and Appendix A describe work in progress of which I was the lead investigator, responsible for all major areas of concept formation, experimental design, data collection, and data analysis. Daniel Goldman contributed to concept formation, experimental design, and data analysis. Xiaofeng Zhao, Peter Macpherson, Tom Jirkew, and Remu Gangji contributed to data collection.

Table of Contents

List of Figures

List of Tables

List of Abbreviations

5-dAza	5-Aza-2'-Deoxycytidine
5-meC	5-Methylcytosine
AID	Activation Induced Cytidine Deaminase
ApoB	Apolipoprotein B
Apobec	Apolipoprotein B mRNA Editing Complex
Apoc1	Apolipoprotein C-1
Ascl1a	Achaete-Scute Complex-Like 1a
BER	Base Excision Repair
BrdU	5-Bromo-2'-Deoxyuridine
C-myc	V-myc Avian Myelogytomatosis Viral Oncogene Homolog
C1qb	Complement Component 1, q Subcomponent, B Chain
C1qc	Complement Component 1, q Subcomponent, C Chain
Cebp	CCAAT/Enhancer Binding Protein
CMZ	Ciliary Marginal Zone
CNS	Central Nervous System
DAPI	4',6-Diamidino-2-Phenylindole, Dihydrochloride
DIG	Digoxigenin
DMB	Differentially Methylated Base
Dnmt	DNA Methyltransferase
DPI	Days Post Injury
ESC	Embryonic Stem Cell
FACS	Fluorescence-Activated Cell Sorting
Gadd45	Growth Arrest and DNA-Damage-Inducible Protein 45
Gapdh	Glyceraldehyde-3-Phosphate Dehydrogenase
GCL	Ganglion Cell Layer
Gfap	Glial Fibrillary Acidic Protein
GFP	Green Fluorescence Protein
GS	Glutamine Synthetase
Hbegf	Heparin-Binding EGF-like Growth Factor
HRP	Horseradish Peroxidase
Hsp70	Heat Shock Cognate 70-kd Protein
HuC/D	HUC RNA-Binding Protein HuC
INL	Inner Nuclear Layer
Insm1a	Insulinoma-Associated 1a
iPSC	Induced Pluripotent Stem Cell

Klf4	Kruppel-Like-Factor 4
MBD4	Methyl-CpG Bindng Domain Protein 4
Mfap4	Microfibrillar-Associated Protein 4
MG	Müller glia
MGPC	Müller glia Progenitor Cell
MO	Morpholino
Mpeg1	Macrophage Expressed 1
NEI	National Eye Institute
NIH	National Institute of Health
ONH	Optic Nerve Head
ONL	Outer Nuclear Layer
Pax6	Paired Box 6
PCNA	Proliferating Cell Nuclear Antigen
PCR	Polymerase Chain Reaction
PGC	Primordial Germ Cell
Plek	Pleckstrin
Pou6F2	POU Class 6 Homeobox 2
Pparg	Peroxisome Proliferator-Activated Receptor Gamma
Ptpn6	Protein Tyrosine Phosphate, Non-Receptor Type 6
RGC	Retinal Ganglion Cell
RPC	Rod Progenitor Cell
RPE	Retinal Pigment Epithelium
RRBS	Reduced Representation Bisulifite Sequencing
RT-PCR	Reverse Transcription Polymerase Chain Reacion
Sox2	Sex Determining Region Y-Box 2
Spi1	Spleen Focus Forming Viurs Proviral Integration Oncogene
SV40	Simian Vacuolating Virus 40
TA	Tibialis Anterior
TDG	Thymine DNA Glycosylase
Tet	Ten-Eleven-Translocation Methylcytosine Dioxygenase
Tnfa	Tumor Necrosis Factor Alpha
Tnfb	Tumor Necrosis Factor Beta
Topors	Topoisomerase 1 Binding, Arginine/Serine-Rich, E3 Ubiquitin Protein Ligase
Tuba1a	Tubulin, Alpha 1a
Tunel	Terminal Deoxynucleotidyl Transferase dUTP Nick End Labeling
Ubc9	E2 SUMO-Conjugating Protein Ubc9
Ube2i	Ubiquitin-Conjugating Enzyme E2I
Uhrf1	Ubiquitin-Like With PHD and Ring Finger Domains 1
UTR	Untranslated Region

Abstract

Despite a high degree of similarity in retinal structure and function, zebrafish respond to retina and optic nerve damage with a regenerative response, while mammals do not. Moreover, the cell types responsible for these regenerative events, Müller glia (MG) and retinal ganglion cells (RGCs), are present in both zebrafish and mammalian retinas. The key to stimulating endogenous regeneration in mammals following retina or optic nerve damage likely resides in the ability to coax mammalian MG or RGCs into responding similarly to their zebrafish counterparts. To this end, zebrafish have been used as a model system in an attempt to understand the causative events and the cellular changes occurring in MG and RGCs during regeneration.

This work describes the identification and characterization of Apolipoprotein B mRNA Editing Complex 2a and 2b (Apobec2a,2b) as components of these regenerative events in zebrafish. Although Apobec2 proteins were first identified over 13 years ago, their function has remained unresolved. Other members of the Apobec protein family participate in cytosine deaminase-dependent DNA/RNA mutagenesis and DNA demethylation. The experiments described in this work were designed with the goal of learning about the events accompanying retina and optic nerve regeneration and about the biochemical function of Apobec2 proteins, simultaneously. Herewith, the following is characterized during regeneration: gene expression programs, the regulation of DNA methylation, the poised programming state of quiescent MG, changes in mRNA editing, and the activation of the immune response in the progression of regeneration. Furthermore, we demonstrate that Apobec2a,2b are necessary for zebrafish retina and optic nerve regeneration and that they function independent of DNA demethylation, RNA editing, and likely cytosine deamination. We show that their biochemical function is conserved and dependent on the proper binding of zinc, and we identify Apobec2 interacting proteins and characterize potential roles for these interactions. Finally, a working model is proposed in which Apobec2a,2b function

independent of cytosine deamination during retina and optic nerve regeneration. Cumulatively, this work serves as a valuable resource to the current understanding of zebrafish retina and optic nerve regeneration and the biochemical function of Apobec2 proteins, and opens multiple avenues for future research.

Chapter 1:
Introduction

The work described in this dissertation is focused on characterizing the role of Apobec2 proteins during zebrafish retina and optic nerve regeneration. In order to place this work within the context of the scientific literature, here I include background and a historical overview covering the topics of zebrafish retina and optic nerve regeneration, DNA methylation, and the Apobec protein family.

1.1 Zebrafish Retina and Optic Nerve Regeneration

According to a recent survey by the NIH's National Eye Institute (NEI), most Americans report that, of all debilitating diseases, the loss of eyesight would have the greatest impact on their daily lives, ranking ahead of the loss of memory, speech, limb, and hearing. The NEI also reports that one in 28 people in the United States suffer from low vision or blindness (http://www.nei.nih.gov/kap/). This represents a major public health problem, decreasing the productivity and quality of life of those affected and extracting a large national economic toll. Three of the leading causes of vision loss (glaucoma, macular degeneration, and diabetic retinopathy) are neural degenerations, characterized by irreversible damage of the retina due to the death of neurons residing there. Many approaches are being developed to treat vision loss resulting from retinal diseases and degenerations, including prosthetic devices, cell transplantation, and gene therapies. While these techniques have shown some success, one can imagine how advantageous it would be to treat these retinopathies by awakening the intrinsic regenerative capabilities of endogenous retinal cells, which have demonstrated this regenerative potential in other vertebrates.

1.1.1 Retina Structure and Biology

The retina is an extension of the central nervous system (CNS) that lines the inner surface of the eye. This tissue is responsible for the detection of light. Other tissues, such as

the cornea and lens, are responsible for focusing light prior to its reaching the retina (Figure 1.1A). Once detected, light stimulates a cascade of events and cellular communications between the neurons that reside in the retina, which ultimately transmit this information to the brain.

The structure of the retina is divided up into three cellular layers: the outer nuclear layer (ONL), the inner nuclear layer (INL), and the retinal ganglion cell layer (GCL). Rod and cone photoreceptors residing in the ONL sense light entering the eye and relay this information on to the retinal ganglion cells (RGCs) residing in the GCL via connections with INL interneurons (bipolar cells, amacrine cells and horizontal cells). The axons of RGCs converge and form the optic nerve, which extends to the brain and facilitates the transmission of the visual information detected by the eye to the brain (Figure 1.1A).

Müller glia (MG) and microglia are two non-neural, glia cell types residing in the retina, with MG playing the more significant role in retinal homeostasis. While the nuclei and cell bodies of MG reside in the INL, their processes are unique in that they extend into all retinal layers and span the entire width of retina, allowing them to form contacts with neighboring retinal neurons and blood vessels and to contribute to the outer and inner limiting membranes (Magalhaes and Coimbra, 1972; Reichenbach and Reichelt, 1986) (Figure 1.1A). This unique structure allows MG to perform their many functions such as 1) to maintain retinal homeostasis by recycling neurotransmitters and controlling the extracellular ionic balance (Pow and Crook, 1996; Schutte and Werner, 1998; Bringmann et al., 2009); 2) to support neurons by releasing trophic factors (Seki et al., 2003) and by participating in the cone-specific visual cycle (Long et al., 1986; Wang et al., 2005; Wang and Kefalov, 2011); 3) to serve as barriers and conduits for the transfer of molecules between cells (Tout et al., 1993; Nagelhus et al., 1999; Shen et al., 2012); and 4) to act as optical fibers, guiding light to photoreceptors (Franze et al., 2007).

1.1.2 Mammalian Retina Injury Response (Protective and Regenerative Responses)

Damage to the retina can come from a variety of sources: trauma, cancer, ischemia, hematoma, retinal disease, etc. After insult, the primary objective of the retina is to prevent further damage, and because of this, a neuroprotective program is initiated. This neuroprotective function is largely carried out by MG through gliosis (Bringmann and

Reichenbach, 2001; Bringmann et al., 2006). During gliosis, MG undergo morphological, biochemical, and physiological changes that vary with the type and severity of insult. Neuroprotection can involve: 1) the production of neurotrophic factors, growth factors, cytokines, and erythropoietin that protect neurons from death (Wen et al., 1995; Cao et al., 1997; Harada et al., 2000; Yasuhara et al., 2004a; Yasuhara et al., 2004b; Fu et al., 2008); 2) the reestablishment of extracellular ion levels (Bringmann et al., 2006); 3) the uptake of excess glutamate which is neurotoxic (Bringmann et al., 2009); and 4) the phagocytosis of exogenous substances and cell debris (Faude et al., 2001; Chang et al., 2006; Kaur et al., 2007). However, gliosis can also have detrimental effects including 1) the impairment of the normal supportive functions of MG; 2) the release of proinflammatory cytokines resulting in cytotoxic effects (Tezel and Wax, 2000; Yuan and Neufeld, 2000); and 3) the formation of inhibitory glial scars (Lewis and Fisher, 2000; Fisher and Lewis, 2003; Francke et al., 2005; Sethi et al., 2005).

Because retinal damage can result in neuronal cell death, a regenerative response is needed in addition to a neuroprotective response to generate new neurons, and ultimately to restore proper vision. But, the mammalian retina lacks an active retinal progenitor population, limiting its ability to produce new neurons. In addition, injuries or diseases that result in damage to the optic nerve require a regenerative response to stimulate the axonal outgrowth of RGCs to regain proper communication between the retina and the brain. Yet, mammalian RGCs' intrinsic capacity for axon growth declines shortly after birth (Goldberg et al., 2002). Furthermore, injured or diseased axons that fail to regenerate successfully often succumb to neuronal death or atrophy (Goldberg and Barres, 2000). Other factors impacting mammalian retina and optic nerve regeneration include the formation of glial scars (as mentioned above) and inhibitory signals (Schwab, 2004; Silver and Miller, 2004; Yiu and He, 2006). Current work using model systems is being directed towards stimulating a mammalian regenerative response.

1.1.3 Model Systems for Studying Retina and Optic Nerve Regeneration

In order to restore vision following retinal neuron cell death or optic nerve damage, a series of events needs to occur, but key to the success of these regenerative events is the

generation of a retinal progenitor population and the establishment of an axonal growth-permissive state, respectively.

Although MG do not function as neural progenitors during development (Weissman et al., 2003), recent work using model systems has shown that under special conditions, these MG can become activated and undergo a reprogramming event that allows them to proliferate and generate a population of proliferating progenitors (MGPCs) to regenerate lost neurons and glia (Fausett and Goldman, 2006; Raymond et al., 2006; Bernardos et al., 2007; Fausett et al., 2008; Ramachandran et al., 2010a). While mammalian MG do not demonstrate this ability *in vivo*, increasing evidence hints that they have an intrinsic regenerative potential and suggests that they could be coaxed to adopt these retinal progenitor characteristics (Das et al., 2006; Lawrence et al., 2007; Roesch et al., 2008; Jadhav et al., 2009). For example, while not acquiring a progenitor state, mammalian MG can respond to injury, proliferate, and express some retinal stem cell associated markers (Roesch et al., 2008; Jadhav et al., 2009). Furthermore, primary cultures of mammalian MG can be stimulated to generate retinal neurons and glia (Das et al., 2006; Lawrence et al., 2007).

For optic nerve regeneration, RGCs must enter into an axonal growth-permissive state. While mammalian RGCs seem to lose their intrinsic capacity for axon growth after birth (Goldberg et al., 2002), an abundance of evidence gathered using model systems suggests that this potential for axonal regrowth can be stimulated (Fischer, 2012; Fischer and Leibinger, 2012).

Model systems are essential for our ability to learn how to increase the human visual regenerative potential. For choice of a model organism, one can choose a system that regenerates endogenously and study how this occurs (newts, frogs, goldfish, zebrafish, postnatal chicks, etc), or one can choose a system that lacks a regenerative response and attempt to stimulate one (mice, rats, cats, etc). Both approaches have led to great discoveries in the field of regeneration.

The work described in this dissertation employs the use of zebrafish, which have emerged as a powerful model system for studying regeneration. Zebrafish research has dominated the field of retina regeneration and has made key contributions to the field of optic nerve regeneration. Teleosts, including zebrafish, respond to retinal damage with a robust

regenerative response (Mensinger and Powers, 1999; Senut et al., 2004; Fausett and Goldman, 2006; Bernardos et al., 2007; Sherpa et al., 2008). This, in combination with the ease with which they are bred, maintained, and genetically manipulated, provides definite advantages over other model systems. Importantly, because of the high degree of structural and functional similarity between the zebrafish and the mammalian retina, it is likely that discoveries made in zebrafish will be applicable to mammals.

In contrast to the mammalian retina (which does not contain a source of retinal progenitors and grow very little after birth), the teleost retinal environment is highly amenable to progenitor cell formation/maintenance and boasts three sources of progenitor cells, which are necessary for the continued grow of their retinas throughout life: 1) a circumferential ring known as the ciliary marginal zone (CMZ) houses progenitors that provide neurons and glia to the extreme periphery of the retina as it grows (Johns, 1977); 2) rod precursors in the ONL produce rod photoreceptors during retinal growth (Johns and Fernald, 1981); and 3) MG replenish the rod precursor populations and can be stimulated to generate retinal progenitors (MGPCs) following injury (Fausett and Goldman, 2006; Bernardos et al., 2007; Fimbel et al., 2007; Thummel et al., 2008a) (Figure 1.1A).

1.1.4 MG and Retina Regeneration

While the regenerative capacity of the teleost fish retina has been long recognized (Braisted and Raymond, 1992; Hitchcock et al., 1992; Otteson et al., 2001), it was not until recently that the source of progenitors acting during retina regeneration was identified. Through the use of zebrafish transgenics, MG were identified as this source of progenitors (Fausett and Goldman, 2006; Bernardos et al., 2007; Fimbel et al., 2007). Importantly, BrdU and CreER/LoxP lineage tracing experiments demonstrated that these MGPCs regenerate all of the major retinal cell types and that these cells remain stably integrated in the retina for extended periods of time (Fausett and Goldman, 2006; Ramachandran et al., 2010b).

Much has been learned about the regenerative response of MG in the relatively short period of time since then. This regenerative response can be roughly divided into three phases: 1) the activation and reprogramming of MG to acquire stem cell-like properties; 2) the generation of MGPCs; and 3) the differentiation of these progenitors (Figure 1.1B). While some information has been gathered for the final phase of this process (Qin et al.,

2009; Craig et al.; Ramachandran et al., 2012; Wan et al., 2012; Nagashima et al., 2013), the majority of the research effort has been dedicated to how MG become activated and generate MGPCs (Kassen et al., 2007; Fausett et al., 2008; Qin et al., 2009; Ramachandran et al., 2010a; Thummel et al., 2010; Ramachandran et al., 2011; Nelson et al., 2012; Powell et al., 2012; Wan et al., 2012; Lenkowski et al., 2013; Nagashima et al., 2013; Nelson et al., 2013; Powell et al., 2013). These events have been described in recent reviews (Nelson and Hyde, 2012; Lenkowski and Raymond, 2014).

While much can be said about how these early phases occur, I will limit this discussion to a few factors that were among the first identified and that were more relevant to the design of my project. One of the first factors identified as being necessary for MG activation and progenitor formation was the basic helix-loop-helix transcription factor Ascl1a (Fausett et al., 2008), which has since been identified as a central hub in the regenerative response and was recently shown to reprogram mouse MG into progenitors in cell culture (Pollak et al., 2013). Soon after the initial characterization of Ascl1a during zebrafish retina regeneration, it was determined that one of its functions is the activation of a Lin28/let-7 miRNA signaling pathway which impacts the activation of other pluripotency factors (Ramachandran et al., 2010a). This work was in development when I joined the Goldman lab. The fact that many of these pluripotency factors were transcriptionally regulated during MG activation played a large role in my thought process as I developed my project and is further discussed below (Section: DNA Methylation).

1.1.5 Retinal ganglion cells and Optic Nerve Regeneration

While the majority of my work focused on the processes of MG activation and MGPC formation during retina regeneration, some of my data was gathered studying optic nerve regeneration. Because of this, I include a short overview of optic nerve regeneration.

Like the MG response during retina regeneration, optic nerve regeneration can be divided into three phases: 1) the generation of a growth-permissive state; 2) axonal regrowth and path finding; and 3) the reestablishment of synaptic connections with the optic tectum (superior colliculus) of the brain (Figure 1.1C). Contrary to retina regeneration, no proliferative event is needed during optic nerve regeneration (provided that no neurons are lost).

Understanding and stimulating the first phase of this process has been the focus of much of the research in this field. Many molecules have been shown to stimulate and/or be necessary for a regenerative response following optic nerve damage and are discussed in a number of recent reviews (de Lima et al., 2012; Fischer, 2012; Fischer and Leibinger, 2012; Zhu et al., 2013). Two key events occur during the generation of a growth-permissive state: 1) the activation of an intrinsic developmental axonal growth program and 2) the overcoming of growth-inhibitory signals.

The study of regeneration in zebrafish has led to useful insights into ways to augment the regenerative capacity of mammals. It is anticipated that unraveling the mechanisms underlying retina and optic nerve regeneration in zebrafish will suggest novel strategies for stimulating these processes in an injured or diseased mammalian retina. Revealing the mechanisms by which MG and RGCs change their cellular identities as they reprogram to a multipotent progenitor or axonal growth-permissive state is one of the keys to the success of this strategy.

1.2 DNA Methylation

Although each cell type of an organism contains essentially the same genetic information, each is unique and has an identifiable appearance and biochemical signature. A number of variables contribute to cellular identity, but differential gene expression is the cornerstone of this identity. Epigenetic information, including modified DNA nucleotides, histone modifications, and non-coding RNAs, determines which genes are “on” and “off” in any particular cell.

One epigenetic modification, 5-methylcytosine (5-meC), occurs when a methyl group is appended to the C5 position of cytosine bases in DNA (Figure 1.2A). This modification is a well-studied form of DNA methylation and is a stable epigenetic mark that can be inherited mitotically and meiotically. It is present in diverse forms of life from prokaryotes to eukaryotes and was discovered in mammals as early as DNA was identified as genetic material (Avery et al., 1944; McCarty and Avery, 1946). It performs a variety of functions, the first of which was characterized in bacteria where it was found to control restriction-modification systems (Boyer, 1964; Uetake et al., 1964; Lederberg, 1965; Casadesus and Low, 2006), which are thought to have evolved as a form of cellular defense, targeting

foreign DNA for degradation. Since then, a number of important processes have been attributed to DNA methylation in mammals: genomic imprinting (Hata et al., 2002; Kaneda et al., 2004; Kato et al., 2007), X-chromosomal inactivation (Barakat and Gribnau, 2012), inhibition of retrotransposition (Walsh et al., 1998; Bourc'his and Bestor, 2004), and regulation of gene expression (Weber et al., 2007; Farthing et al., 2008; Mohn et al., 2008). Mechanistically, DNA methylation is thought to regulate gene expression by recruiting proteins involved in gene repression or by inhibiting the binding of transcriptional activators to DNA. DNA methylation in mammals has been shown to be essential as its loss leads to cellular growth arrest or apoptosis in normal cells and cancer cells (Jackson-Grusby et al., 2001; Chen et al., 2007). Because of this, multiple drugs have been developed to perturb DNA methylation as a way to treat cancer.

In mammals, 5-meC most commonly occurs within the context of a CpG dinucleotide. Non-CpG methylation has recently been identified, but its function is still unclear (Lister et al., 2009). The specific role that CpG methylation plays appears to be dependent on its position in the DNA sequence relative to gene coding regions (Jones, 2012). More than half of the genes in vertebrate genomes contain short CpG rich regions known as CpG islands, while the rest of the genome is relatively depleted for CpGs. The function of DNA methylation in proximity to gene coding regions has been characterized most carefully, and there is a growing consensus for its role. In mammals, most CpG islands are not methylated when located near the transcriptional start site of a gene, but when these regions are methylated, it is associated with long-term gene silencing through the inhibition of transcription initiation. This type of regulation occurs in the control of some pluripotency and tissue specific genes. In addition, CpG islands in gene bodies are sometimes methylated in a tissue-specific manner. Non-CpG island methylation is more dynamic and tissue-specific than CpG island methylation (Han et al., 2011; Jones, 2012). Because of the role that DNA methylation plays in the regulation of gene expression, enzymes that modulate DNA methylation have a large impact on cellular identity.

1.2.1 Establishment of DNA Methylation

Although the earliest events of development are marked with the global erasure of DNA methylation (with the exception of certain imprinted regions), resulting in an overall

hypomethylated state (Monk et al., 1987; Santos et al., 2002; Jones, 2012; Saitou et al., 2012), the establishment of DNA methylation at later events is needed to induce and/or maintain the silencing of pluripotency and germ line-specific genes (Shen et al., 2007; Weber et al., 2007; Farthing et al., 2008; Mohn et al., 2008) and to regulate and/or stabilize lineage-specific gene expression during differentiation (Hemberger et al., 2009).

With the exception of the targeting of DNA methylation (which in plants is aided by small RNAs), the mechanistic establishment of DNA methylation has been well-characterized biochemically and genetically. DNA methylation is catalyzed by a family of DNA methyltransferases (Dnmts) that transfer a methyl group from S-adenosylmethionine (AdoMet or SAM) to the C5 position of cytosine forming 5-meC. In mammals there are three such enzymes: Dnmt1, Dnmt3a, and Dnmt3b. A structurally related protein, Dnmt3l, is catalytically inactive and serves as a cofactor for Dnmt3a and Dnmt3b and stimulates their activity (Chedin et al., 2002; Gowher et al., 2005; Jia et al., 2007). Another enzyme recognized by sequence homology, Dnmt2, was later found to methylate RNA instead of DNA (Goll et al., 2006).

Dnmt3 enzymes can establish new methylation patterns to unmodified DNA and are thus known as *de novo* methyltransferases (Figure 1.2C). They are responsible for creating the DNA methylation landscape during development (Okano et al., 1999) . Dnmt1 functions during DNA replication to propagate the methylation landscape from parent to daughter strand by acting on hemimethylated DNA (Jones and Liang, 2009). The recruitment of Dnmt1 to hemimethylated DNA is aided by Uhrf1 (Achour et al., 2008; Arita et al., 2008; Avvakumov et al., 2008) (Figure 1.2B). Dnmt3 proteins cooperate with Dnmt1 to efficiently maintain DNA methylation during replication at sites that were missed by Dnmt1 (Arand et al., 2012).

1.2.2 DNA Demethylation

The knowledge of how 5-meC is removed from DNA has lagged behind the knowledge of its establishment, and much has yet to be learned about the process of DNA demethylation. In the simplest sense, DNA demethylation can occur in a replication-dependent fashion, independent from any enzymatic activity. Thus by undergoing a series of rapid proliferative events, it would be possible to demethylate the genome (Figure 1.2D).

While this may be the case in some instances, there is mounting evidence for a replication-independent or an active mechanism of DNA demethylation. For example, within the first hours after fertilization, the paternal DNA undergoes a rapid loss of 5-meC in the zygote before the first cell division (Mayer et al., 2000; Oswald et al., 2000; Saitou et al., 2012). Evidence for active DNA demethylation is also found in studies of primordial germ cells (PGCs) (Hajkova et al., 2002; Popp et al., 2010), where global DNA demethylation is important for setting up pluripotent states in the early embryo and for erasing parental-origin-specific imprints (Feng et al., 2010).

Although the exact mechanism of DNA demethylation remains unclear, it is evident that it is more complicated than the process of DNA methylation, in that it likely requires multiple intermediate steps and enzymes. Many proteins have been associated with decreases in DNA methylation including Gadd45 (Barreto et al., 2007; Rai et al., 2008; Ma et al., 2009a; Schmitz et al., 2009), Apobec/AID (Morgan et al., 2004; Rai et al., 2008; Bhutani et al., 2009; Popp et al., 2010; Santos et al., 2013), Tet (Ito et al., 2010; Guo et al., 2011; He et al., 2011; Mohr et al., 2011), and DNA glycosylase proteins (Rai et al., 2008; Ma et al., 2009a; Zhu, 2009; Cortellino et al., 2011; Santos et al., 2013). Models of DNA demethylation include processes of deamination, oxidation, or both (Figure 1.2E). While mechanisms involving Tet enzymes appear to be used most frequently (Wu and Zhang, 2014), it is likely that these different mechanisms function either jointly or at different times (Santos et al., 2013).

In addition to development, active DNA demethylation has been associated with other reprogramming events including nuclear transfer (Simonsson and Gurdon, 2004; Jullien et al., 2011), heterokaryon formation (Bhutani et al., 2009), induced pluripotency stem cell (iPSC) generation (Meissner et al., 2008; Mikkelsen et al., 2008; Polo et al., 2012; Hackett et al., 2013; Kumar et al., 2013b), and cancer (Ehrlich, 2009; Ehrlich and Lacey, 2013; Kristensen et al., 2013). This is particularly true for promoter regions of pluripotency genes (Mikkelsen et al., 2008; Bhutani et al., 2009; Polo et al., 2012).

Because MG reprogram and activate the expression of pluripotency genes during retina regeneration and because RGCs reawaken a developmental growth potential following optic nerve injury, I hypothesized that DNA demethylation was an important event regulating these transitions. This led me to perform a preliminary survey where I measured mRNA

levels of genes correlated with DNA demethylation (listed above) at multiple times following injury to the retina. These preliminary data indicated that Apobec2 proteins might be important for zebrafish retina regeneration.

1.3 Apobec Protein Family

The underlying genetic mechanism of evolution is the generation of random mutations and the selection of those that provide a benefit to life. In some instances, nonspecific mutations in DNA are unfavorable and can arise due to replication errors, incidental DNA damage, or the movement of viruses or transposable elements. These mutations can have devastating effects on cellular function, manifest in developmental defects, disease, and cancer. But, there are a limited number of cases where controlled, targeted mutations are beneficial to life.

1.3.1 Apobec Proteins, Cytosine Deaminases

Apobec proteins are a vertebrate-specific group of zinc-dependent enzymes capable of introducing mutations in DNA and RNA through cytosine deamination. This catalytic activity only occurs within the context of polynucleotides and results in the conversion of cytosine or 5-meC to uracil or thymine, respectively (Figure 1.2E and 1.3A). The family is named after Apolipoprotein B Editing Complex 1 (Apobec1), the first Apobec protein identified (Teng et al., 1993). Apobec1 is a mammalian enzyme that was first shown to deaminate C6666 in Apolipoprotein B (ApoB) mRNA, a major component in lipid transport, changing a glutamine codon into a stop codon resulting in a truncated form of ApoB that is involved in the assembly of chylomicrons (Navaratnam et al., 1993; Teng et al., 1993). Its ability to edit other RNAs has been demonstrated (Skuse et al., 1996; Mukhopadhyay et al., 2002), as well as its ability to act on DNA substrates (Skuse et al., 1996; Harris et al., 2002a; Petersen-Mahrt and Neuberger, 2003; Gee et al., 2011). After the discovery of Apobec1 a number of other Apobecs were identified with varying functions.

Activation Induced Cytidine Deaminase (AID), an Apobec found in jawed vertebrates, was found to be essential for antigen-driven diversification of immunoglobulin genes in the adaptive immune system (Muramatsu et al., 1999). Subsequent genetic experiments revealed its central role in class-switch recombination, somatic hypermutation,

and gene conversion (Muramatsu et al., 2000; Arakawa et al., 2002; Harris et al., 2002b). As mentioned previously, AID has also been shown to function during multiple reprogramming events, by participating in a multistep process of DNA demethylation (Morgan et al., 2004; Bhutani et al., 2009; Popp et al., 2010; Santos et al., 2013).

APOBEC3 proteins where first identified as paralogs to Apobec1 and are found in placental mammals (Jarmuz et al., 2002). Humans encode seven APOBEC3s: 3A, 3B, 3C, 3D/E, 3F, 3G, and 3H. These proteins are highly divergent. APOBEC3B, D/E, F and G differ from APOBEC3A, C, H, and all other Apobecs in that they contain two deaminase domains instead of one within a single polypeptide (Jarmuz et al., 2002). One of these domains is generally acidic while the other is basic. Although the acid domain of these bi-domain APOBEC3s is catalytic, the basic domain is not; nonetheless, this basic domain contributes to cytosine deamination by stimulating the binding of APOBEC3s to polynucleotides (Figure 1.3A) (Hakata and Landau, 2006; Bogerd et al., 2007). APOBEC3G was identified as the factor involved in HIV restriction (Sheehy et al., 2002) and has since become the most studied Apobec protein. After infection, APOBEC3G is packaged into the HIV virion and mutates the nascent first DNA strand produced by reverse transcription, inhibiting its integration into the host genome or mutating it to the point of no functionality (Harris et al., 2003; Lecossier et al., 2003; Mangeat et al., 2003; Mariani et al., 2003; Zhang et al., 2003). Because of their ability to mutate mobile elements, including endogenous retroelements and exogenous viruses, it has become clear that a major function of APOBEC3 proteins lies in the innate immunity (Conticello, 2008; Koito and Ikeda, 2012; Smith et al., 2012).

Other Apobec proteins (Apobec2, Apobec4, and Apobec5) have received considerably less attention. Apobec5s, the most recently identified Apobec proteins, have yet to be analyzed (Severi et al., 2011). They are present in non-placental vertebrates and are speculated to be functional homologues of the APOBEC3s (Severi et al., 2011). Interestingly, in biochemical analyses used to demonstrate deamination by other Apobec proteins, Apobec2 and Apobec4 (both found in jawed vertebrates) appear unable to deaminate cytosine (Harris et al., 2002a; Mikl et al., 2005; Lada et al., 2011). While this may be due to the context of the experimental design, it raises the possibility that Apobec proteins perform functions independent of deamination.

1.3.2 Cytosine Deaminase-Independent Function of Apobecs

Although the majority of the research on Apobec proteins has focused on characterizing their cytosine deaminase-dependent functions, evidence for deaminase-independent functions has been reported. Apobec1 has been shown to bind the 3' untranslated region (UTR) of Cox-2 and c-myc mRNA, stabilizing their turnover (Anant and Davidson, 2000; Blanc et al., 2007), and APOBEC3 proteins have been found to block viral replication, specifically during elongation (Iwatani et al., 2007; Aguiar and Peterlin, 2008; Narvaiza et al., 2009).

Evolutionary analyses of Apobec proteins suggest that AID, Apobec2, and Apobec4 are the ancestral members of the Apobec family, with all other members likely stemming from AID (Conticello et al., 2005; Conticello, 2008; Severi et al., 2011). Although no function has been identified for Apobec2 or Apobec4 proteins, their sequences are conserved, particularly in mammals. While Apobec2 is evolutionarily much older than Apobec1, substitution rates indicate that it is much more highly conserved (Liao et al., 1999). This is similar to comparisons to the Apobec3 proteins, which demonstrate a high degree of sequence diversity (Sawyer et al., 2004; Zhang and Webb, 2004). This suggests that Apobec2 and Apobec4 proteins may possess an ancestral function that is independent of cytosine deamination.

1.3.3 Apobec2 Proteins

Apobec2 was the second Apobec protein identified, through its sequence homology to Apobec1 (Liao et al., 1999; Anant et al., 2001a), and was the first Apobec for which structural data was obtained (Prochnow et al., 2007). Other Apobec crystal structures currently available include those of the C-terminal catalytic domain of APOBEC3G (Chen et al., 2008; Holden et al., 2008; Shandilya et al., 2010), the C-terminal catalytic domain of APOBEC3F (Bohn et al., 2013), and APOBEC3C (Kitamura et al., 2012). These structures reveal a five-stranded ß-sheet core surrounded by six α-helices. This is very similar to the structures of free nucleotide cytidine deaminases (CDAs), which also possess a five-stranded ß-sheet core but differ in the number of flanking α-helices. These Apobec structures also provide glimpses of their cytosine deaminase active sites, which contain a zinc ion coordinated by two cysteines and a histidine and a catalytic glutamate residue (Figure 1.3B).

Interestingly, the APOBEC2 crystal structure provides evidence for Apobec oligomerization, and it is anticipated that this oligomerization aids in its ability to engage long polynucleotides (Prochnow et al., 2007; Shandilya et al., 2010). Similarly, dimerization and tetramerization of CDAs has been reported and is required for their function (Johansson et al., 2002; Costanzi et al., 2006). Other groups have reported evidence for oligomerization of Apobec1 (Teng et al., 1999), Apobec2 (Sato et al., 2009; Etard et al., 2010), APOBEC3 (Burnett and Spearman, 2007), and AID (Wang et al., 2006). While it is evident that Apobec proteins have the potential to oligomerize, it is unclear how physiological this oligomerization is, as other groups report their lack of oligomerization (Brar et al., 2008; Chen et al., 2008; Holden et al., 2008; Krzysiak et al., 2012).

It is possible that the differences seen in Apobec oligomerization are dependent on the portion of the protein studied, the protein and salt concentrations, and substrate availability (Bransteitter et al., 2009; Chaurasiya et al., 2014). This may be particularly true for APOBEC2, whose crystal structure lacked 41 amino acids of its N-terminus (Prochnow et al., 2007). This N-terminus is very unique and is a distinguishing factor of all Apobec2 proteins (Figure 1.3A). Notably, another Apobec2 structural study, which used the full-length protein instead of the N-terminally truncated protein, suggested that Apobec2 is a monomer in solution and demonstrated that a flexible N-terminal region (removed with the N-terminal truncation for the crystal structure) precludes its ability to oligomerize (Krzysiak et al., 2012).

Unlike other characterized Apobecs, biochemical studies of purified Apobec2 suggest that its ability to bind polynucleotides is limited (Anant et al., 2001a; Sato et al., 2009). Interestingly, in comparison to most other Apobec proteins, Apobec2 proteins are highly acidic which may hinder their binding to highly negatively charged DNA or RNA. This alone could explain their lack of deaminase activity in previous biochemical assays (Harris et al., 2002a; Mikl et al., 2005; Lada et al., 2011). While this data would suggest that Apobec2 does not regulate polynucleotides, it is possible that these results are dependent on the context of the experiments, which may lack a key component necessary for these events to occur. This would not be entirely unexpected, as one would assume that a potential DNA or RNA mutator would be highly regulated. Such is the case for Apobec1, whose function is

highly modulated by Apobec1 complementation factor (ACF) (Mehta et al., 1996; Lau et al., 1997; Teng et al., 1999).

While biochemical data for Apobec2 is lacking, a considerable amount of molecular data has been gathered. Apobec2 expression is highest in cardiac and skeletal muscle, but it is also seen in many other cell types (Lau et al., 1997; Anant et al., 2001a). Pro-inflammatory cytokines (Matsumoto et al., 2006) and the tumor suppressor p53 (Kostic and Shaw, 2000) have been shown to induce Apobec2 expression, and Apobec2 appears to inhibit TGFß signaling, though the mechanism of this inhibition is unknown (Vonica et al., 2011). Increased Apobec2 expression, whether endogenous or exogenous, is correlated with a number of processes including 1) cellular differentiation (Sato et al., 2009; Pennings et al., 2011; Vonica et al., 2011), 2) inflammation (Iio et al., 2010), 3) liver and lung tumorigenesis (Okuyama et al., 2011), and 4) skeletal muscle aging (Piec et al., 2005). Forced reduction of Apobec2, through knockdown or knockout technologies, has been shown to: 1) cause a dystrophic muscle phenotype in zebrafish (Etard et al., 2010); 2) decrease body mass, alter muscle fiber type ratios, and cause myopathies in mice (Sato et al., 2009); and 3) perturb developmental left-right axis specification in frogs and zebrafish (Vonica et al., 2011). Although no direct biochemical data exists that shows Apobec2 possesses cytosine deaminase activity, these studies all hypothesize that Apobec2 is acting in these processes by catalytically editing RNA.

At the onset of my dissertation research, the most compelling evidence of a biochemical function for Apobec2 proteins suggested that they participate in a multiprotein complex to engage DNA and carry out DNA demethylation during zebrafish development (Rai et al., 2008). This paper demonstrated that the expression of Apobec2 proteins was regulated by the presence of exogenously introduced methylated DNA, and that Apobec2 proteins, directly or indirectly, impacted its demethylation. Furthermore, overexpression of Apobec2 proteins in conjunction with MBD4 increased global genomic DNA methylation levels as measure by mass spectrometry. Because this paper provided the most thorough analysis of Apobec2 function, it guided a lot of my early thought processes as I designed my project.

1.4 Central Goal and Specific Aims of Dissertation

With this background in mind, I hypothesized that Apobec2 proteins were necessary for zebrafish retina and optic nerve regeneration and that they functioned to regulate cellular identity through the process of DNA demethylation. To test this hypothesis, I formulated a number of specific aims:

SPECIFIC AIM 1: Characterize the expression of Apobec2 genes during retina and optic nerve regeneration and determine their necessity for these events.

SPECIFIC AIM 2: Characterize changes in genomic DNA methylation as MG reprogram for retina regeneration and determine if Apobec2 proteins impact DNA demethylation.

SPECIFIC AIM 3: Perform mRNA comparisons of MGPCs with and without knockdown of Apobec2 and identify any mRNA that is edited in an Apobec2-dependent fashion.

SPECIFIC AIM 4: Determine if the catalytic activity of Apobec2 is necessary for regeneration and if the regenerative function of zebrafish Apobec2 proteins is conserved in human APOBEC2.

SPECIFIC AIM 5: Identify and characterize Apobec2 interacting proteins during the regenerative response, including the possibility of Apobec2 protein oligomerization.

Experiments designed to test these specific aims are described in Chapters 2 through 5. At the completion of these research chapters, a conclusion chapter is included to summarize what has been learned through this work and to describe future directions that could build upon these results.

1.5 Figures

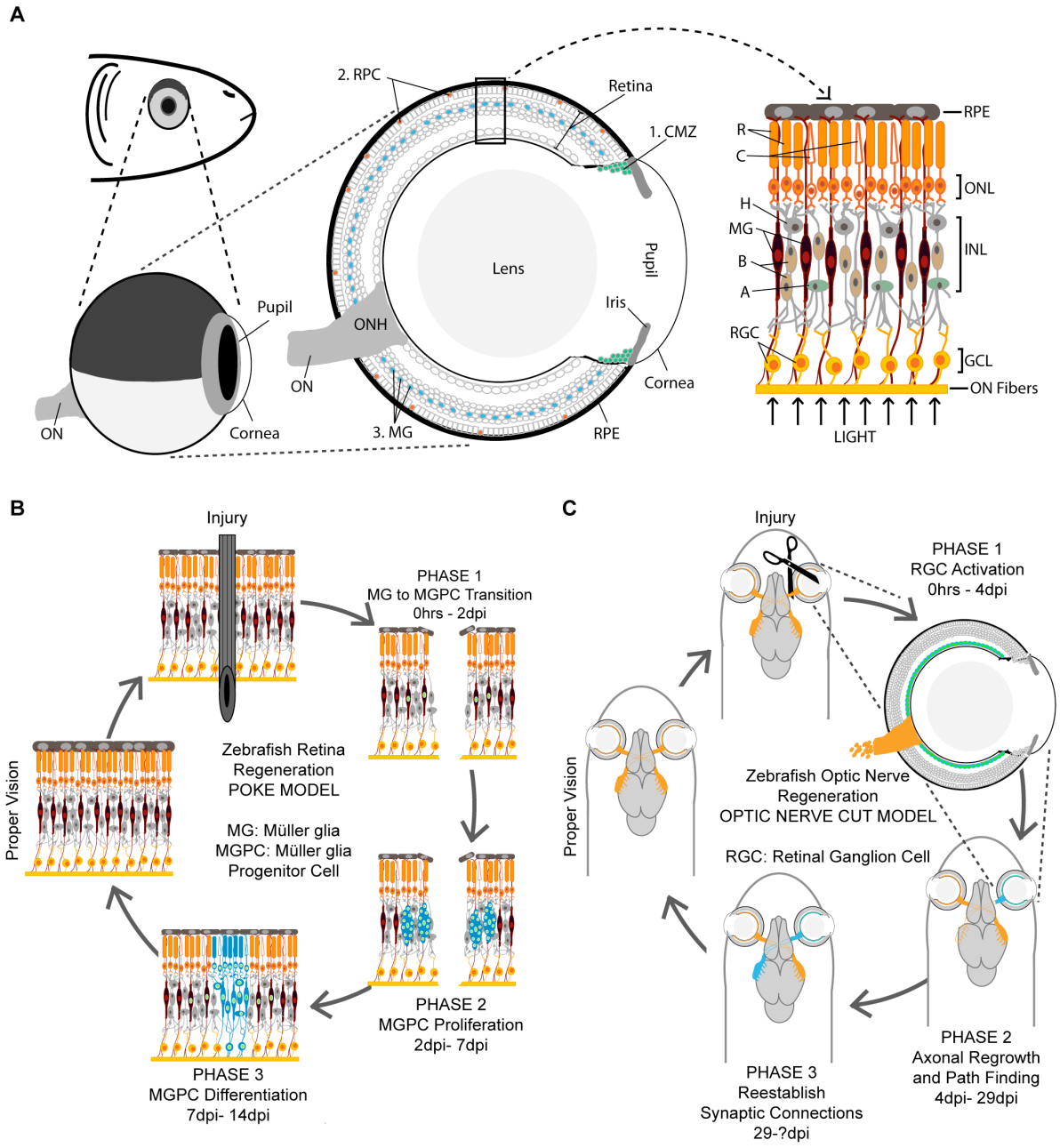

Figure 1.1 Zebrafish retina and optic nerve regeneration

(A) Structure of the zebrafish eye and retina. Also listed and located are the zebrafish endogenous sources of retinal progenitors (CMZ, RPC, MG). (B) Diagram showing the phases of MG-dependent, zebrafish retina regeneration following mechanical lesion with a 30-gauge needle. (C) Diagram showing the phases of RGC-dependent, zebrafish optic nerve regeneration following optic nerve cut. ON, optic nerve; ONH, optic nerve head; CMZ, ciliary marginal zone; RPC, rod precursor cells; MG, Müller glia; RPE, retina pigment epithelium; ONL, outer nuclear layer; INL, inner nuclear layer; GCL, ganglion cell layer; R,

rod photoreceptor; C, cone photoreceptor; H, horizontal cell; B, bipolar cell; A, amacrine cell; RGC, retinal ganglion cell.

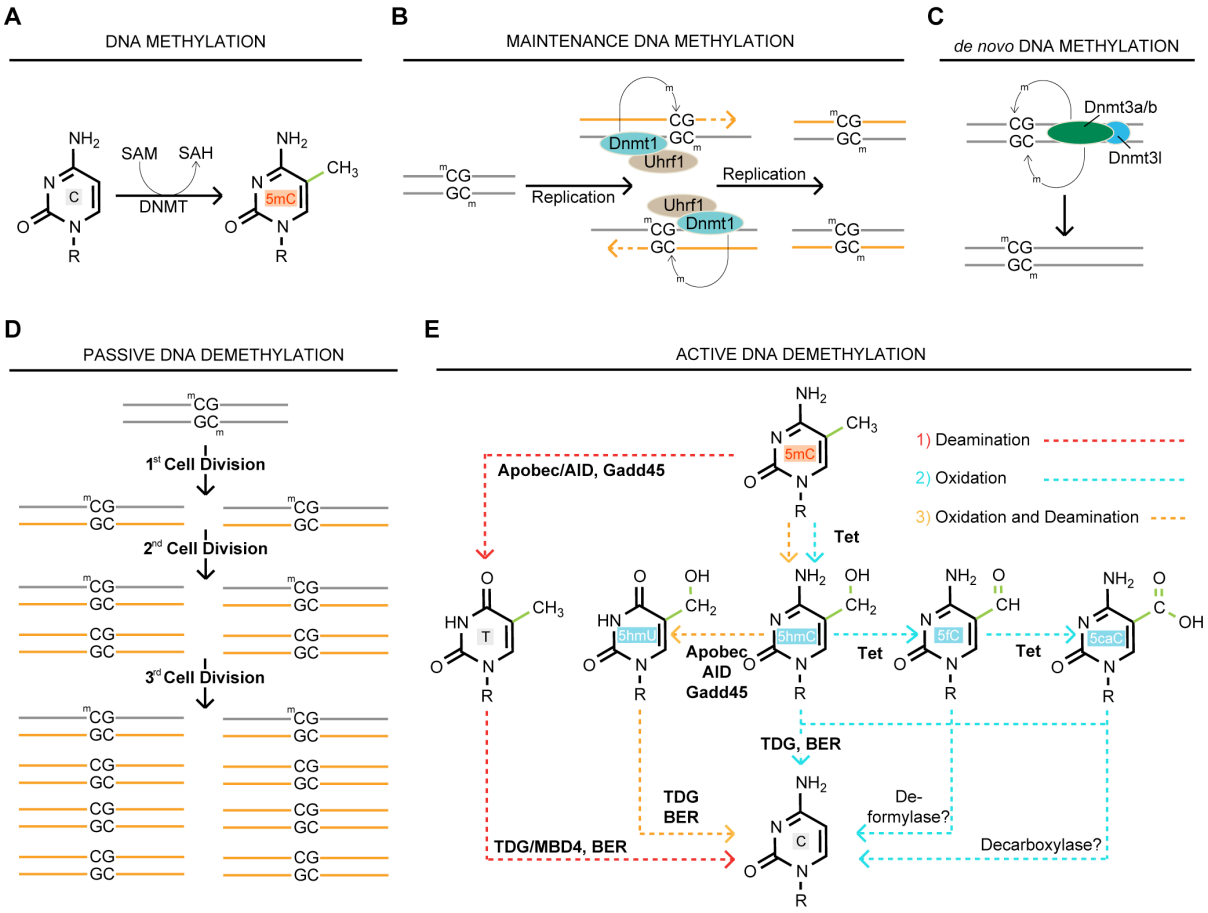

Figure 1.2 Mechanisms of DNA methylation and demethylation

(A) 5mC is formed through the transfer of a methyl group from SAM, resulting in its conversion to SAH, to the C5 position of cytosine by Dnmts. (B and C) Mechanisms of DNA methylation. (B) Dnmt1-mediated maintenance of DNA methylation during replication. (C) Dnmt3-mediated mechanism of *de novo* DNA methylation. (D and E) Mechanisms of DNA demethylation. (D) A rapid series of DNA replications in the absence of maintenance methylation results in passive genome-wide DNA demethylation. (E) Models of active DNA demethylation include: 1. Apobec/AID-dependent deamination of 5mC generates a thymine, resulting in a base-pair mismatch. This mismatch is sensed and excised by a DNA glycosylase (TDG or MBD4) and repaired through BER. Gadd45 proteins function to recruit and coordinate the activity of these enzymes. 2. Tet-dependent oxidation of 5mC converts it to 5hmC, 5fC, or 5caC, which can be sensed and excised by the DNA glycosylase TDG and repaired through BER. An unknown deformylase or decarboxylase may act on 5fC or 5caC, respectively, converting them to C. 3. Tet-dependent oxidation of 5mC converts it to 5hmC, which is then deaminated by Apobec/AID proteins to form 5hmU. 5hmC is a better substrate for Apobec-dependent deamination than 5mC. TDG functions to excise 5hmU followed by repair through BER. C, cytosine; G, guanosine; 5mC, 5-methylcytosine; SAM, S-adenosylmethionine; SAH, S-adenosylhomocysteine; T, thymine; 5hmU, 5-hydroxymethyluracil; 5hmc, 5-hydroxymethylcytosine; 5fc, 5-formylcytosine; 5caC, 5-carboxycytosine; BER, base excision repair.

A

Gene Name	Gene Structure	Location	Species Restriction	Protein Size	ZDD Motif	pI	Substrate
Hs AID		12p13	Jawed Vertebrates	198 aa	CD1- SWSPCYDC	9.65	DNA
Hs APOBEC1		12p13.1	Mammals	236 aa	CD1- SWSPCWEC	8.85	DNA, RNA
Hs APOBEC2		6p21	Jawed Vertebrates	224 aa	CD1- SSSPCAAC	4.51	N.A.
Hs APOBEC3A		22q13.1	Placental Mammals	199 aa	CD1- SWSPCFSWGC	6.81	DNA
Hs APOBEC3B		22q13.1	Placental Mammals	382 aa	CD1- SWTPCPDC CD2- SWSPCFSWGC	5.93	DNA, N.A.? DNA
Hs APOBEC3C		22q13.1	Placental Mammals	190 aa	CD1- SWSPCPDC	7.51	DNA
Hs APOBEC3D/E		22q13.1	Placental Mammals	386 aa	CD1- SWNPCLPC CD2- SWSPCPEC	8.42	N.A. DNA
Hs APOBEC3F		22q13.1	Placental Mammals	373 aa	CD1- SWTPCPDC CD2- SWSPCPEC	7.19	N.A. DNA
Hs APOBEC3G		22q13.1	Placental Mammals	384 aa	CD1- SWSPCTKC CD2- SWSPCFSC	7.99	N.A. DNA
Hs APOBEC3H		22q13.1	Placental Mammals	182 aa	CD1- TWSPCSSC	9.09	DNA
Hs APOBEC4		1q25.3	Jawed Vertebrates	367 aa	CD1- SNNSPCNEANHC	7.96	N.A.
Dr AID		Chr 16	Jawed Vertebrates	210 aa	CD1- SWSPCYDC	9.22	DNA
Dr Apobec2a		Chr 22	Jawed Vertebrates	249 aa	CD1- SSSPCYDC	4.50	N.A.
Dr Apobec2b		Chr 23	Jawed Vertebrates	273 aa	CD1- SSSPCYDC	5.01	N.A.

Location of zinc-coordinating domain | Sequence unique to particular Apobec | ZDD Motif: Zinc-Dependant Deaminase Motif | CD: Catalytic Domain | N.A.: No Demonstrated Activity

B

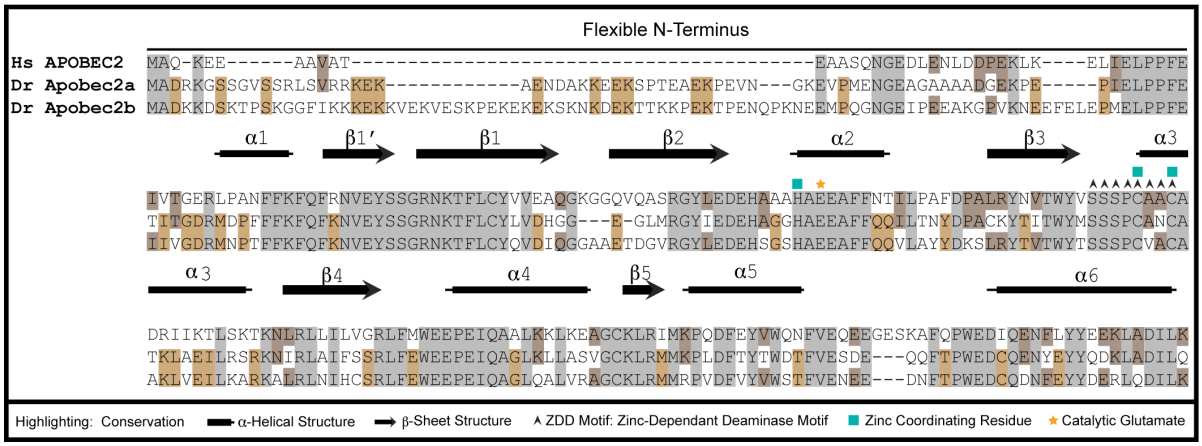

Figure 1.3 Comparisons of Apobecs

(A) Comparisons of the human and zebrafish Apobec genes and proteins. Exon boundaries are demonstrated in the gene structure comparisons. Translated and untranslated portions of the transcripts are indicated with filled or empty boxes, respectively. Portions of the zebrafish *apobec2a*,*2b* untranslated regions are uncharacterized and are denoted with dotted lines. The locations of the sequences coding for zinc-coordinating domains are shown in blue. Sequences coding for unique Apobec protein regions are shown in green; Apobec2 proteins have unique N-termini, and Apobec1 proteins have unique C-termini. The ZDD motif is a distinguishing factor of zinc-dependent deaminases. The core residues of this motif are highlighted. In all Apobecs with demonstrated catalytic activity, there is a W at the second position (underlined). (B) ClustalW sequence alignments comparing human and zebrafish Apobec2 proteins. Secondary structures as identified by the APOBEC2 crystal

structure are diagrammed (Prochnow et al., 2007). Conservation and key residues are identified. Dr, Danio rerio; Hs, Homo sapiens.

Chapter 2:
Injury-dependent Müller glia and ganglion cell reprogramming during tissue regeneration requires Apobec2a and Apobec2b.[1]

2.1 Abstract

Unlike mammals, adult zebrafish are able to regenerate multiple tissues including those of the CNS. In the zebrafish retina, injury stimulates Müller glia (MG) reprogramming/activation and the generation of multipotent Müller glia derived progenitors (MGPCs) that are capable of regenerating all lost cell types. This reprogramming is driven by the reactivation of gene expression programs that share many characteristics with those that operate during early development. Although the mechanisms underlying the reactivation of these programs remain unknown, it is likely that changes in DNA methylation play a significant role. To begin investigating whether DNA demethylation may contribute to retina regeneration, we characterized the expression of genes associated with DNA demethylation in the uninjured and injured retina. We found that two cytidine deaminases (*apobec*2a and *apobec*2b) were expressed basally in the uninjured retina and that they were induced in MGPCs. The maximal induction of *apobec2b* required Ascl1a, but was independent of Lin28, and therefore defines an independent signaling pathway stemming from Ascl1a. Strikingly, when Apobec2a or Apobec2b was knocked down by antisense morpholino oligonucleotides, the proliferative response of MG following injury was significantly reduced and injury-dependent induction of *ascl1a* and its target genes were inhibited, suggesting the presence of a regulatory feedback loop between Apobec proteins and *ascl1a*. Finally, Ascl1a, Apobec2a, and Apobec2b were found to be essential for optic nerve regeneration. These data identify an essential role for Apobec proteins during retina and optic nerve

[1] This chapter was published as Powell C, Elsaeidi F, Goldman D (2012) Injury-dependent Muller glia and ganglion cell reprogramming during tissue regeneration requires Apobec2a and Apobec2b. J Neurosci 32:1096-1109.

regeneration and suggest DNA demethylation may underlie the reprogramming of cells to mount a regenerative response.

2.2 Introduction

While all the cells of an organism are genetically equivalent, each has its own unique identity. Part of this identity is established by epigenetic marks such as 5-methylcytosine (5-meC). DNA methylation predominantly occurs at CpG dinucleotides, and its presence in promoter regions is highly correlated with the repression of gene transcription (Herman and Baylin, 2003; Deaton and Bird, 2011). DNA demethylation is an early event in reprogramming somatic cells to a pluripotent state as seen in nuclear transfer studies (Simonsson and Gurdon, 2004; Jullien et al., 2011), heterokaryon formation (Bhutani et al., 2009) and induced pluripotent stem cell generation (Mikkelsen et al., 2008).

During zebrafish retina regeneration, MG undergo multiple shifts in identity as they reprogram, generate a population of MGPCs, and finally differentiate to regenerate new neurons and glia (Fausett and Goldman, 2006; Raymond et al., 2006; Bernardos et al., 2007; Fimbel et al., 2007; Fausett et al., 2008; Ramachandran et al., 2010a; Ramachandran et al., 2010b). These cell transitions are associated with the activation and inhibition of specific gene regulatory programs. Although the mechanisms underlying these programming changes are largely unknown, we hypothesize that one such mechanism is the active modification of the DNA methylation landscape.

While the events of DNA methylation are well characterized, those of DNA demethylation remain unresolved. Developmental DNA demethylation in zebrafish is thought to occur through the coupling of an Apobec cytidine deaminase, a glycosylase, and a Gadd45 protein (Rai et al., 2008). In this mechanism 5-meC is converted to a thymidine through deamination by an Apobec protein. More recently, it was proposed that 5-meC is first converted to 5-hydroxymethylcytosine (5hmC) by TET proteins (Ito et al., 2010; Mohr et al., 2011), which can then be deaminated by Apobec proteins (Guo et al., 2011; He et al., 2011). Next, MBD4 and TDG DNA glycosylases remove the modified base (Zhu et al., 2000; Zhu, 2009; He et al., 2011), and base excision repair processes replace the abasic site with an unmethylated cytosine. Although a number of studies have suggested roles for these proteins in DNA demethylation (Morgan et al., 2004; Bhutani et al., 2009; Ma et al., 2009a;

Ma et al., 2009b; Popp et al., 2010; Wu and Zhang, 2010; Cortellino et al., 2011; Guo et al., 2011), none have investigated if these proteins contribute to gene expression changes during Müller glia dedifferentiation and zebrafish retina regeneration.

In this study, we begin to characterize the potential role of DNA demethylation during zebrafish retina regeneration by analyzing injury-dependent transcriptional regulation of genes correlated with DNA demethylation. We show that during retina regeneration the expression of *apobec2a* and *apobec2b* (*apobec2a,2b*) is induced in MGPCs and that during optic nerve regeneration *apobec2b* is induced in retinal ganglion cells (RGCs). Importantly, we found that retina and optic nerve regeneration were significantly attenuated following knockdown of Apobec2a and/or Apobec2b. Finally, we provide evidence for signaling components upstream and downstream of these Apobec proteins during regeneration.

2.3 Results

2.3.1 Genes correlated with DNA demethylation are regulated during retina regeneration

To begin to characterize the potential role of DNA demethylation during retina regeneration, we determined the transcriptional regulation of the zebrafish Apobec family members (*aid, apobec2a, apobec2b*), Gadd45 family members (*gadd45α, αl, β, βl, γ, γl*), DNA glycosylases (*mbd4, tdg*), DNA methyltransferases (*dnmt3, dnmt4*), and DNA hydroxylases (*tet2l*, *tet3*) during retina regeneration (Figure 2.1A). With the exception of *aid,* all of the transcripts were expressed in the uninjured and injured adult retina. However, only a subset of these genes exhibited injury-dependent regulation (Figure 2.1A and B). The expression of *gadd45β, gadd45βl*, and *gadd45γ* was induced by 6 hours post injury (hpi), while the expression of *gadd45γl* was highly induced beginning around 2 days post injury (dpi). *tdg*, *dnmt3*, *dnmt*4, and *apobec2a* mRNA levels were moderately increased following retinal injury. Interestingly, *apobec2b* was highly induced around 6-15hpi and peaked around 2-4dpi. Because of the high induction of *apobec2b* and because zebrafish Apobecs contribute to DNA demethylation during zebrafish development (Rai et al., 2008; Rai et al., 2010), we centered the remainder of our experiments on the regulation and signaling of *apobec2a* and *apobec2b* during zebrafish regeneration.

2.3.2 The increased expression of apobec2a and apobec2b after retinal injury is localized to activated MG

Because previous findings largely localized vertebrate Apobec2 to muscle tissue (Etard et al.; Liao et al., 1999; Anant et al., 2001), we sought to confirm our RT-PCR results by examining the spatial pattern of *apobec2a,2b* expression in the retina at 4dpi using *in situ* hybridization. Analysis of *apobec2b* expression showed injury-dependent transcriptional induction in cells localized to the injury site within the inner nuclear layer (INL) (Figure 2.2A, arrows) and also ganglion cells residing in the ganglion cell layer (GCL) at the injury site and flanking it on the side distal to the optic nerve head (ONH) (Figure 2.2A, black arrowheads). On the side of the ONH that did not receive a needle poke injury, we found low levels of *apobec2b* expression in cells residing in the GCL and INL (Figure 2.2A, white arrowheads in upper right corner) similar to what we saw when using *in situ* hybridization to assay *apobec2b* expression in the uninjured retina. Therefore, it appeared that *apobec2b* was induced in RGCs when their axons were severed by the needle poke.

The injury-dependent induction of *apobec2b* in the INL at the injury site is characteristic of genes expressed in MGPCs. To test this idea, fish were injected with bromodeoxyuridine (BrdU) 3.5hrs before harvesting at 4dpi. *In situ* hybridization assays combined with immunofluorescence against the MG-specific marker glutamine synthetase (GS) or the cell proliferation markers BrdU and PCNA showed that these *apobec2b* expressing cells were proliferating MGPCs (Figure 2.2B and C). Quantification revealed that approximately 79% of the proliferating cells at the injury site expressed *apobec2b*. *apobec2b* expression was largely absent from the proliferating cells of the ciliary marginal zone (CMZ), suggesting that Apobec2b is not needed for stem cell maintenance in the retina (data not shown).

Like *apobec2b*, analysis of *apobec2a* expression 4dpi showed injury-dependent transcriptional induction in cells localized to the injury site within the INL (Figure 2.2D, arrows). Low basal levels of *apobec2a* expression was seen in all three retinal nuclear layers flanking the injury site (Figure 2.2D, white arrowheads). *In situ* hybridization assays combined with GS, BrdU, and PCNA immunofluorescence identified the cells with increased *apobec2a* expression levels as MGPCs (Figure 2.2E and F). Quantification revealed that approximately 76% of the proliferating cells at the injury site expressed *apobec2a*.

2.3.3 The promoter of apobec2b is regulated during retinal regeneration

To determine if the injury-dependent induction of *apobec2b* seen by RT-PCR (Figure 2.1) results from increased *apobec2b* promoter activity, we generated *apobec2bP+I;gfp* transgenic fish that harbor 1.85 kb of 5' flanking *apobec2b* DNA, exon 1, intron 1, and 63 bp of exon 2 in frame with the *gfp* sequence (Figure 2.3A). Developmentally, the *apobec2bP+I:gfp* transgenic fish showed a *gfp* expression pattern that was largely localized to the muscle tissue (Figure 2.3B) very similar to previously published *apobec2b* expression analyses in zebrafish (Etard et al., 2010; Rai et al., 2010). Adult transgenic fish retained high levels of expression in most muscle tissues including those of the jaw, mouth, eyes, and body. In contrast the fins, operculum, eye, and cranial region of the fish showed little GFP labeling (Figure 2.3C). Sections through the adult uninjured retina revealed that basal *apobec2b* expression localized to a small population of amacrine cells dispersed throughout the INL as assessed by co-staining with the amacrine and ganglion cell specific HuC/D antibody (Figure 2.3D). Expression was absent from the CMZ where adult stem cells reside (Figure 2.3E). After injury, the *apobec2bP+I:gfp* transgenic fish showed a pattern of expression very similar to that of the endogenous *apobec2b* gene (compare Figure 2.3F and 2.2A) with transgene induction in pillar-like columns of cells at the site of injury in the INL (white arrows, Figure 2.3F) and in injured ganglion cells (white arrowheads, Figure 2.3F). GS and BrdU immunofluorescence showed that GFP+ cells in the INL were MGPCs (Figure 2.3G). Five independent lines showed equivalent staining before and after injury (data not shown), further supporting the evidence of *apobec2b* induction and localization during retina regeneration.

2.3.4 apobec2a and apobec2b regulate MG reprogramming

The above data shows that the expression of *apobec2a* and *apobec2b* is induced early during the process of retina regeneration and is localized to proliferating MGPCs at 4dpi. Here we tested if this increase of Apobec2a and/or Apobec2b is necessary for the conversion of the fully differentiated MG to a progenitor state. To this end, we designed lissamine-tagged antisense morpholinos targeting *apobec2a* and *apobec2b* to knockdown translation of their transcripts during retina regeneration using previously validated morpholino sequences (Rai et al., 2008). To further validate the functionality of the *apobec2a* morpholino, a

construct was created that harbored the *apobec2a* morpholino (MO) binding sequence followed by the *gfp* sequence (pCS2p+ *apobec2a* MO bs-gfp). The pTal *apobec2bP+I:gfp* construct (used for the creation of the transgenic fish) was used to validate *apobec2b* morpholino functionality. Microinjection of these constructs with their respective morpholinos demonstrated a complete GFP knockdown while microinjection with control MO had no effect (Figure 2.4A and B). To determine the efficiency of morpholino knockdown in an injured retina, Apobec2a and Apobec2b protein levels were measured 4 days after administration and electroporation of 0.25 mM morpholino. Treatment with *apobec2a* or *apobec2b* morpholino resulted in an approximate 35% and 70% knockdown in their protein levels relative to a control, respectively (Figure 2.4C and D). Both Apobec2a and Apobec2b protein is found basally in the retina, and their levels increase according to their mRNA induction following injury (data not shown). The apparent low efficiency of Apobec2a knockdown compared to Apobec2b is likely due to the lower level of *apobec2a* induction at the site of injury where the morpholino is present. Thus, the basal Apobec2a levels present in the uninjured, morpholino deficient portion of the retina likely partially mask the effect of the morpholino. Finally, treatment of the *apobec2bP+I:gpf* with *apobec2b* morpholino largely blocked the induction of the transgene at the site of injury (Figure 2.4E).

To determine the impact of Apobec2a and Apobec2b knockdown on retina regeneration, we first analyzed the impact of morpholino incorporation on GFP transgene expression in *1016 tuba1a:gfp* transgenic fish, which was previously shown to label MGPCs in the injured retina (Fausett and Goldman, 2006; Fausett et al., 2008; Ramachandran et al., 2010a). Fish eyes were injected at the time of injury with 0.25 mM lissamine-tagged control or 0.25 mM lissamine-tagged *apobec2a,2b*-targeting morpholinos (0.125 mM of *apobec2a* and *apobec2b* morpholino). As shown previously, administration of the control morpholino (MO) had no noticeable effect on transgene induction following injury (Figure 2.5A top panels). Strikingly, when Apobec2a,2b were knocked down, transgene expression was dramatically reduced in the lissamine+ INL cells when compared to the control (Figure 2.5A bottom panel and Figure 2.5C). When we analyzed the effect of each morpholino individually (injections of 0.25 mM *apobec2a* or 0.25 mM *apobec2b* MO) on the process of regeneration, we were surprised to see that *1016 tuba1a:gfp* transgene expression was

suppressed in both cases (Figure 2.5C) suggesting that these proteins may not act redundantly.

To confirm these results, we repeated these morpholino knockdown experiments using wild type zebrafish to determine if the knockdown of Apobec2a, Apobec2b, or Apobec2a and Apobec2b would inhibit the proliferation of MGPCs using PCNA immunofluorescence as a marker of dividing cells. As seen with *tuba1a:gfp* transgene expression, PCNA labeling was greatly reduced upon injection of any of the experimental morpholinos (Figure 2.5B and D). These results indicate that both Apobec2a and Apobec2b regulate MG reprogramming and proliferation of MGPCs following injury.

We were curious to know if this reduced regenerative response seen after knockdown of Apobec proteins could be attributed to increased cell death at the site of injury. Tunel assays were performed to measure cell death by apoptosis following morpholino treatment and knockdown. No difference was seen between control and experimental knockdown at 2 or 4 days following injury (Figure 2.5E and F). Similar results were seen after staining for activated caspase-3 (data not shown).

2.3.5 Ascl1a activates apobec2b expression during retina regeneration

We next investigated potential mechanisms underlying the injury-dependent activation of *apobec2a* and *apobec2b*. Previous studies suggested that in zebrafish, *cebpβ* overexpression increased the expression of multiple genes correlated with DNA demethylation developmentally, including *apobec2a* and *apobec2b* (Rai et al., 2010). Therefore, we assayed the transcriptional regulation of *cebpβ* following retina injury and compared it with other regeneration-associated genes. Interestingly, *cebpβ* was induced very early after injury, peaking around 15hpi and then declining (Figure 2.6A). Most importantly, *cebpβ* induction appeared to coincide with the induction of *apobec2b* and other regeneration-associated genes like *tuba1a, ascl1a,* and *lin28* (Fausett et al., 2008; Ramachandran et al., 2010a). To test if this induction was necessary for injury-dependent *apobec2a* and *apobec2b* expression, Cebpβ was knocked down by administration of a previously validated *cebpβ* specific antisense morpholino oligonucleotide (Rai et al., 2010). The functionality of the *cebpβ* MO was validated through the creation of a construct harboring the binding sequence followed by the *mCherry* sequence (pCS2p+ *cebpβ* MO bs-*mCherry*, Figure 2.6B).

Following knockdown of Cebpβ during retina regeneration, gene expression was assayed 2dpi when MG are reprogrammed and just beginning to enter the cell cycle (Fausett and Goldman, 2006). Surprisingly, Cepbβ knockdown had no discernable effect on *apobec2a* or *apobec2b* expression in the injured retina (Figure 2.6C and F).

Besides Cebpβ, others have reported that human APOBEC2 expression is enhanced by NF-κB signaling (Matsumoto et al., 2006). To test if NF-κB signaling operates in the zebrafish retina to regulate injury-dependent *apobec2b* expression, zebrafish eyes were injected intravitreously with chemical inhibitors of NF-κB signaling, wedelolactone or ethyl pyruvate (Daroczi et al., 2009), at the time of injury, and the expression of *apobec2a* and *apobec2b* was assessed 2 days later. No difference between drug and vehicle injected samples was observed (data not shown).

Next, we looked for the regulation of *apobec2a* and *apobec2b* expression by genes that are induced in reprogramming MG very early following retinal injury and that are required for regeneration. One such gene is *ascl1a* whose expression is induced within 4hpi and is represented in approximately 80% of the MGPCs (Fausett et al., 2008; Ramachandran et al., 2010a). The injury-dependent increase of *apobec2b* largely parallels the induction of *ascl1a* and its downstream targets *tuba1a* (Fausett et al., 2008) and *lin28* (Ramachandran et al., 2010a) (Figure 2.6A). To determine if Ascl1a regulates *apobec2a* and/or *apobec2b* expression in the injured retina, we knocked down its expression with previously validated *ascl1a* MOs (Fausett et al., 2008; Ramachandran et al., 2010a). Interestingly, the induction of *apobec2b*, but not *apobec2a*, was significantly attenuated following Ascl1a knockdown (Figure 2.6D and F). However, knockdown of Lin28 had no noticeable impact on *apobec2b* expression (Figure 2.6E and F), suggesting that Ascl1a/Apobec2b signaling is a novel, previously uncharacterized, signaling pathway stemming from Ascl1a.

Knockdown of Ascl1a in the *apobec2bP+I:gfp* transgenic fish largely blocked the induction of the transgene in the INL (Figure 2.6G) but had no noticeable impact on the transgene levels in RGCs whose axons were injured with a poke (Figure 2.6H) suggesting that Ascl1a signaling doesn't activate *apobec2b* expression in injured RGCs. Overexpression of *ascl1a* during zebrafish development did not lead to a significant increase in *apobec2b* mRNA 2 days post fertilization or a noticeable increase of GFP in the *apobec2bP+I:gfp*

transgenic fish suggesting that the Ascl1a/Apobec2b signaling cascade may be specifically operative in the regenerating retina (data not shown).

2.3.6 Apobec2a and Apobec2b participate in a feedback loop to regulate ascl1a during retina regeneration

We next sought to identify genes whose expression is regulated by Apobec2a and/or Apobec2b signaling. These efforts were complicated due to the lack of a clear molecular function of Apobec2 proteins and no known targets of their signaling. We began by analyzing the impact of Apobec2a and Apobec2b knockdown on the expression of genes transcriptionally induced at or before 2dpi. Those assayed included: *ascl1a*, *lin28*, *klf4*, *oct4*, *olig2*, *atoh*, *tuba1a, tuba1b, nanog, dnmt4*, *pax6a*, and *pax6b*. Interestingly, when Apobec2a and Apobec2b were knocked down, the transcriptional induction of *ascl1a* was reduced in a concentration-dependent manner (Figure 2.7A). In addition, the induction of the Ascl1a target genes *lin28, tuba1a*, and *apobec2b* were attenuated while injury-dependent induction of *pax6a* and *pax6b* remained unaffected (Figure 2.7B). Apobec2a and Apobec2b knockdown had no detectable effect on *atoh, oct4, olig2, klf4, tuba1b, dnmt4,* and *nanog* expression (data not shown). Similar results were seen when Apobec2a or Apobec2b was knocked down individually at concentrations of 0.25 mM (Figure 2.7C), but lower concentrations showed no effect (Figure 2.7D). These results indicate that a feedback mechanism exists between Ascl1a and Apobec2b/Apobec2a (Figure 2.7E).

Knockdown or overexpression of Apobec2a and Apobec2b did not have a significant impact on the levels of *ascl1a* mRNA in developing zebrafish 2 days post fertilization (data not shown), indicating that the feedback regulation observed in the adult retina is specific to retina regeneration.

2.3.7 ascl1a and apobec2b mRNAs are regulated during optic nerve regeneration

Curiously, *apobec2b* appeared to be induced in RGCs when optic axons were injured with a needle poke (Figure 2.2A and 2.3F). Indeed, we found that optic nerve lesion induced *apobec2b* expression in RGCs (Figure 2.8). The expression of *apobec2b* increased during the first 24hrs following optic nerve lesion and reached its peak around 2dpi (Figure 2.8A and B). Optic nerve lesion in *apobec2bP+I:gfp* transgenic fish showed that *apobec2b*

promoter activity was increased in RGCs that were regenerating their optic axons (Figure 2.8C). *apobec2a* expression was largely uninduced during optic nerve regeneration (Figure 2.8A and B).

During retina regeneration, *apobec2b* induction was dependent on Ascl1a expression (Figure 2.6C and E). Surprisingly, we found that the expression of *ascl1a* was slightly induced following optic nerve cut (Figure 2.8A and B). To determine if Ascl1a signaling was necessary for the induction of *apobec2b* during optic nerve regeneration, Ascl1a was knocked down with *ascl1a* MOs applied to the lesioned optic nerve stump as previously described (Veldman et al., 2007; Veldman et al., 2010). Two days post optic nerve lesion, injury-dependent induction of *apobec2b* was quantified. Ascl1a knockdown had no apparent effect on injury-dependent *apobec2b* induction following optic nerve lesion (Figure 2.9A). This is similar to what we saw in the ganglion cells that were injured after injection of *apobec2bP+I:gfp* transgenic fish with the *ascl1a* MO (Figure 2.6H). Likewise, Cebpβ knockdown had no impact on *apobec2b* induction (Figure 2.6H). Interestingly, when we knocked down Apobec2a and Apobec2b together, but not each individually, we observed a significant decrease (40%) in the injury-dependent induction of *ascl1a* (Figure 2.9B). These results suggested that Apobec2a and Apobec2b contribute to *ascl1a* expression during optic nerve regeneration.

2.3.8 Ascl1a, Apobec2a, and Apobec2b regulate axonal growth during optic nerve regeneration

To investigate if Ascl1a, Apobec2a, and Apobec2b are necessary for optic nerve regeneration, we combined *in vivo* morpholino-mediated RGC protein knockdown with retinal explants to assay ganglion cell axon regeneration (Veldman et al., 2010). For these experiments, Gelfoam impregnated with *apobec2a, apobec2b*, *ascl1a,* or control MO was applied to the lesioned optic nerve stump overnight. 4 days later the retinas were harvested, diced and cultured as explants for 4 days, after which retinal ganglion cell axonal growth was quantified as previously described (Veldman et al., 2010). Retinal explants prepared from control MO treated retinas displayed robust axonal outgrowth, while knockdown of Ascl1a, Apobec2a or Apobec2b caused a significant suppression of optic axon regrowth (Figure 2.9C

and D). Therefore, similar to retina regeneration, Ascl1a, Apobec2a and Apobec2b also regulate optic axon regeneration.

2.4 Discussion

DNA demethylation is a key event in the reprogramming of fully differentiated somatic cells to acquire pluripotency (Simonsson and Gurdon, 2004; Mikkelsen et al., 2008; Bhutani et al., 2009; Jullien et al.). Similarly, we hypothesize that following retina injury DNA demethylation underlies the reprogramming of Müller glia to acquire characteristics of a multipotent retinal progenitor. Many proteins have been implicated in the process of DNA demethylation including Apobec proteins, Gadd45 proteins, MBD4, TDG, and Tet proteins (see introduction). Recent work suggests that these factors participate in a multistep process to carry out DNA demethylation (Guo et al., 2011; He et al., 2011). Importantly, Apobec proteins, Gadd45 proteins and DNA glycosylases have been implicated in DNA demethylation during zebrafish development (Rai et al., 2008).

To begin investigating if these components participate in retina regeneration we measured their expression levels in uninjured and injured retinas. Although many of these genes showed constitutive expression, some demonstrated injury-dependent induction. Of particular note, we report that *apobec2a* and *apobec2b* are induced in reprogramming MG during retina regeneration and that *apobec2b* is induced in damaged RGCs after injury. In MG, the increased expression of *apobec2b* is dependent on an early increase of Ascl1a (Fausett et al., 2008), but is independent of Lin28 (Ramachandran et al., 2010a). Knockdown of Apobec2b, like knockdown of Ascl1a and Lin28, significantly reduces the ability of Müller glia to respond to injury by reprogramming and generating MGPCs. Thus, *apobec2b* represents an independent signaling pathway stemming from Ascl1a that is important for zebrafish retina regeneration. When the levels of Apobec2a were perturbed by morpholino knockdown, retina regeneration was also reduced. This suggests that Apobec2a and Apobec2b may act in a non-redundant fashion. The crystal structure of human APOBEC2 indicates that it functions as a dimer or tetramer (Prochnow et al., 2007), so it is possible that zebrafish Müller glia reprogramming requires the oligomerization of Apobec2a and Apobec2b. When the levels of Apobec2a and/or Apobec2b were knocked down by antisense morpholino, the levels of *ascl1a* also decreased. This could explain why a similar

knockdown of *ascl1a* and its target genes was seen after knockdown of Apobec2a and Apobec2b individually or in combination. We hypothesize that an early increase of Ascl1a is required for the induced expression of *apobec2b* and that Apobec2a and Apobec2b then function through oligomerization to actively demethylate gene promoters through a multistep reaction. One such promoter could be that of *ascl1a*. But, it is equally likely that Apobec2a and Apobec2b are acting on *ascl1a* indirectly, acting to demethylate the promoters of other unknown genes that then feedback and activate *ascl1a*.

The expression of *apobec2b* and *ascl1a* (to a small extent) is also regulated during optic nerve regeneration, but unlike retina regeneration, knockdown of Ascl1a during optic nerve regeneration had no impact on the expression of *apobec2b*. The induction of *apobec2b* in injured RGCs likely explains why knockdown of Ascl1a during retina regeneration only results in a ~77% reduction in the levels of *apobec2b* at 2dpi, the residual increase of *apobec2b* being attributed to the injured ganglion cells. Although the mechanisms mediating injury-dependent *apobec2b* induction differ during retina and optic nerve regeneration, both involve Ascl1a, Apobec2a and Apobec2b expression and show regulation of *ascl1a* expression by Apobec2a and Apobec2b.

2.4.1 The role of zebrafish Apobec2a and Apobec2b during regeneration

That *apobec2a* and *apobec2b* were regulated during regeneration was somewhat surprising because previous work had largely localized Apobec2 to muscle tissue (Liao et al., 1999; Etard et al., 2010). The exact role that these proteins may play during retina regeneration remains unknown. Apobec proteins have traditionally been associated with cytidine deamination and editing of DNA and/or RNA (Conticello, 2008; Prochnow et al., 2009; Blanc and Davidson, 2010). However, unlike many mammalian APOBEC proteins with an assigned function, APOBEC2 remains an enigma with no clear mechanism of action and relatively few functions assigned. Human APOBEC2 appears to play a role in muscle development and may contribute to its adaptability (Sato et al., 2009; Etard et al., 2010). In *Xenopus*, Apobec2 has been reported to regulate left-right axis specification (Vonica et al., 2011), and in developing zebrafish Apobec2b stimulates DNA demethylation (Rai et al., 2008).

Early *in vitro* studies suggested that APOBEC2 had cytosine deaminase activity (Liao et al., 1999; Anant et al., 2001a), but later studies refuted those findings (Mikl et al., 2005). APOBEC2 structural data demonstrate its potential to bind polynucleotides (Prochnow et al., 2007; Bransteitter et al., 2009), but no studies have confirmed this binding. When considering the highly conserved amino acids in the Apobec family, Apobec2 would appear to be a fully functional deaminase. Importantly, transfection of cultured HEK293 cells with human APOBEC2 and TET1 stimulated DNA demethylation while overexpression of each individually did not (Guo et al., 2011). Likewise, overexpression of Apobec2b and hMBD4 during zebrafish development stimulated global DNA demethylation, but overexpression of each individually had no effect (Rai et al., 2008). Whether a similar scenario acts during retina regeneration or if Apobec2a and Apobec2b function to modify RNA is unknown; nonetheless our data indicates that many of the components controlling DNA demethylation are induced following retina injury.

2.4.2 Cellular reprogramming during regeneration

The cellular reprogramming events of MG during retina regeneration and RGCs during optic nerve regeneration likely have similarities and differences. Retina regeneration requires extensive MG reprogramming, resulting in their generation of MGPCs capable of regenerating all major retinal cell types (Fausett and Goldman, 2006; Raymond et al., 2006; Fimbel et al., 2007; Ramachandran et al., 2010b). Optic nerve regeneration differs from retina regeneration in that only one cell type is involved, and it occurs in the absence of proliferation. Yet, during optic nerve regeneration RGCs likely require a high degree of reprogramming to reach an early developmental state allowing for correct axonal growth, path finding and synapse formation. These differences may contribute to the variation in amount of Apobec2a and Apobec2b present and their regulation.

This study establishes Apobec2a and Apobec2b as important components for retina and optic nerve regeneration. Whether Apobec2a and Apobec2b participate in active DNA demethylation during retina and optic nerve regeneration remains to be determined. To make this connection, two routes are possible. First, one could identify targets of Apobec2a or Apobec2b and characterize their methylation levels. This approach is limited because of the difficulty distinguishing between a direct and an indirect target. Alternatively, one could

identify the regions of DNA undergoing DNA demethylation during retina regeneration, and determine if Apobec proteins are required for their demethylation. Until one of these approaches is taken, the void existing between these proteins and DNA demethylation will remain. Further studies will attempt to close this gap using zebrafish retina regeneration as a model system.

2.5 Methods

2.5.1 Animals

Zebrafish were kept at 26-28 °C on a 14/10 hr light/dark cycle. Fish of either sex were used in all experiments. Transgenic *1016 tuba1a1016:gfp* fish were previously described (Fausett and Goldman, 2006). The *apobec2bP+I:gfp* expression vector contains 1.85 kb of 5' flanking *apobec2b* DNA, exon 1, intron 1, and 63 bp of exon 2 (8.934 kb total, Figure 2.3A) that was amplified from zebrafish DNA with Phusion DNA Polymerase (New England Biolabs) using apobec2bP+I-F and apobec2bP+I-R primers that harbor a Sal1 and a BamH1 site at their 5' ends, respectively (Table 2.1). This PCR fragment was cloned within the *pT2AL200R150G* Tol2 vector (Urasaki et al., 2006) in frame to the *gfp* sequence followed by an *SV40 polyA* signal sequence. The construct was injected into single-cell zebrafish embryos, which were raised to adulthood and screened for transgenic progeny. Five independent lines were selected and grown to adulthood, each exhibiting a similar phenotype.

2.5.2 RNA isolation and PCR

Total RNA was isolated using TRIzol reagent (Invitrogen) and treated with DNase (Invitrogen). cDNA synthesis was performed using 1 μg of purified RNA, 500 ng of random hexamer primers (Invitrogen) and M-MuLV Reverse Transcriptase (New England Biolabs). PCR reactions were done using Taq DNA polymerase and gene specific primers (Table 2.1). The *gadd45β*, *gadd45γ*, *mbd4*, and *tdg* real-time specific primers were designed using previously validated sequences (Rai et al., 2008) and the *ascl1a, lin28*, *pax6a*, *pax6b*, *gapdh*, *l24* (ribosomal protein L24), and *β-actin* primers have been described previously (Ramachandran et al., 2010a; Veldman et al., 2010). Real-time PCR reactions were carried out in triplicate with SYBR green fluorescein on an iCycler real-time PCR detection system (BioRad).

2.5.3 Retina injury, optic nerve lesions, and morpholino-mediated gene knockdown

Fish were anesthetized in 0.02% tricaine methane sulfonate before retina and optic nerve surgeries. Eye lesions were performed as described previously (Ramachandran et al., 2010a). Briefly, while anesthetized, fish were placed under a dissecting microscope for visualization and the right eye was gently rotated in its socket and stabbed through the sclera with a 30-gauge needle eight times (twice in each quadrant) when total RNA was isolated for RT-PCR, six times when RNA was isolated after morpholino injection and electroporation (three times in each hemisphere), and four times (1 time in each quadrant) for immunohistochemistry and *in situ* hybridization.

To deliver morpholinos to the injured retina, a 30-gauge needle was attached to a Hamilton syringe and approximately 0.7 μl was injected into the vitreous at the time of injury. The untagged control, 3'-lissamine-tagged control, *ascl1a* and *lin28* MOs have been described previously (Fausett et al., 2008; Ramachandran et al., 2010a). The 3'-lissamine-tagged *apobec2a* and *apobec2b* and the 3'-carboxyfluorescein *cebpβ* MOs (Gene Tools, LLC) were designed using previously validated target sequences (Rai et al., 2008; Rai et al., 2010). Morpholino delivery to cells was facilitated by electroporation as previously described (Ramachandran et al., 2010a). For immunohistochemical studies on morpholino injected samples, eyes were harvested 4 days post injury (dpi) to analyze the effect of the morpholino on MG proliferation. When RNA was collected for expression studies of morpholino injected samples, retinas were isolated 2dpi to negate any transcriptional difference occurring solely due to potential differences in Müller glia proliferation. We previously showed that MG proliferation begins at around 2dpi and is at its maxima at 4dpi (Fausett et al., 2008).

Optic nerve lesion and retinal explants were performed as described previously (Veldman et al., 2010). Briefly, explants were carried out four days following optic nerve transection and morpholino treatment, retinas were isolated and cut into 0.5 mm squares with a razor blade and digested with hyaluronidase (1 mg/ml) for 15 min at room temperature. Explants were rinsed 3x with L15 culture media and plated, one retina per plate that was precoated with poly-L-lysine and laminin. Explants were cultured in 0.5 ml L15 media containing 8% fetal calf serum, 3% zebrafish embryo extract and 1x antibiotic/antimycotic at 28 °C for 4 days in a humidified ambient air incubator. Adherent explants were quantified for neurite length and density as previously described (Veldman et al., 2010). Morpholino

mediated knockdown in adult retinal ganglion cells following optic nerve transection was accomplished by placing a small piece of Gelfoam, soaked in morpholino (1 μl of a 1 mM morpholino) onto the lesioned optic nerve stump for one day and subsequently removed.

2.5.4 Morpholino validation constructs and western blots

To validate the functionality of the antisense morpholinos introduced in our study, constructs were created that included the binding sequence of each morpholino preceding the sequence of *mCherry* or *gfp*. The *apobec2a* morpholino binding site was cloned into the pcs2p+ vector preceding the sequence of *gfp* using the *gfp* sequence as template and the apobec2aMobsgfp-F and the mcherry/gfp-R primers (Table 2.1) and the restriction enzymes EcoR1 and Xba1 (pcs2p+ *apobec2a* MO bs-gfp). The *cebpβ* morpholino binding site was cloned into the pcs2p+ vector preceding the sequence of *mCherry* using the *mCherry* sequence as template and the cebpβMobsmcherry-F and the mcherry/gfp-R primers (Table 2.1) and the restriction enzymes EcoR1 and Xba1 (pcs2p+ *cebpβ* MO bs-*mCherry*). The ptal *apobec2bP+I:gfp* vector that includes the binding site for the apobec2b morpholino was used for the validation of the *apobec2b* MO. Purified constructs were microinjected into single cell embryos at a concentration of 2 ng/ml in conjunction with 0.125 mM lissamine-tagged (*apobec2a* and *apobec2b*) or fluorescein-tagged (*cebpβ*) experimental morpholino or 0.125 mM lissamine-tagged or untagged control morpholino. Microinjections were analyzed for mCherry and GFP expression 1 day post fertilization. Experimental morpholino injections demonstrated a complete block of GFP (*apobec2a* and *apobec2b* MOs) or mCherry (*cebpβ* MO) while control MO showed no effect.

To determine the efficiency of morpholino knockdown in the injured retina, western blots were performed on protein isolated from retinas harvested 4 days post intraocular injection and electroporation of 0.25 mM morpholino. Six injections were performed to each eye. Retinas were harvested into nuclei lysis buffer (50 mM Tris-HCl pH 7.5, 10 mM EDTA, 1% SDS) including a protease inhibitor cocktail (Thermo) and sonicated on ice. Protein concentrations were measured using the BCA assay (Peirce), and 40 mg of protein was run for each sample on a 10% polyacrylamide gel. Rabbit anti-Apobec2a and anti-Apobec2b antibodies were provided by David Cairns (Rai et al., 2008) and were used at a dilution of 1:2000. After probing for the deaminases, the blots were stripped for 30 minutes

at 70 °C (50 mM Tris-HCl pH7.5, 2% SDS, 50 mM DTT) and reprobed for glutamine synthetase (GS) as a loading control (1:2000, Chemicon/Millipore). Anti-rabbit and anti-mouse HRP secondary antibodies were used and chemiluminescence (Roche) for protein detection. Western blots were quantified by densitometry using Image J software. Protein levels were normalization to GS expression.

2.5.5 Bromodeoxyuridine (BrdU), wedelolactone, and ethyl pyruvate injections

To identify dividing cells, fish were injected intraperitoneally with 15 μl of 20 mM BrdU stock 3.5 hours before harvesting at 4dpi. Eyes were sectioned and assayed for BrdU immunofluorescence.

Wedelolactone (Calbiochem) and ethyl pyruvate (Sigma Aldrich), inhibitors of NF-κB signaling (Daroczi et al., 2009), were injected intravitreously into the eye at the time of injury at concentrations of 2 μM and 25 mM stock respectively using a 30-gauge needle attached to a Hamilton syringe. Six injections of 1 μl drug were performed for each eye analyzed, followed by retina harvest at 2dpi. Gene expression analysis was then carried out on retina RNA and compared to control vehicle injections (20% DMSO).

2.5.6 Tissue preparation

Fish were given an overdose of tricaine methane sulfonate, and the eyes from adult fish were enucleated, followed by the removal of the lens and immersion into fresh 4% paraformaldehyde in 0.1 M phosphate buffer, pH 7.4, for 4hrs at room temperature or overnight at 4 °C. After fixation, tissues were cryoprotected in phosphate-buffered 20% sucrose for 6-12hrs before embedding with Tissue-Tek O.C.T. compound (Sakura, Finetek). Embedded samples were kept frozen at -80 °C until sectioned to 10 microns on a CM3050S cryostat (Leica). Sections were collected on Superfrost/Plus slides (Fisher Scientific), dried and stored at -80 °C.

2.5.7 Immunofluorescence

Immunofluorescence was performed as described previously (Ramachandran et al., 2010a) using the following primary antibodies: rat anti-BrdU (dividing cell marker, 1:400, Abcam), mouse anti-PCNA (dividing cell marker, 1:500, Sigma), rabbit anti-GFP (1:1000,

Invitrogen), rabbit anti-cleaved caspase-3 (cell death marker, 1:50, Cell Signaling) and mouse anti-GS (Müller glia marker, 1:500, Chemicon/Millipore). Secondary anti-mouse, anti-rabbit, or anti-rat antibodies were conjugated to Alexa 488 (1:1000, Invitrogen) or cyanine 3 (1:250, Jackson ImmunoResearch). Antigen retrieval for BrdU and PCNA staining was performed by either boiling the sections in 10 mM sodium citrate and 0.05% Tween 20 for 20 min and cooling for another 20 min or by pretreating the sections with 2 N HCl for 22 min at 37 °C followed by two 5 min washes with 100 mM sodium borate. Blocking was performed for 1 h with 3% donkey serum (Invitrogen) in PBS-0.1% Tween. Following immunofluorescent staining, slides were rinsed with water and allowed to dry in the dark prior to cover-slipping with 2.5% PVA (PVA-polyvinyl alcohol/DABCO (1,4 diazabicyclo [2.2.2]octane).

2.5.8 In situ hybridization

In situ hybridizations were performed with antisense digoxigenin (DIG)-labeled RNA probes as described previously (Ramachandran et al., 2010a). Sense control probes were generated and showed no signal above background (data not shown). Clones of *apobec2a* and *apobec2b* were kindly provided by Dr. David Jones (Rai et al., 2008). Full length antisense DIG labeled probes were created using restriction endonuclease linearized plasmid, SP6 RNA polymerase (Promega), and DIG rNTPs (Roche) as described previously (Fausett and Goldman, 2006).

2.5.9 Tunel assay

Tunel was performed on 10 micron retina sections harvested 2 and 4 day post intraocular injection and electroporation of 0.25 mM morpholino. After digestion for 20 min with Proteinase K (Roche) at 37 °C (10 ug/ml Proteinase K, 10 mM Tris-HCl pH 7.5), slides were analyze for Tunel staining using the *In situ* Cell Death Detection Kit, Fluorescein (Roche). The number of Tunel+ cells on each retinal section containing an injury site was quantified, and the total number of Tunel+ cells for each eye was then divided by the number of sections analyzed to give an average number of Tunel+ cells per section containing an injury site.

2.5.10 Imaging and statistics

Slides were examined using a Zeiss Axiophot, Axio Observer Z.1, or Olympus Fluoview FV1000 laser scanning confocal microscope. Images were captured using a digital camera adapted onto the microscopes. Images were processed and annotated with Adobe Photoshop CS. P-values were calculated using the student T-test.

2.6 Acknowledgments

We would like to thank Dr. David Jones for generously providing us with clones of zebrafish *apobec2a* and *apobec2b* and antibodies against zebrafish Apobec2a and Apobec2b. We would also like to thank the Goldman Lab for helpful comments on this work. This work was supported by NEI grant RO1 EY018132 (DG) and the University of Michigan Genetics Training Grant 5T32GM007544-33 (CP).

2.7 Figures

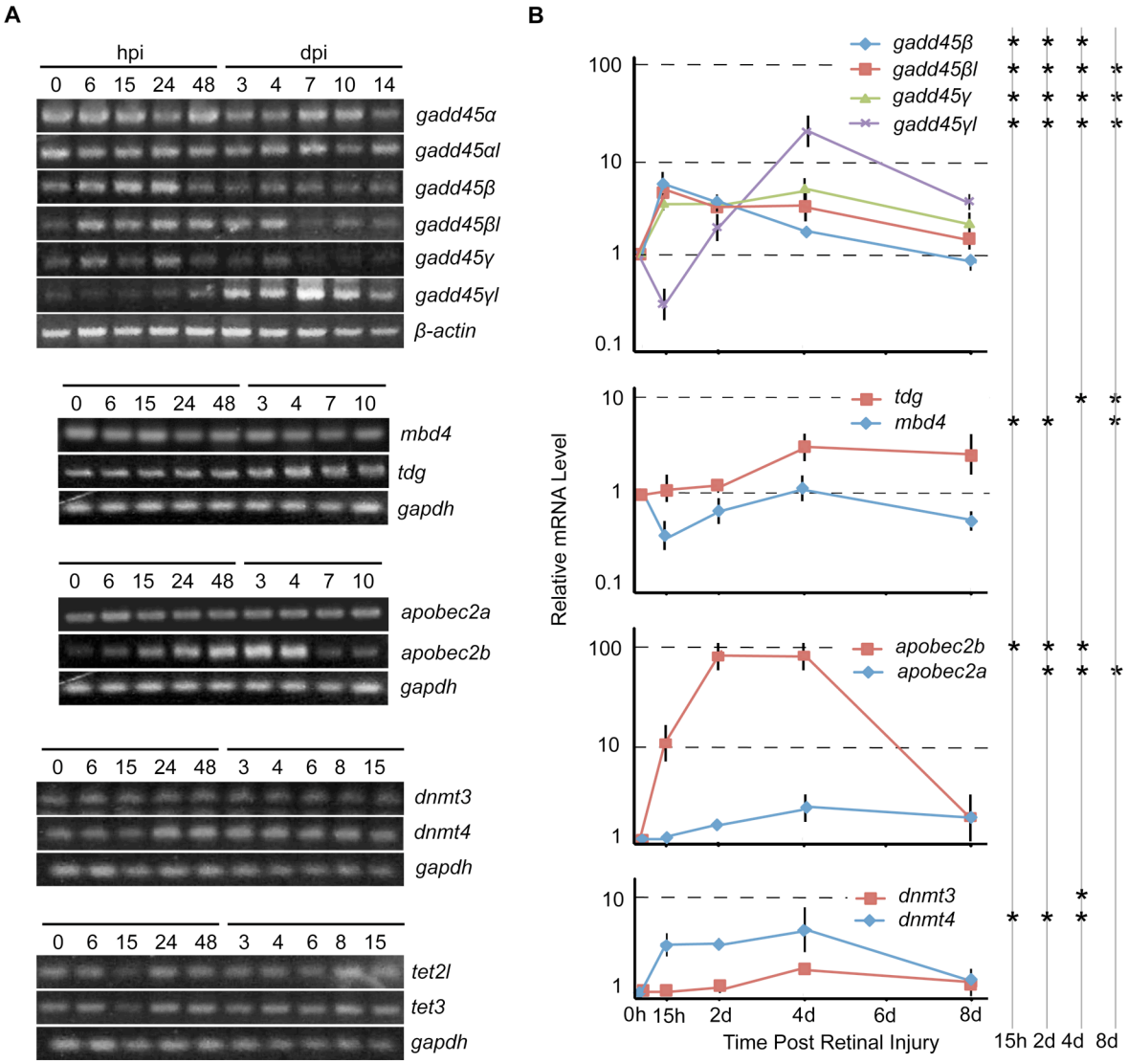

Figure 2.71 Injury-dependent regulation of genes correlated with DNA demethylation

(A) RT-PCR analysis of indicated mRNAs isolated from retina at various times post injury (hours post injury, hpi; days post injury, dpi) by poke with a 30-gauge needle. The expression of *β-actin* and *gapdh* served as the internal controls. One representative of three independent time courses is shown. (B) Real-time PCR quantification of indicated mRNAs isolated from retina at various times post injury (labeled on the bottom *X*-axis). *Y*-axis is fold induction in log scale and is normalized to 0 hours (0h), i.e. the uninjured retina, which was assigned a value of 1. The expression of *gapdh* served as the internal control. Data represents means ± s.d. (n=3 individual cDNA sets; compared with control, time points marked with an asterisk have a $P < 0.05$).

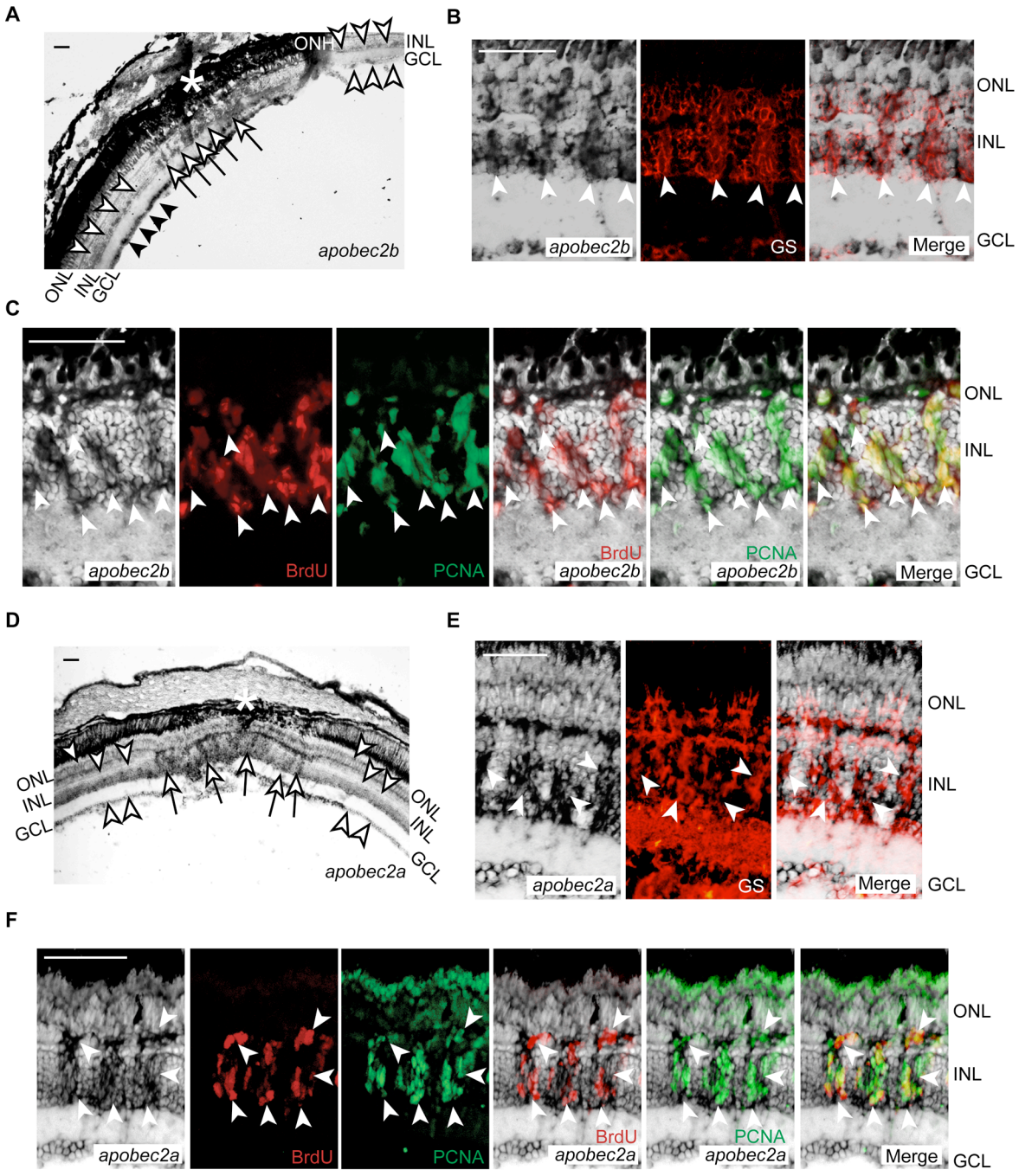

Figure 2.72 *apobec2a* and *apobec2b* are induced in MGPCs following retinal lesion

(A) In situ hybridization at 4dpi shows injury-dependent induction of *apobec2b* mRNA in the INL and GCL. Shown is a representative image of an injury site (*) and surrounding retina tissue. Cells within the INL that show induced *apobec2b* expression at the injury site are marked with white arrows. Injured RGCs at and flanking the injury site on the side distal to the optic nerve head (ONH) are distinguished with black arrowheads. Cells in the INL and GCL expressing basal levels of *apobec2b* are marked with white arrowheads. (B) Combined *apobec2b* in situ hybridization and GS immunofluorescence shows injury-

dependent induction of *apobec2b* in MG. White arrowheads indicate co-localization of *apobec2b* mRNA and GS+ cells. (C) Combined *apobec2b* in situ hybridization and BrdU and PCNA immunofluorescence shows injury-dependent induction of *apobec2b* in proliferating cells. White arrowheads indicate co-localization of *apobec2b* mRNA in BrdU+ and PCNA+ cells. The scale bar is equal to 50 μm. (D) In situ hybridization at 4dpi shows injury-dependent induction of *apobec2a* mRNA in the INL. Shown is a representative image of an injury site (*) and surrounding retina tissue. INL cells that show induced *apobec2a* expression at the injury site are marked with white arrows. Cells expressing basal levels of *apobec2a* are marked with white arrowheads. (E) Combined *apobec2a* in situ hybridization and GS immunofluorescence shows injury-dependent induction of *apobec2a* in MG. White arrowheads indicate co-localization of *apobec2a* mRNA and GS+ cells. (F) Combined apobec2a in situ hybridization and BrdU and PCNA immunofluorescence shows injury-dependent induction of *apobec2a* in proliferating cells. White arrowheads indicate co-localization of *apobec2a* mRNA in BrdU+ and PCNA+ cells. The scale bar is equal to 50 μm. Abbreviations: ONL, outer nuclear layer; INL, inner nuclear layer; GCL, ganglion cell layer; GS, glutamine synthetase.

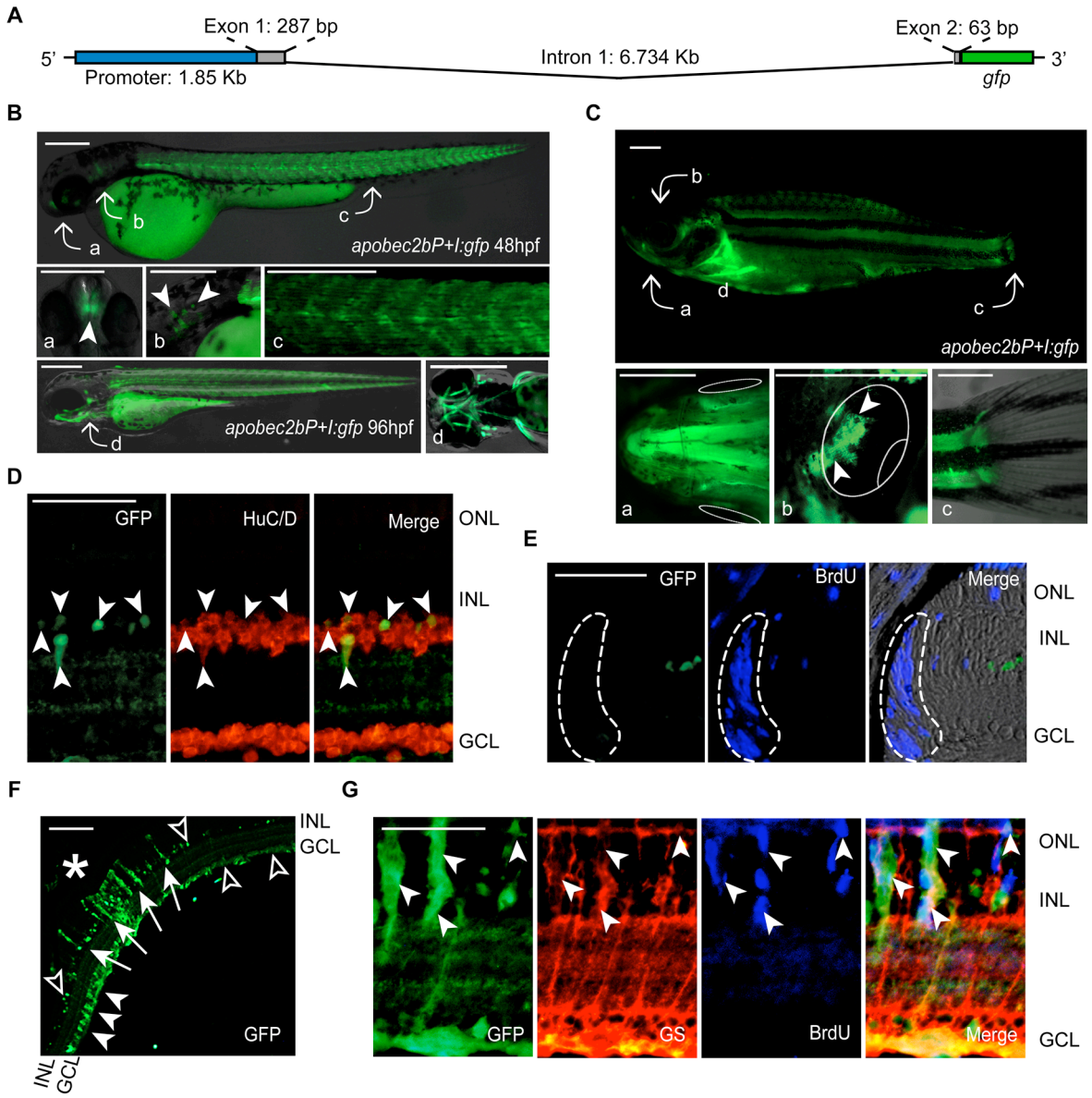

Figure 2.73 *apobec2bP+I:gfp* transgenic fish label MGPCs following injury

(A) Map of the *apobec2bP+I:gfp* transgene. (B) Representative images of 48 and 96 hours post fertilization (hpf) *apobec2bP+I:gfp* transgenic embryos showing GFP expression in the a) telencephalon, b) pharyngeal arches, c) somites, and d) muscles of the jaw and eyes. Scale bar is equal to 400 μm. (C) GFP expression in 3-month-old adult *apobec2bP+I:gfp* transgenic fish. a) Ventral view showing expression in the muscles of the jaw and mouth. b) Dorsal view showing expression in the muscles of the eye. c) Posterior view showing the lack of expression in the caudal fin. d) High expression seen in pectoral fin musculature. Scale bar is equal to 1 mm. (D) Transgene expression in the uninjured retina of adult *apobec2bP+I:gfp* fish is confined to a subset of HuC/D+ cells in the INL. Retinal sections were co-labeled with antibodies specific for GFP and the amacrine and ganglion cell specific HuC/D protein. White arrowheads indicate co-localization of GFP+ and HuC/D+ cells. The scale bar is equal to 50 μm. (E) Lack of transgene expression in the retina's circumferential

germinal zone (CMZ) of adult *apobec2bP+I:gfp* fish. Retinal sections were examined for GFP and BrdU immunofluorescence. The fish was given an intraperitoneal injection of BrdU 3.5hrs before harvest, and BrdU incorporation identified the CMZ (dotted area). The scale bar is equal to 50 μm. (F) Retinal injury in *apobec2bP+I:gfp* fish results in increased transgene expression in the INL and GCL (4dpi). Shown is an immunofluorescence image using antibodies specific to GFP. Cells within the INL that show induced *apobec2b* expression at the injury site (*) are marked with white arrows. Injured RGCs are distinguished with white arrowheads. Cells in the INL and GCL expressing basal levels of *apobec2b* are marked with black arrowheads. The scale bar is equal to 100 μm. (G) Triple immunofluorescence using antibodies specific to GFP, GS and BrdU shows injury-dependent transgene induction in MGPCs. Fish were given an intraperitoneal injection of BrdU 3.5hrs before harvest. White arrowheads indicate co-localization GFP, GS and BrdU. The scale bar is equal to 50 μm. Abbreviations are as in Figure 2.2.

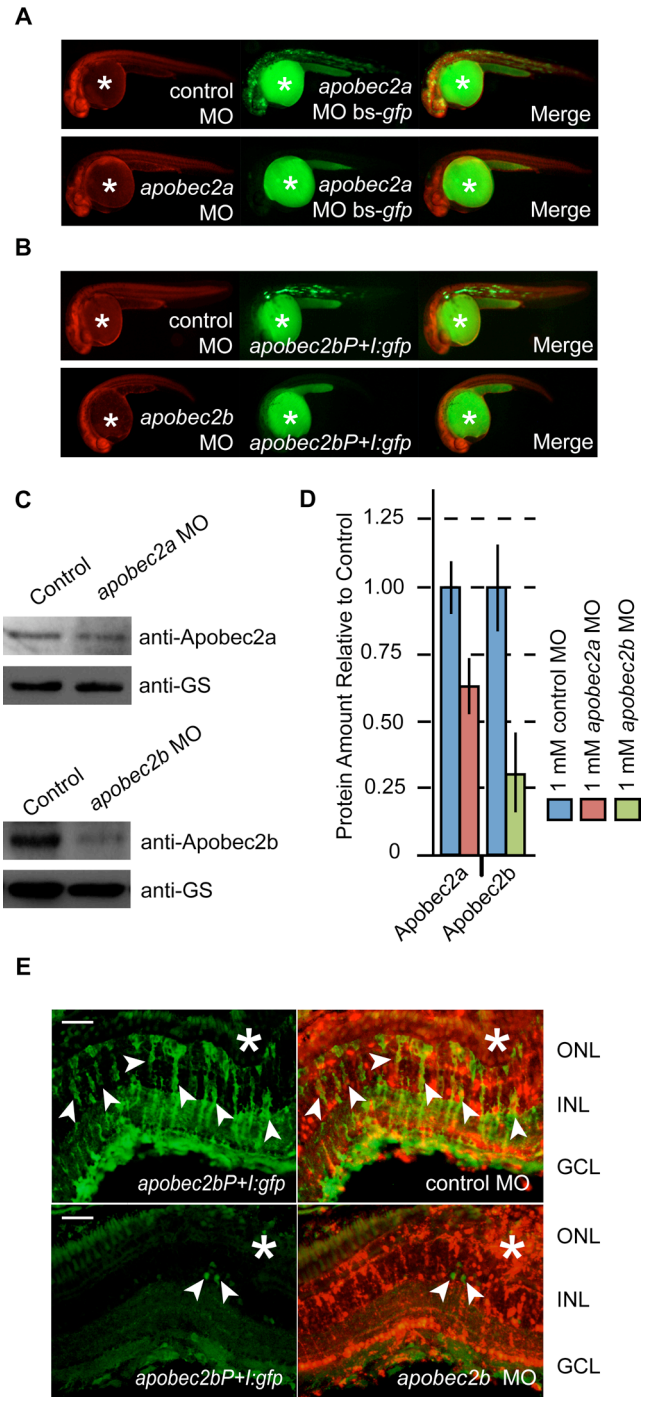

Figure 2.74 Validation of *apobec2a* and *apobec2b* MOs

(A) 24 hours post fertilization embryos microinjected at the single cell stage with pCS2p+ *apobec2a* MO bs-*gfp* (expression vector with *apobec2a* MO target sequence appended to the amino terminus of GFP) in combination with lissamine-tagged control or *apobec2a* MO showing knockdown of GFP with the *apobec2a* MO but not the control MO. An asterisk marks autofluorescence in the zebrafish yolk sac. (B) 24 hours post fertilization embryos microinjected at the single cell stage with ptal *apobec2bP+I:gfp* in combination

with lissamine-tagged control or *apobec2b* MO showing knockdown of GFP with the *apobec2b* MO but not the control. An asterisk marks autofluorescence in the zebrafish yolk sac. (C) Western blot of protein isolated from a 4 days post injury retina showing knockdown of Apobec2a and Apobec2b by their respective morpholinos. GS served as a loading control. (D) Quantification of Apobec2a and Apobec2b knockdown after morpholino treatment. Densitometry was calculated from Western blots using Image J. *Y*-axis is relative protein amount and is normalized to the control, which was assigned a value of 1. GS served as the internal control (control and Apobec2a, n=3 individual retinas; Apobec2b, n=2 individual retinas). (E) GFP immunofluorescence shows *apobec2b* MO treatment suppresses injury-dependent GFP expression in *apobec2bP+I:gfp* transgenic fish. Eyes were isolated 4dpi. The injury site is marked with an asterisk. Arrowheads indicate GFP+ cells within INL harboring lissamine-tagged morpholino. The scale bar is equal to 50 μm. Abbreviations: MO, morpholino; ONL, outer nuclear layer; INL, inner nuclear layer; GCL, ganglion cell layer; GS, glutamine synthetase.

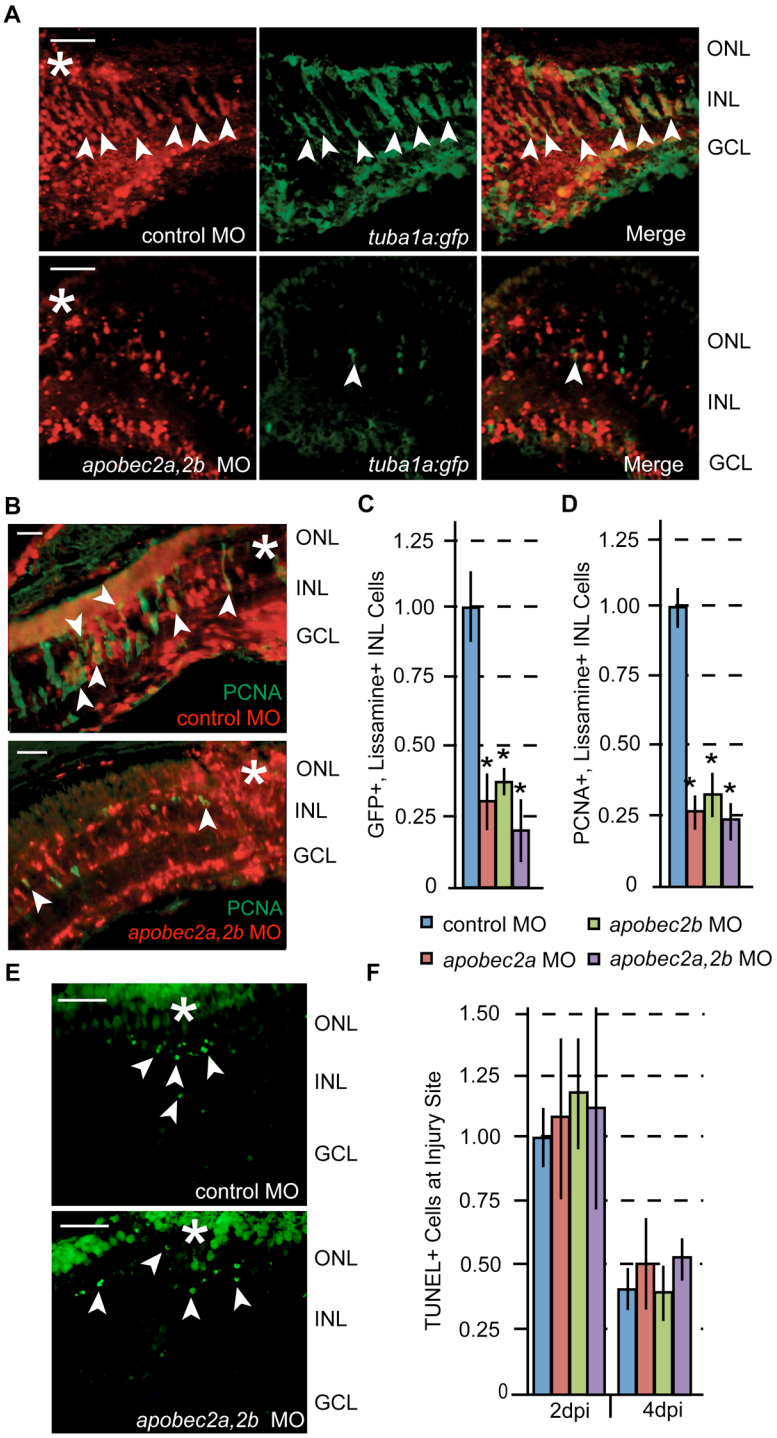

Figure 2.75 Knockdown of Apobec2a or Apobec2b blocks *1016 tuba1a:gfp* transgene expression and MGPC proliferation

(A) GFP immunofluorescence shows Apobec2a,2b knockdown suppresses injury-dependent GFP expression in *1016 tuba1a:gfp* fish. Arrowheads indicate GFP+ cells within INL harboring lissamine-tagged morpholino. Eyes were isolated 4dpi. The scale bar is equal to 50 μm. (B) PCNA immunofluorescence shows Apobec2a,2b knockdown suppresses cell

proliferation in the injured retina. Arrowheads indicate PCNA+ cells within the INL harboring lissamine-tagged morpholino. Eyes were isolated 4 days post injury. The scale bar is equal to 50 μm. (C and D) Quantification of the percentage of the total number of morpholino+ cells within the INL that are GFP+ (*1016 tuba1a:gfp*) (C) or are proliferating (wt) as indicated by PCNA staining (D) following Apobec2a, Apobec2b, or Apobec2a,2b knockdown. The data was normalized to the value of the control MO, which was given a value of 1. Data represents means ± s.d. (n=3 individual fish; compared with control MO, *apobec2a*, *apobec2b, and apobec2a,2b* MO oligonucleotides $*P < 0.0012$ for GFP and $*P < 0.0002$ for PCNA quantifications). (E) Tunel staining identifies cells undergoing apoptosis at the site of injury (*) following treatment with control or apobec2a and apobec2b MO. Eyes were isolated 2 days post injury. Arrowheads indicate Tunel+ cells. (F) Quantification of the Tunel+ cells at the site of injury. Samples were isolated 2 and 4 days post injection and electroporation of the indicated morpholino. The data was normalized to the value of the control MO at 2dpi, which was given a value of 1. Data represents means ± s.d. (n=3 individual fish). Abbreviations are as in Figure 2.4.

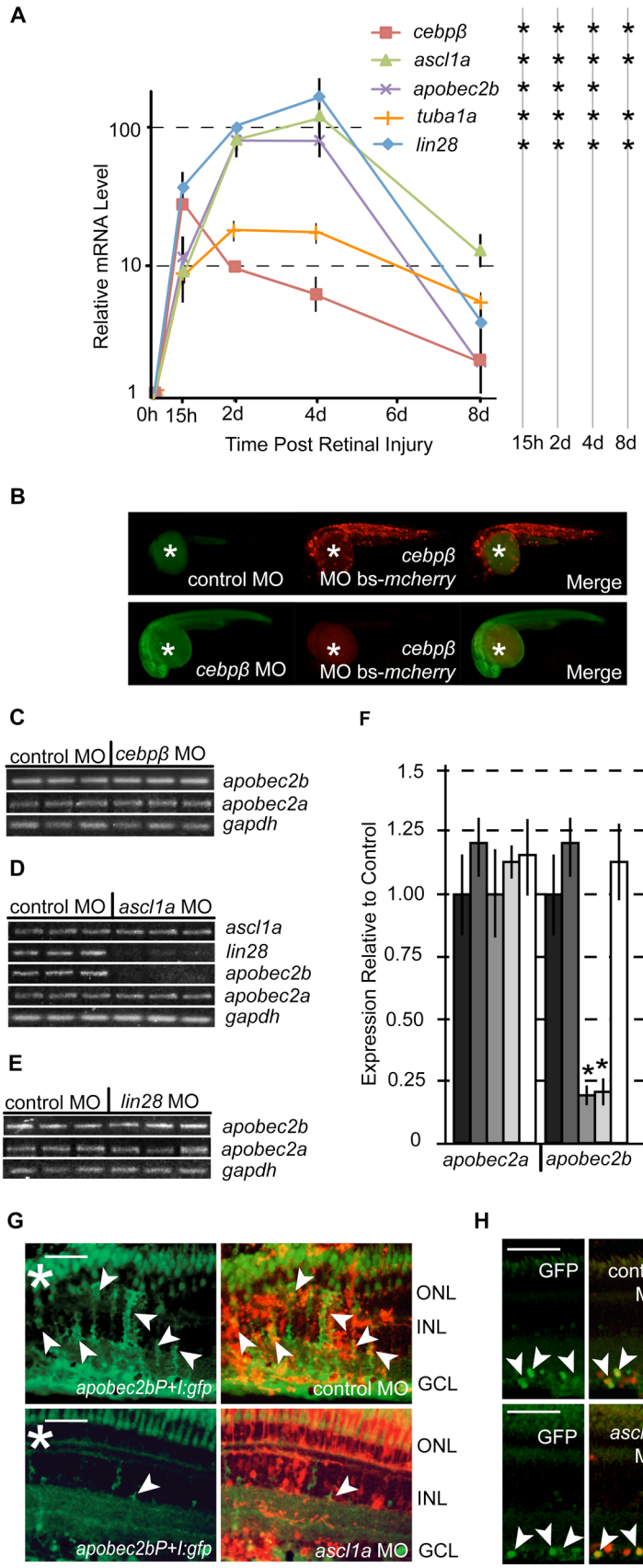
A
cebpβ
ascl1a
apobec2b
tuba1a
lin28
Relative mRNA Level
100
10
1
0h 15h 2d 4d 6d 8d
Time Post Retinal Injury
15h 2d 4d 8d
B
control MO
cebpβ
MO bs-mcherry
Merge
cebpβ MO
cebpβ
MO bs-mcherry
Merge
C
control MO | cebpβ MO
apobec2b
apobec2a
gapdh
D
control MO | ascl1a MO
ascl1a
lin28
apobec2b
apobec2a
gapdh
E
control MO | lin28 MO
apobec2b
apobec2a
gapdh
F
Expression Relative to Control
1.5
1.25
1.00
0.75
0.50
0.25
0
apobec2a
apobec2b
1 mM ascl1a MO2
1 mM lin28 MO
1 mM control MO
1 mM cebpβ MO
1 mM ascl1a MO1
G
apobec2bP+l:gfp
control MO
ascl1a MO
ONL
INL
GCL
H
GFP
control MO
ascl1a MO
ONL
INL
GCL

Figure 2.76 Injury-dependent Ascl1a signaling results in the increased expression of *apobec2b*

(A) Real-time PCR quantification of indicated mRNAs isolated from retina at various times post injury (*X*-axis). *Y*-axis is fold induction in log scale and is normalized to 0 hours (0h, i.e. uninjured control) which was assigned a value of 1. The expression of *gapdh* served as the internal control. Data represents means ± s.d. (n=3 individual cDNA sets; compared with control, time points marked with an asterisk have a $P < 0.037$). (B) 24 hours post fertilization embryos microinjected at the single cell stage with *cebpβ* MO bs-*mCherry* (expression vector harboring MO target sequence appended to the amino terminus of mCherry) in combination with untagged control or fluoroscein tagged *cebpβ* MO showing knockdown of mCherry with the *cebpβ* MO but not the control. An asterisk marks autofluorescence in the zebrafish yolk sac. (C) RT-PCR indicates Cebpβ knockdown has no effect on injury-dependent *apobec2a* or *apobec2b* expression at 2dpi. (D) RT-PCR indicates Ascl1a knockdown blocks injury-dependent induction of *lin28* and *apobec2b* mRNAs at 2dpi. (E) Lin28 knockdown shows no effect on injury-dependent induction of *apobec2a* and *apobec2b* mRNAs at 2dpi. (C and E) Each agarose gel lane represents a sample prepared from an independent fish. The expression of *gapdh* served as the internal control. (F) Real-time PCR quantification of *apobec2a* and *apobec2b* mRNA levels after injury and treatment with the indicated morpholinos. *ascl1a* MO 1 is specific to its ATG translational start region and *ascl1a* MO 2 is specific to its 5'UTR. The mRNA fold induction was normalized to the value of the control MO, which was given a value of 1. *gapdh* served as the internal control. Data represents means ± s.d. (n=3 individual fish; compared with control MO, *ascl1a* MO 1 and 2 $*P < 0.01$). (G) GFP immunofluorescence shows *ascl1a* MO treatment suppresses injury-dependent GFP expression in cells of the INL of *apobec2bP+I:gfp* transgenic fish. Eyes were isolated 3dpi. The injury site is marked with an asterisk. Arrowheads indicate GFP+ cells within INL harboring lissamine-tagged morpholino. The scale bar is equal to 50 μm. (H) GFP immunofluorescence shows *ascl1a* MO treatment has no impact on injury-dependent GFP expression in injured ganglion cells of *apobec2bP+I:gfp* transgenic fish. Shown is a region flanking an injury site. Eyes were isolated 3dpi. Arrowheads indicate GFP+ cells within GCL harboring lissamine-tagged morpholino. The scale bar is equal to 50 μm. Abbreviations are as in Figure 2.4.

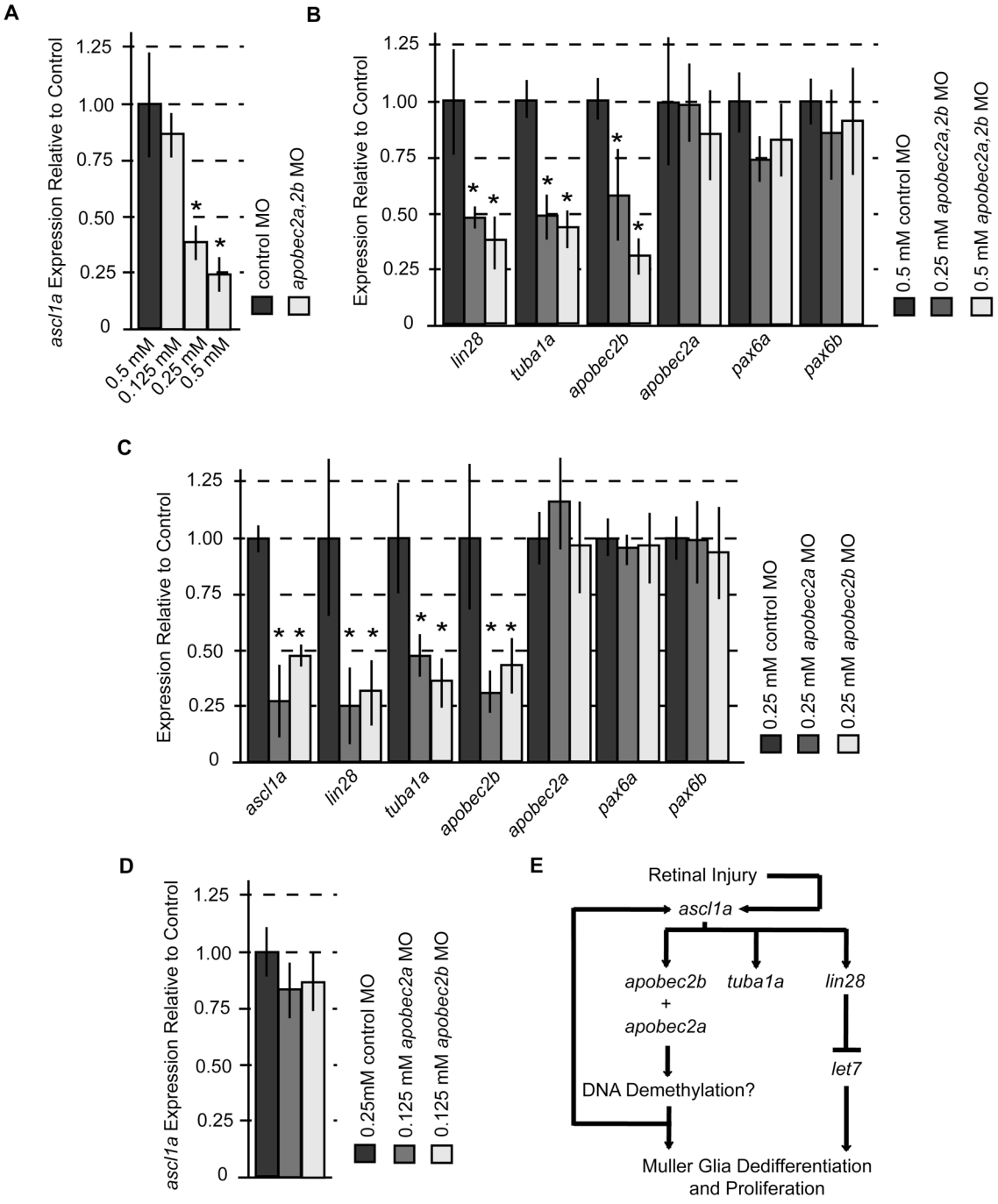

Figure 2.77 Apobec2a and Apobec2b regulate injury-dependent *ascl1a*, *lin28* and *tuba1a* expression

(A and C) Real-time PCR quantification of the effects of Apobec2a and Apobec2b knockdown either together (A and B) or individually (C and D) on the indicated mRNAs. mRNA levels were normalized to the control MO, which was given a value of 1. The expression of *gapdh* served as the internal control. Data represents means ± s.d. (A)

Knockdown of Apobec2a and Apobec2b blocks injury-dependent *ascl1a* induction (n=3 individual fish; compared with control MO, *apobec2a,2b* MO $*P < 0.011$). (B) Knockdown of Apobec2a and Apobec2b blocks injury-dependent induction of *lin28*, *tuba1a* and *apobec2b* (n=3 individual fish; compared with control MO, *apobec2a,2b* MO knockdown of *lin28* $*P < 0.018$, knockdown of *tuba1a* $*P < 0.004$, knockdown of *apobec2b* $*P < 0.027$). (C) Knockdown of Apobec2a and Apobec2b independently shows similar effects on gene expression as knocking them both down together (n=3 individual fish; compared with control MO, *apobec2a* and *apobec2b* MO individually block the induction of *lin28*, *tuba1a*, and *apobec2b* $*P < 0.04$). (D) The decreased expression of *ascl1a* after the independent knockdown of Apobec2a and Apobec2b is concentration-dependent, as lower concentrations of morpholino do not significantly alter *ascl1a* levels. **(**E) Summary of knockdown data placed in context of known signaling during retina regeneration.

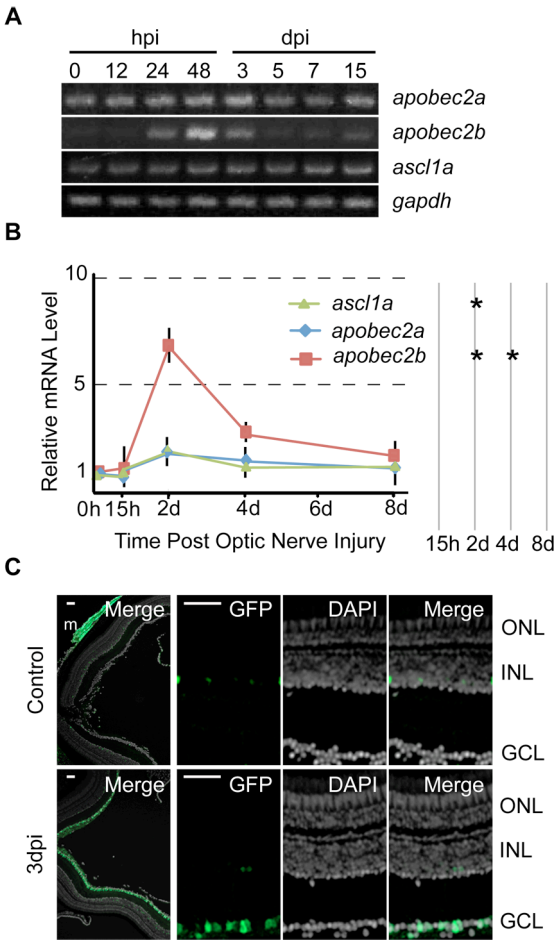

Figure 2.78 *apobec2b* and *ascl1a* mRNA levels are induced during optic nerve regeneration

(A) RT-PCR analysis of indicated mRNAs isolated from the retina at various times post optic nerve lesion (hours post injury: hpi, days post injury: dpi). The expression of *gapdh* served as the internal control. One representative of three independent time courses is shown. (B) Real-time PCR quantification of indicated mRNAs levels isolated from retina at the indicated times post injury (*X*-axis). *Y*-axis is normalized to 0 hours (0h), i.e. the uninjured retina, which was assigned a value of 1. The expression of *gapdh* served as the internal control. Data represents means ± s.d. (n=3 individual cDNA sets; compared with control, time points marked with an asterisk have a $P < 0.0053$). (C) GFP immunofluorescence shows injury-dependent transgene induction in retinal ganglion cells of *apobec2bP+I:gfp* transgenic fish at 3dpi. GFP expression in an ocular muscle exterior to the eye is marked with an "m" in the control (top) panel. The scale bar is equal to 50 μm. Abbreviations are as in Figure 2.4.

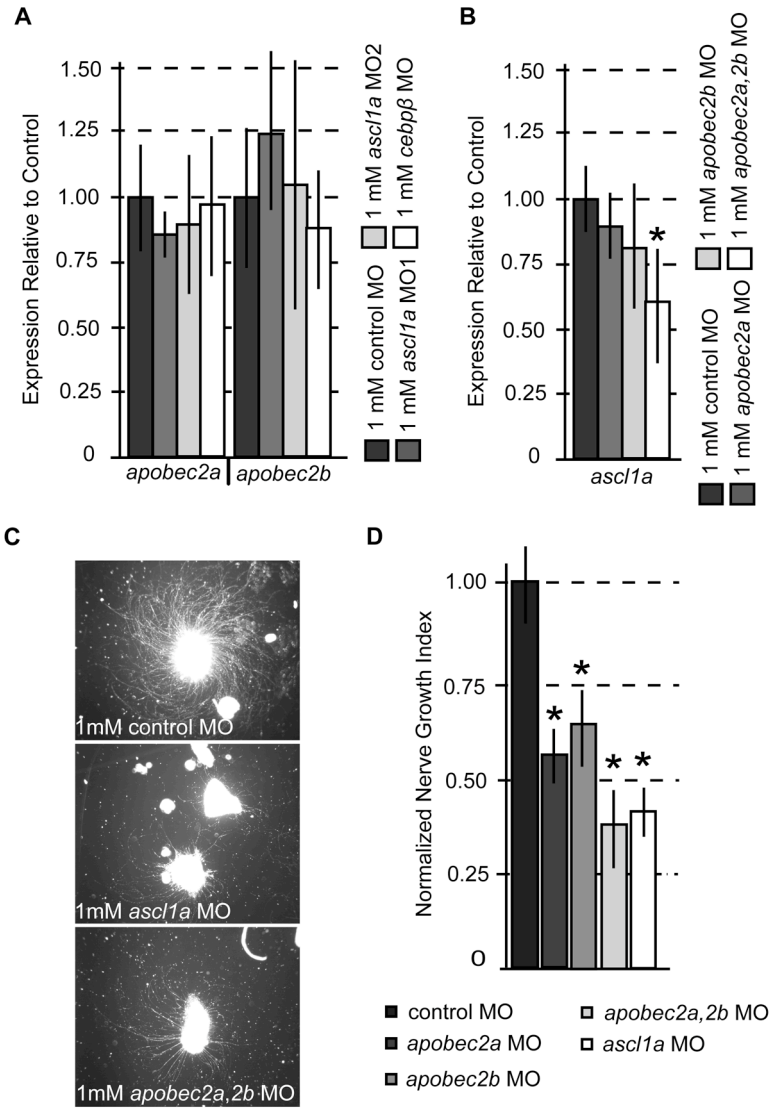

Figure 2.79 Ascl1a, Apobec2a, and Apobec2b regulate axonal growth during optic nerve regeneration

1 mM of the indicated morpholinos were delivered to retinal ganglion cells *in vivo* by placing morpholino-soaked Gelfoam on the optic nerve stump following lesion. (A and B) Retinas were isolated 2 days post optic nerve lesion and morpholino treatment for expression analysis. The expression of *gapdh* served as the internal control. The data was normalized to the value of the control MO, which was given a value of 1. (A) Knockdown of Cebpβ or Ascl1a did not significantly affect *apobec2a* or *apobec2b* expression. Data represents means ± s.d. (n=3 individual fish). (B) Knockdown of Apobec2a and Apobec2b, but not each individually, reduced the levels of *ascl1a*. Data represents means ± s.d. (n=3 individual fish for the *apobec2a* and *apobec2b* MO samples, n=4 individual fish for control and *apobec2a,2b* MO samples; compared with control MO, *apobec2a,2b* MO knockdown of ascl1a $*P < 0.024$). (C) Representative images of axonal outgrowth following treatment with the indicated morpholinos. Retinas were isolated 4 days after morpholino treatment, diced,

and cultured for 4 days prior to analysis of neurite outgrowth. (D) Quantification of Nerve Growth Index (see Material and Methods) values following morpholino treatment and explant. Values were normalized to control MO treated samples, which were given a value of 1. Data represents means ± s.d. (n=3 individual fish for control, *ascl1a,* and *apobec2a,2b* MO samples; n=4 individual fish for *apobec2a* and *apobec2b* MO samples; compared with control MO, samples marked with an asterisk have a $P < 0.01$).

2.8 Tables

Primer Name	Application	Sequence
gadd45α	SQ RT-PCR	F, GTGTGGAGATAACGCAACGGAAAGAATGG
		R, GGATGAACGCGACAATATAAATACAGTGAA
gadd45αI	SQ RT-PCR	F, GCCAGAGAAAGAACACCAACGAGAACT
		R, ACGTCCTCAGAAAGTCCCACAAACAAA
gadd45β	SQ RT-PCR	F, TCAGGCACAGAGAAGCGAGTAAAGGAA
		R, AATAGTTCAGCGTTCTTGCAGGGACAG
gadd45βI	SQ RT-PCR	F, TCCACTGACAATAACGCCAATGAACC
		R, TGCATCCTTTCAGAGCTACGACACAGT
gadd45βI-RT	Real-Time PCR	F, GATCCACTTCACGCTCATCCA
		R, GGCAATAGAAGGCACCCACTG
gadd45γ	SQ RT-PCR	F, GCGAAACGCGACCTAAAGTGGAT
		R, AGAACTTCTTCACCTCCGACAATCTCTC
gadd45γI	SQ RT-PCR	F, GTTCTGCTCTCTGCAACCTGTGGAAT
		R, CTCTCGTGGCATACCTGACCTCGTT
gadd45γI-RT	Real-Time PCR	F, TTTCTGCCAAAGCAAACGACT
		R, CAGTGAGCATCTTCAAAATCTTCAG
aid	SQ RT-PCR	F, GGACAGTGTGCTCATGACCCAGAAGAAAT
		R, GATGTTCACAATGATCACGTTAATGC
apobec2a	SQ RT-PCR and Real-Time PCR	F, GACCCGGCCTGCAAATACACC
		R, AGCGCAATTGTTTTCGATGTGATGTA
apobec2b	SQ RT-PCR	F, GGCAGACAAAAAGGACAGCAAGAC
		R, CACAGGCCTCATCATGCGTAGTTT
apobec2b-RT	Real-Time PCR	F, ATGAGGAGTTTGAGCTAGAGCCGATG
		R, ATCCTCCAGGTAACCACGAACGC
aid	SQ RT-PCR	F, GTTAGCAAGTTTCGACTTTCGGAATGAT
		R, GATGTTCACAATGATCACGTTAATGCTACAG
mbd4	SQ RT-PCR	F, CTTCAACATGAACATTATCTGCAAATCCTG
		R, GAGACGCTCTTCCATGACCCCTG
tdg	SQ RT-PCR	F, GCAGACGCTTCAGGCTCAGTATCC
		R, CCAGGCCGAGGTCAAAGGTGTAG
dnmt3	SQ RT-PCR and Real-Time PCR	F, GCTTGTTGATGCCGTGAAAGTGAGTC
		R, ATCAACCTTCCCACGATTATTCCAAACT
dnmt3-RT	Real-Time PCR	R, TCATGGTGACGGGGAAATGTGC
dnmt4	SQ RT-PCR and Real-Time PCR	F, CAGAGCAGAGACGGCCAATCAGAG
		R, TGGCCACCACATTCTCAAACATCC
dnmt4-RT	Real-Time PCR	R, CATTACAGGGACTTCCACCAATCACC
tet2I-RT	SQ RT-PCR and Real-Time PCR	F, CACACCCAACTCTAAAACGGACAACAC
		R, ATGGTGGGGAAGCGTAAGAAGGA
tet3-RT	SQ RT-PCR and Real-Time PCR	F, GGACTGTCGTCTGGGCTGTAGGG
		R, GCCAGCAGCCGCACTTCTCTT

cebpβ-RT	Real-Time PCR	F, CCTCAAGCGGGCGGTAAAATG
		R, CTGCTCCACGCGCTTCTGTAACC
tuba1a-RT	Real-Time PCR	F, GGCTGCCCTGGAGAAAGATTATGA
		R, AGGATTGACCTTTTAGCCAGTTGACA
mmp9	SQ RT-PCR	F, ACAACCACTGCTTCCACCACAACTCA
		R, AAGCTGCATCAGTGAATCGAGGGTATC
apobec2bP+I	Cloning	F, CGAGGTCGACGTGAAGCGGGGACAACAAG
		R, CGGTGGATCCCGCCCGGACGAGTACTCCACAT
apobec2aMobsgfp	Cloning	F, TTCGAATTCGATGGCCGATAGAAAGGGAGCAGCATGGTGAGCAAGGGCGAGGA
cebpβMobsmcherry	Cloning	F, TTCGAATTCATGCGCAATCCGGCGGGTGTTAAGATCATGGTGAGCAAGGGCGAGGA
mcherry/gfp	Cloning	R, CTTTCTAGATTACTATTACTTGTACAGCTCGTCCATGC

Table 2.81 List of primers used in this study and their applications

Chapter 3:
Analysis of DNA methylation reveals a partial reprogramming of the Müller glia genome during retina regeneration[2]

3.1 Abstract

Upon retinal injury, zebrafish Müller glia (MG) transition from a quiescent supportive cell to a progenitor cell (MGPC). This event is accompanied by the induction of key transcription and pluripotency factors. Because somatic cell reprogramming during iPSC generation is accompanied by changes in DNA methylation, especially in pluripotency factor gene promoters, we were interested in determining if DNA methylation changes also underlie MG reprogramming following retinal injury. Consistent with this idea, we found that genes encoding components of the DNA methylation/demethylation machinery were induced in MGPCs and that manipulating MGPC DNA methylation with 5-aza-2'-deoxycytidine altered their properties. A comprehensive analysis of the DNA methylation landscape as MG reprogram to MGPCs revealed that demethylation predominates at early times, while levels of *de novo* methylation increase at later times. We found that these changes in DNA methylation were largely independent of Apobec2 protein expression. A correlation between promoter DNA demethylation and injury-dependent gene induction was noted. In contrast to iPSC formation, we found that pluripotency factor gene promoters were already hypomethylated in quiescent MG and remained unchanged in MGPCs. Interestingly, these pluripotency factor promoters were also found to be hypomethylated in mouse MG. Our data identify a dynamic DNA methylation landscape as zebrafish MG transition to a MGPC and suggest that DNA methylation changes will complement other regulatory mechanisms to ensure gene expression programs controlling MG reprogramming are appropriately activated during retina regeneration.

[2] This chapter was published as Powell C, Grant AR, Cornblath E, Goldman D (2013) Analysis of DNA methylation reveals a partial reprogramming of the Muller glia genome during retina regeneration. Proc Natl Acad Sci U S A 110:19814-19819.

3.2 Introduction

Induced pluripotent stem cells (iPSCs) can be generated through the forced expression of pluripotency factor genes, like *Oct4*, *Klf4*, *Sox2*, *c-Myc*, *Lin28*, and *Nanog*, which are normally expressed in embryonic stem cells (ESCs) (Takahashi and Yamanaka, 2006; Stadtfeld and Hochedlinger). Pluripotency factor gene expression in ESCs and iPSCs is associated with chromatin that is in an "open" accessible state, while their repression in somatic cells is associated with less accessible, condensed chromatin (Gaspar-Maia et al.). DNA methylation has a significant impact on chromatin structure (Gaspar-Maia et al., 2011). DNA demethylation of pluripotency factor promoter regions is correlated with increased expression during iPSC formation (Mikkelsen et al., 2008; Polo et al.). Similar epigenetic changes are seen in other cellular reprogramming events such as nuclear transfer (Simonsson and Gurdon, 2004), heterokaryon formation (Bhutani et al., 2009), and carcinogenesis (Suva et al.).

Tissue regeneration provides another avenue to study cellular reprogramming. Unlike mammals, zebrafish can regenerate multiple tissues including the retina. During zebrafish retina regeneration, Müller glia (MG) reprogram to generate progenitor cells (MGPCs) capable of replacing all lost neural cell types (Fausett and Goldman, 2006; Raymond et al., 2006; Bernardos et al., 2007; Fimbel et al., 2007). The role that MG play during this regenerative event can be roughly divided into three phases: the replication-independent transition of MG to MGPCs occurring by 2 days post injury (dpi), the proliferative amplification of MGPCs between 2 and 7dpi, and the differentiation of these progenitors following 7dpi. MGPC formation is accompanied by the increased expression of pluripotency factors (Ramachandran et al., 2010a) and other key signaling molecules (Fausett et al., 2008; Thummel et al.; Ramachandran et al.; Meyers et al.; Nelson et al.; Ramachandran et al.; Wan et al.). The induction of pluripotency genes, along with the finding that the putative cytidine deaminases Apobec2a and Apobec2b (Apobec2a,2b) are necessary for MGPC formation (Powell et al., 2012), is consistent with the idea that active modification of the DNA methylation landscape may underlie the reprogramming of MG to MGPCs.

To test this idea, we compared the methylation profiles of MG with MGPCs using reduced representation bisulfite sequencing (RRBS). This comprehensive analysis identified

a changing DNA methylation landscape underlying MG reprogramming and progenitor formation. Surprisingly, unlike the reprogramming of fibroblasts to iPSCs, promoters of genes encoding pluripotency factors were hypomethylated in MG and remained so in MGPCs. Furthermore, we were surprised to find that Apobec2a,2b had little impact on site-specific DNA demethylation. These studies provide an unprecedented view of the DNA methylation landscape as MG reprogram to a MGPC and will serve as an important resource for understanding the function of DNA methylation during cellular reprogramming and tissue regeneration.

3.3 Results

3.3.1 Modulators of DNA methylation are transcriptionally regulated during MG reprogramming

Previous studies suggested that many of the genes encoding regulators of DNA methylation were induced in the injured retina (Powell et al., 2012). To assess whether these genes were specifically induced in MGPCs, we used FACS to isolate MG from uninjured *gfap:gfp* transgenic fish retinas and MGPCs from injured *1016 tuba1a:gfp* transgenic fish retinas at 4 days post injury (dpi) (Figure 3.6A and B) (Ramachandran et al., 2011). We have shown previously that mechanical lesion with a 30-gauge needle results in the activation of MG only at the site of injury and that *1016 tuba1a:gfp* transgenic fish specifically label MGPCs at 4dpi (Ramachandran et al., 2011). Quantitative real-time PCR showed increased expression of genes associated with DNA demethylation, like *gadd45β*, *gadd45βl, gadd45γ, gadd45γl, apobec2a, apobec2b, tdg,* and *tet3* in MGPCs (Figure 3.1A-C). Of those associated with DNA methylation, we found increases of *dnmt1, dnmt4, dnmt5,* and *dnmt7* (Figure 3.1A and D). Expression analyses using mRNA prepared from whole retina likewise showed injury-dependent induction of these *dnmt* mRNAs (Figure 3.6C and D). Basal expression levels of these and other DNA methylation-associated genes were observed in quiescent MG (Figure 3.1A). These results suggest that the regulation of DNA methylation may be important for MGPC formation.

3.3.2 Dnmt inhibition perturbs MG reprogramming and MGPC proliferation, migration, and differentiation

Treatment of zebrafish embryos with 5-aza-2'-deoxycytidine (5-dAza) has been shown to induce global DNA hypomethylation (Martin et al., 1999) and alter gene expression (Potok et al.). To investigate if DNA methylation regulates MGPC formation and properties, we treated injured *1016 tuba1a:gfp* transgenic fish daily with 5-dAza. Because the inhibition of Dnmts by 5-dAza requires its incorporation into DNA, de novo DNA methylation events occurring prior to the beginning of the first DNA replication will not be perturbed.

GFP expression in these fish report MG reprogramming to a MGPC (Fausett and Goldman, 2006). Interestingly, 5-dAza treatment caused a dramatic increase in GFP expression in MGPCs, whose identity was confirmed by co-labeling with PCNA (Figure 3.2A, 3.7A and B). However, treatment with 5-dAza also reduced MGPC proliferation (Figure 3.2B and C) and perturbed the localization of PCNA+ cells in the outer nuclear and ganglion cell layers (Figure 3.2B and D). While the majority of PCNA+ cells at the site of injury likely derive from MGPCs, as indicated by their co-localization with GFP (Figure 3.7A and B), we cannot rule out the possibility that some of the reduced proliferation in the outer nuclear layer is due to a decrease in rod progenitor proliferation at the injury site. Treatment with 5-dAza did not seem to impact the number of MG responding to injury as it did not alter the number of MGPC columns at 2dpi when MG are just beginning to proliferate (Figure 3.7C). In addition, 5-dAza perturbed the migration and differentiation of MGPC derived progeny (Figure 3.8A-D). 5-dAza treatment without injury did not impact GFP expression or proliferation in *1016 tuba1a:gfp* transgenic fish (Figure 3.8I).

To determine if the effects of 5-dAza were due to a cytotoxic effect on MG, Tunel assays were performed. 5-dAza treatment did not increase the absolute number of Tunel+ nuclei at the injury site at any time point analyzed (Figure 3.8E). However, on rare occasions we did note a 1016 *tuba1a:gfp*, GFP+/Tunel+ cell in the 5-dAza sample, but never in controls (Figure 3.8F). This data, along with the fact that many MGPCs survive to 10dpi (Figure 3.8C), indicates that 5-dAza is only weakly cytotoxic to MGPCs. We then confirmed that 5-dAza actually caused hypomethylation of the MGPC genome by performing restriction PCR with McrBC, a methylation-sensitive endonuclease (Figure 3.8G and H). Together these results suggest that DNA demethylation may activate genes, like *tuba1a*, that are associated with MG reprogramming, and may also impact genes contributing to MGPC proliferation, migration, and differentiation.

3.3.3 Comparison of MG and MGPC DNA methylation landscapes at 4dpi

To determine if DNA methylation changes underlie the conversion of a MG to MGPCs, we used RRBS to identify site-specific DNA methylation changes in these two cell types. For this analysis, MG were FACS purified from uninjured *gfap:gfp* fish retinas and MGPCs were FACS purified from injured *1016 tuba1a:gfp* fish retinas at 4dpi. These fish have been bred to the same wild-type background for many generations, and we confirmed that they have highly homologous backgrounds using in depth SNP analyses (see Materials and Methods).

Genomic DNA was isolated from MG and MGPCs and their methylation profiles were compared by RRBS (Figure 3.9 and 3.10 and Table 3.1). The methylation level of 611,434 individual cytosines within the CpG context were quantitatively compared between the two cell populations, and of those, 9,554 were differentially methylated bases (DMBs) (Figure 3.3A). This represents a difference of 1.56% between the methylation profiles. 54.0% and 46.0% of these DMBs were increasing and decreasing methylation, respectively (Figure 3.3B). Validation of a subset of these DMBs was performed by restriction PCR after digesting MG and 4dpi MGPC gDNA with the methylation-sensitive restriction enzyme HpaII (Figure 3.11A-D). Consensus sequences for methylated and demethylated sites were analyzed using 10 bp flanking the DMB, and no clear consensus was found outside of the centrally located CpG.

Interestingly, DMBs were not congregated within the genome, but were thinly dispersed along all chromosomes (Figure 3.10D). Most DMBs, regardless of the direction of change in methylation, were localized to intergenic and intronic regions, while relatively few were localized to exonic and promoter regions (Figure 3.3C). There was a dearth of DMBs localized to CpG islands and shores, suggesting that the bulk of the methylation changes are occurring in CpG-poor regions (Figure 3.3C). Surprisingly, no DMBs were localized to the promoters of pluripotency factors and previously characterized retina regeneration-associated genes suggesting that promoter methylation/demethylation was not involved in their regulation. This differs from previously studied reprogramming events that correlated pluripotency factor promoter region demethylation with increased gene expression (Simonsson and Gurdon, 2004; Bhutani et al., 2009; Polo et al., 2012).

While DNA methylation predominantly occurs within the CpG context, non-CpG methylation can occur in the contexts of CHG and CHH (H represents A, C, or T). The methylation level of 775,005 CHG and 1,554,382 CHH cytosines were quantitatively compared by RRBS and of those, 440 and 635 were differentially methylated, respectively (Figure 3.12). This represents changes of only 0.057% and 0.041% in their levels, respectively. Like DMBs in the CpG context, CHG and CHH DMBs were also predominantly localized to CpG poor intergenic and intronic regions (Figure 3.12C and F).

3.3.4 Promoter DMBs that are decreasing methylation are correlated with increases in gene expression

Because DNA methylation is thought to regulate gene transcription (Reddington et al., 2013), we decided to further analyze the DMBs that are localized to promoter regions. Specifically, we sought to determine if promoters with DMBs that are decreasing methylation show increased expression levels and vice versa. 6,210 promoters were analyzed by RRBS, and of those, 292 contained at least one DMB (4.7%) (Figure 3.11E). Previous microarray expression data comparing MG and 4dpi MGPC cell populations quantitatively compared the expression of 8,339 genes, of which 1,361 were increasing expression and 262 were decreasing expression in MGPCs (Figure 3.11F) (Ramachandran et al., 2012). Comparison of these data sets revealed little correlation between promoter DMBs with increasing methylation and gene expression. However, we did find a correlation between promoter DMBs with decreasing methylation and increased gene expression (Figure 3.3D and 3.11G). To confirm these trends, the expression levels of a random subset of genes (whose promoters contained at least one DMB) were analyzed using cDNA prepared from FACS purified MG and 4dpi MGPCs (Figure 3.11H and I). These results support the correlations found in the RRBS/microarray comparison.

3.3.5 Apobec2-independent DNA demethylation predominates as MG transition to MGPCs

We previously showed that Apobec2a,2b are required for MGPC formation and hypothesized that they participate in active DNA demethylation of the MG genome following injury (Powell et al., 2012). We sought to use RRBS to directly test if they regulate DNA demethylation. Our RRBS dataset comparing MG and 4dpi MGPCs cannot differentiate

between DMBs arising passively (replication-dependent) and actively (replication-independent). The knockdown of Apobec2 proteins blocks MGPC proliferation, so analyzing their effects at 4dpi may bias our results due to a block of passive DNA demethylation. Furthermore, because the knockdown of Apobec2a,2b blocks *1016 tuba1a:gfp* transgene induction, an alternate method was needed to purify MGPCs following knockdown.

To overcome these obstacles, we injected and electroporated control or *apobec2a,2b* lissamine-tagged antisense morpholino-modified oligonucleotides (MOs) into *gfap:gfp* transgenic fish and performed 6 additional lesions post electroporation resulting in the activation of MG across the entire retina. GFP+, lissamine+ cells were then isolated by FACS at 2dpi (Figure 3.13A and B). This protocol resulted in the isolation of all MG that have MO, not only those responding to injury (MG and MGPC). To estimate this enrichment, GFP+/lissamine+ MGPCs were isolated from control MO-treated *1016 tuba1a:gfp* or *gfap:gfp* fish at 4dpi and *ascl1a* mRNA levels (a transcript restricted to MGPCs) compared (Figure 3.14D). This analysis indicates that ~60% of the GFP+/lissamine+ sorted cells from *gfap:gfp* fish are MGPCs.

At 2dpi, MGPCs are just beginning their proliferative response (Fausett and Goldman, 2006), so the majority of DMBs identified by RRBS should result from active demethylation. RRBS libraries were prepared using 2dpi MGPC populations treated with control or *apobec2a,2b* MO (Figure 3.13 and 3.14 and Table 3.1). We first compared the methylation profiles of FACS-purified MG (uninjured) with 2dpi MGPCs electroporated with control MO (Figure 3.4A-C and 3.13A-D). We analyzed a total of 360,448 CpGs and found 7,535 DMBs (Figure 3.4A). Unlike 4dpi, the majority of DMBs at 2dpi were decreasing methylation (73.6%) (Figure 3.4B), but similar to 4dpi, the DMBs were predominantly localized to CpG poor promoter and intronic regions (Figure 3.4C). In addition to changes in CpG methylation, 317 and 613 DMBs were found in the context of CHG and CHH, respectively (Figure 3.15C and D). These results suggest that DNA methylation is actively regulated during MGPC formation.

When we compared the methylation profiles of 2dpi MGPCs from control and *apobec2a,2b* MO-treated retinas (Figure 3.4D and 3.16), a total of 283,572 CpGs were analyzed and only 66 DMBs were found, a difference of only 0.023% (Figure 3.4D). In addition, 63.6% of the DMBs identified were more demethylated following knockdown of

Apobec2a,2b; opposite from what one would expect if they were participating in DNA demethylation (Figure 3.16E). Non-CpG methylation was largely unaffected, with no CHG DMBs and only 1 CHH DMB (Figure 3.16C and D). Methylation comparisons of MG and 2dpi *apobec2a,2b* MO-treated MGPC were very similar to those between MG and 2dpi control MO-treated MGPCs (Figure 3.15G-K). These results strongly suggest that Apobec2 proteins do not participate in site-specific active DNA demethylation during MG reprogramming. When we compared the overall genomic methylation of these cell populations, we did see that the 2dpi MGPC, *apobec2a,2b* MO-treated cell population was slightly more methylated than the 2dpi MGPC, control MO-treated population, suggesting that Apobec2a,2b may directly or indirectly regulate global DNA methylation levels (Figure 3.16G).

3.3.6 Pluripotency factor and regeneration-associated gene promoters are hypomethylated in quiescent MG

As mentioned previously, the promoter methylation levels of genes encoding pluripotency factors and select regeneration-associated genes remained unchanged upon MGPC formation. Surprisingly, when we looked at the basal (quiescent MG) promoter methylation of these genes (including *ascl1a, insm1a, hbegfa, lin28, sox2, oct4, nanog, c-mycb,* and *klf4*), we found that they were hypomethylated (Figure 3.5B). When we compared RRBS basal promoter methylation levels with our microarray expression data, we found that genes highly induced in 4dpi MGPCs tended to have lower than average promoter (Figure 3.5C) and intragenic (Figure 3.5D) methylation levels. We confirmed the basal hypomethylation of a number of these promoters by bisulfite (Figure 3.5E and F) and restriction (Figure 3.5H, 3.17) PCR. Slight discrepancies seen between RRBS, bisulfite PCR, and restriction PCR may be attributed to the regions targeted for analysis (outlined in Figure 3.5A). Surprisingly, both MG and non-MG had similar restriction PCR profiles (Figure 3.5H and 3.17). These results suggest that pluripotency factor and many regeneration-associated genes may be poised for activation in quiescent MG, though further work is needed to analyze other epigenetic marks. Thus, zebrafish MG may require only limited reprogramming, and may be more stem cell in nature than previously thought.

The regenerative capability of mammalian MG is very limited compared to zebrafish MG and is lost with age (Lamba et al., 2008). We wondered if this may be due to differences in methylation of regeneration-associated gene promoters. To assess whether the basal promoter methylation levels differ between zebrafish and mouse MG, we isolated mouse MG from uninjured retina by staining with an anti-GLAST-PE antibody followed by FACS. MG enrichment was confirmed by PCR (Figure 3.5G). When we analyzed the methylation levels of a limited number of mouse promoters by restriction PCR, we found that like zebrafish MG, mouse promoter methylation levels of pluripotency factors and genes associated with regeneration in zebrafish, had low methylation levels (Figure 3.5I, 3.17). This suggests that like zebrafish MG, mouse MG may be somewhat poised for a regenerative response if provided the proper stimulation.

3.4 Discussion

During zebrafish retina regeneration, MG transition from a quiescent supportive cell to a MGPC. This transition is accompanied by the increased expression of pluripotency and other regeneration-associated genes (Fausett et al., 2008; Ramachandran et al., 2010a; Thummel et al., 2010; Ramachandran et al., 2011; Nelson et al., 2012; Powell et al., 2012; Ramachandran et al., 2012; Wan et al., 2012). Previously studied somatic cell reprogramming events found strong correlations between the increased expression of pluripotency factors and decreases in their promoter methylation levels (Meissner et al., 2008; Rai et al., 2008; Bhutani et al., 2009). Likewise, we hypothesized that the regulation of DNA methylation would accompany the reprogramming of MG to MGPCs in the injured retina. Indeed, we found that as MG transition to a MGPC, their genome undergoes dynamic changes in DNA methylation. This unprecedented analysis of the MG DNA methylation landscape as it transitions from a differentiated support cell to a MGPC provides unique insight into the reprogramming process as it takes place in an intact animal.

When we began these studies, we suspected that MG reprogramming may share characteristics with somatic cell reprogramming based on the common need to reawaken gene expression programs silenced during development. Quite surprisingly, and unlike somatic cell reprogramming, we found pluripotency factor gene promoter methylation levels do not change during MG reprogramming, but rather are already locked into a

hypomethylated state. Similarly, we found that genes that are highly induced and necessary for MG reprogramming harbor hypomethylated promoters that remain unchanged throughout the reprogramming event. These observations suggest that MG are (to an extent) preprogrammed for a regenerative response and may be more stem cell-like than previously thought (Jadhav et al., 2009). This type of cellular preprogramming has also been noted during zebrafish development (Potok et al.). The basal hypomethylation of MG may aid the regenerative process by increasing the speed and efficiency of MGPC formation, both of which are higher than those seen during iPSC generation. Interestingly, blocking DNA methylation improves the efficiency of iPSC generation (Mikkelsen et al., 2008).

With these thoughts in mind, we investigated the methylation status of a subset of these promoters in mice to ascertain whether DNA methylation at these locations could account (at least partially) for the limited regenerative potential of mouse MG. Surprisingly, these mouse promoters also exhibited low methylation levels similar to their zebrafish counterparts. Thus, understanding why they remain repressed and devising ways to neutralize this repressive environment may facilitate mammalian MG reprogramming. One candidate for this repression, *let-7*, appears to inhibit regeneration in both zebrafish and *C. elegans* (Ramachandran et al., 2010a; Zou et al., 2013). Interestingly, ascl1a inhibits *let-7* expression during zebrafish MG reprogramming (Ramachandran et al., 2010a) and its overexpression in postnatal mouse MG enhanced their reprogramming (Pollak et al., 2013). We suspect that this latter effect is mediated by inhibition of *let-7* and hypothesize that *let-7* is a key factor contributing to the limited regenerative potential of mammalian MG.

While we did not find methylation changes occurring in the promoters of pluripotency factor and early-induced regeneration associated genes, we did identify a changing DNA methylation landscape as MG reprogram to MGPCs. During MGPC formation (0-2dpi), DNA demethylation predominates and may underlie some of the gene expression changes noted during this time. Indeed many promoter demethylation events are associated with increased gene expression. However, other mechanisms must also be at play since some of the best-studied regeneration-associated genes do not undergo changes in DNA methylation. These genes may be directly regulated by other events like histone modifications and availability of transcription factors. Thus, changes in DNA methylation may be necessary for MG reprogramming but may not be sufficient.

The predominance of DNA demethylation as MG transition to a MGPC is intriguing, and we suspected that Apobec2 proteins were involved in this process based on previous studies showing their knockdown inhibits retina regeneration (Powell et al., 2012) and that they contribute to DNA demethylation in zebrafish embryos and adult mouse brains (Rai et al., 2008; Guo et al., 2011). Surprisingly, our studies suggest they do not have a significant impact on site-specific active DNA demethylation during MG reprogramming. Thus, other genes potentially involved in DNA demethylation, like Gadd45 (Barreto et al., 2007; Rai et al., 2008; Ma et al., 2009b) and Tet proteins (Pastor et al., 2013), may be better targets for investigating the impact of DNA demethylation during MG reprogramming. The role that Apobec2 proteins play during MG reprogramming remains to be determined. It is possible that these proteins, as other Apobecs, catalytically edit RNAs, but it is also possible that they perform some function that is independent of a deaminase activity. Indeed, some have questioned if Apobec2 proteins are catalytically active and if they bind polynucleotides (Anant et al., 2001a; Mikl et al., 2005; Conticello, 2008; Sato et al., 2009). Further work is needed to shed light on the mechanism of these proteins.

From 2-4dpi, when MGPCs are expanding, the DNA methylation landscape shifts from one that is predominately driven by demethylation (2dpi), to one with increasing levels of de novo methylation (4dpi). We note that at this time, MGPCs are at the peak of their proliferative phase and may be preparing for differentiation. Perhaps the increased methylation noted at 4dpi contributes to the differentiation of MGPCs as they begin to repair a damaged retina. Consistent with this idea, pharmacological inhibition of this methylation was detrimental to proper lamination and differentiation of these MGPCs.

In summary, our comprehensive analysis of the DNA methylation landscape as MG transition to a MGPC and generate progenitors for retinal repair provides a novel view of the reprogramming process and provides an important resource for understanding the function of DNA methylation in cellular reprogramming and retina regeneration.

3.5 Materials and Methods

3.5.1 Animals

Zebrafish were kept at 26-28 °C on a 14/10 hr light/dark cycle. Transgenic *gfap:gfp* (Kassen et al., 2007) and *1016 tuba1a:gfp* (Fausett and Goldman, 2006; Powell et al., 2012)

fish have been described previously. Fish were harvested by treatment with a lethal dose of tricaine methane sulfonate (Sigma). Only adult fish (>2.5 months of age) were used in this study. To estimate the background variation between the *gfap:gfp* and *1016 tuba1:gfp* lines (while they have been maintained for multiple generations by breeding with the same wt fish, they may have been generated in different zebrafish backgrounds) we used the RRBS sequencing data (see below) to call SNPs relative to the reference genome and quantify the percentage of positions at which the strains share SNPs versus where they are polymorphic. To call SNPs we mapped pooled reads from MG and 4dpi samples to the Zv9 reference genome using the Burrows-Wheeler Aligner (BWA) (Li and Durbin, 2009), deduplicated using Picard's MarkDuplicates function (Li et al., 2009) and called variants with SAMtools mpileup function (Li et al., 2009). We filtered indels, low-coverage calls, and variants that might be the result of bisulfite treatment (C-to-T, T-to-C, and their complements). Using this methodology we identified 5,982 SNPs relative to the reference genome. 347 (5.8%) of which were also polymorphic between the two lines. By contrast, different zebrafish strains have been reported to have between 29.9% and 64.2% polymorphic SNPs (Stickney et al., 2002). This confirmed that the background of the *gfap:gfp* and the *1016 tuba1:gfp* lines is highly homologous.

Mice were harvested by treatment with a lethal dose of isoflurane (VetOne). 7 week old, C57BL/6 female mice were used in this study. Fish and Mice were handled in accordance with the University of Michigan Committee on Use and Care of Animals.

3.5.2 Retina Injury, Morpholino-Mediated Gene Knockdown, and Drug Delivery

Retina lesions have been described previously (Fausett and Goldman, 2006; Powell et al., 2012). Briefly, fish were anesthetized in 0.02% tricaine methane sulfonate (Sigma) and under microscopic visualization eyes were gently rotated in their sockets and stabbed through the sclera with a 30-gauge needle to the depth of the bevel. Lissamine-tagged morpholino antisense oligonucleotides (MOs) (Gene Tools) were delivered at the time of injury by using a Hamilton syringe. MO delivery to cells was facilitated by electroporation as described (Powell et al., 2012). The control, *apobec2a*, and *apobec2b* targeting MOs were described previously (Rai et al., 2008; Powell et al., 2012). The *apobec2a* and *apobec2b* (*apobec2a,2b*) MOs were injected in combination at a working concentration of 0.25 mM

(0.125 mM of each) (Powell et al., 2012) and compared to injections of 0.25 mM control MO. 5-Aza-2'-deoxycytidine (Sigma) was resuspended in sterile water to a concentration of 20 mM and aliquoted to avoid multiple freeze thaws. Aliquots were stored at -80° C. Fish were injected intraperitoneally with 20 µl of 20 mM stock daily (0-7dpi).

3.5.3 Fluorescence Activated Cell Sorting

GFP+ MG were purified from uninjured *gfap:gfp* and injured (4dpi), *1016 tuba1a:gfp* (12 lesions per eye) transgenic fish as described previously (Ramachandran et al., 2012). Negative populations were also obtained. GFP+, lissamine+ MG were purified by FACS of dissociated *gfap:gfp* transgenic fish retinas 2 days following administration of 0.25 mM lissamine-tagged control or *apobec2a,2b*-targeting MO (6 x 0.7 ml MO injections per eye, followed by 6 lesions post electroporation). Zebrafish retinas were collected in 0.8 mL Leibovitz's L15 medium, treated for 15 min with 1 mg/mL hyaluronidase (Sigma) at room temperature, and then dissociated in 0.01% (vol/vol) trypsin with frequent trituration. A single-cell suspension was confirmed by microscopy and cells were washed in Leibovitz's L15 medium before sorting.

Mouse retinas were collected in 0.8 mL Leibovitz's L15 medium and dissociated using the Neural Tissue Dissociation Kit (Miltenyi Biotec) according to the manufacturer's manual dissociation protocol. The cells were then stained with an anti-GLAST PE (ACSA-1) antibody (Miltenyl Biotec) as directed by the manufacturer (Jungblut et al., 2012). A single-cell suspension was confirmed by microscopy and cells were washed in Leibovitz's L15 medium before sorting. MG (PE+) and non-MG (PE-) cell populations were obtained. Cell sorting was performed by the University of Michigan Flow Cytometry Core on a BC Biosciences FACSAria 3 laser high-speed cell sorter.

3.5.4 RNA Isolation, RT-PCR, and Real-Time PCR

Total RNA was isolated using TRIzol (Invitrogen) and was DNase treated (Invitrogen). cDNA synthesis was performed by using random hexamers and SuperScript-II reverse transcriptase (Invitrogen). PCR reactions used Taq and gene-specific primers (Table 3.2). Real-time PCR reactions were carried out in triplicate with ABsolute SYBR Green Fluorescein Master Mix (Thermo Scientific) on an iCycler real-time PCR detection system

(Bio-Rad). The ΔΔCt method was used to determine relative expression of mRNAs in control and injured retinas and normalized to *gapdh* mRNA expression levels. Student T tests were performed to determine statistical differences between samples.

3.5.5 Tissue Preparation, Immunofluorescence, Tunel assay and Imaging

The eyes from adult zebrafish were enucleated, followed by the removal of the lens and immersion into fresh 4% paraformaldehyde in 0.1 M phosphate buffer, pH 7.4, for 3 h at room temperature. After fixation, tissues were cryoprotected in phosphate-buffered 20% sucrose for 6-12 h before embedding with Tissue-Tek O.C.T. compound (Sakura, Finetek). Embedded samples were kept frozen at -20 °C until they were sectioned to 12 microns on a CM3050S cryostat (Leica). Sections were collected on Superfrost/Plus slides (Fisher Scientific), dried and stored at -20 °C.

Immunofluorescence was performed as described previously (Ramachandran et al., 2010a) using the following primary antibodies: mouse anti-PCNA (dividing cell marker, 1:500, Sigma), rat anti-BrdU (dividing cell marker, 1:500, Abcam), rabbit anti-GFP (1:1000, Invitrogen), mouse anti-Zpr1 (red/green cones, 1:250, Invitrogen), mouse anti-GS (Müller glia, 1:500, Millipore), and mouse anti-HuC/D (1:300, amacrine and ganglion cells, Invitrogen). The following secondary antibodies were used: Alexa Flour 555 donkey anti-mouse IgG (1:1000, Invitrogen), Alexa Four 488 goat anti-rabbit IgG (1:1000, Invitrogen), Cy5 donkey anti-mouse (1:1000, Invitrogen), and Cy3 donkey anti-rat (1:1000, Jackson Immunoresearch). Antigen retrieval for PCNA and BrdU staining was performed by either boiling the sections in 10 mM sodium citrate for 20 min and cooling for another 20 min or treating the sections with 2 N HCl at 37°C for 25 min, followed by a rinse with 0.1 M sodium borate solution (pH 8.5) for 10 min.

Tunel assays were performed on slides treated for 20 min with Proteinase K (Roche) at 37 °C (10 ug/ml Proteinase K, 10 mM Tris-HCl pH 7.5). Slides were then analyzed for Tunel staining using the *In situ* Cell Death Detection Kit, Fluorescein (Roche).

Images were examined using a Zeiss Axiophot, Axio Observer Z.1. Images were captured using a digital camera adapted onto the microscope and were processed/annotated with Adobe Photoshop CS4. Student T tests were performed to determine statistical differences between samples.

3.5.6 DNA Isolation and Quantification

Genomic DNA was isolated using the Purelink Genomic DNA Mini Kit (Invitrogen) according to the manufacturer's recommendations. The time between the harvest and DNA isolation of any sample did not exceed 3 hrs. The quantity of dsDNA from each sample was measured using a Qubit 2.0 Fluorometer at the University of Michigan DNA Sequencing Core (UMDSC).

3.5.7 RRBS Library Preparation and Sequencing

RRBS library preparation was carried out with minor modifications to previously published methods (Gu et al., 2011). Briefly, genomic DNA samples (isolated from independent cell sorts) were digested for 4 hrs with MspI, purified, and end-repaired and A-tailed with Klenow fragment 3'->5' exo- (NEB). The samples were then purified and resuspended in TruSeq DNA Sample Preparation (Illumina) Resuspension Buffer and submitted to a second round of adenylation followed immediately by ligation to bar-coded Illumina adapters using the reagents and instructions of the Illumina TruSeq DNA Sample Preparation kit. The samples were then size selected on a 3% Nusieve 3:1 TBE gel and run at 5V/cm. Fragment sizes ranging from 160-340 bp (corresponding to 40-220 bp without adapter sequence) were excised from the gel and purified. Samples were then bisulfite converted using the EZ DNA Methylation-Direct Kit (Zymo), followed by amplification using PfuTurbo Cx Hotstart DNA Polymerase (Agilent) using the primers provided in the Illumina TruSeq DNA Sample Preparation kit. The libraries were then submitted to a second step of size selection on a 3% Nusieve 3:1 TBE gel, quality checked on an Agilent 2100 Bioanalyzer, DNA 1000 Tapestation and dsDNA quantified with a Qubit 2.0 Fluorometer. 50 ng of the final libraries were submitted for sequencing at the UMDSC. Two independent libraries were prepared for each time point, and 4 libraries were multiplexed in one lane for each sequencing reaction. Sequencing was performed on an Illumina HiSeq 2000 by the UMDSC. The starting template amount, multiplexing barcode, sequencing method, and the number of sequence reads for each sample are listed in Table 3.1. Detailed sequencing data is available on the GEO database (GSE50717).

3.5.8 RRBS Data Analysis

FASTQC (www.bioinformatics.babraham.ac.uk/projects/fastqc/) was used to determine initial quality metrics, and sequence trimming was performed to remove PCR primers, adapter sequences, and low-quality base calls using TRIM_GALORE (www.bioinformatics.babraham.ac.uk/projects/trim_galore/). The number of reads retained after trimming for each sample is listed in Table 3.1. FASTQC analysis post trimming showed elimination of low-quality positions, less enrichment of adapters, and a striking bias for C/TGG (or CAA for paired end) at the 5' end (over 80% of reads, as expected for RRBS) (Gu et al., 2011). Estimates of bisulfite conversion rates for each sample were determined using a modified TRIM_GALORE protocol based on a previously described approach (Krueger et al., 2012). All samples showed high bisulfite conversion rates (Figure 3.10E and 3.14C). In preparation for mapping, a zebrafish chromosomal genome (UCSC ZV9) index for BISMARK (Krueger and Andrews, 2011) was prepared. Experimental sample reads were then aligned to the genome index using BISMARK. Mapping efficiencies for each sample are listed in Table 3.1. The BISMARK script METHYLATION_EXTRACTOR was used to extract methylation calls for every C. CpG context files were processed using the MethylKit R package (Akalin et al., 2012) to compute statistics about individual samples (Figure 3.9, 3.10A-D, 3.13C-F, and 3.14A and B). Samples were filtered based on coverage so that positions with coverage below 5 and positions with coverage higher than the 99.9 percentile of coverage for that sample were discarded. Samples were then combined to perform analyses only at locations common between them. MethylKit was then used to identify locations of differential methylation using logistic regression to estimate p-values. The p-values were adjusted to q-values using the SLIM method. The differentially methylated positions reported in this study have a maximum q-value cutoff of 0.01 and a minimum methylation difference of 1 percent.

3.5.9 Basal Promoter Methylation Levels and Global Methylation Analysis

To calculate the basal promoter methylation levels, the methylation of all CpGs quantified by RRBS was averaged across defined promoter regions, 5 Kb upstream and 1.0 Kb downstream of the transcription start site (TSS). To compare the global methylation levels of the 2dpi *gfap:gfp* control MO and the 2dpi *gfap:gfp apobec2a,2b* MO samples, two analyses were performed. First, the overall methylation for each sample was determined

using every position call (CpG) to calculate the total number of Cs (not converted by bisulfite treatment, and thus methylated) compared to total calls (Figure 3.16G, columns T). Second, the overall methylation for each sample was determined using only positions covered in all samples to calculate the total number of Cs compared to total calls (Figure 3.16G, columns S). To test the hypothesis that there was no difference between the samples, the replicates were pooled to perform a Chi-square test.

3.5.10 Microarray Data Analysis

Statistics were performed using data from a previously published microarray dataset (Ramachandran et al., 2012) with the limma package in BioConductor (computes an empirical Bayes adjustment for the t-test) (Smyth, 2004). To correct for multiple testing, Benjamini and Hochber's method to control for false discovery rate (FDR) was used (Benjamini and Hochberg, 1995). Genes identified as differentially expressed had an FDR of 5% and change in expression larger than or equal to 2-fold (Figure 3.11F and G).

3.5.11 Bisulfite and Restriction PCR

Bisulfite PCR primer sets were designed using the BiSearch primer design tool and are listed in Table 3.2. gDNA was bisulfite treated using the EZ DNA Methylation-Direct Kit (Zymo), and target regions were amplified with bisulfite specific primers using PfuTurbo Cx Hotstart DNA Polymerase (Agilent). The amplicons were gel excised and cloned into pGEMT-Easy (Promega) and transformed into *E. coli.* 10 independent clones were selected for sequencing following miniprep using M13FOR and SP6 sequencing primers at the UMDSC. Restriction PCRs were performed following gDNA digestion (or mocks without digestions) with HpaII at 37 °C for 4 hrs (Figure 3.11 C and D), with McrBC at 37 °C for 2hrs (Figure 3.8H), or with an enzyme cocktail including HpaII, HpyCH4IV, and BstuI at 37 °C for 2 hrs and 60 °C for 30 min (Figure 3.5H and I; Figure 3.17A and B). Following digestion, gDNA was purified by phenol:chloroform, ethanol precipitated, and resuspended in ddH2O. Target regions were then amplified with site-specific primers (Table 3.2) using Phusion DNA Polymerase (NEB).

3.6 Acknowledgments

This work was supported by NEI Grants RO1 EY018132, 1R21 EY022707 (D.G.), and the University of Michigan Vision Research Training Grant 5T32EY13934-10 (C.P.). We thank the University of Michigan Flow Cytometry Core; the University of Michigan DNA Sequencing Core; the University of Michigan Bioinformatics Core; R. Karr for fish care; P. Macpherson for help with mice; members of the Goldman lab for helpful comments.

3.7 Figures

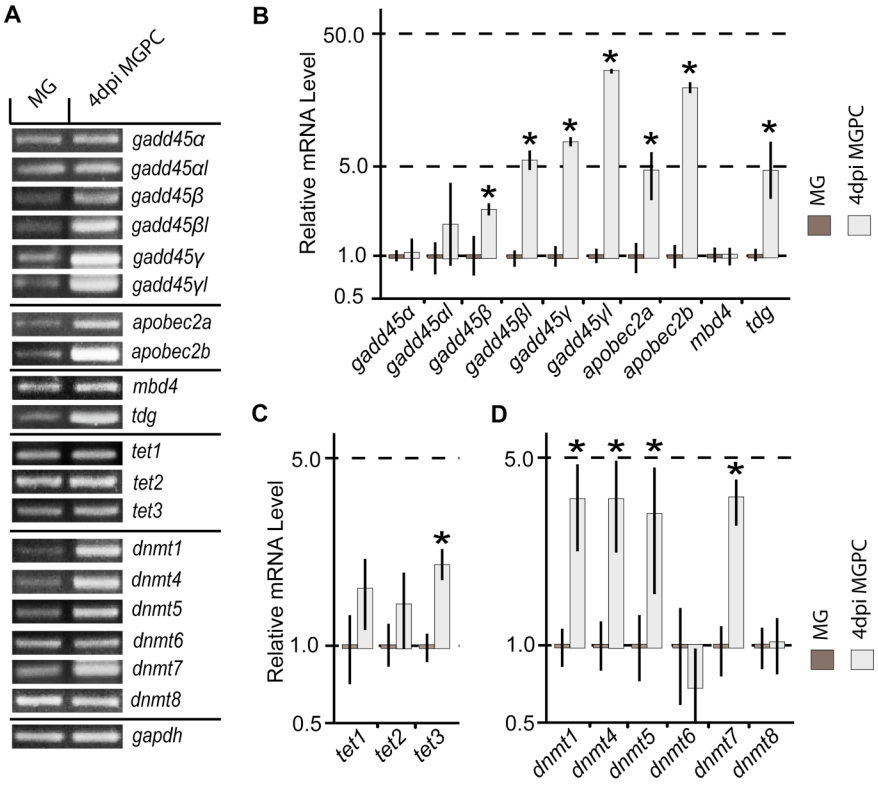

Figure 3.1 The transcript levels of potential regulators of DNA methylation are induced during MGPC formation

(A) RT-PCR gene expression comparisons of quiescent MG (*gfap:gfp*) and 4dpi MGPC (*1016 tuba1a:gfp*) cell populations targeting genes correlated with the regulation of DNA methylation. (B and C) Quantification of potential DNA demethylase mRNAs in (A) by qPCR. **P* < 0.02403. (D) Quantification of DNA methyltransferase mRNAs in (A) by qPCR. **P* < 0.04117.

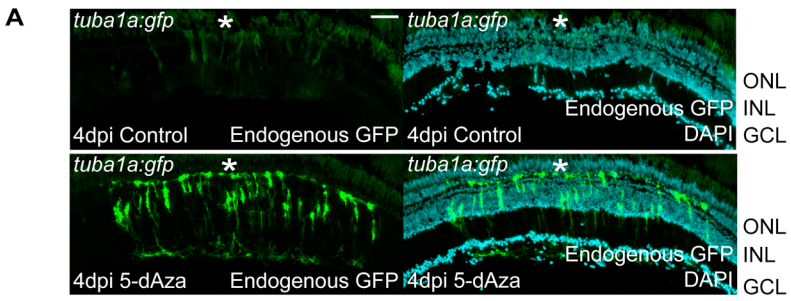
A
tuba1a:gfp
4dpi Control
Endogenous GFP
4dpi Control
DAPI
ONL
INL
GCL
4dpi 5-dAza

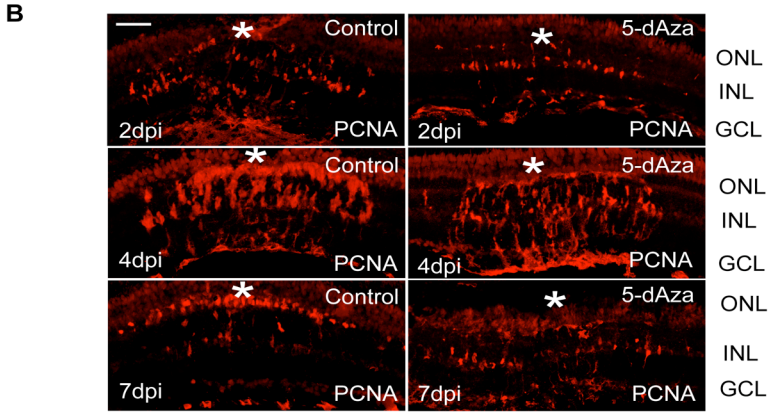
B
Control
5-dAza
2dpi
4dpi
7dpi
PCNA
ONL
INL
GCL

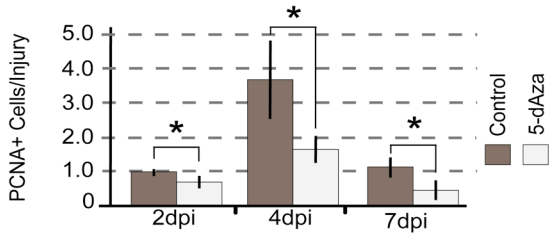
C
PCNA+ Cells/Injury
5.0
4.0
3.0
2.0
1.0
0
2dpi
4dpi
7dpi
Control
5-dAza

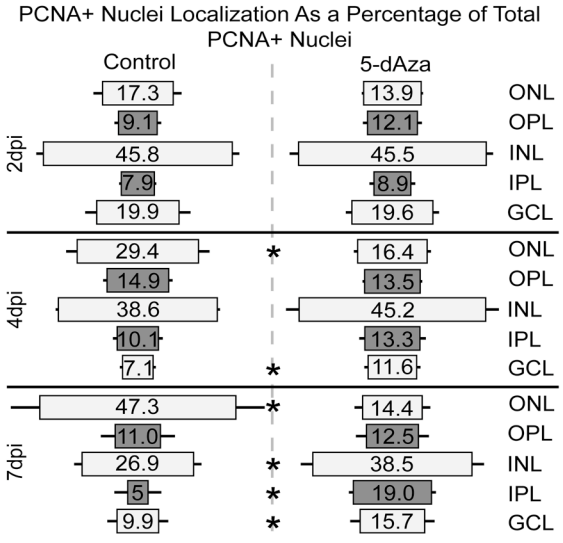
D
PCNA+ Nuclei Localization As a Percentage of Total PCNA+ Nuclei
Control
5-dAza
2dpi
17.3
9.1
45.8
7.9
19.9
13.9
12.1
45.5
8.9
19.6
4dpi
29.4
14.9
38.6
10.1
7.1
16.4
13.5
45.2
13.3
11.6
7dpi
47.3
11.0
26.9
5
9.9
14.4
12.5
38.5
19.0
15.7
ONL
OPL
INL
IPL
GCL

Figure 3.2 Inhibition of Dnmts suggests that the regulation of DNA methylation is important for MG reprogramming

(A) 4dpi *1016 tuba1a:gfp* transgenic fish treated with 5-dAza show increased levels of endogenous (unstained) GFP. (B) 5-dAza inhibits the generation of and localization of PCNA+ MGPCs. (C) Quantification of PCNA+ nuclei per injury site. The value is normalized to the value of 2dpi control. *$P < 0.02873$. (D) Graphic depicting the localization of PCNA+ nuclei within the retina at the indicated time points. 5-dAza perturbs the localization of PCNA+ nuclei at 4 and 7dpi. Lines extending from the box represent error. *$P < 0.04128$. ONL, outer nuclear layer; OPL, outer plexiform layer; INL, inner nuclear layer; INL, inner plexiform layer; GCL, ganglion cell layer. Scale bars, 50 μm.

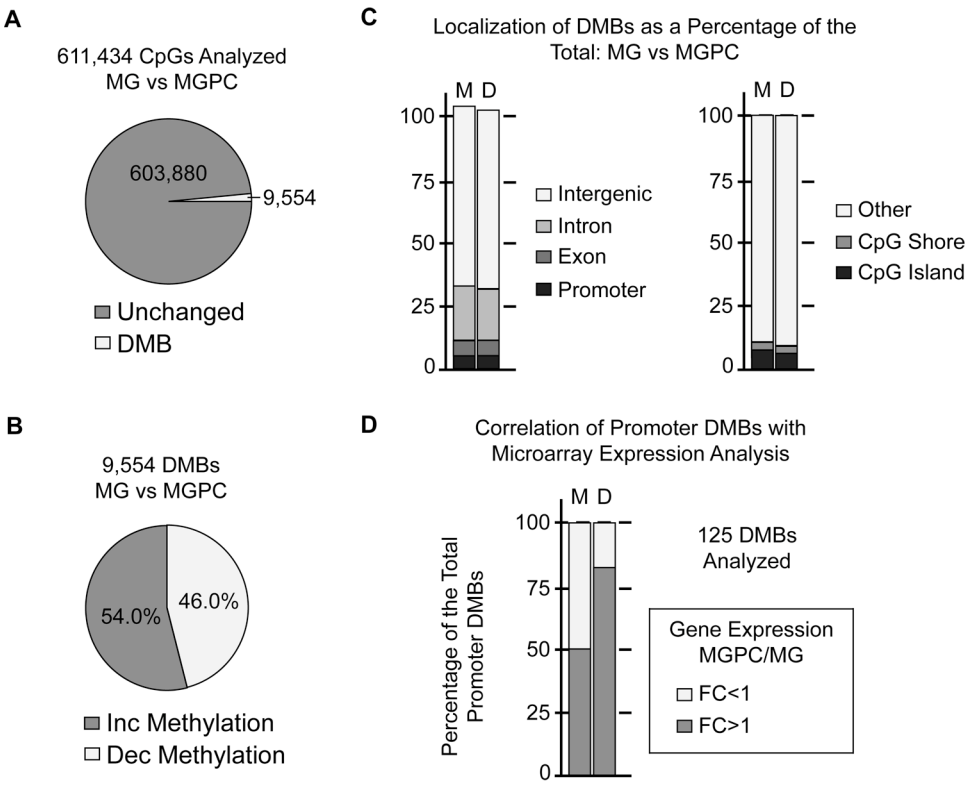

Figure 3.3 Site-specific regulation of DNA methylation accompanies MG reprogramming

(A, B, and C) RRBS comparison of quiescent MG (*gfap:gfp*) and 4dpi MGPCs (*1016 tuba1a:gfp*). Quantification (A) and classification (B) of DMBs. (C) Localization of DMBs by type: M, methylated; D, demethylated (some DMBs fall into multiple classes so the total exceeds 100%). Most DMBs are localized to intergenic, CpG-poor regions. (D) Correlation of RRBS promoter DMBs with previously obtained microarray gene expression data (Ramachandran et al., 2012). Classification of DMBs by their localization to gene promoters increasing (FC>1) or decreasing (FC<1) expression during MG reprogramming. No correlation is seen between gene expression and DMBs that are increasing methylation (**M**), while a correlation is seen between increased gene expression and DMBs that are decreasing methylation (**D**). DMB, differentially methylated base; FC, fold change. Promoters were defined as 5 Kb upstream and 1.0 Kb downstream of TSS.

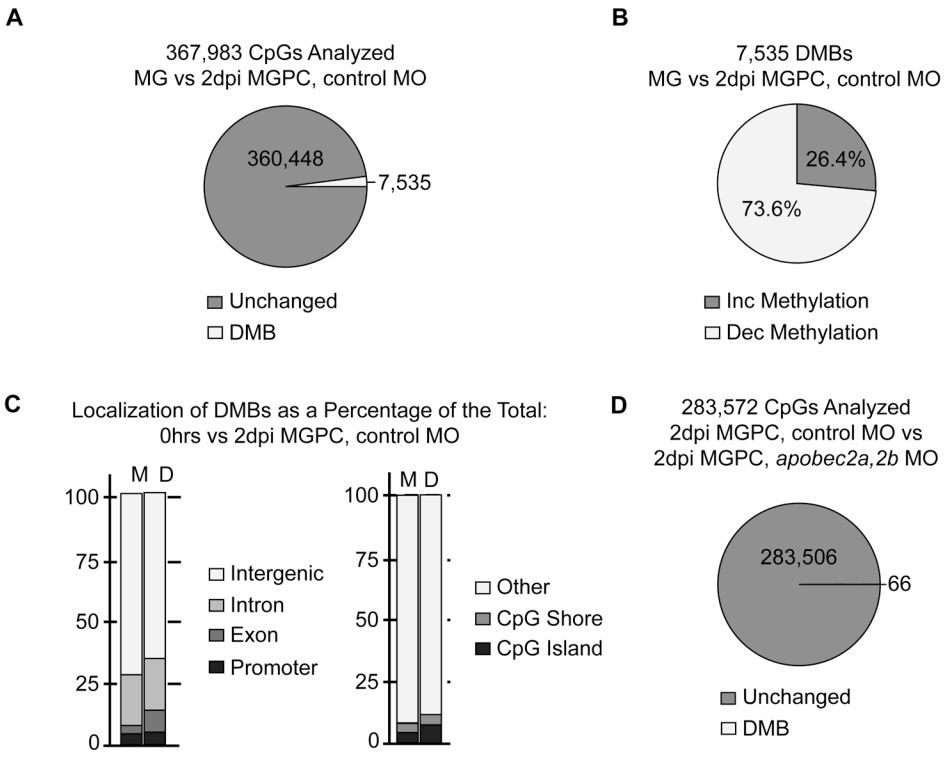

Figure 3.4 Site-specific, active DNA demethylation predominates at 2dpi and is independent of Apobec2a,2b

(A, B, and C) RRBS comparison of quiescent MG (*gfap:gfp*) and 2dpi MGPCs treated with control MO. Quantification (A), classification (B), and (C) localization of DMBs as performed in Figure 3.2. DNA methylation is regulated by 2dpi (incipience of MG proliferative response) suggesting that these changes are actively made (Fausett and Goldman, 2006). Most DMBs are localized to intergenic, CpG-poor regions. **(**D) RRBS comparison of 2dpi MGPCs treated with control or *apobec2a,2b* MO indicates that the knockdown of Apobec2a,2b does not impact site-specific DNA demethylation. Abbreviations are as in Figure 3.3.

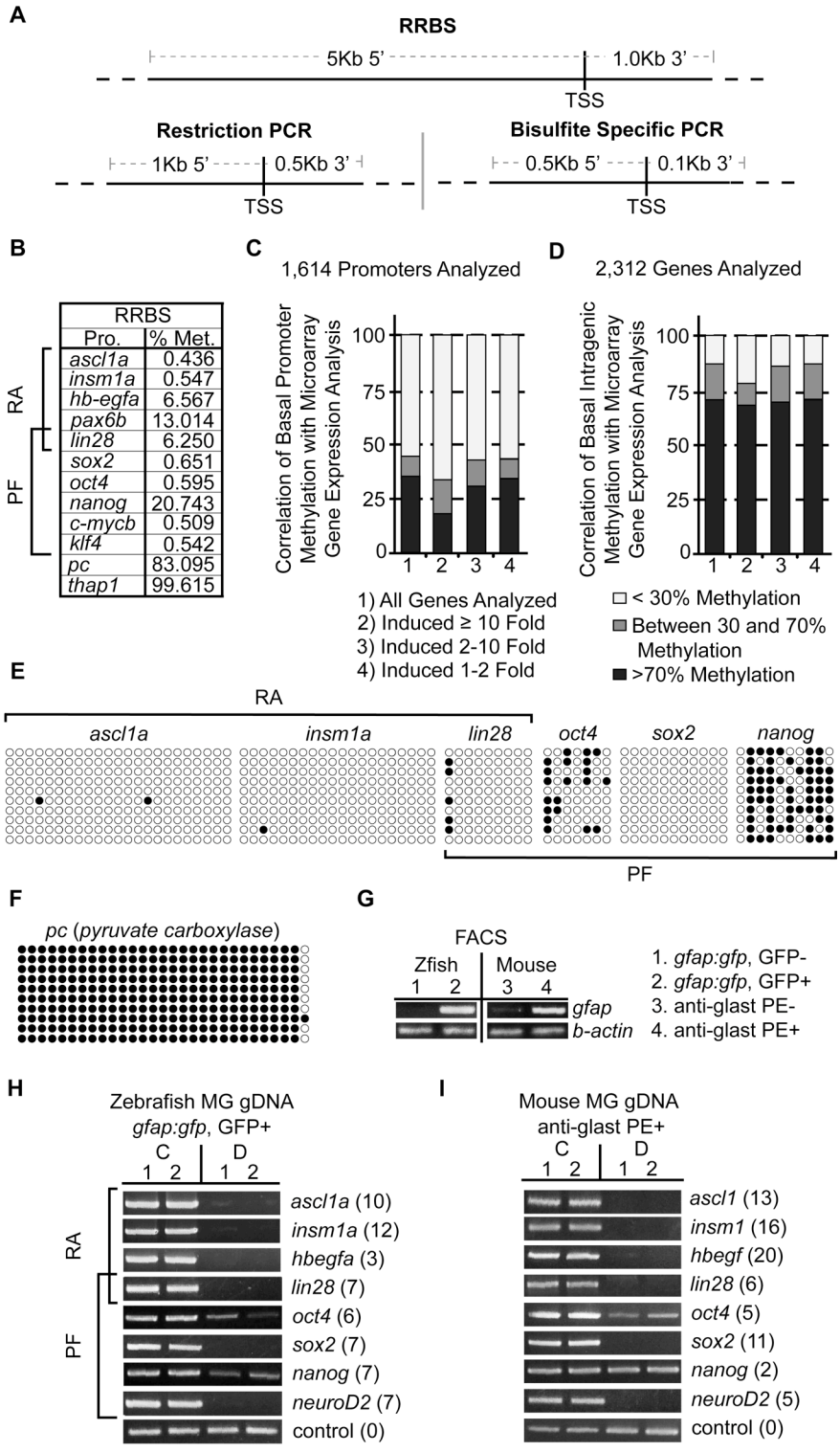

Figure 3.5 MG basal DNA methylation profile suggests that they are to an extent poised for a rapid regenerative response

(A) Graphic depicting target regions analyzed by RRBS, bisulfite PCR, and restriction PCR. (B) Average promoter methylation levels calculated using quiescent MG RRBS data indicate that many pluripotency factor (PF) and regeneration-associated (RA) genes have low basal methylation levels. (C and D) Correlation of basal promoter methylation levels with microarray gene expression data indicates that highly induced genes have lower than average promoter (C) and intragenic (D) methylation levels. (E and F) Bisulfite PCR analysis of promoters regions characterized as having low (E) or high (F) basal methylation levels by RRBS. Each horizontal line of circles represents an independent clone. Filled and unfilled circles represent methylated and unmethylated cytosines, respectively. (G) Validation of MG enrichment following FACS of zebrafish *gfap:gfp* transgenic fish retinas (GFP- and GFP+ populations) and mouse retinas (anti-GLAST PE- and anti-GLAST PE+ populations) using RT-PCR. (H) Zebrafish promoter restriction PCR following genomic digest with HpaII, HpyCH4IV, and BstuI (**D**) or mock/control, undigested (**C**) using MG (*gfap:gfp*, GFP+) gDNA. The number of potential restriction cut sites is indicated next to each target name. (I) Restriction PCR was carried out as in *H* using mouse MG (anti-GLAST PE+) gDNA. PF and RA gene promoters of both zebrafish and mouse MG appear to be lowly methylated. TSS, transcription start site.

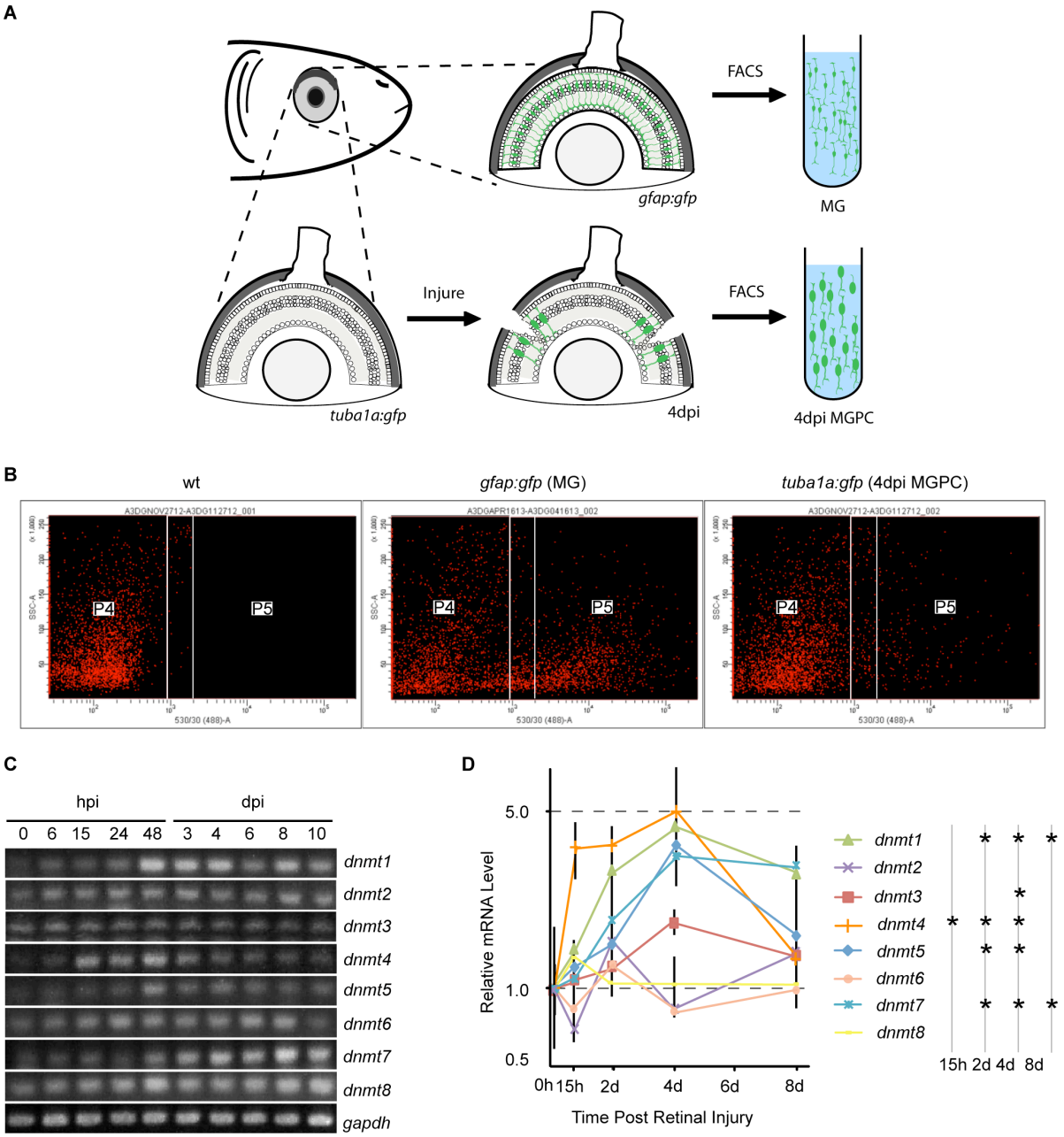

Figure 3.6 Poke model, FACS, and gene expression comparisons

(A) Graphic depicting the method of targeted cell population isolation. (B) Representative scatter plots used to FACS-purify GFP-expressing cells. Wild-type (wt) retinal cells do not fall into the P5 window, whereas GFP+ retinal cells from *gfap:gfp* and *1016 tuba1a:gfp* transgenic fish retinas readily sort into this window. P4 and P5 are arbitrary names assigned to the cell sorting windows. (C) RT-PCR using cDNA prepared from whole retinas harvested at the indicated time points shows the injury-dependent regulation of DNA

methyltransferases. (D) Quantification of select time points from C by quantitative PCR. *P < 0.04092. Error bars represent standard deviation. hpi, hours post injury; MGPC, Müller glia progenitor cell.

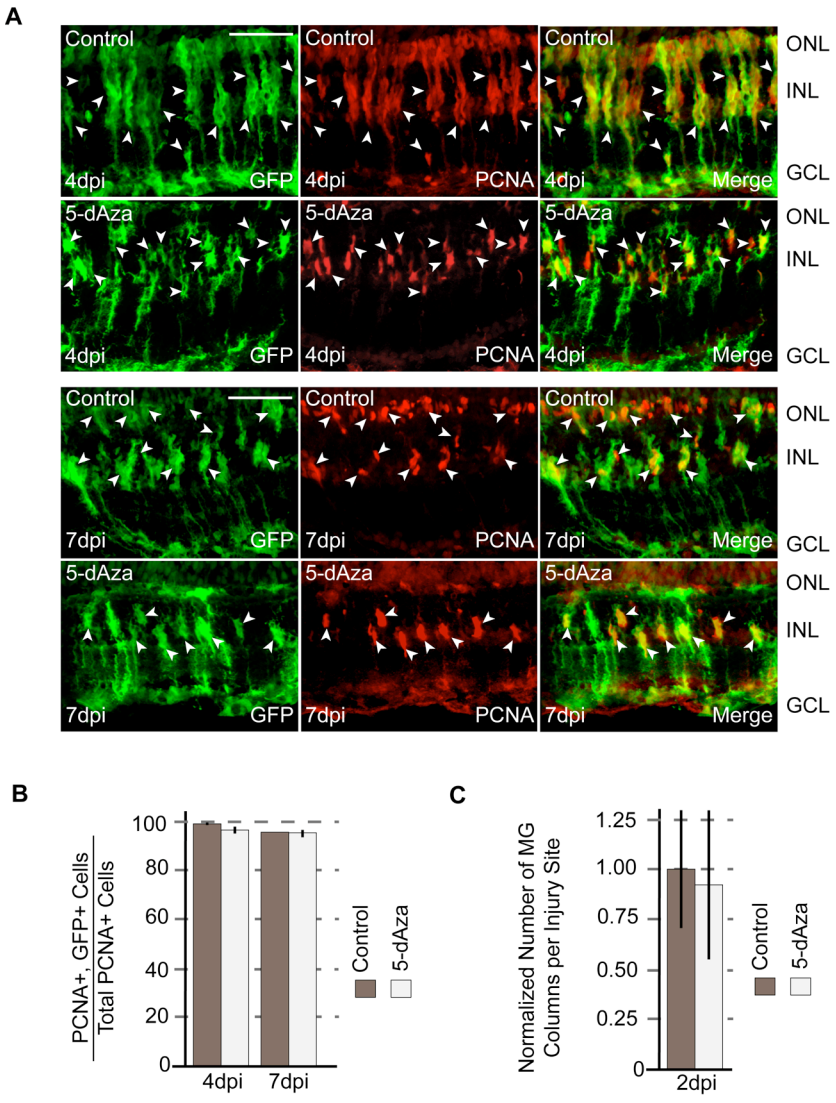

Figure 3.7 Inhibition of Dnmts results in genomic hypomethylation and impacts MGPC migration and differentiation

(A) Both control and 5-dAza-treated (daily intraperitoneal injection with 20 µl of 20 mM 5-dAza) *1016 tuba1a:gfp* transgenic fish have a high correlation between PCNA+ and GFP+ cells at 4 and 7dpi. (B) Quantifications of *A*. (C) Quantification of the number of MGPC columns that form per injury site 2dpi as an indication of the number of MG that are responding with a proliferative response. ONL, outer nuclear layer; INL, inner nuclear layer; GCL, ganglion cell layer; dpi, days post injury; Scale bars, 50 µm.

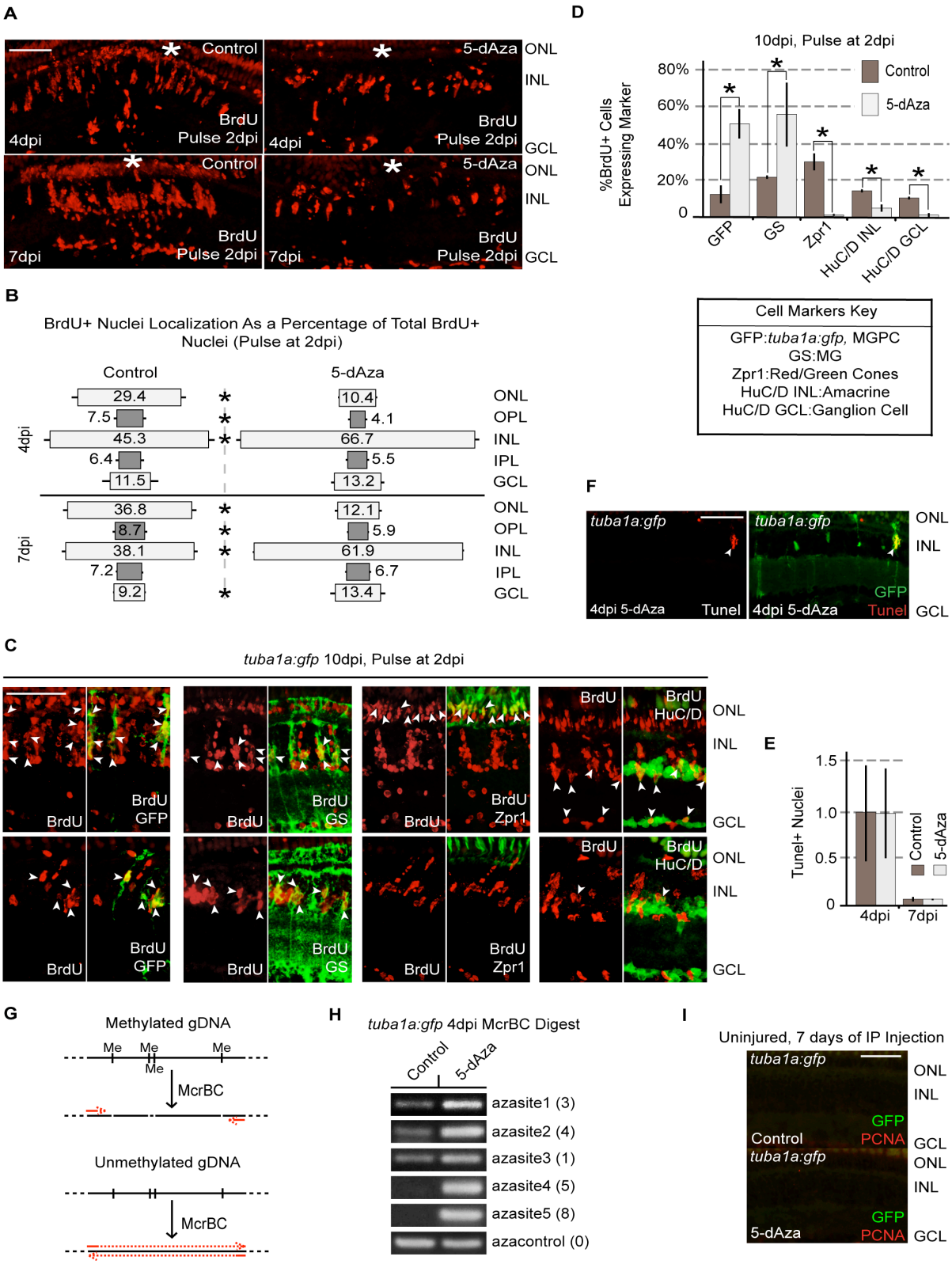
A
Control
5-dAza
BrdU
Pulse 2dpi
4dpi
7dpi
ONL
INL
GCL
B
BrdU+ Nuclei Localization As a Percentage of Total BrdU+ Nuclei (Pulse at 2dpi)
Control
5-dAza
4dpi
7dpi
29.4
7.5
45.3
6.4
11.5
36.8
8.7
38.1
7.2
9.2
10.4
4.1
66.7
5.5
13.2
12.1
5.9
61.9
6.7
13.4
ONL
OPL
INL
IPL
GCL
D
10dpi, Pulse at 2dpi
%BrdU+ Cells Expressing Marker
80%
60%
40%
20%
0
Control
5-dAza
GFP
GS
Zpr1
HuC/D INL
HuC/D GCL
Cell Markers Key
GFP:tuba1a:gfp, MGPC
GS:MG
Zpr1:Red/Green Cones
HuC/D INL:Amacrine
HuC/D GCL:Ganglion Cell
F
tuba1a:gfp
4dpi 5-dAza
Tunel
GFP
ONL
INL
GCL
C
tuba1a:gfp 10dpi, Pulse at 2dpi
BrdU
BrdU GFP
BrdU GS
BrdU Zpr1
BrdU HuC/D
E
Tunel+ Nuclei
1.5
1.0
0.5
0
Control
5-dAza
4dpi
7dpi
G
Methylated gDNA
Me
McrBC
Unmethylated gDNA
H
tuba1a:gfp 4dpi McrBC Digest
Control
5-dAza
azasite1 (3)
azasite2 (4)
azasite3 (1)
azasite4 (5)
azasite5 (8)
azacontrol (0)
I
Uninjured, 7 days of IP Injection
tuba1a:gfp
Control
5-dAza
GFP
PCNA
ONL
INL
GCL

Figure 3.8 Inhibition of Dnmts results in genomic hypomethylation and impacts MGPC migration and differentiation

(A, B, C, and D) Fish treated with control or 20 mM 5-dAza were given a pulse of BrdU (20 μl IP injection of 20 mM BrdU) at 2dpi. The BrdU+ cells were then traced. (A) 5-dAza treatment blocks the migration of BrdU+ cells. (B) Quantifications of (A). Lines extending from the box represent error. $*P < 0.03600$. (C) Treatment with 5-dAza blocks MGPC differentiation as determined by co-labeling with cell specific markers. (D) Quantifications of (C). $*P < 0.02730$. (E) 5-dAza treatment did not significantly increase the number of Tunel+ cells at the injury site at 4 or 7dpi. (F) While the total number of Tunel+ cells did not change, on rare occasions, a *1016 tuba1a:gfp*, GFP+ cell would stain for Tunel following 5-dAza treatment. This was not noted in the control and indicates that 5-dAza is weakly cytotoxic to MG. (G) Design of restriction PCR following genomic digestion with McrBC which selectively cleaves methylated DNA. (H) gDNA was isolated from FACS purified GFP+ retinal cells isolated from 4dpi *1016 tuba1a:gfp* transgenic fish treated with either control vehicle or 20 mM 5-dAza. Restriction PCR was then carried out following genomic digest with McrBC. Locations were chosen based on high genomic methylation levels as determined by RRBS (Figure 3.9 and 3.10). The number of potential McrBC cut sites for each amplicon is indicated in parentheses. These results confirm that treatment with 5-dAza induces hypomethylation of MGPCs. (I) Uninjured fish injected for five consecutive days with either vehicle or 5-dAza showed no increase in GFP or PCNA staining. ONL, outer nuclear layer; INL, inner nuclear layer; GCL, ganglion cell layer; dpi, days post injury; MG, Müller glia; MGPC, Müller glia progenitor cell. Scale bars, 50 μm.

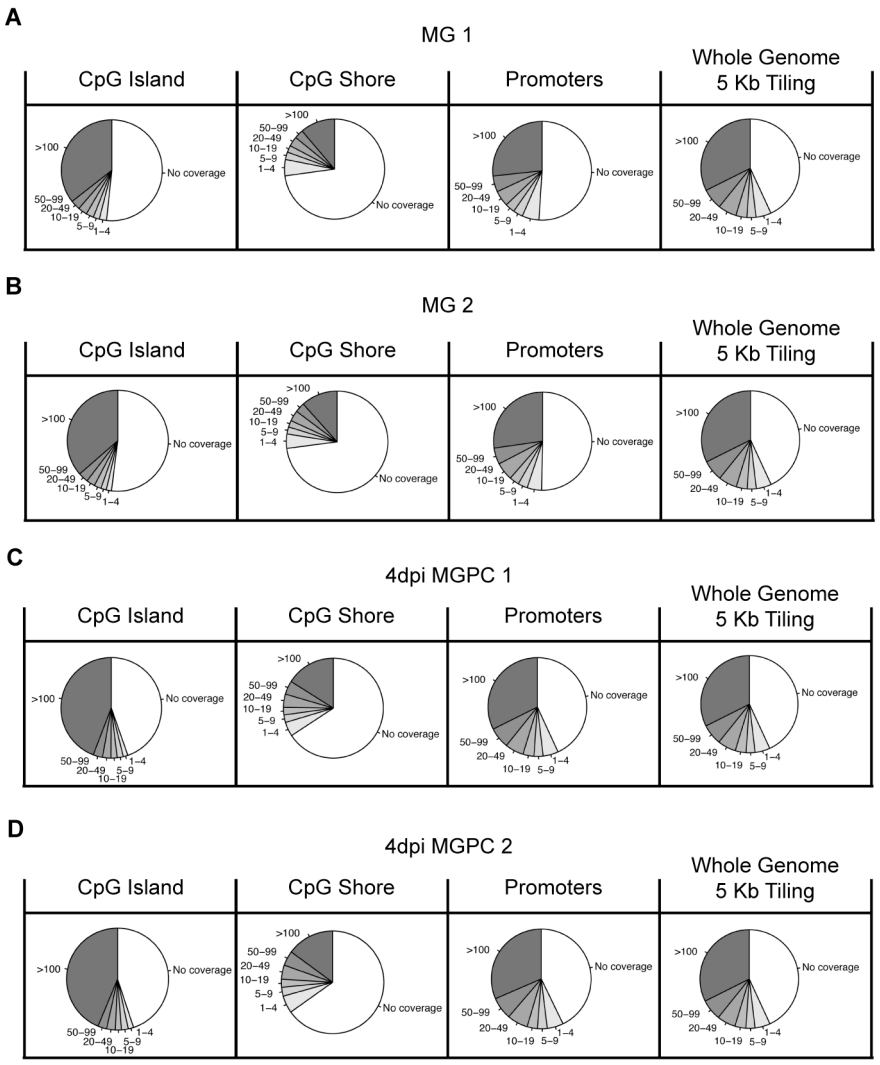

Figure 3.9 MethylKit analysis of *gfap*:*gfp* (MG) and 4dpi *1016 tuba1a*:*gfp* (4dpi MGPC) RRBS libraries

(A, B, C, and D) Experimental coverage of the indicated libraries.

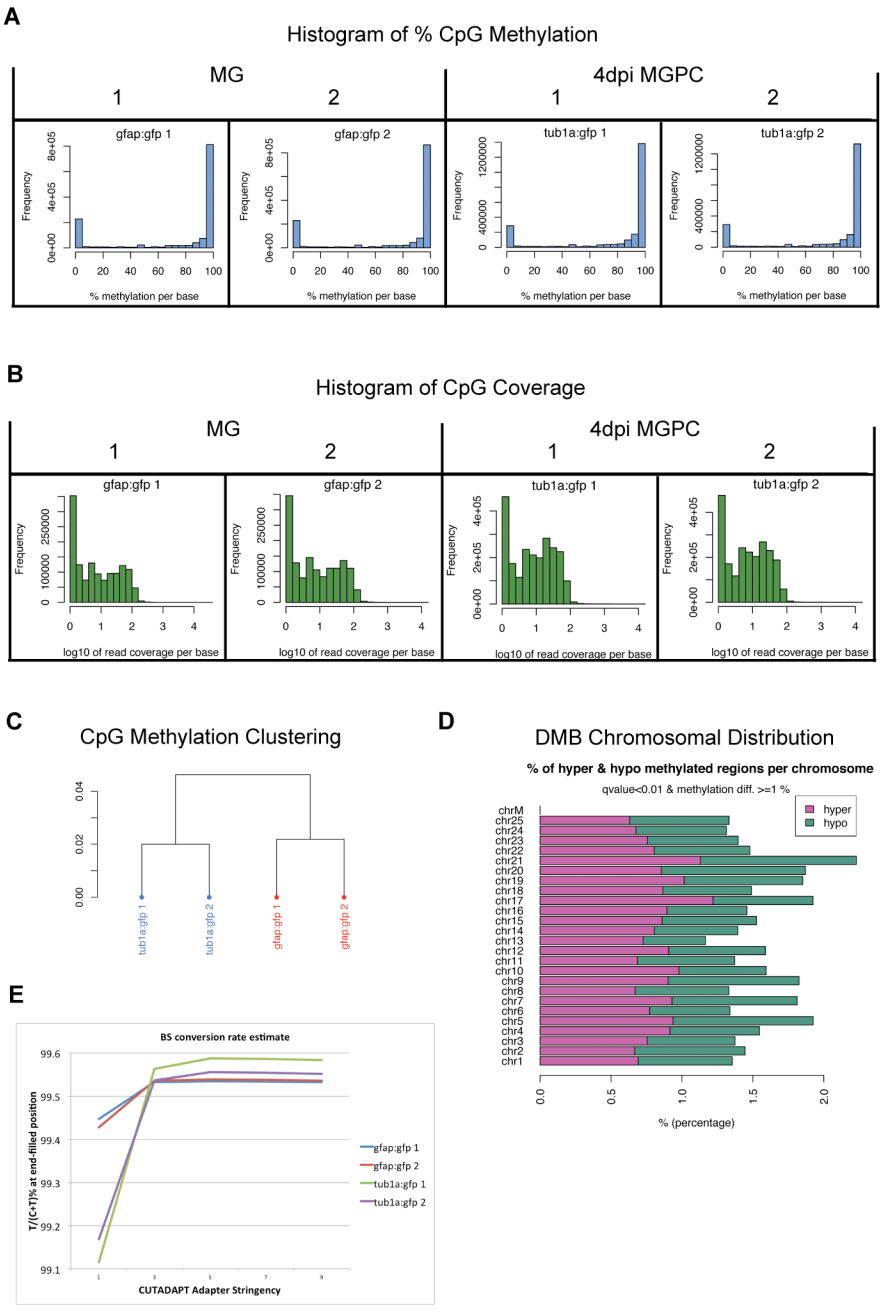

Figure 3.10 MethylKit analysis of *gfap*:*gfp* (MG) and 4dpi *1016 tuba1a*:*gfp* (4dpi MGPC) RRBS libraries, continued

(A) Histograms of percent CpG methylation for each library. These histograms should (and do) have two peaks on both ends; any given CpG will or will not be methylated in a cell. (B) Histograms of CpG coverage for each sample. PCR duplication problems occurring during final library amplification will be manifest by secondary peaks towards the right side of the histogram. The samples did not show noticeable duplication problems. (C) Dendogram of samples clustered according to their methylation profiles. Replicates cluster

together. (D) Chromosomal distribution of DMBs, showing percentages of hypo/hypermethylated bases over all covered positions of a given chromosome. (E) Estimation of bisulfite conversion rates for each library (Gu et al., 2011).

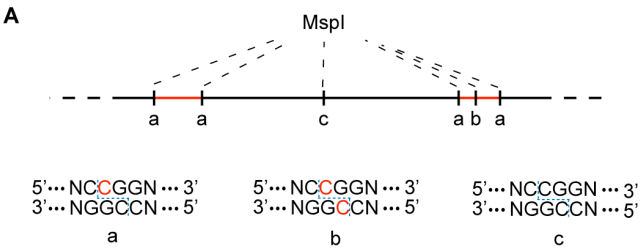

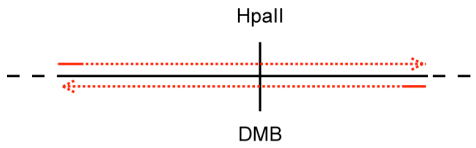

B

Sample	Cut Type	Base ID	% Me MG 1	% Me MG 2	% Me 4dpi MGPC 1	% Me 4dpi MGPC 2	Fold Diff
mesite1	a	chr11.18126837	0.00	0.00	100.00	100.00	1E+08
mesite2	b	chr16.56171078	9.38	7.32	70.00	52.94	7.37
		chr16.56171079	8.57	4.65	73.02	53.06	9.53
mesite3	b	chr19.25838912	2.86	10.53	40.74	45.45	6.44
		chr19.25838913	5.56	6.67	66.67	57.89	10.19
mesite4	a	chr16.44907805	30.00	29.03	72.41	84.85	2.66
mesite5	b	chr21.44117213	40.91	18.75	91.67	68.75	2.69
		chr21.44117214	32.00	27.27	85.00	61.90	2.48
mesite6	a	chr13.17805288	9.09	4.76	70.00	64.29	9.69
dmesite1	a	chr25.20672952	91.67	97.83	37.04	44.00	2.34
dmesite2	b	chr3.8384686	94.12	89.66	8.33	45.00	3.45
		chr3.8384687	82.05	77.88	21.43	34.48	2.86
dmesite3	a	chr3.58429271	96.15	100.00	23.26	20.00	4.53
dmesite4	b	chr1.59980835	82.35	86.11	19.05	11.11	5.59
		chr1.59980836	88.89	65.63	12.00	8.00	7.73
dmesite5	a	chr6.19595717	100.00	81.25	8.33	25.00	5.44
dmesite6	b	chr8.41635362	98.06	94.37	59.76	63.24	1.56
		chr8.41635363	96.30	88.46	12.82	28.21	4.50
dmesite7	b	chr17.167647	100.00	85.71	3.85	35.29	4.74
		chr17.167648	90.91	94.92	42.11	62.75	1.77

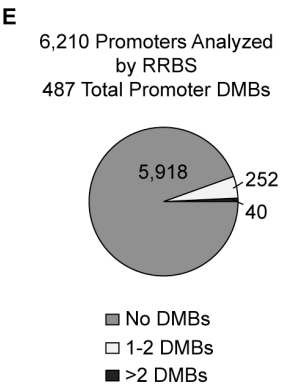

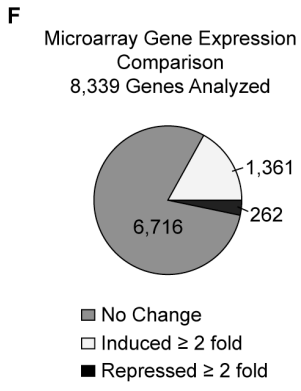

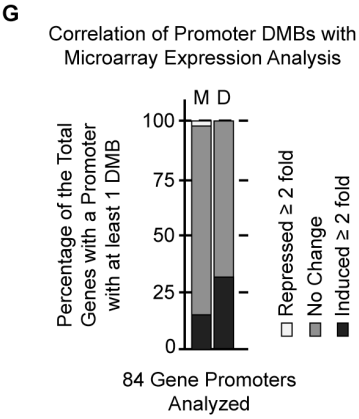

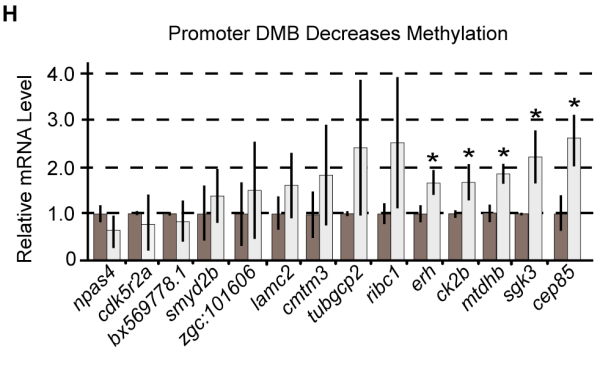

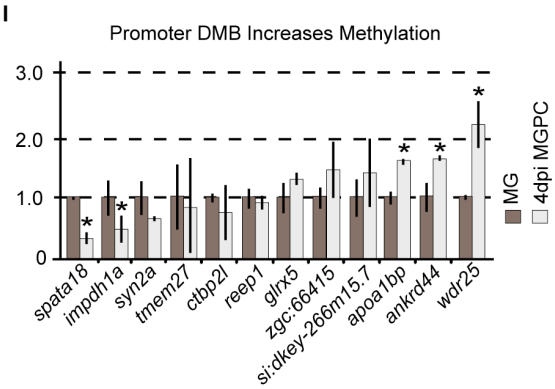

Figure 3.11 Validation of the DMBs identified by RRBS and correlation of RRBS promoter DMBs with microarray gene expression data

(A) Graphic classifying three possible MspI cut sites. Red lines depict fragment sizes selected by RRBS. Because of this selection, regions with few MspI restriction sites (CpG poor regions, large fragments) are not included in the RRBS library (c). Some sites will contain a read from one of the two possible methylated cytosines (a) and others will be read at both cytosine positions (b). Cytosines analyzed by RRBS are shown in red. (B) RRBS data of DMBs analyzed by restriction PCR. (C) Graphic depicting the design of site-specific restriction PCR using the methylation-sensitive restriction enzyme HpaII that cleaves the same consensus sequence as MspI. (D) Site-specific restriction PCR shows that the RRBS data is highly reproducible. The control is a region that doesn't contain an HpaII restriction site. (E) Classification of all promoters analyzed by RRBS. (F) Overview of data generated from a previous microarray gene expression comparison of quiescent MG (*gfap:gfp*) and 4dpi MGPCs (*1016 tuba1a:gfp*). (G) Correlation of promoter DMBs with the microarray gene expression comparison. Classification of genes whose promoter contains at least one DMB that is being methylated (M) or demethylated (D) by their changes in expression during MG activation. (*H* and *I*) Expression comparisons of quiescent MG (*gfap:gfp*) and 4dpi MGPCs (*1016 tuba1a:gfp*) performed by qPCR targeting genes whose promoter contains: (H) at least one DMB that is decreasing methylation (**P* < 0.02046) and (I) at least one DMB that is increasing methylation (**P* < 0.03623). A correlation is seen with decreased methylation and increased expression. Mesite, methylated site; dmesite, demethylatated site; DMB, differentially methylated base. Other abbreviations as in Figure 3.8.

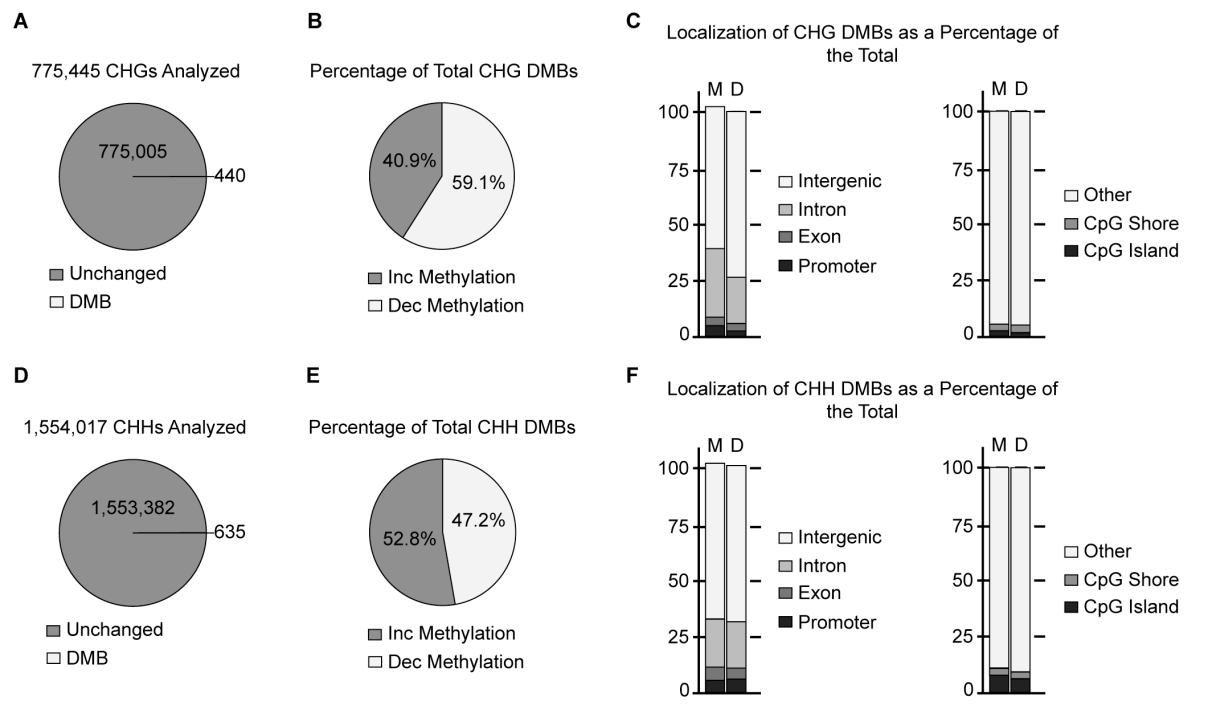

Figure 3.12 Non-CpG methylation changes seen in RRBS comparison of quiescent MG and 4dpi MGPCs

Quantification (A and D), classification (B and E), and localization (C and F) of DMBs within the CHG and CHH contexts, respectively. Abbreviations as in Figure 3.7.

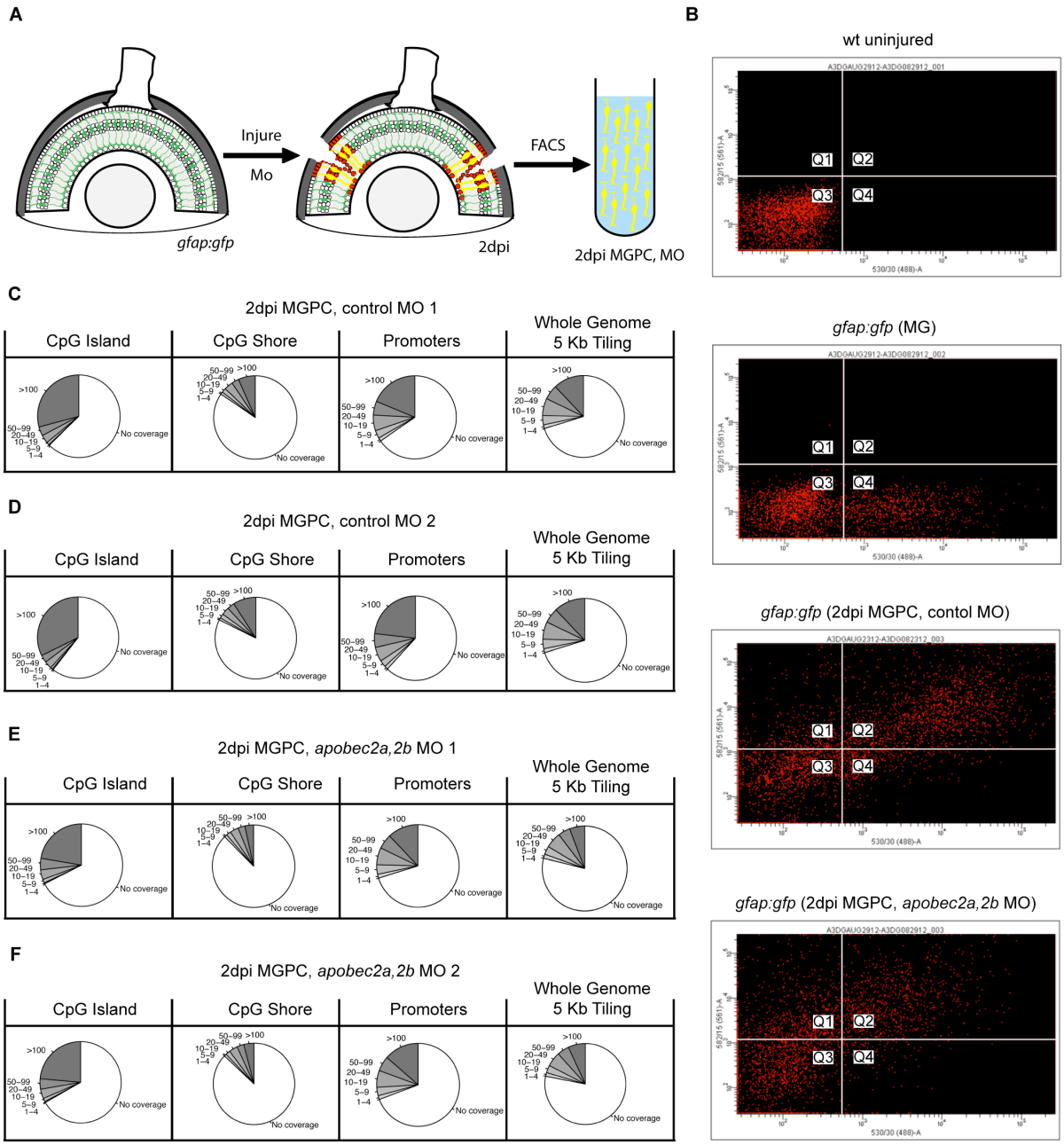

Figure 3.13 FACS and MethylKit analysis of 2dpi MGPC, control MO and 2dpi MGPC, *apobec2a,2b* MO RRBS libraries

(A) Graphic depicting method of targeted cell population isolation. (B) Representative scatter plots used to FACS purify lissamine+, GFP-expressing cells. Wild type (Wt) and uninjured *gfap:gfp* retinal cells do not fall into the Q2 window, whereas lissamine+, GFP+ retinal cells from 2dpi *gfap:gfp* fish treated with control or *apobec2a,2b* MO readily sort into this window. (C, D, E, and F) Experimental coverage of the indicated libraries.

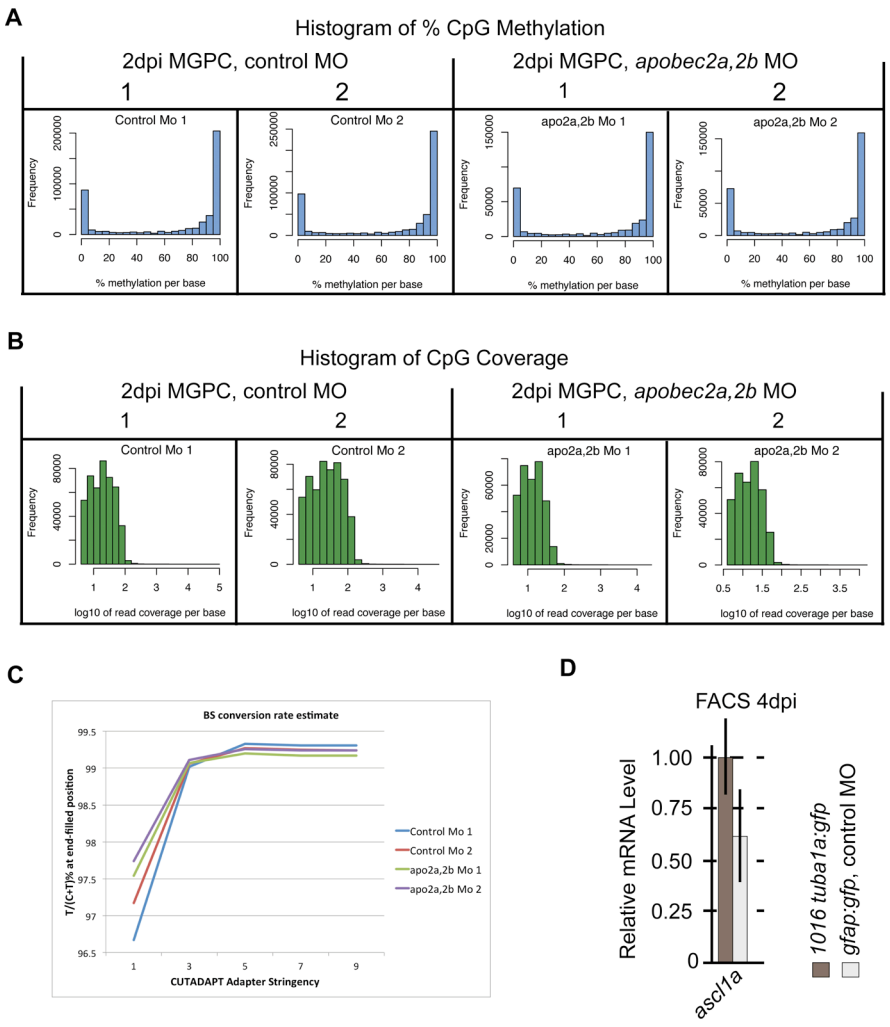

Figure 3.14 MethylKit analysis of 2dpi MGPC, control MO and 2dpi MGPC, *apobec2a,2b* MO RRBS libraries, continued

(A and B) MethylKit analyses of 2dpi MGPC, control MO and 2dpi MGPC, *apobec2a,2b* MO RRBS libraries as done in Figure 3.10. (C) Estimation of bisulfite conversion rates for each library (Gu et al., 2011). (D) *ascl1a* expression comparisons of 4dpi GFP+ (*1016 tuba1a:gfp*) and 4dpi GFP+, lissamine+ (*gfap:gfp*, control MO) cell populations. Because *ascl1a* expression is specific to MGPCs at 4dpi, we can use this expression comparison as a metric to determine the percentage of cells isolated in the *gfap:gfp*, control MO sort that are MGPCs (as this sort will isolate all MG that have MO, not necessarily only those responding to injury). In this way we estimate that ~60% of the cells isolated in the *gfap:gfp*, MO sorts are MGPCs.

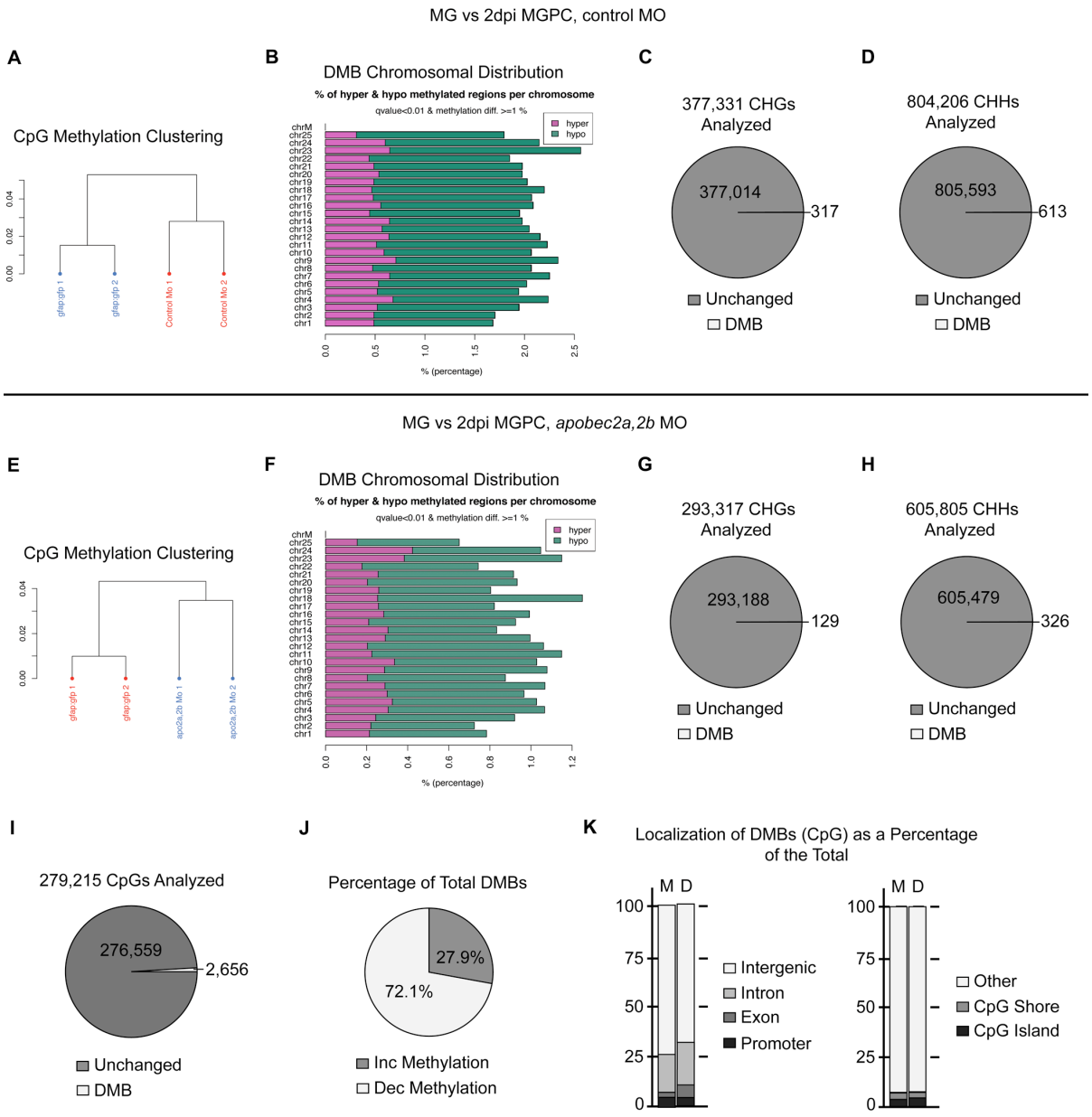

Figure 3.15 MO RRBS library comparisons

(A, B, C, and D) Comparisons of MG and 2dpi MGPC, control MO RRBS libraries. (A and B) MethylKit comparisons as done in Figure 3.10. (C and D) Quantification of DMBs within the CHG (C) and CHH (D) contexts. (E, F, G, H, I, J and K) Comparisons of MG and 2dpi MGPC, *apobec2a,2b* MO RRBS libraries. (E and F) MethylKit comparisons as done in Figure 3.10. (G and H) Quantification of DMBs within the CHG (G) and CHH (H) contexts. Quantification (I), classification (J), and localization (K) of DMBs within the CpG context.

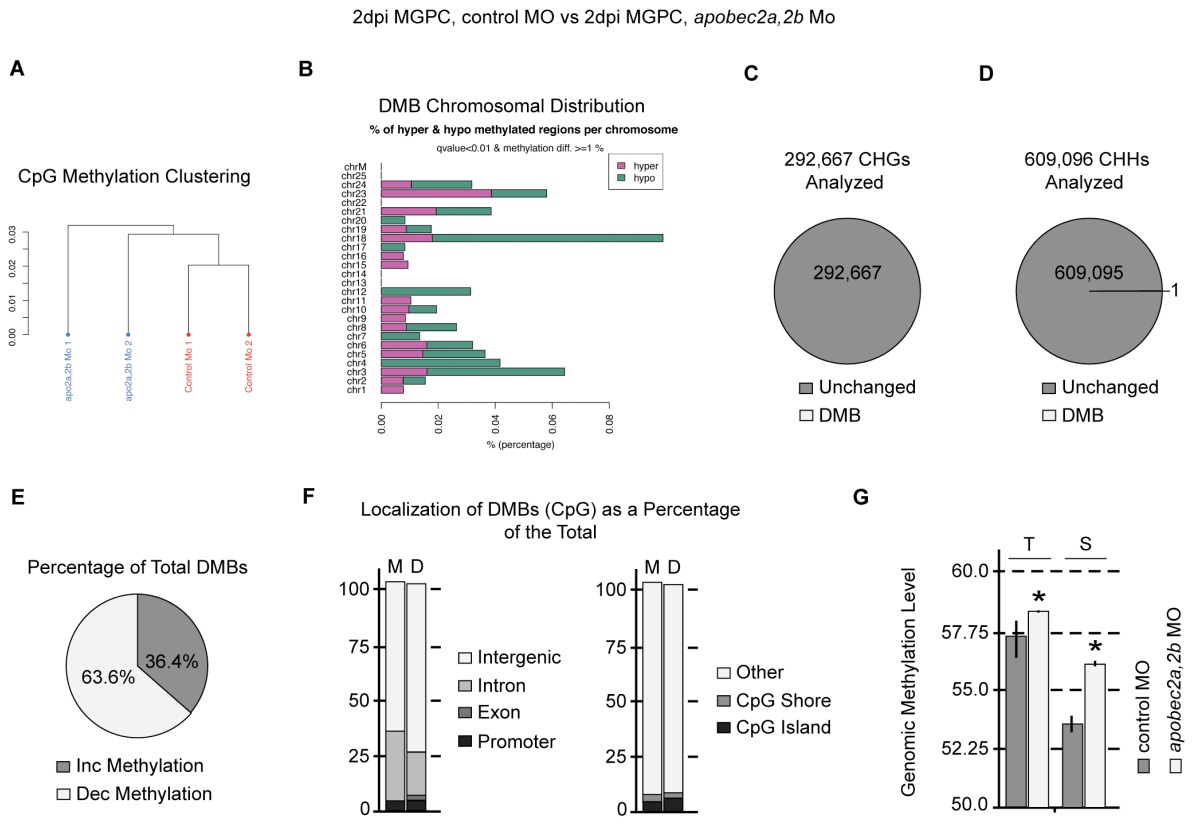

Figure 3.16 MO RRBS library comparisons, continued

RRBS comparisons of 2dpi MGPC treated with control or *apobec2a,2b* MO. (A and B) MethylKit comparisons as done in Figure 3.10. (C and D) Quantification of DMBs within the CHG (C) and CHH (D) contexts. Classification (E) and (F) localization of DMBs (CpG) indicate that the knockdown of Apobec2a,2b does not regulated site-specific DNA demethylation. (G) Genome wide methylation level comparison of 2dpi MGPC, control MO and 2dpi MGPC, *apobec2a,2b* MO RRBS libraries suggests that the knockdown of Apobec2a,2b causes increased global methylation. *$P < 2.2e\text{-}16$.

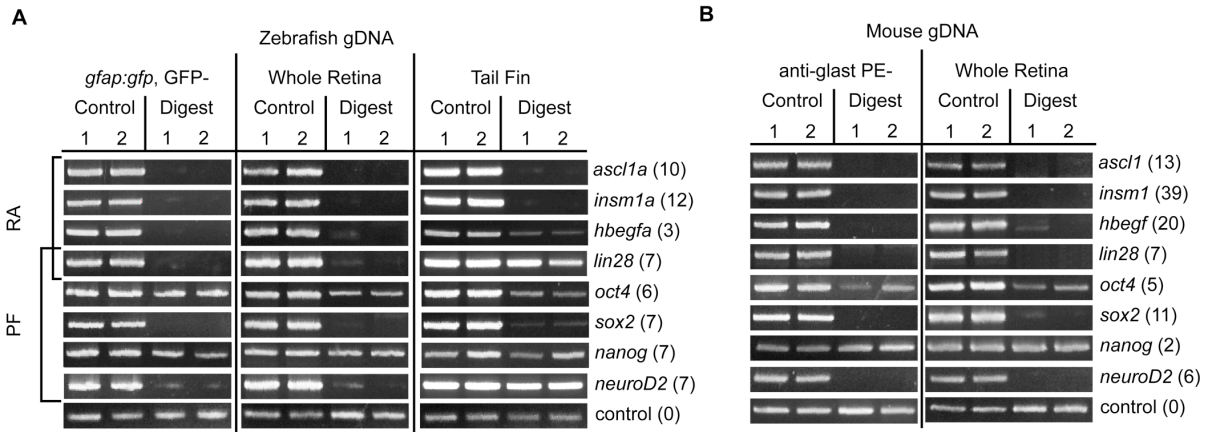

Figure 3.17 Restriction PCR

Targeted promoter restriction PCR following genomic digest (or mock/control, undigested) with HpaII, HpyCH4IV, and BstuI using the indicated zebrafish (A) and mouse (B) gDNAs. The number of potential restriction cut sites are indicated next to each target name. PF, pluripotency factor; RA, regeneration-associated.

3.8 Tables

						# of Reads		Mapping (%)		
Sample	**Tg Fish**	**ng gDNA Template**	**S.R.**	**M.Bar**	**Sequencing Method**	**Original**	**Post Trim**	**U**	**R**	**NA**
MG 1	*gfap:gfp*	400	1	TGACCA	paired-end, 101 cycle	32,314,872	25,924,585	36.3	48.1	15.6
MG 2	*gfap:gfp*	400	1	ACAGTG	paired-end, 101 cycle	29,862,784	24,887,592	37.4	46	16.6
4dpi MGPC 1	*1016 tuba1a:gfp*	400	1	GCCAAT	paired-end, 101 cycle	26,239,980	23,739,757	39.9	38.1	22
4dpi MGPC 2	*1017 tuba1a:gfp*	400	1	CAGATC	paired-end, 101 cycle	27,977,999	22,338,255	38.4	41.2	20.4
2dpi MGPC, control MO 1	*gfap:gfp*	50	2	AGTCAA	single-end, 52 cycle	23,549,077	14,110,476	32.8	42.4	24.8
2dpi MGPC, control MO 2	*gfap:gfp*	50	2	AGTTCC	single-end, 52 cycle	39,547,145	27,330,082	29.3	39.4	31.2
2dpi MGPC, *apobec2a,2b* MO 1	*gfap:gfp*	50	2	ATGTCA	single-end, 52 cycle	14,840,658	8,131,173	29.2	44.4	26.4
2dpi MGPC, *apobec2a,2b* MO 2	*gfap:gfp*	50	2	CCGTCC	single-end, 52 cycle	15,955,560	8,595,116	31.5	45.1	23.3

Table 3.1 Overview of RRBS library sequencing and alignment

S.R., sequencing run; M. Bar, multiplexing barcode; U, unique alignment; R, redundant alignment; NA, no alignment

Primer Set	Application	Sequence 5'->3'
gapdh	SQ RT-PCR and Real-Time PCR	F, ATGACCCCTCCAGCATGA
		R, GGCGGTGTAGGCATGAAC
gadd45a	SQ RT-PCR and Real-Time PCR	F, GTGTGGAGATAACGCAACGGAAAGAATGG
		R, CAACAGAAGGCTTGAATCAGGGTAAAAT
gadd45al	SQ RT-PCR and Real-Time PCR	F, GCCAGAGAAAGAACACCAACGAGAACT
		R, GCACCACGTTATCAGGGTCCACAT
gadd45b	SQ RT-PCR and Real-Time PCR	F, TCTCACAGTCGGCGTTTATG
		R, CGGCTCTCCTCACAGTAGGT
gadd45bl	SQ RT-PCR and Real-Time PCR	F, GATCCACTTCACGCTCATCCA
		R, GGCAATAGAAGGCACCCACTG
gadd45g	SQ RT-PCR and Real-Time PCR	F, CAACGACATCAACATCGTTCG
		R, TCAGCGTTCAGGCAGAGTAA
gadd45gl	SQ RT-PCR and Real-Time PCR	F, TTTCTGCCAAAGCAAACGACT
		R, CAGTGAGCATCTTCAAAATCTTCAG
apobec2a	SQ RT-PCR and Real-Time PCR	F, CTGCTGCAGACGGAGAAAAACCA
		R, CCAGCGTGCTCGTCCTCAATGTA
apobec2b	SQ RT-PCR and Real-Time PCR	F, ATGAGGAGTTTGAGCTAGAGCCGATG
		R, ATCCTCCAGGTAACCACGAACGC
mbd4	SQ RT-PCR and Real-Time PCR	F, GAACATGAAACAAACAAGCCAAGAAACAGC
		R, CGAGTCATTGCCGTATTTGCCGAT
tdg	SQ RT-PCR and Real-Time PCR	F, ATGGATGAAAGGCTGTATGGATC
		R, TCCTCTGGATGTACAGGCAT
tet1	SQ RT-PCR and Real-Time PCR	F, GGACTGTCGTCTGGGCTGTAGGG
		R, GCCAGCAGCCGCACTTCTCTT
tet2	SQ RT-PCR and Real-Time PCR	F, CACACCCAACTCTAAAACGGACAACAC
		R, ATGGTGGGGAAGCGTAAGAAGGA
tet3	SQ RT-PCR and Real-Time PCR	F, GATAGGTATGGGGAGAAGGGGGAAG
		R, GCCAGGATGACAACAACGATGACA
dnmt1	SQ RT-PCR and Real-Time PCR	F, TATGGCCGCCTGGAATGGGA
		R, GGAGAGGGGTGGAGGAACAGCAT
dnmt2	SQ RT-PCR and Real-Time PCR	F, GAAATATGGAGAACACGGAGCGACTG
		R, AATTCAGCCTGTCAAAATCCTGTAACG
dnmt3	SQ RT-PCR and Real-Time PCR	F, GCTTGTTGATGCCGTGAAAGTGAGTC
		R, TCATGGTGACGGGGAAATGTGC
dnmt4	SQ RT-PCR and Real-Time PCR	F, CAGAGCAGAGACGGCCAATCAGAG
		R, CATTACAGGGACTTCCACCAATCACC
dnmt5	SQ RT-PCR and Real-Time PCR	F, GCTGACATAAGCCGCTTTCTGGAAT
		R, TCAGTATGTTTGGCCGTGTGGTAATG
dnmt6	SQ RT-PCR and Real-Time PCR	F, GGAGCGTTATGTGGCCTCAGAAGTG
		R, CGGTGCCCTCGTAGAGACCTTTTC
dnmt7	SQ RT-PCR and Real-Time PCR	F, GCAGTCGCTATGAGGTTTTGGGTTG
		R, CCGAAAAGCTGCCTGAAGAAGACT

dnmt8	SQ RT-PCR and Real-Time PCR	F, GAATCGCGCCGATACACCAAGAG
		R, ACACACATCATAGACAGTTTTCCATCACC
mesite1	Restriction PCR	F, ACACGCCAACTCGAGGGATTCAT
		R, CATACAAAACGGAGAGAGTGTAACGGTG
mesite2	Restriction PCR	F, CGAAACCCTTCCCCATAAAACAATAA
		R, GTGGCCACAGCTGAAGAAAATCCTA
mesite3	Restriction PCR	F, TGCTGATTGGCTGCATGTGAGTTT
		R, GCGTAACGGGAATATCTGGAATGTG
mesite4	Restriction PCR	F, GCTACTGCAGGCCGAACAGAAAA
		R AGCAGACACTTAGGTGGGAACAACATT
mesite5	Restriction PCR	F, CACAATATCTAAATGAGAAAGGAAACGGTG
		R, AAGCTGCTTCTGAAGGCTCTGCG
mesite6	Restriction PCR	F, TATACGTGCAGAATCGCCCAGAGA
		R, CAGAAATCAGCAGCATAGCCAGTGA
dmesite1	Restriction PCR	F, TAATCATGTTGACACATTACATTGAGGCTC
		R, CAGTTTTGGGTGCGCAGTAACGA
dmesite2	Restriction PCR	F, TCATCGATTCCCATACGATTCATTCA
		R, GTCTAAAACCACATTGATAACGAAACACG
dmesite3	Restriction PCR	F, AACTCGAAGATAGAAACCCCACTG
		R, AAACTCGATCTTCTGCAGCAACACCT
dmesite4	Restriction PCR	F, GCAGATGTGTTGTGTTGGGGTTTTC
		R, GAGCTGCAGCCGAAGCGTTTAG
dmesite5	Restriction PCR	F, TCGGGGCCTGCTAAATCATCTTC
		R, GAACAACGTGCGGTAACAGAAAATCC
dmesite6	Restriction PCR	F, CACAACCTCATCATCCCCATCTCAT
		R, CGCAAGTCGCTGGCATGTCTATC
dmesite7	Restriction PCR	F, AGTCATTCTAGCCGGTAGGGTATTTCAG
		R, ACGCAGCGTTAGCCTGTACACTCTG
methcontrol	Restriction PCR	F, ACCGAACCCCATGTGTCAGCA
		R, AAAAGATGTCAGGAATGGATCAGTGTG
azacytsite1	Restriction PCR	F, ACAGACTGAGAAACACCGGCAATAAAG
		R, ATGATCCTCCAAACCTCCATCCAG
azacytsite2	Restriction PCR	F, GCCAGTTCTATGTGCCGGTTATGAG
		R, TCACCTGAAGGCTCTGCTGATTGT
azacytsite3	Restriction PCR	F, GATTGCCAGGGGTGGGTAAGACT
		R, GCTGGCCCGGTAATCCTTTTTCT
azacytsite4	Restriction PCR	F, CCATGCAGCCAGGACTCACAGT
		R, TGTTCAAGAACAAATGAAGGTCAAAAGC
azacytsite5	Restriction PCR	F, CCCCAACTACCAACAATGCCAGAC
		R, GAAGTAGCCGTCTTCGTTTCCGC
azacytcontrol	Restriction PCR	F, TACCAGGACAGCCAGGGAATAAAGG
		R, TGGACCCGGTATGCCAGGAAG
npas4	Real-Time PCR	F, TTCATCGTTGCTATCCACAATGTATCG

		R, CATAAAATGAAAGGAATCCCGTCGTT
cdk5r2a	Real-Time PCR	F, TGGACGTGAACCTGTGACTCTGAAG
		R, GAATGGCGCTTGAGGCTTTTCTC
bx569778.1	Real-Time PCR	F, GCCACCCGCTGTCTGCTAATAAACT
		R, TCGGCTAATGCTGATGACTGTGATG
smyd2b	Real-Time PCR	F, CATATTCATACGTGCTGTCTGTGGGAG
		R, TTCAGCCTGGCGATGATTCTGG
zgc:101606	Real-Time PCR	F, TCGAGGAGAAGACCGCCACTGT
		R, GTGAAATGACCCTGCCTGTGAATG
lamc2	Real-Time PCR	F, TGAAGGGTGGCGAGCAGCAA
		R, GATGTGGAGGGACGACGGACA
cmtm3	Real-Time PCR	F, TTATGCCGATTTGCGAAGAGTGG
		R, CTTCACCGAGAAGCAACAGTCCTTTT
tubgcp2	Real-Time PCR	F, TGTCAGTTTCGCCACTCTTCTACAACAG
		R, ATAAACCTCTGCACCATCTCCCCC
ribc1	Real-Time PCR	F, TGACAGAGCAGAGCAGACAGCAGG
		R, GAGTTGAGGATGGAATGGGATGGT
erh	Real-Time PCR	F, TTGCCGATCTCAGCTGTCTTGTGT
		R, GTCTGTCCTGTGATGAAGCGTAGTTG
ck2b	Real-Time PCR	F, GATTTCTTGGTTTTGTGGTCTACGGG
		R, CCTCCAGCTCCTCATCAGGTTCC
mtdhb	Real-Time PCR	F, TCTGGTTCTCCTGCTGGTCTTATGG
		R, CTGCCGTTTTAACCTCCTCCTGTG
sgk3	Real-Time PCR	F, AGCTGCGTGGTCCATCCTTCAG
		R, GAGTTTGGCACGGTTTCCTCTGTAA
cep85	Real-Time PCR	F, GGACTGTGTTCGCATCATTATTGTCG
		R, CCATGTCCCCACTGTCCACTTTG
spata18	Real-Time PCR	F, GCCATGGCTGACACTTTGAGAAGACTA
		R, CGACTCCTGAATAATGTCCACCCTCT
impdh1a	Real-Time PCR	F, ATTACCTGATCAGCGGGGGAACA
		R, GCCATTGAGGACTCTGTGACTGTGTC
syn2a	Real-Time PCR	F, GAACAGGCTGAGTTTGGCGACAT
		R, TCCAGAGAGTTGATGCTGGGAATACC
tmem27	Real-Time PCR	F, TGAGGCAGAGCAAACATCGCAT
		R, CTTTGGCTTTGGCTCGTCGTCTT
ctbp2l	Real-Time PCR	F, GCCTGCTTCGGCGTTGAATCT
		R, GCATCCTTTGAGTCACCACAGAACC
reep1	Real-Time PCR	F, TCGCCTTTGTGGTTTGGTTACTTTC
		R, ACAGAACGCCCTGGCCCTTAGT
glrx5	Real-Time PCR	F, TCCTCAGCGGGACAGAAGAACCT
		R, ATCGTCGGCCAGTTGGAGAAAGT
zgc:66415	Real-Time PCR	F, GGATCTGTGGAACTGGAGCCTGTC
		R, TGTTCTTCTCCTCATTGTTGTGGT

si:dkey-266m15.7	Real-Time PCR	F, TGCATCCTTCAGACCAGACGAGAG
		R, TTATCATTGGCAACCTGGAAAGTGTT
apoa1bp	Real-Time PCR	F, CCAGGAAACAACGGAGGAGACG
		R, CCACAACCAGGCTATACGCTTCATC
ankrd44	Real-Time PCR	F, CATGAGACCTGTGCCACCCTTTTAT
		R, CCTTCCTTTCTCTGCTGCCATACAA
wdr25	Real-Time PCR	F, CTTTGGACACGAAGCCTTGAGATG
		R, ACCCACACGCAGGTTCAGACG
ascl1a	Real-Time PCR	F, ATTCCAGTCGGGCGTCCTGTCA
		R, CCTCCCAAGCGAGTGCTGATATTTT
ascl1aBS	Bisulfite PCR	F, GTATGGGATGTTTTTATTGTAGT
		R, CACTAAAATTTTCTTTAAACTACCC
ascl1aBSnested	Bisulfite PCR	F, GTTTATTTAGTGGTAGGAGT
		R, AAAATTTTCTTTAAACTACCC
insm1aBS	Bisulfite PCR	F, GAGGAGTTTTTTTTATGAATTATG
		R, RTACCCTACCTTTATCAACA
insm1aBSnested	Bisulfite PCR	F, GAGAGGAGTTTTTTTTATGA
		R, TTTAAAAACTCCTTCACTCT
lin28BS	Bisulfite PCR	F, AGTTTAGTTTTTTTATTGATTAG
		R, TAATAACCCCTACCTTAAAA
lin28BSnested	Bisulfite PCR	F, AGTTTTTTTATTGATTAGGGGT
		R, AACCCCTACCTTAAAAAAAT
oct4BS	Bisulfite PCR	F, AAATATGTATAAGAGGGTAGGAA
		R, CCAAACAAACTAAACTCAAA
oct4BSnested	Bisulfite PCR	F, AAGAGGGTAGGAATGATAAAAT
		R, ATCAAAATAAACCAATAATTCACCACC
sox2BS	Bisulfite PCR	F, TGTGAAGAATTGTGATAATT
		R, CAAAACAAACAACATAAATTCCA
sox2BSnested	Bisulfite PCR	F, GTTAAAGTAGGAGTTATTTTG
		R, CATAAATAAATAAACACTCTC
nanogBS	Bisulfite PCR	F, TATTATTTTTAGGTAAGTGTGGA
		R, AACCRAACTACTAAAAAAAAAAA
nanogBSnested	Bisulfite PCR	F, TTTTTAGGTAAGTGTGGAAT
		R, CCRAACTACTAAAAAAAAAAAC
pcBS	Bisulfite PCR	F, TTGGATAAAGTAAGGAAAGG
		R, TCTTACCAAATCAATATTATCCT
pcBSnested	Bisulfite PCR	F, AAGGAAAGGGTTGGTTTTGT
		R, CAATATTATCCTCTCTTTCCTTC
zfishgfap	SQ RT-PCR	F, GACACCAGCATGGACACTAAACTGACTC
		R, AGAAGCAGGGAAAGTTGGTGAGAAAA
zfishbactin	SQ RT-PCR	F, CATCGTTCACAGGAAGTGCTTC
		R, GGTAAACGCTTCTGGAATGAC
mousegfap	SQ RT-PCR	F, GCCACCAGTAACATGCAAGAGACAGA

		R, GCATTTGCCGCTCTAGGGACTC
mousebactin	SQ RT-PCR	F, ACCACCACAGCTGAGAGGGAAATC
		R, GAACCGCTCGTTGCCAATAGTGAT
zfishascl1apro	Restriction PCR	F, GCCTGTCCTGCTGTGATGATTTCTAA
		R, GAACTGCTGCTGGTTTACGCTTATTTC
zfishinsm1apro	Restriction PCR	F, CCCAACACAGAGAAACGAAAGAGA
		R, ATCACGAAAGCATAGCGGCAGTCT
zfishhbegfapro	Restriction PCR	F, CATAGGCCAACTTTGACCCACAGG
		R, TGAACGCATGAGACCGAAATAAATACA
zfishlin28pro	Restriction PCR	F, TTATCTTCACGGTTTTTGATGGACAGAA
		R, TGTGTGATTGAGATGCGGATTTGC
zfishoct4pro	Restriction PCR	F, GCAATTGGCTTTGTTGTGTCCTATG
		R, AGTCGCCACCTTGCAAATCGTT
zfishsox2pro	Restriction PCR	F, CTCTTGTTATTTTGAAGGAGGCTGTGC
		R, TTTTCCTCCGGGGTCTGTATTTGTAA
zfishnanogpro	Restriction PCR	F, GGTAGCATGTGCCACCATGTTCAGTA
		R, CCTCGGAATCACTGGGTGTATCACT
zfishneurod2pro	Restriction PCR	F, GTGGCTGCTGTGTTTTGTAGTTTATTTTG
		R, CGAGTCGGGTCAGTTTTTTTATTATTCAC
mouseascl1pro	Restriction PCR	F, GGAGGGACAAGGAGGGAAGACTTTC
		R, GCTTGAGCCTGCTTCTGGGATTATT
mouseinms1pro	Restriction PCR	F, TCAGGCATATTAGGGAAAGGAACG
		R, GAATGGCCCCAAATATGTCAGGAG
mousehbegfpro	Restriction PCR	F, TGTCCAAGTTCACACGGTAAAGAGCA
		R, AGCGAGGTTCCACTAAGGCACTGT
mouselin28pro	Restriction PCR	F, GAGGGGGTGTCAAATCTCAAGGTTC
		R, GGAGATAGGGAGGGCCAGGTGAT
mouseoct4pro	Restriction PCR	F, GGGGAGGGAGAACTGAGAATCTTGA
		R, CATCCCTCCGCAGAACTCGTATG
mousesox2pro	Restriction PCR	F, CCTCTTGTGTCAGGGTTGGGAGTTAG
		R, GCCGCGATTGTTGTGATTAGTTTT
mousenanogpro	Restriction PCR	F, CAAAACTCAAACAAACACCACCAACC
		R, CCAACGGCTCAAGGCGATAGATT
mouseneurod2pro	Restriction PCR	F, CACAAACCGCCAATTCCCAGACT
		R, CTCCCTCTCGGACAACTTACCTCAGA
mousemethcontrol	Restriction PCR	F, TCTGTTGGCCTCAAATACCCTAAGACAT
		R, CTAGCAACACAAATCCACCAGAAATCC

Table 3.2 List of primers used in this study and their applications

Chapter 4:
Insights into the mechanism of Apobec2 function during zebrafish retina regeneration

4.1 Abstract

During zebrafish retina regeneration, Apobec2a and Apobec2b (Apobec2a,2b) are required for Müller glia (MG) activation and Müller glia progenitor cell (MGPC) proliferation, but their biochemical function during these events remains unclear. Because studies of other Apobec proteins have revealed roles in mRNA editing, we sought to determine if Apobec2a,2b regulate mRNA editing during zebrafish retina regeneration via cytosine deamination and to identify potential mRNA targets. While evidence of C-to-U mRNA editing was found, this study suggests that it occurs independent of Apobec2a,2b, as their knockdown did not influence this editing. Similar to other previously studied Apobec2s, overexpression of Apobec2a,2b did not induce cytosine deamination-dependent *rpoB* mutations in bacterial mutagenesis assays, putting into question their catalytic activity. Using conditional expressing transgenic fish, we demonstrate that the induction of exogenous Apobec2a,2b and that of exogenous human APOBEC2, after knockdown of endogenous Apobec2a,2b, can rescue a regenerative response, suggesting that the biochemical function that Apobec2a,2b perform during MG activation and MGPC proliferation is conserved between fish and mammals. Interestingly, retina regeneration was not rescued by the conditional expression of Apobec2a,2b harboring mutations impacting zinc binding, indicating that the proper coordination of zinc is essential for their function. To gain further insights into the function of Apobec2a,2b, yeast two-hybrid screens were performed, identifying Ubc9 (an E2 SUMO ligase), Toporsa (an E3 Ubiquitin/SUMO ligase), and Pou6F2 (a homeodomain transcription factor) as conserved Apobec2 interacting proteins. Evidence is provided that Apobec2 subcellular localization can be controlled by their N-terminal sumoylation, facilitated by Ubc9 and Toporsa, and that Apobec2 proteins interact

with the DNA binding domain of Pou6F2, possibly perturbing Pou6F2's association with DNA or altering its subcellular localization. Finally, a mechanistic model is proposed whereby Apobec2a,2b participate in the regenerative response independent of cytosine deamination.

4.2 Introduction

Apobec2 was the second Apobec protein identified, through its sequence homology to Apobec1 (Liao et al., 1999; Anant et al., 2001a). Although the expression of Apobec2 has been correlated with a number of processes (Piec et al., 2005; Sato et al., 2009; Iio et al., 2010; Okuyama et al., 2011; Pennings et al., 2011; Vonica et al., 2011) and the perturbation of Apobec2 expression results in multiple phenotypes (Sato et al., 2009; Etard et al., 2010; Vonica et al., 2011; Powell et al., 2012), little is known about its biochemical function, including whether or not it acts catalytically to mutate DNA and/or RNA through cytosine deamination. Unlike other Apobecs, Apobec2 fails to induce mutations in bacterial and yeast based mutagenesis assays (Harris et al., 2002a; Mikl et al., 2005; Lada et al., 2011). In addition, *in vitro* biochemical assays have demonstrated that the ability of Apobec2 to bind polynucleotides is limited (Anant et al., 2001a; Sato et al., 2009). Still, the question remains as to whether a condition could exist within a cell that would provide the environment necessary for Apobec2 to demonstrate this catalytic activity.

While biochemical data is lacking, prominent models of Apobec2 function suggest a role in DNA demethylation (Rai et al., 2008) and RNA editing (Okuyama et al., 2011). Previously, we demonstrated that Apobec2a and Apobec2b (Apobec2a,2b) are necessary for zebrafish retina and optic nerve regeneration (Powell et al., 2012). Specifically, during retina regeneration, Apobec2a,2b regulate Müller glia (MG) activation and the proliferation of Müller glia derived progenitor cells (MGPCs). One of the ways they influence these events is by directly or indirectly regulating the transcriptional induction of *ascl1a*, a gene that encodes a transcriptional activator necessary for retina regeneration (Fausett et al., 2008; Ramachandran et al., 2011). With this background, we have sought to determine the essential biochemical function that these Apobec2 proteins play in these processes. Interestingly, knockdown of Apobec2a,2b during retina regeneration did not influence

changes in DNA methylation levels accompanying MG activation, indicating that Apobec2 proteins perform an alternate function (Powell et al., 2013).

Here we report the results from a series of experiments designed at further uncovering the biochemical function of these proteins during retina regeneration. We address the possibility that Apobec2a,2b regulate mRNA editing by comparing mRNA profiles of MG with those of MGPCs with and without knockdown of Apobec2a,2b. Although mRNA editing occurs, it happens independent of Apobec2a,2b. Evidence is presented that demonstrates that the function of Apobec2a,2b during retina regeneration is conserved and requires the proper coordination of zinc. Apobec2 interacting proteins are identified and characterized. Finally, a model is proposed whereby Apobec2a,2b regulate MG activation and MGPC proliferation independent of cytosine deamination. Comprehensively, this study contributes greatly to the current understanding of Apobec2 proteins and their mechanism of action.

4.3 Results

4.3.1 Apobec2a,2b-independent mRNA editing occurs during Müller glia activation

To determine if injury-dependent mRNA editing occurs during MG activation and if Apobec2a,2b regulate these editing events (specifically C-to-U editing), mRNA analyses were performed between quiescent MG and MGPCs following control or *apobec2a,2b* MO knockdown. To this end, RNA was purified from MG (isolated by FACS sorting GFP+ cells from uninjured [0 hour, hr] *gfap:gfp* transgenic fish retinas) (Kassen et al., 2007), and from 2 days post injury (dpi) MGPCs following a control or Apobec2a,2b knockdown (isolated by FACS sorting GFP+, lissamine+ cells from *gfap:gfp* transgenic fish 2 days after administration and electroporation of either 0.25 mM control or *apobec2a,2b* MO) (Powell et al., 2013). With these RNA samples, TruSeq libraries were prepared, sequenced, and aligned to the zebrafish reference genome (Table 4.2). Relative to the reference genome, variants of all types were identified within each sample, with a preponderance of T-to-C, C-to-T, A-to-G, and G-to-A variant types (Table 4.3).

Comparisons of regions of high sequencing quality and ≥ 10 X coverage (see materials and methods) in both the 0hr MG and 2dpi MGPC, control MO libraries identified 2,560 C-to-T variants in one or both of the samples (indicative of SNPs relative to the

reference genome or the deamination of C to U) (Figure 4.1A). Most of these variants were localized to translated regions of the mRNA and were synonymous mutations (did not change the resulting protein primary structure) (Figure 4.1A and B). Some of these variants (8.5% of the total) were differentially regulated after injury, with 3.7% decreasing and 4.8% increasing by more than 2 fold during the conversion of MG to MGPC (Figure 4.1C). Importantly, these changes in variant abundance were not due to differences in sequencing depth that could result from variation in library preparation or differences in transcription level (Figure 4.2A). These results suggest that C-to-U mRNA editing is regulated during MG activation.

Comparisons of the 0hr MG and 2dpi MGPC, *apobec2a,2b* MO libraries identified 2,374 C-to-T variants (Figure 4.1D). Like the previous analysis, most of these variants were localized to translated regions of the mRNA and were synonymous mutations (Figure 4.1D and E). Interestingly, 9.4% of these variants were differentially regulated between the samples, with 3.5% decreasing and 5.9% increasing in abundance after injury, indicating that the knockdown of Apobec2a,2b did not repress C-to-U mRNA editing (Figure 4.1F and Figure 4.2B). Likewise, comparisons of the 2dpi MGPC, control MO and 2dpi MGPC, *apobec2a,2b* MO libraries indicated that only 1.5% of the 3,286 variants were differentially regulated between the samples, with roughly equal amounts increasing and decreasing after Apobec2a,2b knockdown (Figure 4.1G-I and Figure 4.2C). Furthermore, the abundances of the most highly regulated C-to-T variants following injury (≥ 3 fold induction) were largely unperturbed following Apobec2a,2b knockdown (Table 4.4). These results demonstrate that while C-to-U mRNA editing is regulated during MG activation, it occurs in an Apobec2-independent fashion. This, in combination with previous data that indicates that Apobec2a,2b do not regulate DNA demethylation during MG activation (Powell et al., 2013), suggests that Apobec2 proteins may not function as RNA or DNA mutators.

4.3.2 Overexpression of Apobec2a,2b does not increase survival in bacterial mutagenesis assays

Previously studied Apobec2 proteins have failed to induce mutations in bacterial and yeast based mutagenesis assays (Harris et al., 2002a; Mikl et al., 2005; Lada et al., 2011). Here we tested if the same is true of zebrafish Apobec2a,2b. While induction of Apobec1

and AID increased the number of rifampicin resistant bacteria colonies, APOBECEC2, Apobec2a, and Apobec2b did not (Figure 4.3A and B). Because the physiological temperature of zebrafish is lower than mammals, it was possible this lack of mutagenic activity seen with Apobec2a,2b induction was due to temperature. Indeed, it has been suggested that the activity of zebrafish AID is impacted by temperature (Dancyger et al., 2011; Abdouni et al., 2013). In contrast to this report of zebrafish AID, performing the mutagenesis assay at 25 °C instead of 37 °C did not increase the ability of Apobec2a,2b to stimulate bacterial resistance (Figure 4.3C).

Comparisons of Apobec protein chemistries and primary structures revealed at least three features unique to Apobec2 proteins: 1) they are the most acidic of all Apobec proteins; 2) they have very unique N-termini; and 3) while they contain an SSS motif within their active sites, all Apobec proteins demonstrated to be catalytically active contain an SWS motif (Figure 4.4A). The acidic nature of these proteins may negatively influence their ability to bind polynucleotides. Indeed, biochemical studies of purified Apobec2 suggest that its ability to bind polynucleotides is limited (Anant et al., 2001b; Sato et al., 2009). How their unique N-termini or their SSS motifs could impact their function in the bacterial mutagenesis assay is less clear, though mutation of the SWS motif to an SSS motif in Apobec1 completely abolishes its mutagenic activity (Figure 4.3B) (Harris et al., 2002a). The N-termini of Apobec2 proteins may regulate their oligomerization, possibly impacting their ability to bind large polynucleotides. The crystal structure of a truncated human APOBEC2 (amino acids 41-224) suggested that it can oligomerize, but the NMR structure of the full-length protein suggested that it is monomeric (Prochnow et al., 2007; Krzysiak et al., 2012).

To test the possibility that these unique Apobec2 features mask or hinder their mutagenic potential, Apobec2s were engineered that harbor N-terminal truncations, Apobec2(T), or that contain mutations converting the SSS motif to an SWS motif. For the truncations of Apobec2 proteins, the first 41, 73, or 93 amino acids was removed from APOBEC2, Apobec2a, and Apobec2b, respectively (this is the case in all the truncations described in this work). Induction of Apobec2s containing S to W mutations did not affect their mutagenic activity at 25 °C or 37 °C (Figure 4.3B and C). Surprisingly, analyses of Apobec2 proteins harboring N-terminal deletions revealed that the induction of Apobec2a(T) at 37 °C and that of Apobec2b(T) at 25 °C slightly increased the number of rifampicin

resistant bacterial colonies, while the induction of APOBEC2(T), Apobec2a(T) at 25 °C, and Apobec2b(T) at 37 °C did not (Figure 4.3B and C). To determine if these increases in rifampicin resistance were due to cytosine deaminase-dependent mutagenesis, we characterized mutations of bacterial *rpoB* and quantified the percentage of dC/dG transitions occurring after induction of Apobec2a(T) at 37 °C or Apobec2b(T) at 25 °C. In comparison to reports of APOBEC1 (100% dC/dG transitions versus 27% dC/dG transitions in the control) (Harris et al., 2002a) and AID (80% dC/dG transitions versus 31% dC/dG transitions in the control) (Petersen-Mahrt et al., 2002), analysis of Apobec2a(T) and Apobec2b(T) revealed dC/dG transitions of 20% and 40% respectively (Figure 4.4B and C), indicating that the differences in rifampicin resistance resultant from their inductions were not due to a preponderance of cytosine deamination. While we were unable to identify the exact mechanism whereby these truncations increase the number of rifampicin resistant colonies, we did note that bacteria expressing Apobec2a(T) and Apobec2b(T) at 37 °C and 25 °C, respectively, grew to higher densities (Figure 4.4D). This may have contributed to the increased number of rifampicin resistant colonies, as more cells would have been added to the plates according to our methods, which were based on volume (see materials and methods).

Thus, while Apobec2a(T) and Apobec2b(T) slightly increased the number of rifampicin resistant colonies, they did so in a cytosine deaminase-independent fashion. These results, in combination with those of full length Apobec2a,2b and APOBEC2 (Figure 4.3) and those reported by others (Anant et al., 2001a; Harris et al., 2002a; Mikl et al., 2005; Sato et al., 2009; Lada et al., 2011; Powell et al., 2013), place doubt in the hypothesis that Apobec2 proteins catalytically function as cytosine deaminases. Indeed, they suggest that the function of Apobec2 proteins may be independent of cytosine deamination.

4.3.3 The biochemical function of Apobec2a,2b required for retina regeneration is conserved and requires the proper coordination of zinc

Apobec proteins are zinc-dependent deaminases. The zinc ion coordinated by Apobecs is critical for their ability to biochemically function as cytosine deaminases. But, it is likely that the importance of zinc binding by Apobec proteins is not limited solely to the mechanism of deamination. Metalloprotein structure is dependent on the proper binding of

the metal. Changes in structure resulting from improper metal binding, or the lack thereof, can disrupt the protein's interactions with other macromolecules and/or alter its stability and/or solubility. While the catalytic activity of Apobec2 proteins has come into question, their sequences contain the conserved residues needed for zinc binding and have been shown to be bona fide zinc binding proteins (Prochnow et al., 2007; Krzysiak et al., 2012). This conservation suggests that zinc binding is important for the function of Apobec2 proteins.

To determine if the biochemical function that Apobec2a,2b perform during retina regeneration is conserved and dependent on the proper binding of zinc, rescue experiments were designed using exogenously introduced, tagged Apobec2 proteins. The ability of these tagged Apobecs to escape morpholino-mediated gene knockdown and to function properly was assessed. The additional 5' mRNA sequence encoding *myc* and *flag* tags allows the induction of these exogenous transgenes to escape *apobec2a/b* MO mediated knockdown (Figure 4.5A and B). Importantly, the N-terminal tags did not hinder their ability to rescue a previously characterized Apobec2a/b knockdown phenotype during zebrafish development (Figure 4.5B). The viral 2a peptide (V2a) allows for polycistronic expression (Provost et al., 2007), and its functionality in zebrafish was demonstrated (Figure 4.5C).

We then created transgenic fish that allow the conditional expression, via heat shock, of N-terminally tagged Apobec2a,2b (*hsp70:zapobec2wt*), mutant Apobec2a,2b (harboring alanine substitutions of a cysteine involved in the coordination of zinc) (*hsp70:zapobec2mut*) (Prochnow et al., 2007), or APOBEC2 (*hsp70:APOBEC2*) (Figure 4.6A). This design allows the induction of exogenous Apobec2 proteins in the adult retina with and without injury. Also included in these transgenic constructs was a *1016 tuba1a:gfp* expression cassette which has been shown to label MGPCs after injury and facilitates transgenic screening (Figure 4.6A) (Fausett and Goldman, 2006).

Analyses of uninjured adult transgenic fish (in the absence of heat shock) showed that they all have basal GFP expression in a subgroup of cells in the inner nuclear layer (INL) and the retinal ganglion cell layer (RGC) (Figure 4.6B-D). Similar to uninjured adult wild type fish, they showed minimal cellular proliferation in the outer nuclear layer (ONL), presumably rod progenitor cells, and extremely limited proliferation in the INL (Figure 4.6E). After injury (in the absence of heat shock), these transgenic fish showed phenotypes highly similar to previously characterized *1016 tuba1a:gfp* transgenic fish, with GFP expression induced at

the site of injury (Figure 4.6B-D). Furthermore, all transgenic fish showed a normal proliferative response following injury (Figure 4.6F). Thus, in the absence of heat shock, these transgenic fish respond to injury normally.

The ability of these transgenic fish to induce the expression of their respective transgenes following heat shock was demonstrated by measuring their basal and post heat shock expression levels (Figure 4.7C-E) and by immunostaining (Figure 4.7B). Heat shock of uninjured *hsp70:zapobec2wt* transgenic fish showed that the induction of Apobec2a,2b was unable to induce a proliferative response (Figure 4.7A). Furthermore, *ascl1a* expression analyses of injured, heat shocked *hsp70:zapobec2wt* and *hsp70:hAPOBEC2* transgenic fish indicated that the exogenous induction of these genes did not impact the expression of *ascl1a* below or beyond its normal levels following injury, indicating that their presence does not stimulate or hinder the normal regenerative response (Figure 4.7F). In contrast, *ascl1a* expression analyses of injured, heat shocked *hsp70:zapobec2mut* transgenic fish demonstrated that exogenous induction of mutant Apobec2a,2b negatively impacted *ascl1a* expression levels slightly, indicating that their presence diminishes the normal regenerative response (Figure 4.7F). This suggests that the proper coordination of zinc is important for the biochemical function of Apobec2a,2b and is consistent with a dominant negative phenotype, where the presence of exogenous mutant Apobec2a,2b precludes the ability of endogenous Apobec2a,2b to perform their functions.

This is supported by experiments using *apobec2a,2b* MO to knockdown endogenous Apobec2a,2b after injury. In preparation for these experiments, we identified the lowest concentration of *apobec2a,2b* MO that consistently reduced the level of injury-dependent *ascl1a* induction (Figure 4.7G), facilitating our ability to see potential rescue. In addition, because it is unclear if Apobec2a,2b act redundantly, as both are required for retina regeneration (Powell et al., 2012), we hoped that a minimal knockdown would allow APOBEC2 to rescue even if it was only compensating for one of the two zebrafish Apobec2 proteins. Rescue experiments were then performed to determine if exogenously introduced Apobec2a,2b, mutant Apobec2a,2b, or APOBEC2 could rescue the previously characterized phenotype following knockdown of endogenous Apobec2a,2b (Powell et al., 2012), namely the diminished transcriptional activation of *ascl1a* and the impediment of MG activation and MGPC proliferation. As expected, heat shock of *hsp70:zapobec2wt* transgenic fish rescued

ascl1a expression and MGPC proliferation after knockdown of endogenous Apobec2a,2b (Figure 4.8A-C). Experiments using *hsp70:hAPOBEC2* transgenic fish showed similar results (Figure 4.8A-C), suggesting that the biochemical function that Apobec2a,2b perform during MG activation and MGPC proliferation is conserved between fish and mammals. On the other hand, *hsp70:zapobec2mut* transgenic fish were unable to rescue retina regeneration following Apobec2a,2b knockdown, again suggesting that the proper coordination of zinc is essential for their biochemical function (Figure 4.8A-C).

4.3.4 Yeast two-hybrid screens identify Apobec2 interacting proteins and suggest that Apobec2a,2b do not oligomerize

With little evidence to support a role for Apobec2 proteins as cytosine deaminases, we hypothesized that the *hsp70:zapobec2mut* transgenic fish failed to rescue regeneration due to the disruption of a protein:protein interaction interface that is essential for proper regeneration. To identify Apobec2 interacting proteins, specifically within the context of a proliferating MGPC, a full-length normalized yeast two-hybrid library was generated using RNA isolated from 4dpi MGPCs, FACS sorted from *1016 tuba1a:gfp* transgenic fish (Powell et al., 2013). Using this library (pVP16 4dpi *1016 tuba1a:gfp*) yeast two-hybrid screens were carried out for Apobec2a and Apobec2b. These screens identified Ubc9, Toporsa, and Pou6F2 as Apobec2a,2b interacting partners as indicated by yeast growth (white cells) on YC-WHULK plates and their staining (blue) in β-Galactosidase filter assays (Figure 4.9A and B). In support of our results that indicate that Apobec2a,2b do not regulate DNA demethylation or RNA editing, none of these proteins have been shown to directly impact RNA editing or DNA demethylation, suggesting an alternate purpose for these interactions. Interestingly, these screens did not identify Apobec2a,2b as interacting partners of Apobec2a,2b, which would be expected if they oligomerize. This result was confirmed through yeast two-hybrid assays (Figure 4.9D), putting into question models proposing a role for Apobec2 dimerization and tetramerization (Prochnow et al., 2007).

Yeast two-hybrid analyses using APOBEC2 indicated that the interaction interfaces with Ubc9, Toporsa, and Pou6F2 are conserved between fish and mammals (Figure 4.9C). Interestingly, each of these interacting proteins plays a role in retinal development or physiology: 1) Ubc9, the only known E2 SUMO ligase, has been shown to control the cell

cycle exit of retinal progenitors during Xenopus development (Terada and Furukawa, 2010); 2) mutations in TOPORS, a multidomain protein and known E3 SUMO ligase, cause retinitis pigmentosa (Chakarova et al., 2007); and 3) the expression of POU6F2, a homeodomain transcription factor, is associated with retinal differentiation (Zhou et al., 1996). These reports support the hypothesis that the interaction between Apobec2a,2b and these proteins plays an important role during retina regeneration.

4.3.5 N-terminal sumoylation of Apobec2 proteins can control their subcellular localization

Because two of the proteins identified as Apobec2 interacting proteins are involved in the regulation of protein sumoylation, predictive analyses were performed, which identified putative sumoylation sites localized to the N-termini of Apobec2a,2b and APOBEC2. Interestingly, although sumoylation was predicted to occur at the N-termini of each of these proteins, the lysines thought to be sumoylated are not conserved (Figure 4.10A). Consistent with the possibility that Ubc9 and Toporsa regulate Apobec2 sumoylation at these sites, N-terminal truncations of Apobec2a,2b and APOBEC2 (T) showed diminished binding to Ubc9 and Toporsa relative to their full-length (FL) protein forms (Figure 4.10B and C). Expression analyses of *ube2i* (the gene which encodes for Ubc9) and *toporsa* during retina regeneration indicated that the expression of *toporsa* was not differentially regulated after injury, while that of *ube2i* was slightly increased (Figure 4.11A-D).

To determine if these Apobec proteins are modified by N-terminal sumoylation, bacterial sumoylation assays were performed in which Apobec proteins were expressed alone or in combination with components of the sumoylation machinery: an E1 SUMO ligase (a fusion of mouse Aos1 and Uba2) (Uchimura et al., 2004a), an E2 SUMO ligase (Xenopus Ubc9), an E3 ligase (zebrafish Toporsa) and hSUMO1 (Uchimura et al., 2004b) (Figure 4.10D). Interestingly, expression of Apobec2a,2b or APOBEC2 in conjunction with components of the sumoylation machinery increased their molecular weights as assayed by denaturing SDS-PAGE and Western blotting (Figure 4.10E-G). This pattern, indicative of protein sumoylation, was more pronounced with inclusion of Toporsa (Figure 4.10E-G). Each Apobec2 protein showed multiple shifts of size, indicating the presence of more than one sumoylation site in each protein. Importantly, these bands had corresponded bands that were positive for SUMO1 staining (Figure 4.11H). Furthermore, sumoylation assays

performed using a catalytic mutant of Ubc9 (preventing sumoylation) completely abolished these banding patterns (Figure 4.11E-G). These results show that Apobec2a,2b and APOBEC2 can be sumoylated by Ubc9 and that Toporsa stimulates this sumoylation. As expected, N-terminal truncations of Apobec2a,2b and APOBEC2 diminished their sumoylation, further confirming that these sumoylation events occur predominantly at the N-termini of these proteins (Figure 4.10H-J).

Protein sumoylation has been shown to regulate a number of processes including protein subcellular localization, protein function, and protein stability (Flotho and Melchior, 2013). To determine if the N-terminal sumoylation of Apobec2 proteins regulates their subcellular localization, tissue culture experiments were performed to monitor the subcellular localization of non-sumoylated and sumoylated GFP-tagged (C-terminal) Apobec2 proteins. While GFP alone was equally abundant in the nucleus and cytoplasm (Figure 4.12A, E, and F), GFP fusions of Apobec2a,2b and APOBEC2, though present in the nucleus, were enriched in the cytoplasm (Figure 4.12B-D). Fusion of an N-terminal SUMO1 to these Apobecs greatly stimulated this nuclear exclusion (Figure 4.12). We hypothesized that the cytoplasmic enrichment of GFP-tagged Apobec2a,2b and APOBEC2 (in the absence of the N-terminal SUMO1 fusion), was partially due to N-terminal sumoylation of these proteins within the cell. Consistent with this hypothesis, N-terminally truncated Apobec2 proteins fused C-terminally with GFP showed less nuclear exclusion than their full-length forms (Figure 4.12E and F). Importantly, the N-terminal regions removed from each of these proteins did not contain any evident nuclear export signal. Furthermore, a single mutation to a putative sumoylation site within the N-terminus of APOBEC2 (K4R), preventing sumoylation at this site, showed a similar effect (Figure 4.12B and E). These results strongly suggest that N-terminal sumoylation of Apobec2 proteins can regulate their presence within the nucleus.

4.3.6 Apobec2 proteins interact with the DNA binding domain of Pou6F2

POU proteins are transcription factors with positive and negative regulatory roles and are characterized by their bipartite DNA binding domain (DBD) consisting of a POU domain and a homeodomain. To begin to characterize the interaction between Apobec2s and Pou6F2, we cloned *pou6f2*. Interestingly, we found three independent transcripts, one of

which includes an alternative exon (Ex) introduced between Ex6 and Ex7 (Figure 4.13A). This exon introduces a premature stop codon, preventing the translation of the DBD located in Ex8 and Ex9. The other two transcripts, characterized previously (Zhou et al., 1996), produce proteins with differing DBDs, specifically differing in their POU domains (Figure 4.13A and B). These differences have been shown to alter POU6F2's preferred DNA binding sequence (Zhou et al., 1996).

Interestingly, yeast two-hybrid analyses indicated that Apobec2a,2b and APOBEC2 specifically interact with the region of Pou6F2 DBD encoded in Ex9 (Figure 4.13C). Because of Apobec2's interaction with the sumoylation machinery, we wondered if Apobec2 binding to Pou6F2 could regulate its sumoylation. Indeed, sumoylation of other POU proteins has been reported (Wei et al., 2007). Truncation of Apobe2a,2b and APOBEC2 did not perturb their binding to Pou6F2, suggesting that Apobec2s could simultaneously interact with Ubc9 and Pou6F2 (Figure 4.13D). Predictive analyses of the Pou6F2 DBD revealed multiple putative sites of sumoylation (Figure 4.13A). To test whether Apobec2a,2b and APOBEC2 could serve as E3 ligases in the potential sumoylation of Pou6F2, bacterial sumoylation assays were performed (Figure 4.13E). While these results indicated that the DBD of Pou6F2 can be sumoylated, the presence of Apobec2a,2b and APOBEC2 did not stimulate or hinder Pou6F2 sumoylation (Figure 4.13F). These results suggest that the interaction of Apobec2s with the DBD of Pou6F2 performs an alternate function, possibly introducing a preference to bind alternative DNA sequences, precluding its ability to bind DNA, or controlling its subcellular localization.

4.4 Discussion

Apobec proteins are a family of cytosine deaminases capable of introducing mutations into DNA or RNA (Conticello et al., 2005; Conticello et al., 2007; Conticello, 2008). While phenotypes have been described following manipulations of their expression, the biochemical function of Apobec2 proteins has remained unresolved. Prominent models of Apobec2 function include cytosine deaminase-dependent DNA demethylation (Rai et al., 2008; Guo et al., 2011) and C-to-U mRNA editing (Etard et al., 2010; Okuyama et al., 2011; Vonica et al., 2011). Previously, we demonstrated that zebrafish Apobec2a,2b are required for MG activation and MGPC proliferation during zebrafish retina regeneration (Powell et

al., 2012). Furthermore, we showed that their function during regeneration is independent of site-specific DNA demethylation (Powell et al., 2013).

Here we address the possibility that Apobec2a,2b regulate C-to-U mRNA editing during MG activation and the generation of MGPCs. While we find evidence of editing, it occurs in an Apobec2a,2b-independent manner (Figure 4.1). How this editing occurs remains unclear, but is unlikely to be a random event as our data suggests that the editing is targeted toward certain cytosines, not a global, random event. It is also unclear what role these editing events play (particularly for synonymous variants), but possible functions may include the editing of potential miRNA binding sites, changes in codon sequences that aid or hinder protein production, or changes in the mRNA stability. While more research is needed to understand how and why these editing events are regulated during MG activation, it is evident from our results that Apobec2a,2b do not regulate C-to-U mRNA editing.

Previous biochemical studies of Apobec2 proteins have questioned their catalytic activity (Harris et al., 2002a; Mikl et al., 2005; Lada et al., 2011) and their ability to bind large polynucleotides (Anant et al., 2001a; Sato et al., 2009). Here we show that Apobec2a,2b, like other previously studied Apobec2 proteins, do not increase survival in bacterial mutagenesis assays (Figure 4.3 and 4.4). Comparisons between the primary protein structures of Apobec2 proteins and other Apobecs suggest that differences in charge, N-termini, and catalytic domains may preclude their ability to act as cytosine deaminases (Figure 4.4A). Cumulatively, data collected through studies of Apobec2 proteins provides compelling evidence that their main function is independent of cytosine deamination.

To gain further insights into what this function may be, we created transgenic fish that allow the conditional expression of Apobec2a,2b, Apobec2a,2b mutants that perturb their binding to zinc, or human APOBEC2. In Apobec2a,2b knockdown rescue experiments using these transgenic fish, we demonstrate that the essential function of Apobec2a,2b during regeneration is conserved with human APOBEC2 and requires the proper binding of zinc (Figure 4.5-4.8). Although the exact reason why the mutants did not rescue regeneration following knockdown of endogenous Abobec2a,2b remains unclear, we hypothesize that it is due to changes in their protein structure that preclude their ability to bind interacting proteins that are essential for their function.

Using a yeast two-hybrid screen, we report that Ubc9, Toporsa, and Pou6F2 are conserved Apobec2 interacting proteins (Figure 4.9). Each of these interacting proteins plays a role in retinal development or physiology (Zhou et al., 1996; Chakarova et al., 2007; Terada and Furukawa, 2010). Surprisingly, our yeast two-hybrid analyses demonstrate that Apobec2a,2b do not oligomerize in yeast (Figure 4.9D). The possibility that Apobec2 proteins oligomerize was first reported by analysis of the crystal structure of N-terminally truncated APOBEC2, and this oligomerization was predicted to augment its ability to bind large polynucleotides (Prochnow et al., 2007). Other studies using purified Apobec2 seem to support a model of oligomerization (Sato et al., 2009; Etard et al., 2010). In contrast to these reports, an NMR structure of full length APOBEC2 indicated that it is a monomer in solution, and that the N-terminal region removed in the crystal structure occupies the region predicted to be the oligomerization surface (Krzysiak et al., 2012). While Apobec2 proteins may have the ability to oligomerize under certain *in vitro* conditions, our data suggests that Apobec2a and Apobec2b do not *in vivo*, at least in yeast. Further work will be needed to clarify these contradictions.

We demonstrate that Ubc9 and Toporsa interact with the N-termini of Apobec2 proteins and facilitate their sumoylation (Figure 4.10 and 4.11). In addition, we show clear evidence that the N-terminal sumoylation of Apobec2 proteins can stimulate their nuclear exclusion, providing context for at least one purpose of this sumoylation (Figure 4.12); although, other functions are possible and may include changing the stability of Apobec2 or enhancing/diminishing its ability to interact with other macromolecules. Furthermore the possible sumoylation of Apobec2 proteins by SUMO2 and SUMO3 remains to be analyzed, and these modifications may perform additional roles. Moreover, the interaction between Apobec2 proteins and Ubc9 or Toporsa may not be limited to sumoylation. Indeed, Ubc9 has been shown to perform sumoylation-independent functions such as a role in transcriptional regulation (Ihara et al., 2008). In addition to its role as an E3 SUMO ligase, Toporsa, a multidomain protein, has been shown to function as an E3 ubiquitin ligase (Seong et al., 2012), and may have other uncharacterized functions.

Studies of the interaction between Apobec2 proteins and Pou6F2 indicate that this interaction is occurring between a non-N-terminal region of Apobec2s and the DNA binding domain of Pou6F2, specifically the sequence encoded by exon 9 (Figure 4.13). The nature of

this interaction remains undefined, but we show that it does not serve to facilitate Pou6F2 sumoylation (Figure 4.13). Interestingly, the expression of Pou6F2 during development is associated with the differentiation of retinal cells (Zhou et al., 1996). Analyses of its binding have also been performed and identified a preference for sequences containing (A/T)AAT. Pou6F2 was also shown to bind the Oct-1 consensus sequence ATGC(A/T)AAT (Zhou et al., 1996). Although searching promoters for regions containing (A/T)AAT likely is not sufficiently stringent, a superficial analysis of genes recently shown to be necessary for MG activation and the proliferation of MGPCs, identified the Oct-1 consensus sequence in the promoters of *lin28*, *insm1a*, and *apobec2a* (Ramachandran et al., 2010a; Powell et al., 2012; Ramachandran et al., 2012). POU proteins have been shown to be both positive and negative regulators of gene expression (Cook and Sturm, 2008). While the transcriptional programs controlled by Pou6F2 are unknown, we speculate that a major function of Pou6F2 is to suppress the stem cell-like nature of MG and to maintain MG in a differentiated state, and as such inhibit regeneration.

Finally, we provide a working model of the cytosine deaminase-independent function of Apobec2a,2b proteins during MG activation and the generation of MGPCs (Figure 4.14). In this model, non-stimulated (no injury) MG are maintained in a differentiated state aided by the binding of Pou6F2 to the promoters of genes required for MG activation and the proliferation of MGPCs, repressing their expression. Differentiated MG have low basal levels of Apobec2a,2b, which are excluded from the nucleus via N-terminal sumoylation facilitated by Ubc9 and Toporsa. After injury, the expression of *apobec2a,2b* is induced, resulting in high levels of Apobec2a,2b some of which are able to enter the nucleus, escaping sumoylation, and interact with the DNA binding domain of Pou6F2, precluding its ability to bind DNA and relieving its inhibitory role. This allows the full activation of genes required for MG activation and the proliferation of MGPCs. Moreover, we hypothesize that a similar model functions during optic nerve regeneration, as we have previously demonstrated that Apobec2a,2b are required for zebrafish axonal regeneration (Powell et al., 2012). In all, this work adds greatly to the understanding of Apobec2 proteins and their conserved function and opens avenues for possibilities of future research.

4.5 Materials and Methods

4.5.1 Animals

Zebrafish were kept at 26-28 °C on a 14/10 hr light/dark cycle. Transgenic *gfap:gfp* (Kassen et al., 2007) and *1016 tuba1a:gfp* (Fausett and Goldman, 2006; Powell et al., 2012) fish have been described previously. Fish were harvested by treatment with a lethal dose of tricaine methane sulfonate (Sigma). Fish were handled in accordance with the University of Michigan Committee on Use and Care of Animals.

In preparation for the construction of *hsp70* transgenic fish, the *1016 tuba1a:gfp SV40* cassette (Fausett and Goldman, 2006) was cloned followed by a second expression cassette encoding 1523 bp of the *hsp70* promoter (Halloran et al., 2000) driving the expression of: 1) *myc-zapobec2b-Viral2apeptide(V2a)-flag-zapobec2a* (*hsp70:zapobec2wt*), 2) *myc-zapobec2b(C180A)-V2a-flag-zapobec2a(C156A)* (*hsp70:zapobec2mut*), or 3) *myc-hAPOBEC2* (*hsp70:hAPOBEC2*) followed by an *SV40* sequence into the *pT2AL200R150G* Tol2 vector (Urasaki et al., 2006). The primers and intermediate clones used in the preparation of these constructs are listed in Table 4.1. Overlap extension PCR was used for the preparation of constructs including V2a peptide sequences (optimized for zebrafish translation) and constructs including mutations. The V2a peptide allows for polycistronic expression (Figure 4.5) (Provost et al., 2007). Tol2 transposase-mediated integration of the transgene was performed by injection into single-cell zebrafish embryos, which were raised to adulthood and screened for transgenic progeny (Powell et al., 2012). Multiple independent lines were selected and grown to adulthood, each exhibiting a similar phenotype (Figure 4.6-4.8).

4.5.2 Site Directed Mutagenesis and Cloning

Site directed mutagenesis was carried out using overlap extension PCR as outlined previously (Ramachandran et al., 2011) and the primers listed in Table 4.1. Cloning was carried out using Phusion DNA Polymerase (NEB) and the primers listed in Table 4.1. Each clone was sequenced by the University of Michigan DNA Sequencing Core (UMDSC). For this study, clones were used in the following applications: mRNA preparation (pCS2 *flag-zapobec2a-V2a-GFP* and pCS3+MT *myc-zapobec2b-V2a-GFP*), creation of transgenic fish

(pTal *hsp70:zapobec2wt*, pTal *hsp70:zapobec2mut*, and pTal *hsp70:hAPOBEC2*), mutagenesis assays (pHis, pHis- (pHis with the His tag removed) *rApobec1*, pHis- *rApobec1(W90S)*, pHis- *hAID*, pHis- *hAPOBEC2*, pHis- *hAPOBEC2(T)*, pHis- *hAPOBEC2(S125W)*, pHis- *zApobec2a*, pHis- *zApobec2a(T)*, pHis- *zApobec2a(S153W)*, pHis- *zApobec2b*, pHis- *zApobec2b(T)*, and pHis- *zApobec2b(S177W*), yeast two-hybrid assays (pLexAADE2Noti(pLexA) *hAPOBEC2*, pLexA *hAPOBEC2(T)*, pLexA *zApobec2a*, pLexA *zApobec2a(T)*, pLexA *zApobec2b*, pLexA *zApobec2b(T)*, pVP16 *zApobec2a*, and pVP16 *Pou6F2DNABindingDomain*(*dbd*)), bacterial sumoylation assays (pT *E1E2S1* (Uchimura et al., 2004b), pT *E1E2(C93A)S1*, pETDuet *flag-Toporsa*, pGST *hAPOBEC2*, pGST *hAPOBEC2(T)*, pGST *zApobec2a*, pGST *zApobec2a(T)*, pGST *zApobec2b*, pGST *zApobec2b(T)*, pETDuet *GST-Pou6f2dbd,* pHis- *hAPOBEC2*, pHis- *zApobec2a*, and pHis- *zApobec2b*), and tissue culture analyses (pEGFP, pCS2 *hSUMO1-gfp*, pCS2 *hAPOBEC2-gfp*, pCS2 *hSUMO1-hAPOBEC2-gfp*, pCS2 *hAPOBEC2(T)-gfp*, pCS2 *hAPOBEC2*(*K4R*)-*gfp*, pCS2 *zApobec2a-gfp*, pCS2 *hSUMO1-zApobec2a-gfp*, pCS2 *zApobec2a(T)-gfp*, pCS2 *zApobec2b-gfp*, pCS2 *hSUMO1-zApobec2b-gfp*, and pCS2 *zApobec2b(T)-gfp*). pCDNA V5 hAPOBEC2 (provided by Dr. Hongjun Song, Johns Hopkins University), pTrc99a hAID (provided by Dr. Michael Neuberger, Medical Research Council Laboratory of Molecular Biology), pTrc99a rApobec1 (provided by Dr. Michael Neuberger, Medical Research Council Laboratory of Molecular Biology), pCRIITopo zApobec2a (provided by Dr. David Jones, University of Utah), and pCRIITopo zApobec2b (provided by Dr. David Jones, University of Utah) served as templates for cloning. *hSUMO1* was cloned using cDNA prepared from HEK293 cells. The pLexA and pVP16 plasmids were provided by Dr. Anne Vojtek (University of Michigan) and pT-E1E2S1 was provided by Dr. Jeremy Henley (University of Bristol).

4.5.3 Retina Injury, BrdU Injections, Morpholino-Mediated Gene Knockdown, and Heat Shock

Retina lesions and BrdU injections have been described previously (Fausett and Goldman, 2006; Veldman et al., 2010; Powell et al., 2012). Lissamine-tagged morpholino antisense oligonucleotides (MOs) (Gene Tools) were delivered at the time of injury by using a Hamilton syringe. MO delivery to cells was facilitated by electroporation as described

(Powell et al., 2012). The control, *apobec2a*, and *apobec2b* targeting MOs have been described previously (Rai et al., 2008; Powell et al., 2012; Powell et al., 2013). Heat shock was carried out carried out at 36.5 °C as has been described (Ramachandran et al., 2012). Unless indicated otherwise, in the analyses of uninjured fish, heat shock was carried out every 12 hours for 1 hour each over a four-day period (Figure 4.8A and B). For analyses of injured fish, heat shock was carried out at 9 hours post injury (hpi, 1 hour heat shock), 24hpi (1 hour heat shock), 28hpi (30 min heat shock), and 33hpi (1 hour heat shock) to mimic the induction of endogenous *apobec2a,2b*, and fish were harvested 48hpi. Analyses were performed using size and age matched fish. Transgenic fish analyzed in this study were heterozygous.

4.5.4 Fluorescence Activated Cell Sorting

FACS sorting of GFP+ cells from uninjured (0 hours, 0hrs) *gfap:gfp* and 4 days post injury (dpi) *1016 tuba1a:gfp* transgenic fish and FACS sorting of GFP+, lissamine+ cells from 2dpi *gfap:gfp* transgenic fish injected/electroporated with lissamine-tagged morpholino was carried out as previously described (Powell et al., 2013). Briefly, zebrafish retinas were collected in 0.8 mL Leibovitz's L15 medium, treated for 15 min with 1 mg/mL hyaluronidase (Sigma) at room temperature, and then dissociated in 0.01% (vol/vol) trypsin with frequent trituration. A single-cell suspension was confirmed by microscopy and cells were washed in Leibovitz's L15 medium before sorting. Cell sorting was performed by the University of Michigan Flow Cytometry Core on a BC Biosciences FACSAria 3 laser high-speed cell sorter.

4.5.5 RNA-seq Library Preparation and mRNA Variant Analyses

RNA was isolated from GFP+ MG or from GFP+, lissamine+ 2dpi MGPCs using the Direct-zol RNA MiniPrep Kit (Zymo Research) and was treated with DNase (Invitrogen). RNA for each sample was submitted to the UMDSC for the generation of RNA-seq libraries according to the Illumina TruSeq protocol. Two independent libraries were prepared for each sample, and all libraries were multiplexed in one lane for sequencing. Sequencing was performed on an Illumina HiSeq 2000 sequencer at the UMDSC. The starting template amount, sequencing method, and the number of sequence reads for each library are listed in

Table 4.2.

In preparation for sequence alignment, BOWTIE indexes were created of the zebrafish genome assembly Zv9 using BOWTIE-BUILD (Langmead et al., 2009). CUFFDIFF indexes were created of the zebrafish transcript annotations Zv9.69 using CUFFCOMPARE (Trapnell et al., 2010). Initial library quality control metrics were performed using FASTQC (www.bioinformatics.babraham.ac.uk/projects/fastqc/), which indicated the presence of some adapter and primer contamination. Sequences were aligned to the genome using TOPHAT2 (Kim et al., 2013). Alignment statistics are listed in Table 4.2. FASTQC quality metrics after alignment indicated that the adapter/primer contamination was no longer problematic.

For variant analyses, variants were called from aligned reads compared to the zebrafish genome (Zv9) using SAMTOOLS/MPILEUP (Li et al., 2009). Variants were filter based on their presence in both replicas. Non-genic variants and variants that fell 5bp from possible splice junctions were filtered employing SNPEFF and SNPSIFT, respectively (http://snpeff.sourceforge.net/). Previous work has reported a propensity for artifactual variant calls near splice junctions (Park et al., 2012). Finally, the variant positions were filtered with the following quality metrics: minimum QUAL (ovariant likelihood, Phred-scaled) of 20, minimum MQ (mapping quality) of 50, and minimum DEPTH (depth of coverage at variant position) of 10. The correct strand for the mRNA was identified to determine what mutation was being called. Table 4.3 lists the total called variants by type for each sample. For analyses of cytosine deamination, the relative abundance of each C-to-T variant for each library was calculated by dividing the number of variant calls by the total sequence calls for that position. The variant abundance of the 0hrs, 2dpi control MO, and 2dpi *apobec2a,2b* MO samples was determined by taking the average variant abundance of their respective replicas. Comparisons between 0hrs and 2dpi control MO, 0hrs and 2dpi *apobec2a,2b* MO, and 2dpi control MO and 2dpi *apobec2a,2b* MO samples were carried out at every C-to-T variant position that met the quality metrics listed above in both sample sets (Figure 4.1 and 4.2).

4.5.6 RNA Isolation, RT-PCR, and Real-Time PCR

Total RNA was isolated using TRIzol (Invitrogen) and was DNase treated

(Invitrogen). cDNA synthesis was performed using random hexamers and either SuperScript-II (Invitrogen) or M-mulv (NEB) reverse transcriptase. PCR reactions used Taq and gene-specific primers (Table 4.1). Real-time PCR reactions were carried out with ABsolute SYBR Green Fluorescein Master Mix (Thermo Scientific) on an iCycler real-time PCR detection system (Bio-Rad). The ΔΔCt method was used to determine relative expression of mRNAs. Student T tests were performed to determine statistical differences between samples.

4.5.7 mRNA Synthesis and Embryo Microinjections

pCS2 *flag-zapobec2a-V2a-GFP* and pCS3+MT *myc-zapobec2b-V2a-GFP* plasmids were linearized with NotI (NEB) and capped mRNAs were synthesized using the mMESSAGE mMACHINE (Ambion). Single cell zebrafish embryos were injected with ~200 pL of solution containing 0.125 mM MO or 0.125 mM MO with 2 ng/μL of mRNA.

4.5.8 Bacterial Mutagenesis and Growth Assays

Bacterial mutagenesis assays were carried out as described (Harris et al., 2002a; Petersen-Mahrt et al., 2002). Briefly, BL21(DE3) cultures harboring the indicated plasmid were grown at 37 °C in 2 mL of LB containing 100 μg/mL ampicillin to an OD 600. 1 ml of LB containing 100 μg/mL ampicillin, 3 mM isopropyl-β-D-thiogalactopyranoside (IPTG) was then added and the culture was grown over night with shaking at either 37 °C or 25 °C (Barreto et al., 2005; Dancyger et al., 2011). The next day, 1 mL of the culture was harvested, spun down, and spread onto a plate containing LB and 100 μg/mL rifampicin. Samples were allowed to grow over night at 37 °C, and the next day the number of growing colonies was quantified. To identify mutations that were occurring in the *rpoB* gene, colony PCR was carried out on rifampicin+ colonies using the rpoB primers (Table 4.1). PCR products were sequenced by the UMDSC. Variants were identified by comparison with the wild type *rpoB* sequence as has been done by others (Harris et al., 2002a; Petersen-Mahrt and Neuberger, 2003). For bacterial growth assays, protein expression was induced overnight as outlined above for the bacterial mutagenesis assay. The following day, the OD 600 for each sample was determined. Student T tests were performed to determine statistical differences between the control and experimental samples.

4.5.9 Tissue Preparation and Immunofluorescence

Zebrafish eyes were prepared, sectioned at 12 micron, and stained as has been done previously (Powell et al., 2012; Powell et al., 2013). The following primary antibodies were used for immunofluorescence: rat anti-BrdU (dividing cell marker, 1:1000, Abcam), mouse anti-PCNA (dividing cell marker, 1:500, Sigma), rabbit anti-GFP (1:1000, Invitrogen), mouse anti-Flag (1:1000, Rockland), and rabbit anti-Myc (1:1000, Sigma). The following secondary antibodies were used: Alexa Flour 555 donkey anti-mouse IgG (1:1000, Invitrogen), Alexa Flour 488 donkey anti-mouse IgG (1:1000, Invitrogen), Alexa Four 488 goat anti-rabbit IgG (1:1000, Invitrogen), and Cy3 donkey anti-rat (1:1000, Jackson Immunoresearch). Antigen retrieval for BrdU and PCNA staining was performed by boiling the sections in 10 mM sodium citrate for 20 min followed by cooling them for another 20 min in solution.

4.5.10 Preparation of Full-Length Normalized Yeast two-hybrid Library

RNA was purified from FACS sorted GFP+ cells isolated from 4dpi *1016 tuba1a:gfp* transgenic fish and treated with DNase (Invitrogen). Library preparation was performed using the EasyClone normalized cDNA library construction package (Dualsystems Biotech) as outlined by the manufacturer. Briefly, 500 ng of RNA was used for the production of cDNA, ds cDNA synthesis was carried out for 21 cycles, and 1200 ng of ds cDNA was used for library normalization. Normalized library amplification was then carried out using Phusion DNA Polymerase (NEB) and the Y2HlibraryascI-F and Y2HlibrarynotI-R primers (Table 4.1). These were cloned into a modified pVP16ascI construct into the AscI (NEB) and NotI (NEB) sites. Library ligation was carried out with 250 ng of template and 250 ng of backbone. To assay the quality of the library, a small aliquot of this ligation was transformed, and the inserts size of 20 independent colonies was measured. Average insert size was ~1330 bp. A large-scale transformation was then performed using DH10B Electromax Ultracompetent Cells (Invitrogen) resulting in ~2 million independent transformants. Transformants were scrapped from their plates, and plasmid and bacterial stocks were prepared of the pVP16 4dpi *1016 tuba1a:gfp* yeast two-hybrid library as outlined by the EasyClone normalized cDNA library construction package.

4.5.11 Yeast Transformations and Yeast two-hybrid Screens

Yeast transformation and large scale yeast two-hybrid screens for Apobec2a (pLexA *zApobec2a*) and Apobec2b (pLexA *zApobec2b*) using the pVP16 4dpi *1016 tuba1a:gfp* yeast two-hybrid library were performed using standard protocols described by others (Bartel and Fields, 1997). The library was screened to 3X coverage. Protein interactions were assessed by two independent assays: growth assays on YC-WHULK plates and β-Galactosidase filter assays. To identify interacting VP16 protein fusions, colony PCR was performed using YC-WHULK+ L40 colonies (transferred and grown on > 4 independent plates for correct plasmid selection in case multiple VP16 clones were transformed in the original screen) using the Y2HVP16CPCR primers listed in Table 4.1 and Phusion DNA Polymerase (NEB). PCR products were then sequenced using the Y2HVP16seqp primer (Table 4.1) by the UMDSC.

4.5.12 Bacterial Sumoylation Assays and Western Blotting

Bacterial sumoylation assays were carried out as described (Uchimura et al., 2004b). Briefly, BL21(DE3) cultures harboring the indicated plasmids were grown at 37 °C in 2 mL of LB containing appropriate antibiotics (100 μg/mL ampicillin, 50 μg/mL kanamycin, and/or 50 μg/mL chloramphenicol) to an OD 600. 1 ml of LB containing appropriate antibiotics and 3 mM IPTG was then added and the culture was grown over night with shaking at 25 °C. Bacteria were then pelleted and stored at -80 °C until use. Predictions of sumoylation sites were performed using SUMOsp 2.0 (Xue et al., 2006) and the SUMOplotTM Analysis Program (www.abgent.com/sumoplot).

In preparation for Western blotting, bacteria were lysed with boiling in 1X denaturing SDS-PAGE loading buffer and spun down to pellet particulate matter. Microinjected zebrafish embryos were lysed by sonication on ice in nuclei lysis buffer (50 mM Tris-HCl pH 7.5, 10 mM EDTA, 1% SDS) including a protease inhibitor cocktail (Thermo). Extract from lysed embryos was then boiled in 1X denaturing SDS-PAGE loading buffer. Proteins were resolved on 8% or 10% SDS-PAGE gels and transferred to nitrocellulose membranes. Blots were blocked for 1 hour in 1X PBS, 0.1% Tween containing 3% donkey serum (Sigma) before probing with antibodies. For the detection of GST-tagged proteins, blots were incubated with primary antibody diluted in blocking solution for 1 hour at room temperature, followed by washing and protein detection. The probing of all other blots was performed as

outlined previously (Powell et al., 2012). The following primary antibodies were used: mouse anti-Flag (1:12.000, Rockland), rabbit anti-Myc (1:12,000, Sigma), rabbit anti-GFP (1:12,000, Invitrogen), mouse anti-SUMO1 (1:10,000, Santa Cruz) and mouse anti-GST conjugated with HRP (1:5,000, Santa Cruz). The following secondary antibodies were used: goat anti-rabbit IgG conjugated to HRP (1:15,000, Rockland) and goat anti-mouse IgG conjugated to HRP (1:15,000). Proteins were detected using Lumi Lights Western Blotting Substrate (Roche) and exposed using X-ray film or a FlourChem M Digital Darkroom.

4.5.13 Tissue Culture

Human embryonic kidney cells (HEK293T) cells were maintained on 100mM dishes in Dulbecco's Modified Eagle's Medium (Life Technologies, USA) supplemented with 4.5 g/L D-glucose, 2mM glutamine, 10% fetal bovine serum (FBS), and penicillin/streptomycin (Life Technologies, USA) at 37º C with 5% CO_2. Cells were seeded on 12 mM cover slip glass in 24-well plates and allowed to grow to 50-70% confluency before transfection with 200 ng of plasmid DNA using Lipofectamine 2000 (Invitrogen). After transfection, cells were either placed at 37 ºC for 24 hours or at 37 ºC for 4 hours and then 28 ºC for 20 hours before fixation with 4% PFA/PBS (w/v) and DAPI staining.

4.5.14 Imaging and Image Analysis

Retinal sections were examined using a Zeiss Axiophot, Axio Observer Z.1 microscope. Images were captured using a digital camera adapted onto the microscope and were processed/annotated with Adobe Photoshop CS4. For the quantification of PCNA+ cells, eyes injured 4X (once in each quadrant) were sectioned across four slides. The total number of PCNA+ cells per slide was quantified for three individual eyes per condition. Student T tests were performed to determine statistical differences between the control and experimental samples.

Cover slips with transfected HEK293T cells were mounted onto glass slides in DABCO and imaged using an Olympus BX62 laser-scanning confocal microscope equipped with 405, 488, and 543 nm lasers and a 60x PlanApo N 1.42 NA oil immersion objective. Densitometric means of cytoplasmic and nuclear GFP signal were calculated in ImageJ. The

ratio of nuclear to cytoplasmic signal was calculated for at least $n \geq 25$ cells per condition. Student T tests were performed to determine statistical differences between samples.

4.6 Acknowledgements

This work was supported by NEI Grants RO1 EY018132, 1R21 EY022707 (D. Goldman), the University of Michigan Vision Research Training Grant 5T32EY13934-10 (C. Powell), and the University of Michigan Predoctoral Fellowship (C. Powell). I thank A. Grant for help with variant analyses; E. Cornblath for help in cloning and experiments done using tissue culture; A. Vojtek for suggestions concerning experiments involving yeast; H. Song, M. Neuberger, D. Jones, A. Vojtek, and J. Henley for providing plasmids; the University of Michigan Flow Cytometry Core; the University of Michigan DNA Sequencing Core; R. Karr and J. Kirk for fish care; Members of the Goldman lab for helpful comments.

4.7 Figures

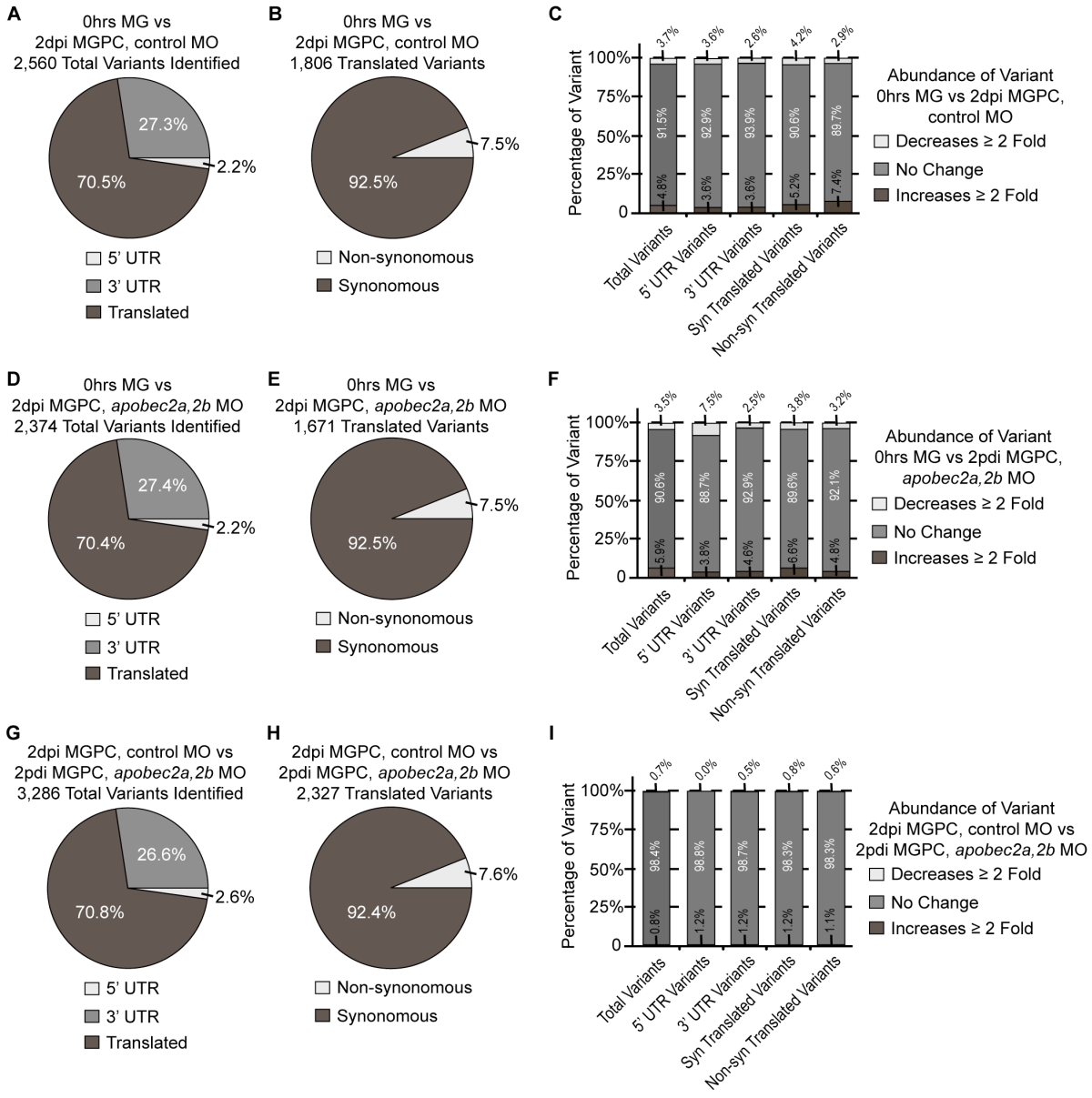

Figure 4.1 mRNA analyses reveal injury-dependent C-to-U editing during MG activation to a MGPC, which occurs independent of Apobec2a,2b

(A, B, C) Comparisons of the 0hr MG and the 2dpi MGPC, control MO libraries. Graph depicting (A) the localization of C-to-T variants within the transcript and (B) the classification of C-to-T variants localized to translated regions of their respective transcript as either synonymous (no change in protein coding) or non-synonymous (changes amino acid codon). (C) Comparison of the abundances of each C-to-T variant suggests that some are differentially abundant, increasing or decreasing ≥ 2 fold as a MG transitions to a MGPC, indicative of changes in C-to-U editing. (D, E, F) Comparisons of the 0hr MG and the 2dpi MGPC, *apobec2a,2b* MO libraries and (G, H, I) comparisons of the 2dpi MGPC, control MO and the 2dpi MGPC, *apobec2a,2b* MO libraries as done in (A, B, C) for their respective

libraries suggests this C-to-U mRNA editing occurs independent of Apobec2a,2b. MGPC, Müller glia progenitor cell; Syn, synonymous; Non-syn, non-synonymous; UTR, untranslated region.

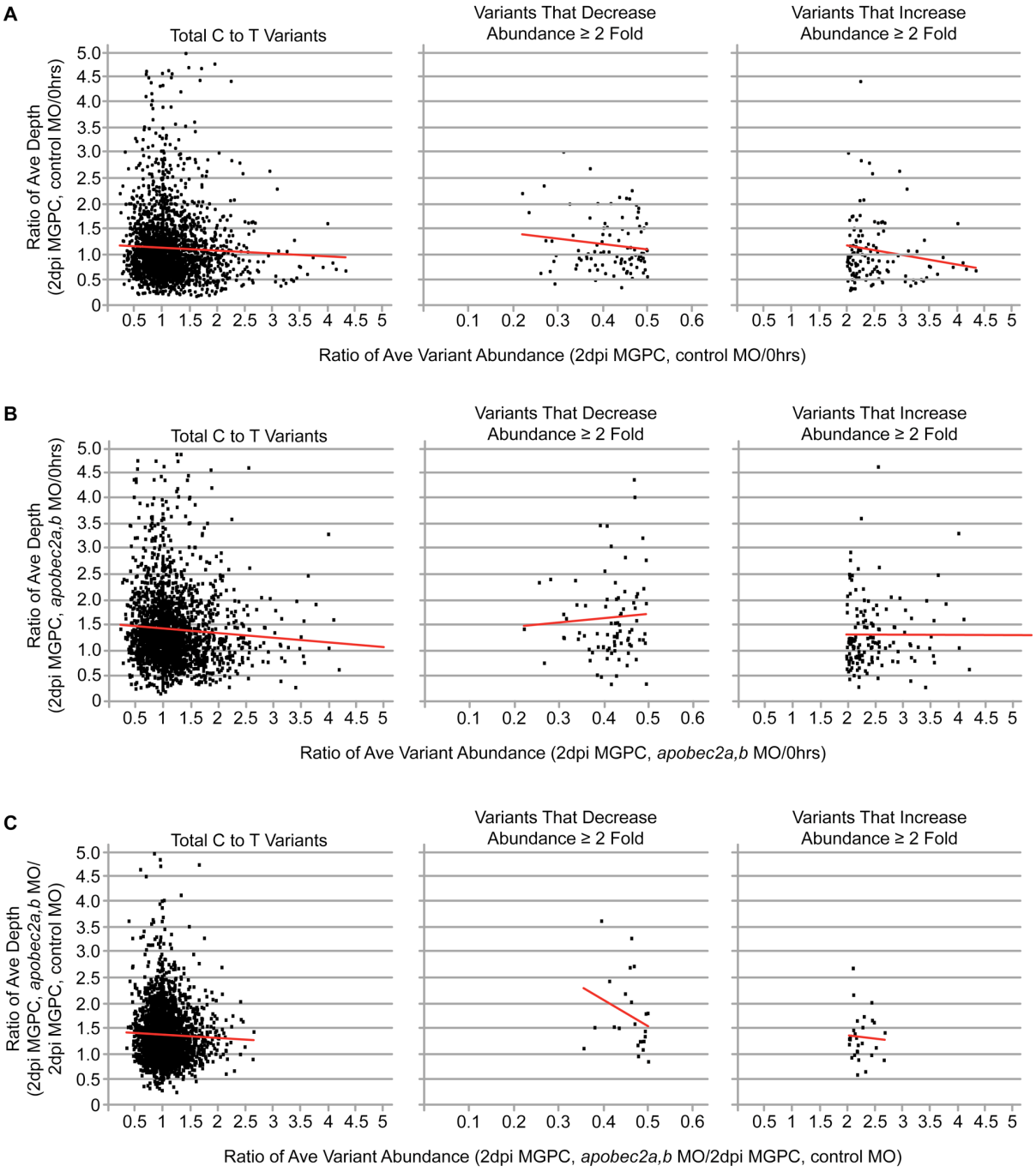

Figure 4.2 Comparisons of variant abundance and variant depth

(A, B, C) Comparisons of the (A) 0hr MG and the 2dpi MGPC, control MO libraries, (B) the 0hr MG and the 2dpi MGPC, *apobec2a*,*2b* MO libraries, and (C) the 2dpi MGPC, control MO and the 2dpi MGPC, *apobec2a*,*2b* MO libraries. Plots of C-to-T variants. Each individual point represents an independent C-to-T variant. The X-axis represents the difference in the abundance of each individual variant (average of both replicas) and the Y-axis represents the difference in the sequencing depth at the position of each variant (average of both replicas). Plots of total C-to-T variants (left) and variants decreasing (middle) or

increasing (right) in abundance by ≥ 2 fold in the indicated comparison demonstrates that differences in abundance are not correlated with differences in depth. Abbreviations as in Figure 4.1.

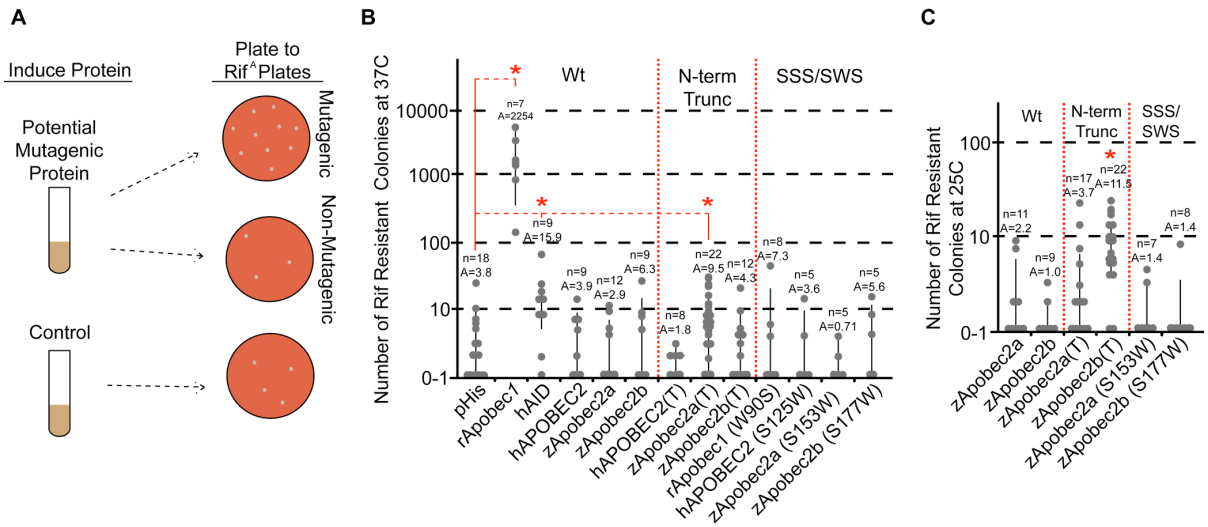

Figure 4.3 Bacterial mutagenesis assays suggest that Apobec2a,2b lack catalytic activity

(A) Graphic providing an overview of the bacterial mutagenesis assay. (B and C) Bacterial mutagenesis assays carried out at (B) 37 °C and (C) 25 °C. Graphs are in log scale. Compared to pHis (empty vector) the induction of rApobec1, hAID, zApobec2a(T) at 37 °C, and zApobec2b(T) at 25 °C resulted in significant increases in bacterial survival. *$P <$ 0.02369. The number of replicas (n) and the average colony number (**A**) is listed for each sample. Wt, wild type; trunc, truncation; Rif, rifampicin.

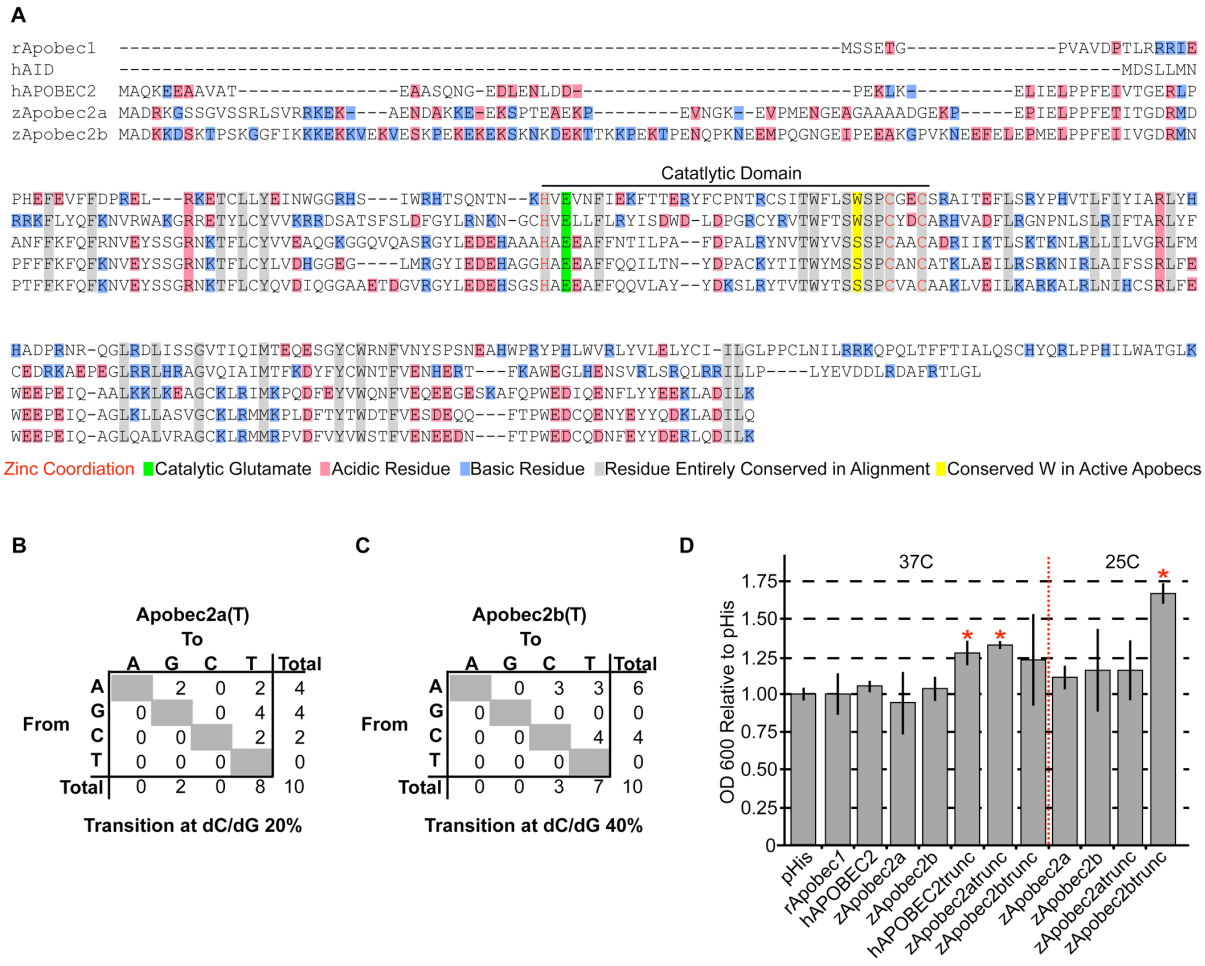

Figure 4.4 Apobec protein alignment, rpoB mutations, and bacterial growth assays

(A) ClustalW alignment of the proteins analyzed in the bacterial mutagenesis assay highlighting differences in protein charge, N-termini, and catalytic domains. Annotations are defined at the bottom of the figure. (B and C) Quantifications of dC/dG transitions in the *rpoB* sequence in rifampicin resistant colonies growing after induction of (B) Apobec2a(T) at 37 °C or (C) Apobec2b(T) at 25 °C, as select mutations in *rpoB* lead to rifampicin resistance. The low abundance of dC/dG transitions (C to T or G to A mutations that are indicative of cytosine deamination), relative to other previously studied Apobecs, suggest that the increased survival of bacteria following inductions of Apobec2a(T) at 37 °C or Apobec2b(T) at 25 °C occurs in a cytosine deaminase-independent manner. (D) Bacterial growth assays comparing the final growth densities of bacteria induced to express the indicated protein. Compared to pHis (empty vector) the induction of hAPOBEC2(T), zApobec2a(T) at 37 °C, and zApobec2b(T) at 25 °C resulted in significant increases in bacterial density. n = 4 for each sample. *$P < 0.00076$.

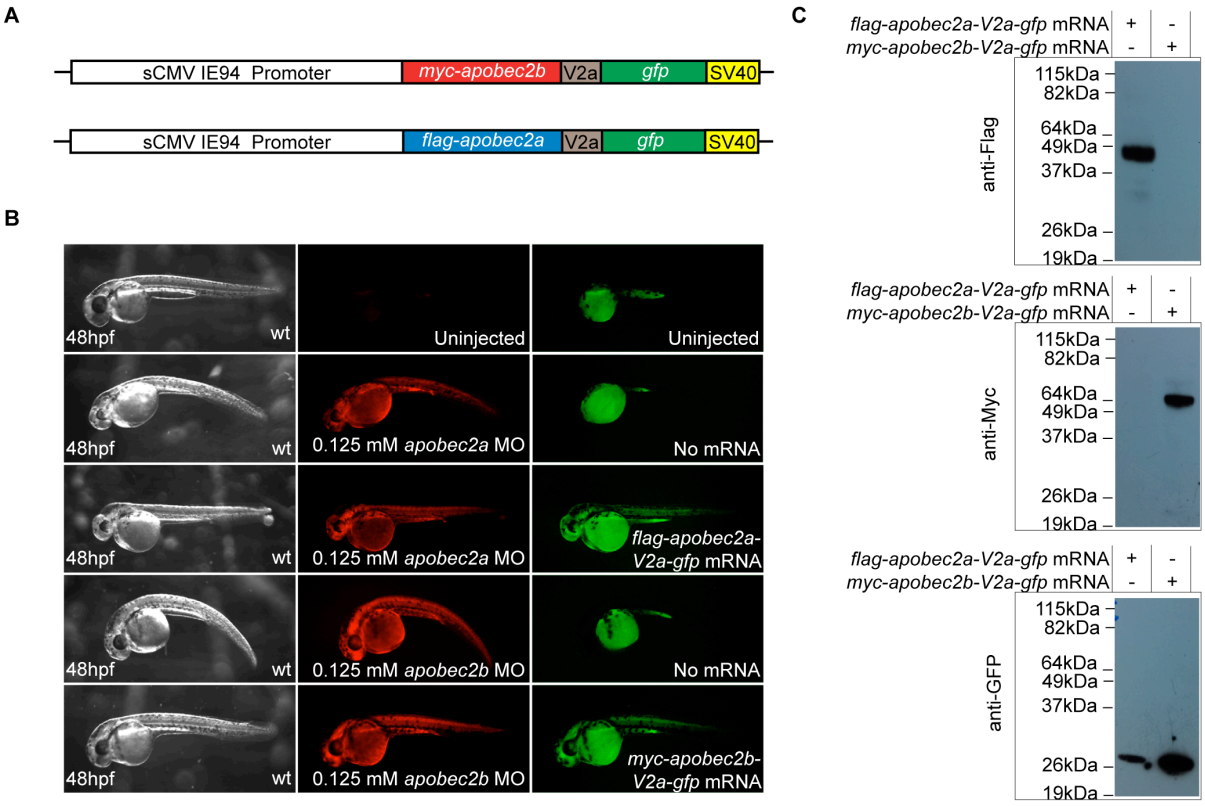

Figure 4.5 N-terminally tagged Apobec2a,2b proteins and the viral 2a peptide are functional in zebrafish

(A) Graphic depicting the makeup of the pCS2 clones used to create *myc-apobec2b-V2a-gfp* and *flag-apobec2a-V2a-gfp* mRNAs for microinjection. (B) The expression of *myc-apobec2b-V2a-gfp* and *flag-apobec2a-V2a-gfp* mRNAs escape MO knockdown, as indicated by the expression of GFP. Furthermore, knockdown of Apobec2a or Apobec2b during zebrafish development has been shown to cause muscle dystrophies manifest by a curved body axis (Etard et al., 2010). Here we show that microinjection of *flag-apobec2a-V2a-gfp* or *myc-apobec2b-V2a-gfp* mRNA rescues the Apobec2a/b developmental knockdown phenotype, suggesting that these tagged proteins function properly. (C) The proper functioning of the viral 2a (V2a) peptide was demonstrated after microinjection of *flag-apobec2a-V2a-gfp* or *myc-apobec2b-V2a-gfp* mRNA. Western blotting showed the proper separation of Apobec2 and GFP proteins. hpf, hours post fertilization.

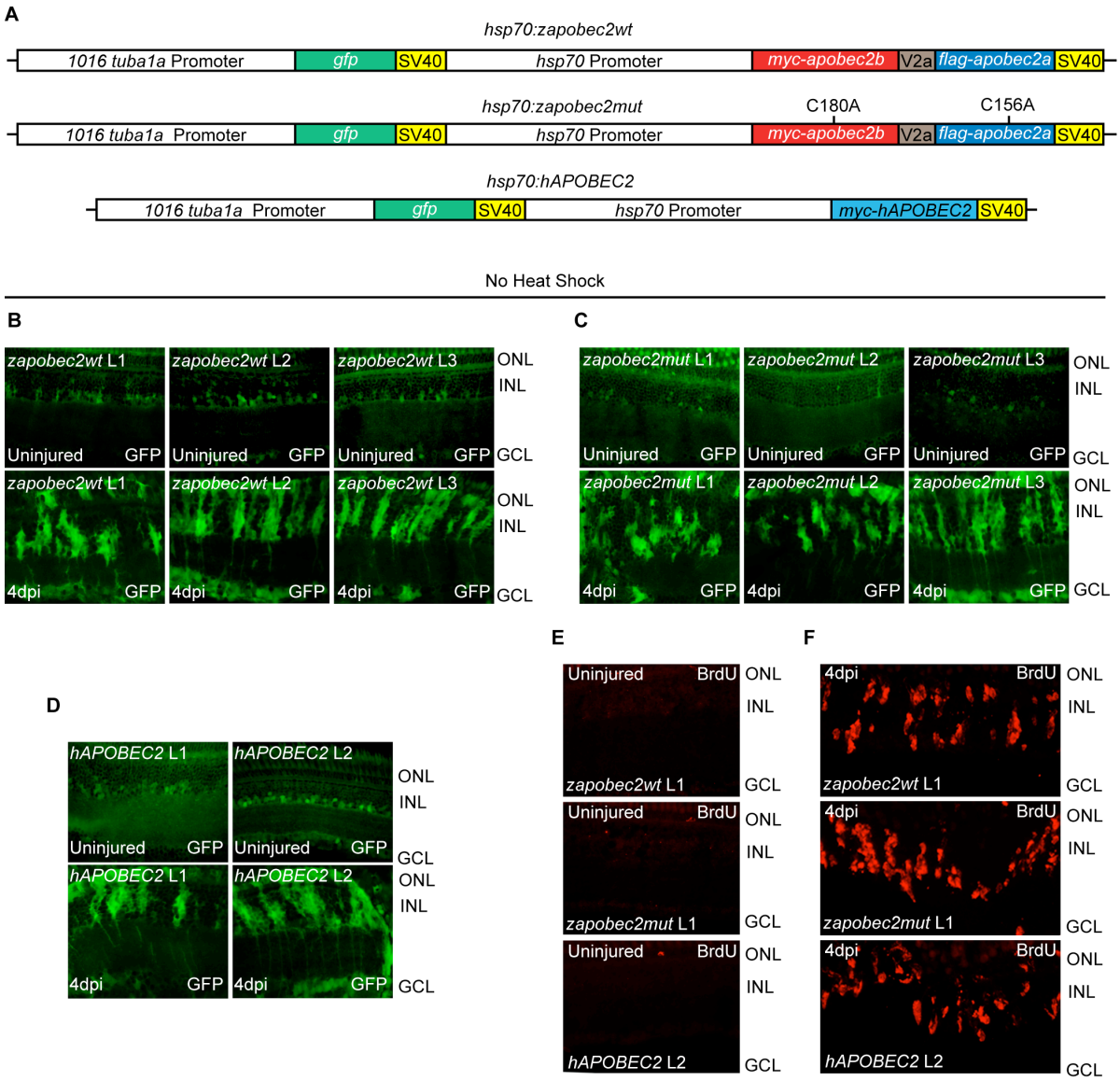

Figure 4.6 Analyses of transgene expression and proliferation in uninjured and injured transgenic fish, in the absence of heat shock

(A) Graphic depicting the composition of the *hsp70:zapobec2wt, hsp70:apobec2mut* and *hsp70:hAPOBEC2* transgenes. (B, C, D) GFP immunostaining of uninjured (top panel) or 4dpi (bottom panel) retinas shows basal and injury-dependent expression of the *1016 tuba1a:gfp* expression cassette in (B) *hsp70:zapobec2wt*, (C) *hsp70:zapobec2mut*, and (D) *hsp70:hAPOBEC2* transgenic fish. (E and F) BrdU immunostaining of (E) uninjured or (F) 4dpi transgenic fish retinas indicates that *hsp70:zapobec2wt, hsp70:zapobec2mut,* and *hsp70:hAPOBEC2* transgenic fish retinas show similar basal and injury-dependent levels of cellular proliferation as wild type fish. Fish were given a pulse of BrdU 3 hours prior to harvest. L, line; ONL, outer nuclear layer; INL, inner nuclear layer; GCL, ganglion cell layer; dpi, days post injury.

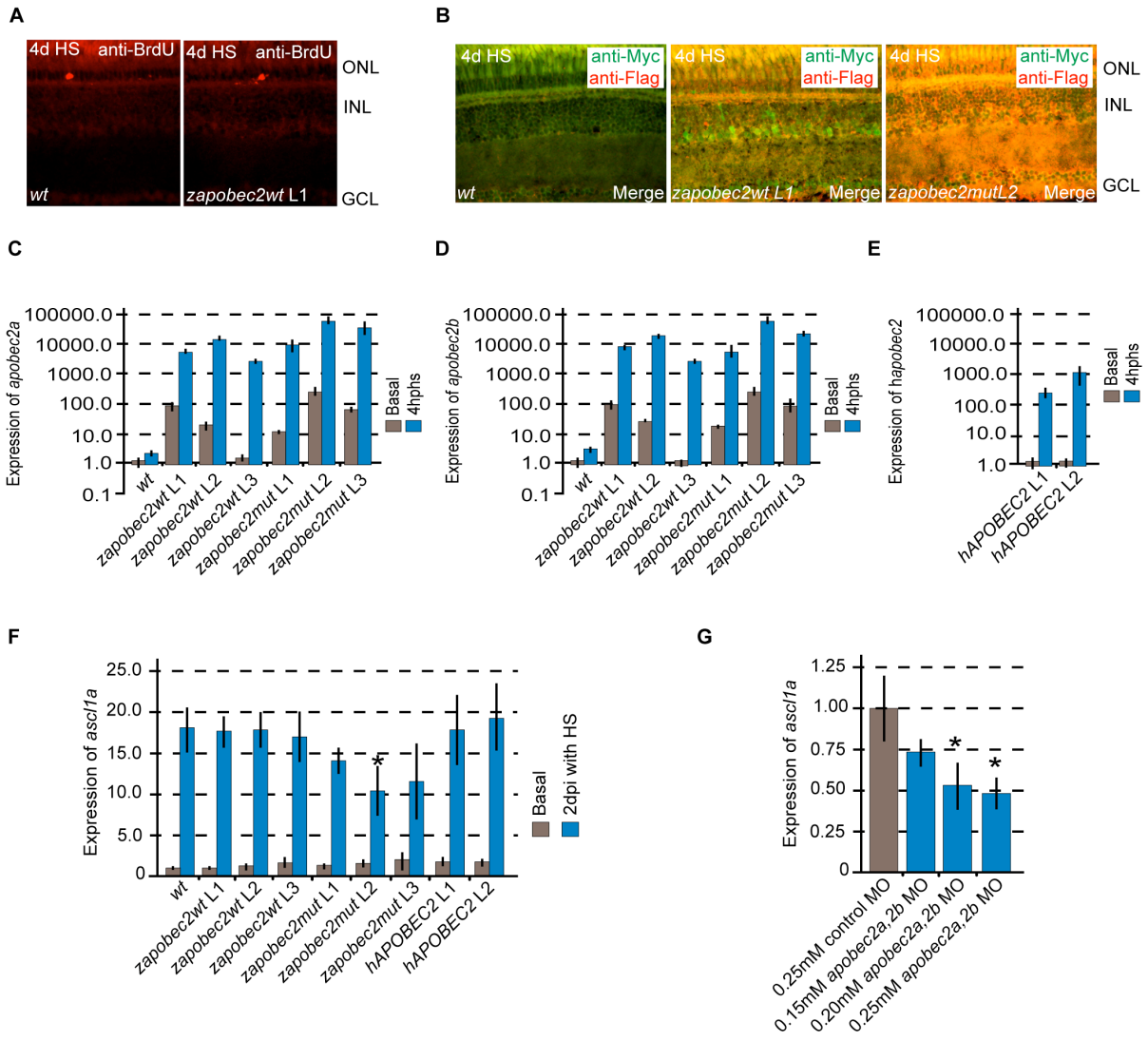

Figure 4.7 Analyses of transgenic fish following heat shock

(A) Four days of heat shock did not induce proliferation in uninjured *zapobec2wt* transgenic fish demonstrating that while Apobec2a,2b are required for retina regeneration, they are not sufficient. Fish were given a pulse of BrdU 3 hours prior to harvest. (B) Heat shock induced the production of transgenic proteins as measured by immunostaining. (C, D, E) Real-time PCR quantifications were carried out to measure basal and 4 hours post heat shock (4hphs) levels of *apobec2a, apobec2b,* and *hAPOBEC2* in retinas isolated from the indicated fish backgrounds. The *apobec2a* and *apobec2b* primers recognize both endogenous and exogenous mRNAs. The expression levels of *apobec2a* and *apobec2b* were normalized to the expression of *gapdh* and compared to the basal levels of wild type (wt) fish, which were given a value of 1. The expression levels of *hAPOBEC2* were normalized to the expression of *gapdh* and compared its basal level in each respective line, which was given a value of 1. Data represents means ± s.d. (n = 3 individual cDNA sets). These results demonstrate that the expression of these transgenes can be controlled through heat shock. While basal and induced levels of these transcripts seem excessive, it is important to realize

that this expression is spread across many retinal cells, which do not normally express these genes, and after injury (in a wild type fish) their endogenous expression is highly induced in a small fraction of the cells residing in the retina. How the MG expression levels (before and after injury) of the exogenous Apobec genes compare to the levels of the endogenous Apobec genes is not clear. (F) Real-time PCR quantifications of basal and injury-dependent (with heat shock) *ascl1a* expression. Transgenic fish show normal levels of *ascl1a* expression in the uninjured, non-heat shocked retina. Analyses performed after injury and with heat shock demonstrate that the activation of the *zapobec2wt* and *hAPOBEC2* transgenes does not impact the injury-dependent activation of *ascl1a,* while the activation of the *zapobec2mut* transgene negatively influences *ascl1a* expression. The expression levels of *ascl1a* were normalized to the expression of *gapdh* and compared to the basal levels of wild type (wt) fish, which was given a value of 1. Data represents means ± s.d. (n = 3 individual cDNA sets). (G) Real-time PCR quantifications of injury-dependent *ascl1a* expression at 2dpi following control or Apobec2a,2b knockdown. 0.20 mM *apobec2a,2b* MO consistently diminished the injury-dependent induction of *ascl1a* expression and was used in the rescue experiments reported in this study (Figure 4.8). *ascl1a* mRNA levels were normalized to the expression of *gapdh* and compared to the value of the control MO, which was given a value of 1. Data represents means ± s.d. (n = 3 individual cDNA sets). $*P < 0.03088$. Abbreviations as in Figure 4.6.

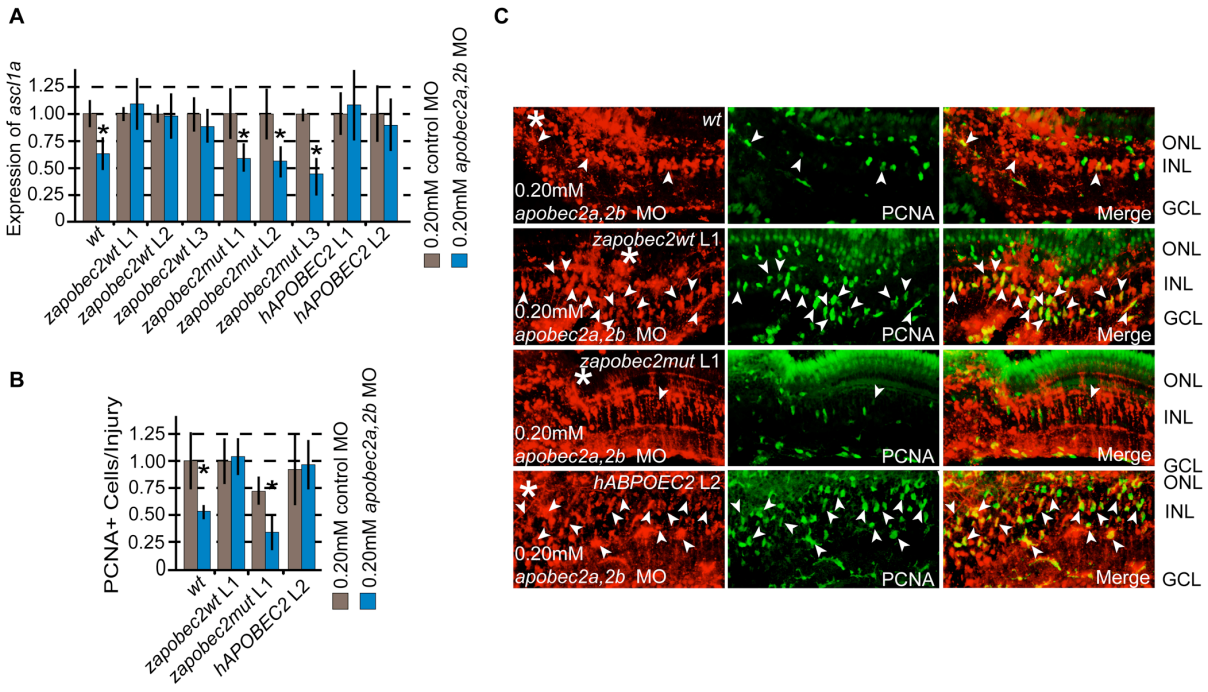

Figure 4.8 Induction of the zapobec2wt and hAPOBEC2 transgenes, but not the zapobec2mut transgene, rescues regeneration following knockdown of endogenous Apobec2a,2b

(A) Real-time PCR quantifications of injury-dependent *ascl1a* mRNA expression levels at 2dpi following control or endogenous Apobec2a,2b knockdown in combination with heat shock to induce the expression of transgenes. The induction of *zapobec2* and *hAPOBEC2,* but not *zapobec2mut*, restores *ascl1a* mRNA levels to that of a normal regenerative response. *ascl1a* mRNA levels were normalized to the expression of *gapdh* and compared to the value of the control MO sample for their respective transgenic line, which was given a value of 1. Data represents means ± s.d. (n = 3 individual cDNA sets). (B) Quantification of the number of PCNA+ cells per injury at 2dpi following control or endogenous Apobec2a,2b knockdown demonstrates that the induction of *zapobec2wt* and *hAPOBEC2,* but not *zapobec2mut*, rescues the proliferative response to the levels of the control MO. Quantifications were normalized to the levels in the wild type control MO sample, which was given a value of 1. Data represents means ± s.d. (n = 3 independent fish). (C) Representative *apobec2a,2b* MO images from (B). Arrowheads designate PCNA+, lissamine+ cells. The induction of the *zapobec2wt* and *hAPOBEC2* transgenes rescues the proliferative response, as indicated by the increase in the number of PCNA+ cells and the increase in co-localization of lissamine and PCNA staining. *$P < 0.04132$. Abbreviations as in Figure 4.6.

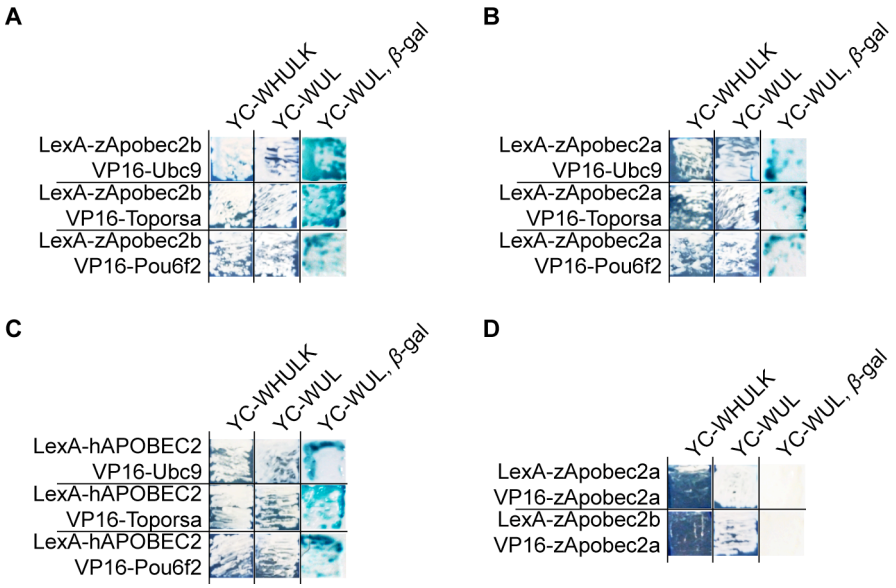

Figure 4.9 Yeast two-hybrid analyses identify conserved Apobec2 interacting proteins

(A, B, C) Yeast two-hybrid assays using two independent analyses to assess protein interactions (growth on YC-WHULK plates [white cells] and blue staining in β-Galactosidase filter assays) demonstrate the conserved interaction between (A) Apobec2b, (B) Apobec2a, and (C) APOBEC2 with Ubc9, Toporsa, and Pou6F2. (D) Yeast two-hybrid assays designed to measure the homo- or heterodimerization of Apobec2 proteins suggest that Apobec2 proteins do not oligomerize within yeast. The omission of tryptophan (W), leucine (L), uracil (U), or lysine (K) from the media maintains selection for the LexA plasmid, the VP16 plasmid, the integrated *lacZ* reporter, or the integrated *HIS3* reporter, respectively. If proteins interact, L40 yeast can grow in the absence of histidine (H) and stain blue in β-Galactosidase filter assays. For the β-Galactosidase filter assays, yeast growing on YC-WUL plates (selecting for the plasmids) were transferred to nitrocellulose membranes. YC-WHULK; media lacking the amino acids W, H, U, L, and K; YC-WUL; media lacking W, U, and L; β-gal, β-Galactosidase.

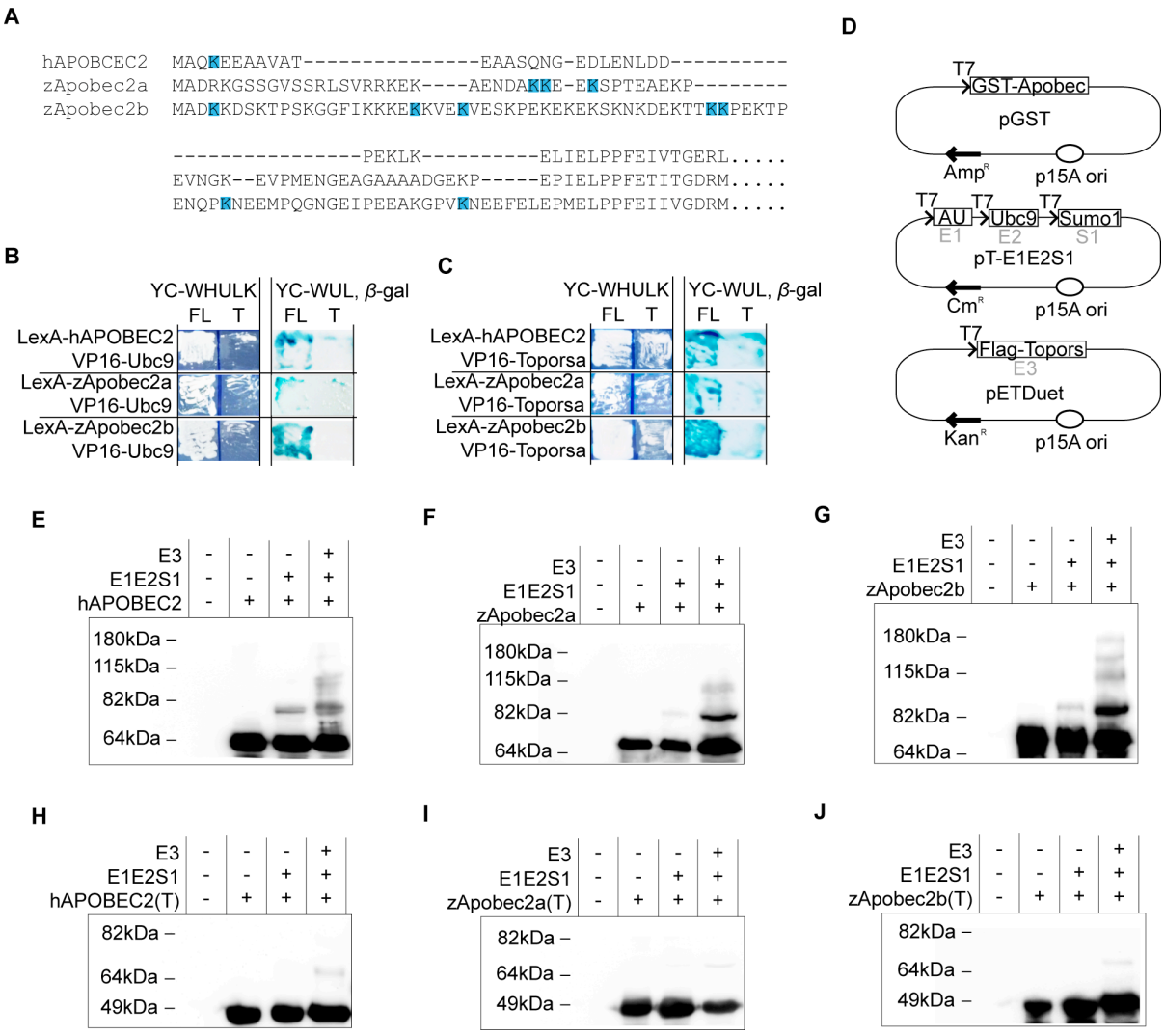

Figure 4.10 Ubc9 and Toporsa interact with the N-termini of Apobec2 proteins and facilitate their sumoylation

(A) ClustalW alignments of the N-termini of Apobec2a,2b and APOBEC2. Lysines (K) that are predicted to be sumoylated are highlighted. (B and C) Yeast two-hybrid assays demonstrate that the interaction between N-terminally truncated Apobec2 proteins and (B) Ubc9 or (C) Toporsa is diminished relative to the full-length Apobec2 proteins. (D) Graphic describing the plasmids used in the Apobec2 bacterial sumoylation assays. (E, F, G, H, I, J) Anti-GST western blots following Apobec2 bacterial sumoylation assays. (E, F, G) Co-expression with Ubc9 stimulates an increase in the mass of (E) APOBEC2, (F) Apobec2a, and (G) Apobec2b, indicative of sumoylation. This pattern is stimulated with co-expression of Toporsa. The presence of multiple bands suggests that these Apobec2s are sumoylated at more than one site. (H, I, J) Removal of the N-terminus of (H) APOBEC2, (I) Apobec2a, and (J) Apobec2b precludes this banding pattern. FL, full length; T, truncation; E1, Aos1/Uba2 fusion protein; E2, Ubc9; S1, SUMO1; E3, Toporsa. Other abbreviations as in Figure 4.9.

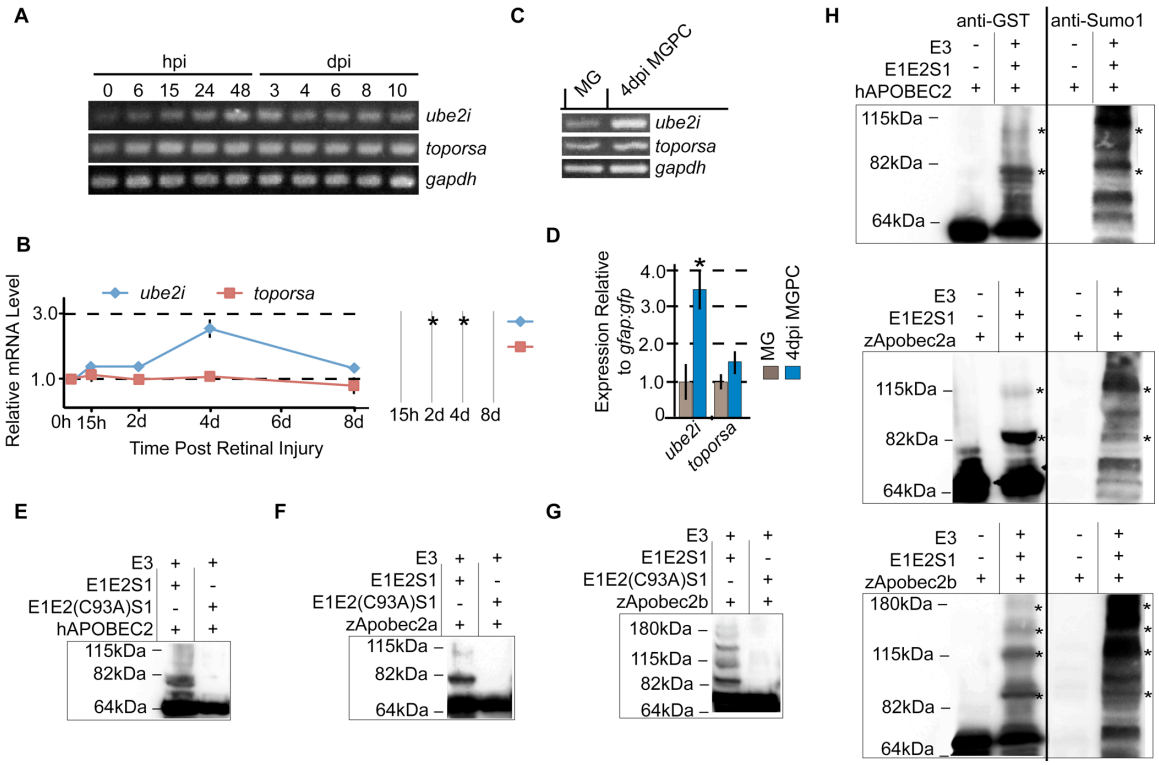

Figure 4.11 Injury-dependent regulation of *ube2i* and *toporsa* expression, and Apobec2 bacterial sumoylation assays, continued

(A) RT-PCR using cDNA prepared from whole retinas harvested at the indicated time points shows the injury-dependent regulation of *ube2i* and *toporsa*. (B) Real-time PCR quantification of select time points from (A) by quantitative PCR. mRNA levels were normalized to the expression of *gapdh* and compared to the value of the control (0h), which was given a value of 1. Data represents means ± s.d. (n = 3 individual cDNA sets). (C) RT-PCR gene expression comparisons of quiescent MG (*gfap:gfp*) and 4dpi MGPC (*1016 tuba1a:gfp*) cell populations targeting *ube2i* and *toporsa* mRNAs. (D) Real-time PCR quantification of (C). mRNA levels were normalized to the expression of *gapdh* and compared to the value of MG, which was given a value of 1. **P* < 0.02814. (E, F, G) Anti-GST western blots following Apobec2 bacterial sumoylation assays demonstrate that using a catalytic mutant of Ubc9 abolishes the banding pattern of Apobecs seen with the co-expression of wild type Ubc9. (H) The banding patterns seen in the Apobec2 bacterial sumoylation assays align with banding of SUMO1 staining. These results strongly suggest that Apobec2 proteins can be sumoylated by Ubc9 and this sumoylation is stimulated by Toporsa. hpi, hours post injury; dpi, days post injury; other abbreviations as in Figure 4.10.

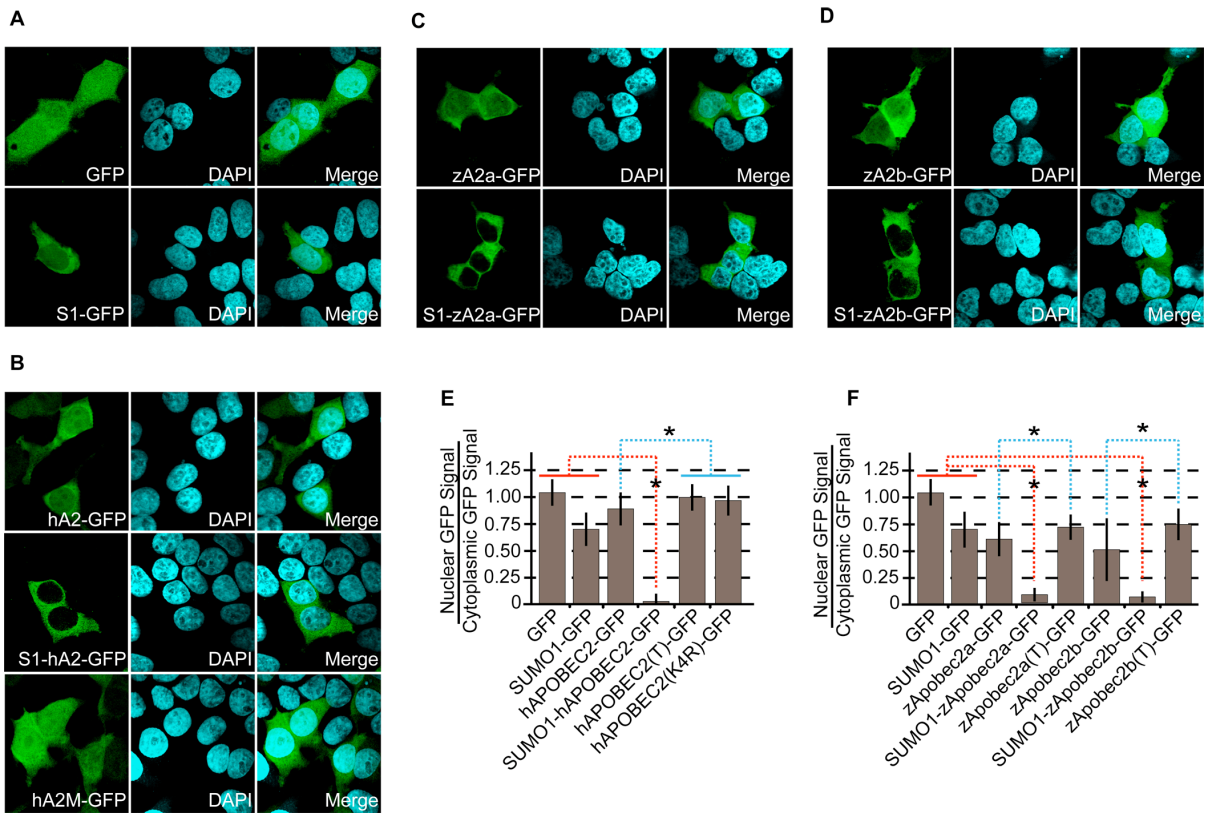

Figure 4.12 Analyses of subcellular localization suggest that the N-terminal sumoylation of Apobec2 proteins promotes their nuclear exclusion

(A, B, C, D) Representative images demonstrating the subcellular localization of (A) GFP, (B) APOBEC2, (C) Apobec2a, and (D) Apobec2b C-terminally tagged with GFP in the absence (top panel) or presence of an N-terminal fusion to SUMO1 (bottom panel in A, C, D; middle panel in B). The bottom panel of B shows a representative image demonstrating the subcellular localization of C-terminally tagged APOBEC2 harboring a (K4R) mutation preventing its sumoylation at that site. (E and F) Quantifications of the nuclear exclusion of the indicated fusion proteins. Experiments with (E) APOBEC2 were performed at 37 °C and those of (F) Apobec2a,2b were performed at 28 °C (see materials and methods). Densitometric means of cytoplasmic and nuclear GFP signal were calculated. The *Y-axis* represents their ratio. Data represents means ± s.d. ($n \geq 25$). Compared to GFP or SUMO1-GFP, the nuclear exclusion of SUMO1-hAPOBEC2-GFP, SUMO1-zApobec2a-GFP, and SUMO1-zApobec2b-GFP is significant. Compared to their wild type forms, truncations of the Apobec proteins show significantly more nuclear signal. Similar results were seen after mutating K4R of APOBEC2. $*P < 0.002381$. S1, SUMO1; hA2, hAPOBEC2; hA2M, hAPOBEC2(K4R); zA2a, zApobec2a; zA2b, zApobec2b.

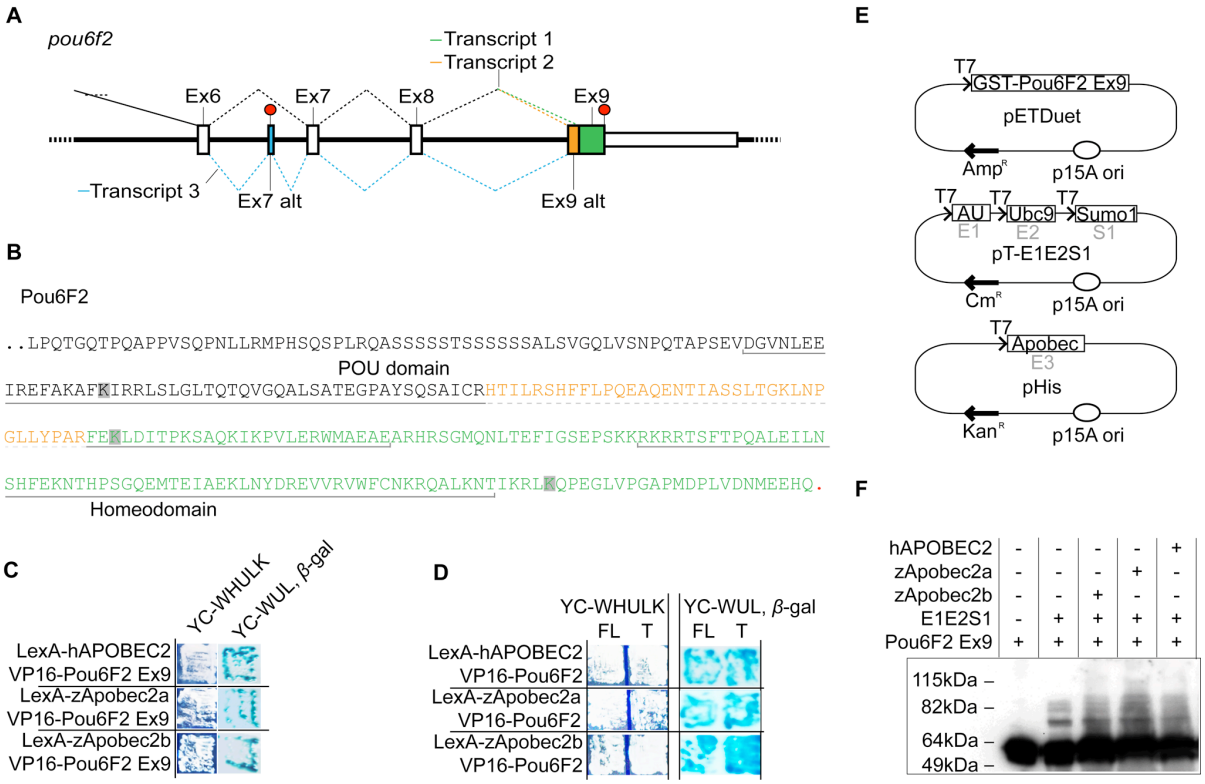

Figure 4.13 Apobec2 proteins interact with the DNA binding domain of Pou6F2

(A) Schematic of the *pou6f2* transcripts identified in its cloning from the retina. Three transcripts were identified. Transcript 2 encodes an alternate exon (Ex) 9 and Transcript 3 encodes an alternate Ex7, which introduces a premature stop signal (red circle). (B) Protein sequence of the DNA binding domain of Pou6F2 Transcript 2. Sequence in black is encoded in Ex8, sequence in yellow is encoded in Ex9 alt, and sequence in green is encoded in Ex9. The inclusion of Ex9 alt introduces 36 amino acids to the center of the POU domain. Lysines (K) predicted to be sumoylated are highlighted. (C and D) Yeast two-hybrid assays indicate (C) that Apobec2 proteins specifically interact with the protein sequence encoded in Ex9 of Pou6F2 and (D) that truncation of Apobec2 proteins does not perturb their binding to Pou6F2. (E) Graphic describing the plasmids used in the Pou6F2 bacterial sumoylation assays. (F) Pou6F2 bacterial sumoylation assays indicate that while the C-terminus of Pou6F2 can be sumoylated, Apobec2 proteins do not impact this sumoylation in a positive or negative manner. Ex, exon; FL, full length; T, truncation; other abbreviations as in Figure 4.9 and 4.10.

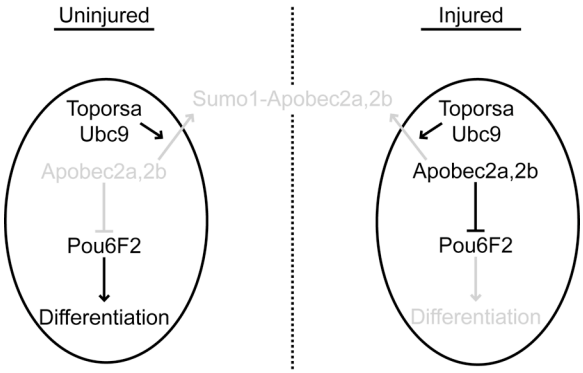

Figure 4.14 Model of the cytosine deaminase-independent role that Apobec2a,2b perform during MG activation and the generation of MGPCs

In the uninjured eye, MG contain low, basal levels of Apobec2a,2b, which are excluded from the nucleus via N-terminal sumoylation facilitated by Ubc9 and Toporsa. In the nucleus, the transcription factor Pou6F2 controls an expression program that maintains MG in a differentiated state. After injury, the expression of *apobec2a,2b* is induced, resulting in high levels of Apobec2a,2b. This abundance of Apobec2a,2b allows them to escape sumoylation and to interact with Pou6F2 in the nucleus via the DNA binding domain of Pou6F2. This interaction induces the dissociation of Pou6F2 from the DNA and disrupts its differentiation program, providing MG the ability, if stimulated, to reprogram and generate MGPCs.

4.8 Tables

Primer Set	Application	Sequence 5'->3'
hAPOBEC2ecori-F	pCS3+MT myc-hAPOBEC2, Cloning	CTTGAATTCAATGGCCCAGAAGGAAGAGGCTGCTGTG
hAPOBEC2xhoi-R	pCS3+MT myc-hAPOBEC2, Cloning	AGGCTCGAGCTACTTCAGGATGTCTGCCAACTTCT
zApobec2abamhi-F	pCMV-3TAg-1a flag-zApobec2a, Cloning	CGCGGATCCATGGCCGATAGAAAGGGCAGCA
zApobec2axhoi-R	pCMV-3TAg-1a flag-zApobec2a, Cloning	CCGCTCGAGTCACTGCAGGATGTCGGCCAG
zApobec2becori-F	pCS3+MT myc-zApobec2b, Cloning	CCGGAATTCAATGGCAGACAAAAAGGACAGCAAG
zApobec2bxhoi-R	pCS3+MT myc-zApobec2b, Cloning	CCGCTCGAGGGCTCTACTTTAAAATATCCTGCAATCTCTC
FlagzApobec2aecori-F	pCS2 flag-zApobec2a, Cloning	CCGGAATTCATGGATTACAAGGATGACGACGATAAG
zApobec2axhoi-R	pCS2 flag-zApobec2a, Cloning	CCGCTCGAGTCACTGCAGGATGTCGGCCAG
zApobec2a,V2a-R	pCS2 flag-zApobec2a-V2a-GFP, PCR Overlap Extension Cloning	CTTCAGCAGGCTGAAGTTTGTAGCTCCGCTTCCCTGCAGGATGTCGGCCAGT
zApobec2b,V2a-R	pCS3+MT myc-zApobec2a-V2a-GFP, PCR Overlap Extension Cloning	CTTCAGCAGGCTGAAGTTTGTAGCTCCGCTTCCCTTTAAAATATCCTGCAATCTCTCATC
V2a-F	V2a PRC Overlap Extension Cloning	GGAAGCGGAGCTACAAACTTCAGCCTGCTGAAGCAGGCTGGAGACGTGGAGGAGAACCCTGGACCT
V2a-gfp-F	pCS2 flag-zApobec2a/b-V2a-GFP, Cloning	CAGGCTGGAGACGTGGAGGAGAACCCTGGACCTATGGTGAGCAAGGGCGAGG
gfpxhoi-R	pCS, flag-zApobec2a/b-V2a-GFP, Cloning	CCGCTCGAGTTACTTGTACAGCTCGTCCATGCC
FlagzApobec2a,V2a-F	pCS3+MT myc-zApobec2a-V2a-flag-zApobec2a-GFP, PCR Overlap Extension Cloning	CAGGCTGGAGACGTGGAGGAGAACCCTGGACCTATGGATTACAAGGATGACGACGAT
tuba1a1016sali-F	pTal, Transgenic Construct Cloning	CTTGTCGACGGCATTCCCTGCTGGGGAAGC
SV40nhei-R	pTal, Transgenic Construct Cloning	CCTGCTAGCGCAGTGAAAAAAATGCTTTATTTGTGAAATTTG
hsp70pronhei-F	pTal, Transgenic Construct Cloning	TGCGCTAGCAGGGGTGTCGCTTGGTGATTT
hsp70probamhi,xmai-R	pTal, Transgenic Construct Cloning	TACGGGATCCCCCGGGTGCAATAAAAAAAACAATTAGAATTAATT
pCS3+/2agei-F	pTal hsp70:zApobec2wt and pTal hsp70:Apobec2mut Cloning	GCTTACCGGTGCTACTTGTTCTTTTTGCAGGATCCCATCG
hAPOBEC2xhoi-R	pTal hsp70:hAPOBEC2 Cloning	AGGCTCGAGCTACTTCAGGATGTCTGCCAACTTCT
zAPOBEC2axhoi-R	pTal hsp70:zApobec2wt/mut Cloning	CCGCTCGAGTCACTGCAGGATGTCGGCCAG
zApobec2a(C156A)-F	pTal hsp70:zApobec2mut, zApobec2a mutagenesis, PCR Overlap Extension Cloning	CCTGGTACATGTCCTCCAGTCCCGCCGCCAACTGCGCAACCAAGCTGGCG
zApobec2a(C156A)-R	pTal hsp70:zApobec2mut, zApobec2a mutagenesis, PCR Overlap Extension Cloning	CGCCAGCTTGGTTGCGCAGTTGGCGGCGGGACTGGAGGACATGTACCAGG
zApobec2b(C180A)-F	pTal hsp70:zApobec2mut, zApobec2b mutagenesis, PCR Overlap Extension Cloning	TGGTACACATCGTCCAGCCCTGCTGTGGCCTGCGCTGCTAAGCTT
zApobec2b(C180A)-R	pTal hsp70:zApobec2mut, zApobec2b mutagenesis, PCR Overlap Extension Cloning	AAGCTTAGCAGCGCAGGCCACAGCAGGGCTGGACGATGTGTACCA

rApobec1ecori-F	pHis- rApobec1 Cloning	CTTGAATTCAATGAGTTCCGAGACAGG CC
rApobec1xhoi-F	pHis- rApobec1/(W90S) Cloning	ACCCTCGAGTCATTTCAACCCTGTGGC C
rApobec1(W90S)-F	pHis- rApobec1(W90S), Mutagenesis, PCR Overlap Extension Cloning	GCTCCATTACCTGGTTCCTGTCCAGCA GTCCCTGTGGGGAGTGCTCCAGG
rApobec1(W90S)-R	pHis- rApobec1(W90S), Mutagenesis, PCR Overlap Extension Cloning	CCTGGAGCACTCCCCACAGGGACTGCT GGACAGGAACCAGGTAATGGAGC
hAIDecori-F	pHis- hAID Cloning	CTTGAATTCAATGGACAGCCTCTTGATG AAC
hAIDxhoi-R	pHis- hAID Cloning	TGCCTCGAGTCAAAGTCCCAAAGTACG AAATGC
hAPOBEC2ecori-F	pHis- hAPOBEC2 and pGST hAPOBEC2 Cloning	CTTGAATTCAATGGCCCAGAAGGAAGA GGCTGCTGTG
hAPOBEC2xhoi-R	pHis- hAPOBEC2/(T) and pGST hAPOBEC2/(T) Cloning	AGGCTCGAGCTACTTCAGGATGTCTGC CAACTTCT
hAPOBEC2(T)ncoi-F	pHis- hAPOBEC2(T) Cloning	GCGCCATGGTTGTCACAGGAGAACGG CTGCCT
hAPOBEC2(S125W)-F	pHis- hAPOBEC2(S125W), Mutagenesis, PCR Overlap Extension Cloning	ACAATGTCACCTGGTATGTGTCCTGGA GCCCCTGTGCAGCGTGTGCTGAC
hAPOBEC2(S125W)-R	pHis- hAPOBEC2(S125W), Mutagenesis, PCR Overlap Extension Cloning	GTCAGCACACGCTGCACAGGGGCTCC AGGACACATACCAGGTGACATTGT
zApobec2aecori-F	pHis- zApobec2a and pGST zApobec2a Cloning	CTTGAATTCAATGGCCGATAGAAAGGG CAG
zApobec2axhoi-R	pHis- zApobec2a(T) and pGST zApobec2a/(T) Cloning	CCGCTCGAGTCACTGCAGGATGTCGGC CAG
zApobec2a(T)ncoi-F	pHis- zApobec2a(T) and pGST zApobec2a/(T) Cloning	GCGCCATGGCCATCACAGGGGATCGC ATGG
zApobec2a(S153W)-F	pHis- zApobec2a(S153W), Mutagenesis, PCR Overlap Extension Cloning	ACACCATCACCTGGTACATGTCCTGGA GTCCCTGCGCCAACTGCGCAACC
zApobec2a(S153W)-R	pHis- zApobec2a(S153W), Mutagenesis, PCR Overlap Extension Cloning	GGTTGCGCAGTTGGCGCAGGGACTCC AGGACATGTACCAGGTGATGGTGT
zApobec2becori-F	pHis- zApobec2b and pGST zApobec2b Cloning	CCGGAATTCAATGGCAGACAAAAAGGA CAGCAAG
zApobec2bxhoi-R	pHis- zApobec2b/(T) and pGST zApobec2b/(T) Cloning	CCGCTCGAGGGCTCTACTTTAAAATATC CTGCAATCTCTC
zApobec2b(T)ncoi-F	pHis- zApobec2b/(T) and pGST zApobec2b/(T) Cloning	GGCGCCATGGTCATTGTAGGAGACCGA ATGAACCCA
zApobec2b(S177W)-F	pHis- zApobec2b(S177W), Mutagenesis, PCR Overlap Extension Cloning	ATACAGTGACTTGGTACACATCGTGGA GCCCTTGTGTGGCCTGCGCTGCT
zApobec2b(S177W)-R	pHis- zApobec2b(S177W), Mutagenesis, PCR Overlap Extension Cloning	AGCAGCGCAGGCCACACAAGGGCTCC ACGATGTGTACCAAGTCACTGTAT
rpoB-F	Mutagenesis Assay	TTGGCGAAATGGCGGAAAACC
rpoB-R	Mutagenesis Assay	CACCGACGGATACCACCTGCTG
Y2Hlibraryasci-F	Generation of Y2H Library	ATTGGCGCGCCCAACGCAGAGTGGCC ATTA
Y2Hlibrarynoti-R	Generation of Y2H Library	TAAGCGGCCGCCTCGCAGAGTGGCCG AGG
Y2HVP16CPCR-F	Yeast Colony PCR	ATGCCGACGCGCTAGACGATTT
Y2HVP16CPCR-R	Yeast Colony PCR	GATTAAGTTGGGTAACGCCAGGGTTT
Y2HVP16seqp-F	Sequencing of Yeast Colony PCRs	TTCGAGTTTGAGCAGATGTTTACCG
Y2HhAPOBEC2ecori-F	pLexA hAPOBEC2 Cloning	TGGAATTCATGGCCCAGAAGGAAGAGG CTG

Y2HhAPOBEC2xhoi-R	pLexA hAPOBEC2/(T) Cloning	AGGCTCGAGCTACTTCAGGATGTCTGC CAACTTCT
Y2HhAPOBEC2(T)ecori-F	pLexA hAPOBEC2(T) Cloning	CTGGAATTCATGGTTGTCACAGGAGAA CGGCTGCCT
Y2HzApobec2abamhi-F	pLexA zApobec2a and pVP16 zApobec2a Cloning	CGGGGATCCGTATGGCCGATAGAAAG GGC
Y2HzApobec2anotii-R	pLexA zApobec2a/(T) and pVP16 zApobec2a Cloning	CTAGCGGCCGCCTACTGCAGGATGTCG GCCAG
Y2HzApobec2a(T)ecori-F	pLexA zApobec2a/(T) Cloning	CTGGAATTCATGGCCATCACAGGGGAT CGCATGG
Y2HzApobec2bbamhi-F	pLexA zApobec2b Cloning	GGGGATCCGTATGGCAGACAAAAAGGA CAG
Y2HzApobec2bnotii-R	pLexA zApobec2b/(T) Cloning	CTAGCGGCCGCCTACTTTAAAATATCCT GCAATCTCTCATC
Y2HzApobec2b(T)ecori-F	pLexA zApobec2b/(T) Cloning	CTGGAATTCATGATCATTGTAGGAGAC CGAATGAACCCA
Y2HPou6F2dbdbamhi-F	pVP16 Pou6F2dbd Cloning	GATGGATCCGTTTCGAGAAGTTGGACA TCACC
Y2HPou6F2dbdnoti-R	pVP16 Pou6F2dbd Cloning	CTAGCGGCCGCCTACCAGTTCTTTAAA GTCCGCAAC
Ube2ixmai-F	pCS2 flag-Ube2i Cloning	AGCCCGGGCGGGATCCTTGGATTCAC GCGAAACAGTGGTCAT
Ube2ixbai-R	pCS2 flag-Ube2i Cloning	AGTTCTAGATGGTTAGGGATTTGATGG CACAGAC
Toporssmai-F	pCS2 flag-Topors Cloning	AAGCCCGGGCGGGATCCCAGATAATG GCACCCTCTAAGATGAAGC
Toporssbai-R	pCS2 flag-Topors Cloning	CAGACCAGCGTAAGAAGTCTAGATGTA TGTG
Flagtoporsmfei-F	pETDuet flag-Topors Cloning	TCTCAATTGTATGGATTACAAGGATGAC GACGA
pCS2avrii-R	pETDuet flag-Topors and pETDuet GST-Pou6f2dbd Cloning	CAGCCTAGGTGTATGTGTTTTAGTTTTA GCTAGCAGTG
Pou6F2dbdecori-F	pGST Pou6F2dbd Cloning	CTTGAATTCAATGGTTGGCCAGCTAGT CAGCAA
Pou6F2dbdxhoi-R	pGST Pou6F2dbd Cloning	GTGCTCGAGCCAGTTCTTTAAAGTCCG CAA
pGST-nhei	pETDuet GST-Pou6f2dbd Cloning	ATGGCTAGCATGTCCCCTATACTAGGTT ATTGGAAA
xUbc9(C94A) F	pE1E2(C93A)S1, Mutagenesis, PCR Overlap Extension Cloning	CGTCTATCCTTCAGGCACAGTGGCCCT GTCTATCTTAGAAGAAGATA
xUbc9(C94A) F	pE1E2(C93A)S1, Mutagenesis, PCR Overlap Extension Cloning	TATCTTCTTCTAAGATAGACAGGGCCAC TGTGCCTGAAGGATAGACG
hSUMO1hindiii-F	pCS2 hSUMO1 Cloning	TTAAAGCTTATGTCTGACCAGGAGGCA AAACCTT
hSUMO1bamhi-R	pCS2 hSUMO1 Cloning	ACAGGATCCAACTGTTGAATGACCCCC CGTTTG
hAPOBEC2ecori-F	pEGFP hAPOBEC2-GFP Cloning	TTAGAATTCATGGCCCAGAAGGAAGAG GCTG
hAPOBEC2bamhi-R	pEGFP hAPOBEC2-GFP Cloning	TCAGGATCCGTCTTCAGGATGTCTGCC AACTTCTCCT
hAPOBEC2clai-F	pCS2 hAPOBEC2-GFP and pCS2 hSUMO1-hAPOBEC2-GFP Cloning	TACATCGATTGATGGCCCAGAAGGAAG AGGCTG
hAPOBEC2(K4R)clai-R	pCS2 hSUMO1-hAPOBEC2/(K4R)-GFP Cloning	TACATCGATTGATGGCCCAGAGGGAAG AGGCTG
gfpxhoi-R	pCS2 hAPOBEC2/(K4R)-GFP and pCS2 hSUMO1-hAPOBEC2/(K4R)-GFP Cloning	CCGCTCGAGTTACTTGTACAGCTCGTC CATGCC
zApobec2acali-F	pCS2 zApobec2a-GFP and pCS2 hSUMO1-zApobec2a-GFP Cloning	TTTATCGATTGATGGCCGATAGAAAGG G

zApobec2aagei-R	pCS2 zApobec2a-GFP and pCS2 hSUMO1-zApobec2a-GFP Cloning	TTTACCGGTCTCTGCAGGATGTCGGC
zApobec2acali-F	pCS2 zApobec2b-GFP and pCS2 hSUMO1-zApobec2b-GFP Cloning	TTTATCGATTGATGGCAGACAAAAAGG ACAGCAAGAC
zApobec2aagei-R	pCS2 zApobec2b-GFP and pCS2 hSUMO1-zApobec2b-GFP Cloning	TTTACCGGTCTCTTTAAAATATCCTGCA ATCTCTCATC
hAPOBEC2(T)ecori-F	pCS2 hAPOBEC2(T)-GFP and pCS2 hSUMO1-hAPOBEC2(T)-GFP Cloning	CTGGAATTCATGGTTGTCACAGGAGAA CGGCTGCCT
zApobec2a(T)ecori-F	pCS2 zApobec2a(T)-GFP and pCS2 hSUMO1-zApobec2a(T)-GFP Cloning	CTGGAATTCATGGCCATCACAGGGGAT CGCATGG
zApobec2b(T)ecori-F	pCS2 zApobec2b(T)-GFP and pCS2 hSUMO1-zApobec2b(T)-GFP Cloning	CTGGAATTCATGATCATTGTAGGAGAC CGAATGAACCCA
GFPbamhi-F	pCS2 hSUMO1-GFP Cloning	TTTGGATCCATGGTGAGCAAGGGCG
gfpxhoi-R	pCS2 Apo(T)-GFP, pCS2 hSUMO1-Apo(T)-GFP, and pCS2 hSUMO1-GFP Cloning	CCGCTCGAGTTACTTGTACAGCTCGTC CATGCC
Pou6F2xmai-F	pCS2 flag-Pou6f2 Cloning	AGCCCGGGCGGGATCCATGATCACAG GGCAGCTGAGCAA
Pou6F2xbai-R	pCS2 flag-Pou6f2 Cloning	AGTTCTAGACCAGTTCTTTAAAGTCCGC AACATCAG
hAPOBEC2	Real-Time PCR	F, AGCTGCCGCCCTTTGAGATTGT
		R, AAGGCTGGCAGGATGGTGTTGA
zapobec2a	Real-Time PCR	F, CTGCTGCAGACGGAGAAAAACCA
		R, CCAGCGTGCTCGTCCTCAATGTA
zapobec2b	Real-Time PCR	F, ATGAGGAGTTTGAGCTAGAGCCGATG
		R, ATCCTCCAGGTAACCACGAACGC
ascl1a	Real-Time PCR	F, ATTCCAGTCGGGCGTCCTGTCA
		R, CCTCCCAAGCGAGTGCTGATATTTT
ube2i	SQ RT-PCR and Real-Time PCR	F, GGCCCACGAGACGATAAACACTG
		R, CAGCATCCGTAACTTAAACAGACCTCC
topors	SQ RT-PCR and Real-Time PCR	F, TGAAGCTGCGTGTGAGGAAGAAAG
		R, TGACGGAGTGGAATATGGAGTGGAA
gapdh	SQ RT-PCR and Real-Time PCR	F, ATGACCCCTCCAGCATGA
		R, GGCGGTGTAGGCATGAAC

Table 4.1 List of primers used in this study and their applications

			# of Reads				
Library	**ng Temp**	**Sequencing Method**	**Original**	**Aligned 1 Time**	**Aligned>1 Time**	**Aligned 0 Times**	**AR**
0hrs MG 1	100	single-end, 52 cycle	23,054,164	2,491,506 (10.81%)	12,608,072 (54.69%)	7,954,586 (34.50%)	65.50%
0hrs MG 2	100	single-end, 52 cycle	30,570,717	3,403,847 (11.13%)	17,206,807 (56.29%)	9,960,063 (32.58%)	67.42%
2dpi MGPC, control MO 1	100	single-end, 52 cycle	20,608,989	2,245,930 (10.90%)	12,185,659 (59.13%)	6,177,400 (29.97%)	70.03%
2dpi MGPC, control MO 2	100	single-end, 52 cycle	26,509,120	3,081,264 (11.62%)	16,731,928 (63.12%)	6,695,928 (25.26%)	74.74%
2dpi MGPC, *apobec2a,2b* MO 1	100	single-end, 52 cycle	21,380,985	1,777,233 (8.31%)	9,667,485 (45.22%)	9,936,267 (46.47%)	53.53%
2dpi MGPC, *apobec2a,2b* MO 2	100	single-end, 52 cycle	43,437,133	5,157,013 (11.87%)	27,649,500 (63.65%)	10,630,620 (24.47%)	75.53%

Table 4.2 Overview of TruSeq library sequencing and alignment

S.R, sequencing run; AR, aligned reads.

Variant Type	0hrs	2dpi MGPC, control MO	2dpi MGPC, *apobec2a,2b* MO
A->C	1,769	1,895	1,538
A->G	6,460	6,913	5,551
A->T	2,218	2,363	1,882
C->A	1,815	1,993	1,599
C->G	1,190	1,298	1,067
C->T	7,038	7,832	6,384
G->A	6,204	6,732	5,599
G->C	1,174	1,254	1,023
G->T	1,455	1,629	1,343
T->A	2,246	2,408	1,895
T->C	7,461	7,627	6,372
T->G	1,565	1,663	1,338

Table 4.3 List of variants by type for each sample

Values provided are averages of the two replicas for each sample.

0hrs vs 2dpi MGPC, control MO							
		Change in:		% Edited			
locus	Gene	Codon	AA	cont0h	contMO	Ratio	Surround.Seq (coding)
chr1:30167073-30186479	eef1a1b	gaC/gaT	D306	31.21	95.24	3.05158603	TTCCCGGCGACAATGTGGGAT
	slc25a3a	**ttC/ttT**	**F290**	**17.28**	**52.84**	**3.05787037**	**CTGGGGTGTTCTGTGCGGTGG**
chr16:33815911-33821400	ndrg1b	Cgt/Tgt	R39C	26.83	82.755	3.084420425	GAAGGGCAACCGTCCCACCAT
chr10:43887067-43905964	actr1	atC/atT	I217	22.16	68.9	3.109205776	TGCGCACCATCAAGGAGGTAT
chr1:44276757-44281942	**CNGA1__2_of_2_**	**aaC/aaT**	**N442**	**16.82**	**53.01**	**3.151605232**	**TTGGCATGAACGTACACTTGG**
chr16:13852337-13923561	clstn3	atC/atT	I769	28.85	92.315	3.19982669	CGGAGTCTATCTCTGTGTATG
chr9:39216184-39344120	**clasp1a**	**gaC/gaT**	**D1337**	**30.065**	**97.5**	**3.242973557**	**CTGTGTGGGACGAACACTTCA**
chr19:36588261-36888387	macf1	caC/caT	H6828	19.005	62.03	3.263877927	GGCTCAGTCACACTCACGCCA
chr13:29044013-29125894	TACC2	ttC/ttT	F321	27.77	92.855	3.343716241	ACGGAGCTTTCGAAACCCCAG
chr13:16279528-16306819	**zgc:110045**	**gaC/gaT**	**D54**	**14.66**	**49.58**	**3.381991814**	**ATATATCTGACGGTTCCAGTC**
chr18:44371429-44400225	**ap2m1b**	**Cta/Tta**	**L184**	**19.13**	**65.01**	**3.398327235**	**TGTGAACTTGCTAATGTCACC**
chr13:29044013-29125894	**TACC2**	**ccC/ccT**	**P375**	**28.265**	**97.22**	**3.439589598**	**ATAGATCTCCCAGTCGCTCTG**
chr23:28586879-28589931	**neurod4**	**-**	**-**	**18.235**	**63.58**	**3.486701398**	**GATCCCTTAACGCTCACTGAG**
chr5:43496833-43615097	**ncor1**	**tcC/tcT**	**S1939**	**20.195**	**70.855**	**3.508541718**	**GCTCCGACTCCTCTAGCAGCA**
chr18:44206153-44266698	**abcc5**	**acC/acT**	**T1353**	**25.48**	**92.645**	**3.635989011**	**ACACAGAGACCGACTGTTTGA**
chr18:10232765-10372507	**mical3a**	**-**	**-**	**19.935**	**74.52**	**3.738148984**	**GGTTTAGAAACGCTTGAGGGA**
chr6:37703110-37798075	**herc2**	**caC/caT**	**H4229**	**14.72**	**57.7**	**3.919836957**	**GACTGGGACACGGCTCAGATG**
chr17:39865234-39907511	**eprs**	**agC/agT**	**S1215**	**17.375**	**69.59**	**4.005179856**	**ATGATGTCAGCGGCTGTTACG**
chr16:35319310-35372930	**snap91**	**-**	**-**	**23.335**	**95.65**	**4.098992929**	**TTTGTGGTCACGTCATTTTTG**
chr13:23113099-23148025	**hk1**	**tgC/tgT**	**C665**	**22.47**	**93.48**	**4.160213618**	**TGATGACCTGCGCATATGAAG**
chr11:20201418-20463289	**cadpsa**	**-**	**-**	**19.16**	**83.07**	**4.33559499**	**TTTTTTACAGCGTAGTGAGAC**

0hrs vs 2dpi MGPC, *apobec2a,2b* MO							
		Change in:		% Edited			
locus	Gene	Codon	AA	cont0h	A2a,bMO	Ratio	Surround.Seq (coding)
chr21:25916057-25925022	adssl	tcC/tcT	S183	29.05	88.805	3.05697074	CTGCATACTCCTCCAAAGCAG
chr10:15844440-15908143	tjp2a	gaC/gaT	D576	20.435	62.79	3.07266944	GCACTGGAGACCAAATAGTCA
chr16:35319310-35372930	**snap91**	**-**	**-**	**23.335**	**73.61**	**3.154488965**	**TTTGTGGTCACGTCATTTTTG**
chr23:28586879-28589931	**neurod4**	**-**	**-**	**18.235**	**57.775**	**3.168357554**	**GATCCCTTAACGCTCACTGAG**
	slc25a3a	**ttC/ttT**	**F290**	**17.28**	**54.76**	**3.168981481**	**CTGGGGTGTTCTGTGCGGTGG**
chr9:39216184-39344120	**clasp1a**	**gaC/gaT**	**D1337**	**30.065**	**95.65**	**3.181440213**	**CTGTGTGGGACGAACACTTCA**
chr18:44371429-44400225	**ap2m1b**	**Cta/Tta**	**L184**	**19.13**	**60.89**	**3.182958704**	**TGTGAACTTGCTAATGTCACC**
chr13:29044013-29125894	**TACC2**	**ccC/ccT**	**P375**	**28.265**	**91.665**	**3.243056784**	**ATAGATCTCCCAGTCGCTCTG**
chr20:51423316-51435380	atp6v1d	-	-	21.43	70.835	3.305412972	TCCCAACAAACGTGTTGCAAA
chr1:44276757-44281942	**CNGA1__2_of_2_**	**aaC/aaT**	**N442**	**16.82**	**57.87**	**3.440546968**	**TTGGCATGAACGTACACTTGG**
chr12:11242670-11254577	psmc5	caC/caT	H377	22.92	79.305	3.460078534	GGAGGGTCCACGTTACCCAGG
chr13:30278772-30366729	spock2	gaC/gaT	D186	18.525	65.13	3.515789474	CTGCTACAGACGTGGACGGCA
chr9:52636192-52713526	slc4a10b	gtC/gtT	V234	14.555	51.55	3.541738234	CAAAAAATGTCCCGTCTCAGG
chr18:44206153-44266698	**abcc5**	**acC/acT**	**T1353**	**25.48**	**91.285**	**3.582613815**	**ACACAGAGACCGACTGTTTGA**
chr1:45294183-45325450	kdm2aa	gaC/gaT	D764	19.205	69.015	3.593595418	GCGAAGAAGACAGGCATGTGA
chr13:29044013-29125894	TACC2	ttC/ttT	F321	27.77	100	3.601008282	ACGGAGCTTTCGAAACCCCAG
	ranbp1	Ctg/Ttg	L180	20.125	73.9	3.672049689	GGCAGAGAAGCTGGAGGAGTT
chr17:39865234-39907511	**eprs**	**agC/agT**	**S1215**	**17.375**	**66.285**	**3.814964029**	**ATGATGTCAGCGGCTGTTACG**
chr13:23113099-23148025	**hk1**	**tgC/tgT**	**C665**	**22.47**	**90.91**	**4.045838896**	**TGATGACCTGCGCATATGAAG**
chr5:43496833-43615097	**ncor1**	**tcC/tcT**	**S1939**	**20.195**	**81.875**	**4.054221342**	**GCTCCGACTCCTCTAGCAGCA**
chr18:10232765-10372507	**mical3a**	**-**	**-**	**19.935**	**82.555**	**4.141208929**	**GGTTTAGAAACGCTTGAGGGA**
chr11:20201418-20463289	**cadpsa**	**-**	**-**	**19.16**	**81.25**	**4.240605428**	**TTTTTTACAGCGTAGTGAGAC**

chr13:16279528-16306819	zgc:110045	gaC/gaT	D54	14.66	73.705	5.027626194	ATATATCTGACGGTTCCAGTC
chr6:37703110-37798075	herc2	caC/caT	H4229	14.72	79.22	5.381793478	GACTGGGACACGGCTCAGATG

Table 4.4 Lists of C-to-T variants whose abundance increase ≥ 3 fold

Tables listing differentially regulated C-to-T variants whose abundance increases ≥ 3 fold in the 0hrs and 2dpi MGPC, control MO (Top) or 0hrs and 2dpi MGPC, *apobec2a,2b* MO library comparisons. Highlighted C-to-T variants are present in both the upper and lower table. The 10 base pairs flanking each C-to-T variant are also listed (Surround.Seq). cont0h, 0hr library; contMO, 2dpi MGPC, control MO library; A2a,bMO, 2dpi MGPC, *apobec2a,2b* MO library; AA, amino acid.

Chapter 5:
Apobec2a and Apobec2b regulate an inflammatory response during zebrafish retina regeneration

5.1 Abstract

Retinal damage stimulates an immune response that includes the production of pro-inflammatory cytokines and the activation of microglia. How this immune response contributes to the regenerative events of zebrafish retina and optic nerve regeneration remains unclear. Here we report that zebrafish retina and optic nerve damage induces the activation of immune and inflammatory gene expression programs and that this activation is localized to immunocompetent cells that migrate to the site of injury. Interestingly, these gene programs occur in a time course that is concurrent with the activation of *apobec2a* and *apobec2b* (*apobec2a,2b*) expression in Müller glia (MG) during retina regeneration and the activation of *apobec2b* expression in retinal ganglion cells (RGCs) during optic nerve regeneration. While we provide evidence that indicates that the activation of these immune response programs and the activation of *apobec2a,2b* expression are occurring in different cells, we demonstrate that the knockdown of Apobec2a,2b negatively influences the injury-dependent activation of immune and inflammatory response genes, suggesting that Apobec2a,2b somehow facilitate cellular communication between the regenerative cells and the immune responsive cells. Finally, we provide evidence that Apobec2 plays a similar role in muscle, the tissue with which Apobec2 proteins are most commonly associated.

5.2 Introduction

Apobec proteins are a vertebrate-specific family of enzymes characterized by their cytosine deaminase domain. The appearance of this family seems to have been concurrent with the evolution of the adaptive and innate immune responses; AID promotes the process of antibody diversification during the events of somatic hypermutation, class switch

recombination, and gene conversion (Muramatsu et al., 2000; Maul and Gearhart, 2010), and APOBEC3 and APOBEC1 proteins regulate innate immunity through mutagenesis of mobile elements including endogenous retroelements and exogenous viruses (Conticello, 2008; Gee et al., 2011; Koito and Ikeda, 2012; Smith et al., 2012).

While the exact biochemical function of Apobec2 proteins remains unclear, the expression of Apobec2 has been correlated with a number of processes (Piec et al., 2005; Sato et al., 2009; Okuyama et al., 2011; Pennings et al., 2011; Vonica et al., 2011), including inflammation (Iio et al., 2010). Interestingly, the pro-inflammatory cytokines tumour necrosis factor-α (TNF-α) and interleukin-1β (IL-1β) were shown to activate *APOBEC2* expression (Matsumoto et al., 2006). Inflammation is one of the first responses of the immune system.

Because the retina is an immune-privileged tissue, a number of mechanisms exist to protect the eye from foreign substances (Kumar et al., 2013a). Retinal glial cells are major contributors to the innate immune response of the retina. Upon activation, microglia travel to areas of damage, phagocytize pathogens and cellular debris, and produce growth factors. Similar to macrophages, microglia can function as antigen presenting cells acting in concert with infiltrating immune cells following retinal damage (Kreutzberg, 1996; Langmann, 2007). MG have been shown to contribute to the immune response through the secretion of pro-inflammatory cytokines, including TNF-α and IL-1β (Kumar and Shamsuddin, 2012), the phagocytosis of foreign particles (Tokuda et al., 1992; Bailey et al., 2010), and the expression of innate immune receptors on their surfaces that can recognize foreign substances and initiate an immune response (Rosenzweig et al., 2009; Shamsuddin and Kumar, 2011; Kumar and Shamsuddin, 2012).

The immune response following retinal damage appears to play a role in retina regeneration as the pro-inflammatory cytokine TNF-α was shown to be necessary for Müller glia derived progenitor proliferation during zebrafish retina regeneration (Nelson et al., 2013). Microglia activation following zebrafish retina injury has also been noted (Craig et al., 2010), though the exact role that this activation plays has yet to be determined. Interestingly, microglia have been demonstrated to be essential for normal retinal growth and neurogenesis during zebrafish development (Huang et al., 2012). In addition, stimulation with complement fragment C3a alone has been shown to induce regeneration in the chick

retina (Haynes et al., 2013), further demonstrating a potential role of the immune response during retina regeneration.

In this study, we characterize the expression of multiple genes associated with the inflammatory immune response during zebrafish retina and optic nerve regeneration. Interestingly, we find evidence that suggests that Apobec2 proteins, previously identified as being necessary for zebrafish retina and optic nerve regeneration (Powell et al., 2012), are somehow connected with this inflammatory response, and that they, like other Apobec proteins, play a role in vertebrate immunity.

5.3 Results

5.3.1 An immune response is initiated following retinal damage and this response occurs concurrent with the activation of apobec2a,2b expression

To begin to analyze the role that the immune response plays during zebrafish retina regeneration, we characterized the expression of genes correlated with the activation of immunocompetent cells and the activation of the complement system. We analyzed two well-characterized expression programs initiated in the activation of macrophages: *tnfb* (with downstream targets such as *apoc1l*) (Gratchev et al., 2008) and *spi1* (with downstream targets such as *plek*, *mfap4*, *mpeg1*, *pparg*, and *ptpn6*) (Zakrzewska et al., 2010), and we analyzed the expression of *c1qc* and *c1qb* as reporters of the complement system (Haynes et al., 2013; Zhang and Cui, 2014).

Following mechanical retina injury, the expression of *tnfb*, *plek*, *c1qb* and *c1qc* is rapidly activated beginning between 15 and 24 hours post injury (hpi) (Figure 5.1A and B). Expression of these genes peaked between 2 and 4 days post injury (dpi) and decreased by 8dpi (Figure 5.1A-B). This is similar to the time course of MGPC proliferation which begins at 2dpi, peaks at 4dpi, and ceases by 8dpi (Fausett and Goldman, 2006). Induced expression of *apoc1l*, *spi1*, *mfap4*, and *ptpn6* was also seen by 2dpi (Figure 5.1C). The activation of *tnfb*, *spi1*, and complement expression programs was also noted following retinal injury instigated by light-mediated photoablation (Figure 5.1D). Furthermore, similar results were found following optic nerve lesion, with expression levels of these genes peaking at 2 days post optic nerve cut (dpONC) and returning to basal levels by 4dpONC (Figure 5.1E-G).

Thus, an immune response accompanies both retina and optic nerve regeneration in zebrafish.

Surprisingly, the activation of immune response genes was concurrent with the activation of *apobec2a* and *apobec2b* (*apobec2a,2b*) gene expression (Figure 5.1B and F). We also noted that the level of activation of the immune response was correlated with the level of activation of *apobec2a,2b* expression (Figure 5.1). These results suggest that the expression of *apobec2a,2b* may be connected, either upstream or downstream, with signaling of the immune response.

5.3.2 The expression of immune response genes after injury is localized to immunocompetent cells at the site of injury

Because of the correlation between increased *apobec2a,2b* expression and increased expression of markers of the immune response, we performed *in situ* hybridization to determine the cellular localization of *tnfb*, *apoc1l*, *spi1*, *plek*, *mfap4*, *mpeg1*, and *c1qc* at 2 days post mechanical lesion. This demonstrated that the expression of these genes was localized to cells at the site of injury, with morphologies typical of immunocompetent cells (Figure 5.2, data not shown). Probing these sections with antibodies against 4C4 (labels microglia in the zebrafish retina) (Craig et al., 2010) and against L-Plastin (lcp1, labels microglia and leukocytes in zebrafish) (Redd et al., 2006) confirmed that these cells were microglia and/or leukocytes (immunocompetent cells) recruited to the injury site (Figure 5.2B). We were unable to detect visible amounts of these transcripts in Müller glia (MG), Müller glia derived progenitor cells (MGPCs), or injured retinal ganglion cells (RGCs) at the site of injury by *in situ* hybridization (Figure 5.2). This is in contrast to previous work that demonstrated that the expression of *apobec2a,2b* is localized to MGPCs during retina regeneration and that the expression of *apobec2b* is localized to RGCs during optic nerve regeneration (Powell et al., 2012).

5.3.3 Immunocompetent cells congregate at the injury site following mechanical retinal injury

Immunostaining with markers of immunocompetent cells indicated that these cells quickly congregate at the injury, entirely filling the lesion site after mechanical injury (Figure

5.3A-C). An *mpeg:gfp* transgenic fish showed similar results (Figure 5.3B) (Ellett et al., 2011). In the uninjured state (control), microglia largely reside in the RGC layer, the inner plexiform layer (proximal to the inner nuclear layer), and the outer plexiform layer (Figure 5.3). Within 6hpi, most of these cells are localized to the injury site or the RGC layer and remain there through 8dpi (Figure 5.3C).

Co-staining retinal sections prepared from injured *apobec2bP+1:gfp* transgenic fish, which label MGPCs and activated RGCs (Powell et al., 2012), for GFP and markers of immunocompetent cells indicated that the transgene activation was not visible in microglia or leukocytes, but suggested that these immunocompetent cells were in close proximity to *apobec2b* expressing MGPCs and activated RGCs (Figure 5.4A and B). Similar results were seen after co-staining injured retinal sections with markers of immunocompetent cells and markers of MG (GFP+ cells from *gfap:gfp* transgenic fish) (Figure 5.4C) or markers of MGPCs at 2dpi (GFP+, PCNA+ cells from *gfap:gfp* transgenic fish) (Figure 5.4D) and 4dpi (GFP+ cells from *1016 tuba1a:gfp* transgenic fish) (Figure 5.4E) (Fausett and Goldman, 2006; Powell et al., 2012). Thus, while MG may be taking part in the inflammatory response during zebrafish retina regeneration, they do not become immunogenic for markers such as 4C4 or L-Plastin, they do not activate *mpeg1* expression as reported by the *mpeg:gfp* transgenic fish, and they do not activate the expression of *tnfb*, *spi1*, or complement expression programs as determined by *in situ* hybridization using probes specific to components of those programs. The same is apparent of RGCs following optic nerve injury, as similar results were seen with activated RGCs damaged at the site of mechanical injury (Figure 5.4).

5.3.4 Apobec2a,2b regulate the expression of immune response genes

Because the expression of *apobec2a,2b* is highly correlated with the activation of these immune response programs (Figure 5.1) and because others have found correlations between *APOBEC2* expression and inflammation (Iio et al., 2010), we sought to test if this immune response program was dependent on the presence of Apobec2a,2b. Surprisingly, when we knocked down Apobec2a, Apobec2b, or Apobec2a,2b, the injury-dependent activation of *tnfb*, *plek*, *c1qc*, and *c1qb* was negatively impacted (Figure 5.5A). *Dnmt4* expression, which is activated after injury in an Apobec2a,2b-independent fashion, served as

a control (Powell et al., 2012). The expression of these genes could be rescued with heat shock of *hsp70:zapobec2wt* transgenic fish, clearly establishing that this effect is dependent on Apobec2a,2b (Figure 5.5B). Furthermore, the heat shock of *hsp70:hAPOBEC2* fish could also rescue the expression of these inflammatory and complement genes, while heat shock of *hsp70:zapobec2mut* fish could not (Figure 5.5B), indicating that the role that Apobec2 proteins play in the immune response is conserved between fish and mammals and that it requires the proper coordination of zinc by Apobec2s.

To validate that these decreases in gene expression occurring following Apobec2a,2b knockdown were not occurring in MG themselves, at a level undetectable by *in situ* hybridization (Figure 5.2) and immunostaining (Figure 5.3 and 5.4), GFP+, lissamine+ cells were isolated from *gfap:gfp* transgenic fish retinas 2 days after administration of either control or *apobec2a,2b* morpholino (Powell et al., 2013). Expression analyses of these cells confirmed that the low level of expression of these genes in MG was not regulated by Apobec2a,2b (Figure 5.5C). These results suggest that the knockdown of Apobec2a,2b perturbs communication between MG and microglia/leukocytes that would ordinarily lead to increased expression of immune response genes in immunocompetent cells. Knockdown of Apobec2a,2b did not impact the localization of microglia/leukocytes to the site of injury indicating that this communication occurs after immunocompetent cells have arrived at the injury site (Figure 5.5D). This result was not entirely unexpected, as microglia/leukocytes have migrated to the injury site and RGC layer within 6hpi (Figure 5.3), at which time the expression of *apobec2b* is just increasing during retina regeneration and before it's expression is induced during optic nerve regeneration (Powell et al., 2012).

5.3.5 Apobec2 expression in muscle regulates immune response genes

Because the expression of *Apobec2* has been reported to be highest in cardiac and skeletal muscle (Liao et al., 1999; Anant et al., 2001a; Powell et al., 2012; Li et al., 2014), and because the knockdown/knockout of Apobec2 leads to muscle phenotypes (Piec et al., 2005; Sato et al., 2009; Etard et al., 2010), we were curious to ascertain whether Apobec2 expression could influence the expression of these immune response genes in muscle fibers (or immunocompetent cells surrounding muscle fibers). Previous reports have demonstrated that *Apobec2* expression is highly repressed following muscle denervation (Sato et al., 2009).

Likewise, we found a greater than 90% decrease in *Apobec2* expression in mouse tibialis anterior (TA) muscle within 3 days following denervation (Figure 5.6A and B). *Myog* expression is highly induced following denervation and served as a positive control (Tang et al., 2009). Interestingly, we found that multiple immune response genes including *TnfB*, *Acvrl1* (a Tnfb receptor), *Apoc1*, *Plek*, and *Mfap4* were decreased concurrently (Figure 5.6C).

To determine if these results were a direct result of a decrease in Apobec2 and not resulting from an alternate path during muscle denervation, *Apobec2* siRNAs were obtained to knockdown Apobec2 in mouse TA muscle in the absence of denervation. siRNA mediated Apobec2 knockdown resulted in decreased expression of *Tnfb*, *Acvrl1*, *Apoc1*, *Plek*, *Mfap4*, and *C1qc,* while the expression of *Myog* was unperturbed (Figure 5.6D). These results further demonstrate the role that Apobec2 proteins play in regulating an immune response program.

5.4 Discussion

While the exact function of the immune response during zebrafish CNS regeneration has not been examined thoroughly, mounting evidence suggests that the immune response plays a critical role (Becker et al., 1998; Craig et al., 2008; Craig et al., 2010; Kroehne et al., 2011; Marz et al., 2011; Kizil et al., 2012; Nelson et al., 2013). Here we begin to characterize this response during zebrafish retina regeneration following mechanical lesion and during zebrafish optic nerve regeneration following optic nerve cut.

After retinal damage (mechanical and light-mediated photoablation), inflammatory and complement gene expression programs are rapidly activated (Figure 5.1A-D). The activation of these programs is highly correlated with the proliferation of MGPCs (Fausett and Goldman, 2006), suggesting that the immune response may influence the proliferation of these progenitors. This potential link is supported by recent evidence that suggests that the pro-inflammatory cytokine TNF-α is required for Müller glia proliferation during zebrafish retina regeneration (Nelson et al., 2013) and that complement factor C3a can induce retina regeneration in the absence of injury in developing chicks (Haynes et al., 2013). Using a combination of *in situ* hybridization, transgenic fish, and immunostaining, we demonstrate that the injury-dependent induction of these immune genes is localized to immunocompetent

cells at the site of injury (Figure 5.2-5.4). These cells migrate to the site of injury by 6hpi and remain there through 8dpi (Figure 5.3). During that time, they are in close proximity to MGPCs and activated RGCs (Figure 5.3 and 5.4).

After zebrafish optic nerve lesion, inflammatory and complement gene expression programs are transiently activated, peaking at 2dpi and returning to basal levels by 4dpi (Figure 5.1E-G). Interestingly, early studies of goldfish retinal explants suggested that a priming event following optic nerve injury is necessary for the optimal axonal outgrowth of explants in tissue culture. It was demonstrated that in comparison to retinal explants prepared following optic nerve crush, explants prepared without prior injury possessed an extremely limited ability for growth (Landreth and Agranoff, 1979). Furthermore, axonal outgrowth increased markedly if they were prepared 4 days or more after injury, suggesting that this priming event occurs in the days immediately following injury and that removing the retina from its natural environment precludes this from happening (Landreth and Agranoff, 1979). It would be interesting if this priming event requires the transient activation of the immune response, which we have begun to characterize here.

Interestingly, the injury-dependent activation of these inflammatory and complement response programs occurs concomitantly with the activation of *apobec2a,2b* expression during retina regeneration and *apobec2b* expression during optic nerve regeneration. Furthermore, the level of induction of this immune program correlates with the level of induction of *apobec2a,2b*, suggesting that one may regulate the other. Others have noted a correlation between APOBEC2 and inflammation (Matsumoto et al., 2006; Iio et al., 2010). Previously, we demonstrated that the expression of *apobec2a,2b* is induced in activated MG following retina damage and in activated RGCs following optic nerve damage and that Apobec2a,2b are necessary for these regenerative events (Powell et al., 2012). Surprisingly, while these immunocompetent cells did not show appreciable levels of *apobec2a,2b* (Powell et al., 2012)(Figure 5.4), the injury-dependent activation of immune response genes was sensitive to Apobec2a,2b knockdown (Figure 5.5) suggesting that Apobec2a,2b may somehow facilitate communication between regenerative cells and immunocompetent cells, and that this communication is important for retina and optic nerve regeneration.

Since its identification, Apobec2 has been most highly associated with muscle tissue (Liao et al., 1999; Anant et al., 2001a; Powell et al., 2012; Li et al., 2014).

Knockdown/knockout of Apobec2 causes multiple phenotypes in muscle, including decreased mass, altered muscle fiber type ratios, and myopathies (Sato et al., 2009; Etard et al., 2010). Surprisingly, no activity-dependent or regenerative research in muscle has focused on Apobec2. But, an inflammatory response has been characterized. In fact, macrophages have been shown to promote muscle growth and regeneration (Arnold et al., 2007; Tidball and Wehling-Henricks, 2007; Deng et al., 2012; Saclier et al., 2013; Zordan et al., 2014). It would be interesting if Apobec2 proteins, similar to their role in zebrafish retina regeneration, regulate immunocompetent cells during times of differential muscle use, muscle growth, and muscle regeneration.

The mechanism by which Apobec2a,2b facilitate communication with microglia/leukocytes during retina and optic nerve regeneration remains unknown. Previously, we proposed a mechanism whereby Apobec2 sumoylation regulates its cellular localization, and that non-sumoylated Apobec2 can enter the nucleus and interact with transcription factors, influencing gene expression (Chapter 5.4). Its possible that one of the gene expression programs controlled through this mechanism involves the production of secretory cytokines that stimulate the activity of immunocompetent cells, which then, through their activity stimulate regeneration. Further work will need to be done in order to fully decipher this mechanism.

In summary, we provide evidence that an immune response accompanies zebrafish retina regeneration following mechanical injury and optic nerve regeneration following optic nerve cut. Furthermore, this work suggests that Apobec2 proteins, like other Apobec proteins, may play a role in the immune response.

5.5 Materials and Methods

5.5.1 Animals

Zebrafish were kept at 26-28 °C on a 14/10 hr light/dark cycle. Transgenic *gfap:gfp* (Kassen et al., 2007), *1016 tuba1a:gfp* (Fausett and Goldman, 2006; Powell et al., 2012), *mpeg1:gpf* (Ellett et al., 2011), *apobec2bP+I:gfp* (Powell et al., 2012), *hsp70:zapobec2wt* (Chapter 4), *hsp70:zapobec2mut* (Chapter 4), and *hsp70:hAPOBEC2* (Chapter 4) fish have been described previously. Fish were harvested by treatment with a lethal dose of tricaine methane sulfonate (Sigma). Only adult fish (>2.5 months of age) were used in this study.

Mice were harvested by treatment with a lethal dose of isoflurane (VetOne). Adult C57BL/6 mice were used in this study. Fish and mice were handled in accordance with the University of Michigan Committee on Use and Care of Animals.

5.5.2 Retina Injury, Morpholino-Mediated Gene Knockdown, and Heat Shock

Mechanical retinal injury has been described previously (Powell et al., 2012; Powell et al., 2013). Photoablation was carried out as described (Thomas et al., 2012). Briefly fish were placed in a glass beaker positioned ~5 cm from the tip of a fiber optic light (X-Cite 120Q metal halide lamp from a Zeiss Axiophot, Axio Observer Z.1 microscope) and exposing them to ~100,000 lux for 30 minutes. Optic nerve lesions have been described previously (Fausett and Goldman, 2006; Veldman et al., 2010; Powell et al., 2012). Lissamine-tagged morpholino antisense oligonucleotides (MOs) (Gene Tools) were delivered at the time of injury by using a Hamilton syringe. MO delivery to cells was facilitated by electroporation as described (Powell et al., 2012). The control, *apobec2a*, and *apobec2b* targeting MOs have been described previously (Rai et al., 2008; Powell et al., 2012; Powell et al., 2013). Heat shock was carried out as outlined previously (Chapter 4).

5.5.3 RNA Isolation, RT-PCR, and Real-Time PCR

Total RNA was isolated using TRIzol (Invitrogen) and was DNase treated (Invitrogen). cDNA synthesis was performed using random hexamers and either SuperScript-II (Invitrogen) or M-mulv (NEB) reverse transcriptase. PCR reactions used Taq and gene-specific primers (Table 5.1). Real-time PCR reactions were carried out with ABsolute SYBR Green Fluorescein Master Mix (Thermo Scientific) on an iCycler real-time PCR detection system (Bio-Rad). The ΔΔCt method was used to determine relative expression of mRNAs. Student T tests were performed to determine statistical differences between samples.

5.5.4 Fluorescence Activated Cell Sorting

FACS sorting was carried out as previously described (Powell et al., 2013). Cell sorting was performed by the University of Michigan Flow Cytometry Core on a BC Biosciences FACSAria 3 laser high-speed cell sorter.

5.5.5 Tissue Preparation, Immunofluorescence, In situ Hybridization, and Imaging

Zebrafish eyes were prepared for sectioning and sectioned as has been done previously (Powell et al., 2012; Powell et al., 2013). *In situ* hybridizations were performed with antisense digoxigenin (DIG)-labeled RNA probes (Powell et al., 2012). Sense control probes were generated and showed no signal above background (data not shown). For cloning of *tnfb*, *plek*, *mpeg1*, *mfap4*, *spi1*, *c1qc*, and *apoc1l* probes, PCR was carried out using Phusion DNA Polymerase (NEB), cDNA prepared with zebrafish retinal RNA, and primers indicated in Table 5.1. PCR products were then adenylated with dATP (Invitrogen) and Taq DNA Polymerase (NEB) and cloned into pGEMT-Easy (Promega). Sequencing at the University of Michigan DNA Sequencing Core validated that these clones were correct. Antisense DIG labeled probes were created using restriction endonuclease linearized plasmid, RNA polymerase [SP6 (Promega) for *tnfb*, *plek*, *mfap4*, *spi1*, and *c1qc* and T7 (Roche) for *mpeg1* and *apoc1l*] and DIG rNTPs (Roche) as described previously (Powell et al., 2012).

Immunofluorescence was performed as described previously (Powell et al., 2012; Powell et al., 2013) using the following primary antibodies: mouse anti-4C4 (gift from Jack Parent, University of Michigan, 1:300), rabbit anti-L-Plastin (gift from Michael Redd, University of Utah, 1:1000), rabbit anti-GFP (1:1000, Invitrogen), and mouse anti-PCNA (dividing cell marker, 1:500, Sigma). The following secondary antibodies were used: Alexa Flour 555 donkey anti-mouse IgG (1:1000, Invitrogen), Alexa Flour 488 donkey anti-mouse IgG (1:1000, Invitrogen), Alexa Four 488 goat anti-rabbit IgG (1:1000, Invitrogen), and AMCA anti-mouse IgG (1:250, Invitrogen). Antigen retrieval for PCNA staining was performed by boiling the sections in 10 mM sodium citrate for 20 min followed by cooling them for another 20 min in solution.

Images were examined using a Zeiss Axiophot, Axio Observer Z.1. Images were captured using a digital camera adapted onto the microscope and were processed/annotated with Adobe Photoshop CS4. Student T tests were performed to determine statistical differences between samples.

5.5.6 Muscle Denervation and siRNA Mediated Gene Knockdown

Tibialis anterior (TA) muscle denervations have been described previously (Tang et al., 2009). Briefly, fur covering the lower back to proximal thigh was removed, the region

was swabbed with Betadine, and a small posterolateral cutaneous incision was made beginning at the approximate region of the sciatic notch. The superficial facia was cut and the hamstring, and gluteal muscles were separated bluntly. With the sciatic nerve exposed, a 1-cm-long section was removed, and the incision closed with wound clips.

Predesigned mouse Apobec2 stealth siRNAs were ordered from Invitrogen (5' to 3'; siRNA1: UCUUUAACACCAUCCUGCCAGCUUU, AAAGCUGGCAGGAUGGUGUUAAAGA; siRNA2: CAGCCUCUCAGAAUGGAGAUGAUUU, AAAUCAUCUCCAUUCUGAGAGGCUG; and siRNA3: UCAUUCUGGUGAGCCGGCUCUUCAU, AUGAAGAGCCGGCUCACCAGAAUGA). Stealth siRNAs and plasmid DNA were delivered into TA muscle by electroporation as described previously (Tang et al., 2009). Briefly, the TA muscle was injected with 20 µl of solution containing 32 µM siRNA, 50 mM NaCl, and 2–5 µg of pCS2EGFP plasmid (marker) with the molar ratio of stealth siRNA to pCS2EGFP being >500-fold so as to ensure all GFP+ fibers harbor siRNA. Nucleic acid uptake was facilitated by placing electrodes, coated with ultrasound transmission gel, on either side of the leg and using a BTX square wave electroporator to deliver six pulses of 140 V/cm of 60-ms duration with an interval of 100 ms. To ensure muscle fibers had recovered form any electroporation-induced damage, animals were allowed to recover 10 days before isolation of GFP+ fibers. For control experiments, 2–5 µg of pCS2EGFP was injected in the absence of siRNAs.

5.6 Acknowledgements

This work was supported by NEI Grants RO1 EY018132, 1R21 EY022707 (D. Goldman), the University of Michigan Vision Research Training Grant 5T32EY13934-10 (C. Powell), and the University of Michigan Predoctoral Fellowship (C. Powell). I thank T. Jurkiw and X. Zhao for help with *in* situ hybridization; E. Cornblath for preparing and analyzing photoablation samples; P. Macpherson for preparing mouse innervation, denervation, and siRNA tissue samples; M. Redd and J. Parent for providing antibodies; the University of Michigan Flow Cytometry Core; the University of Michigan DNA Sequencing Core; R. Karr and J. Kirk for fish care; Members of the Goldman lab for helpful comments.

5.7 Figures

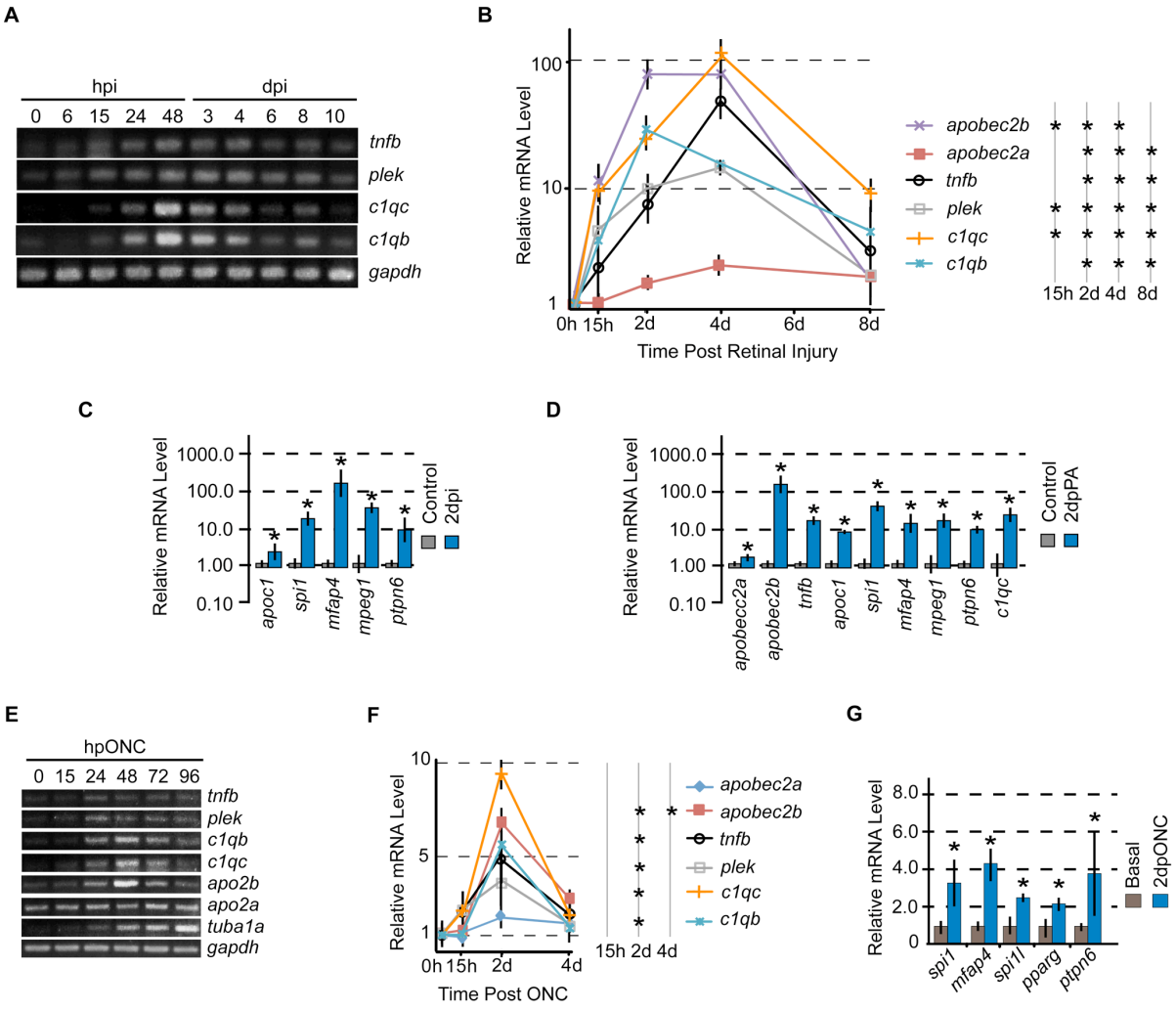

Figure 5.1 Injury-dependent regulation of genes associated with the immune and complement response

(A) RT-PCR analysis and (B and C) real-time PCR quantification of the indicated mRNAs isolated from retinas at various times post mechanical injury by poke with a 30-gauge needle. (D) Real-time PCR quantification of the indicated mRNAs isolated from retinas 2 days post light-mediated photoablation (2dpPA). (E) RT-PCR analysis and (F and G) real-time PCR quantification of indicated mRNAs isolated from retinas at various times post optic nerve cut (ONC). Expression analyses demonstrate that an immune response occurs concurrent with a regenerative response. For RT-PCR and real-time PCR analyses, the expression of *gapdh* served as the internal control. For real-time data, the *Y*-axis represents fold induction and is normalized to 0 hours (0h), i.e. the uninjured retina, which was assigned a value of 1. Data represents means ± s.d. (n=3 individual cDNA sets; compared with control, time points marked with an asterisk have a $P < 0.05$). hpi, hours post injury; dpi, days post injury.

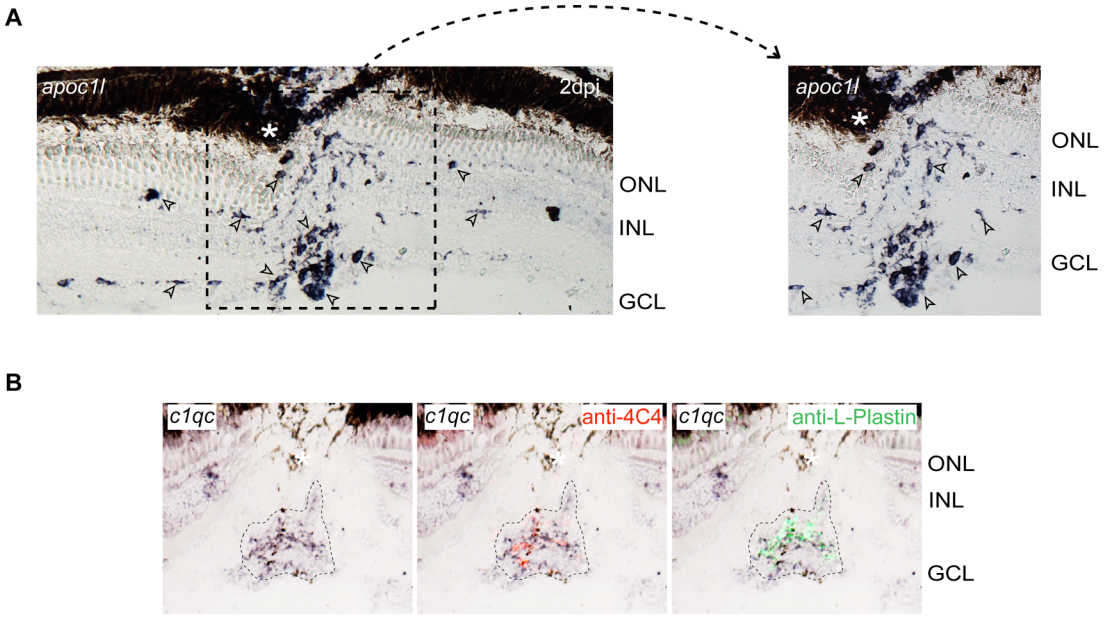

Figure 5.2 Immunocompetent cells at the site of injury express markers of the immune and complement response

In situ hybridization signal at 2dpi mechanical injury using (A) *apoc1l* and (B) *c1qc* probes is localized to cells at the injury site that have morphologies typical of immunocompetent cells (representative cells are designated with arrowheads in A). (B) Co-staining with markers of microglia (4C4 and L-Plastin) and leukocytes (L-Plastin) confirmed the cells stained positive by *in situ* hybridization are immunocompetent cells. Area encircled by dashed lines delineates a region of overlap between *in situ* hybridization and immunostaining signals. The injury site is marked with an asterisk. Dpi, days post injury; ONL, outer nuclear layer; INL, inner nuclear layer; GCL, ganglion cell layer.

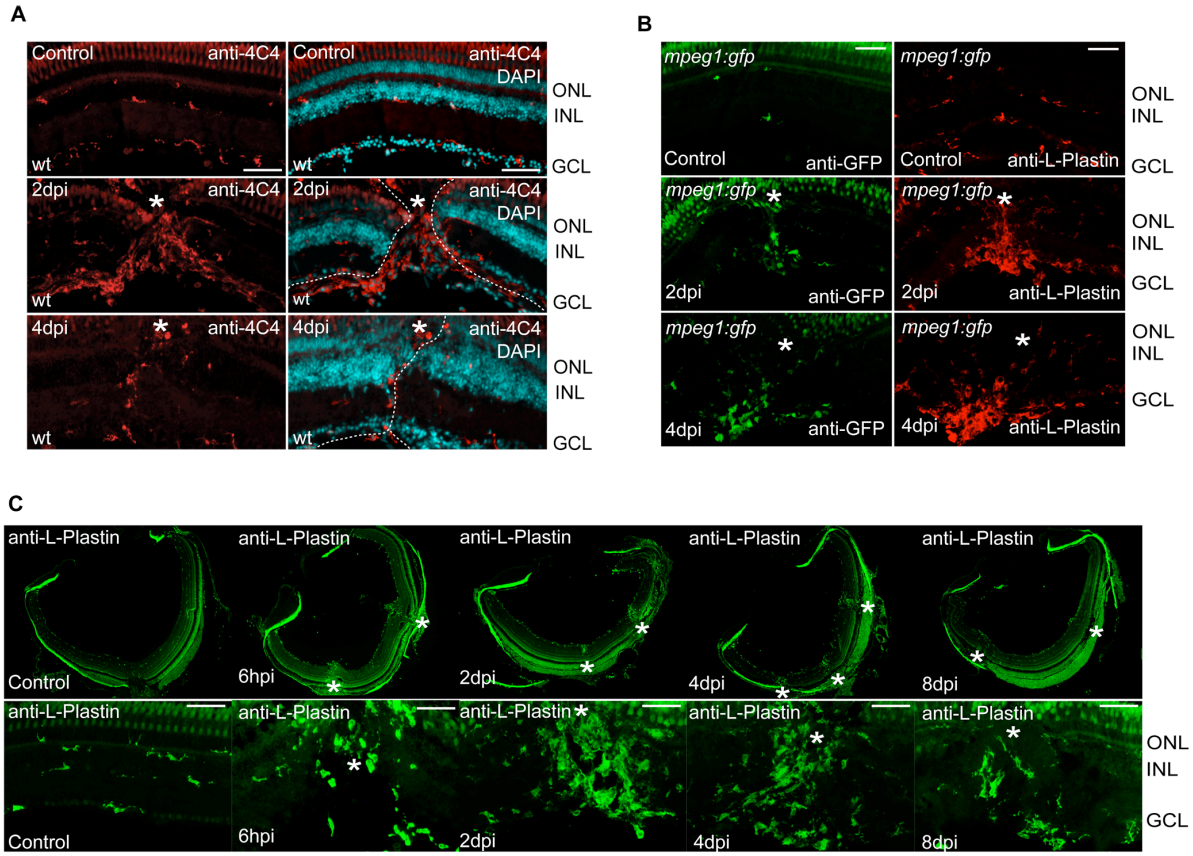

Figure 5.3 Immunostaining identifies the localization of immunocompetent cells during a time course of retina regeneration

Immunostaining using antibodies targeting (A) 4C4 in wt fish, (B) GFP and L-Plastin in *mpeg:gfp* transgenic fish, and (C) L-Plastin in wt fish demonstrate the localization of immunocompetent cells in the uninjured eye (control) and in the injured eye at multiple time points after poke with a 30-gauge needle. Microglia/leukocytes arrive at and fill the injury site within 6hpi and remain there through 8dpi. Abbreviations as in Figure 5.2. The injury site is marked with an asterisk. Scale bars, 50 μm.

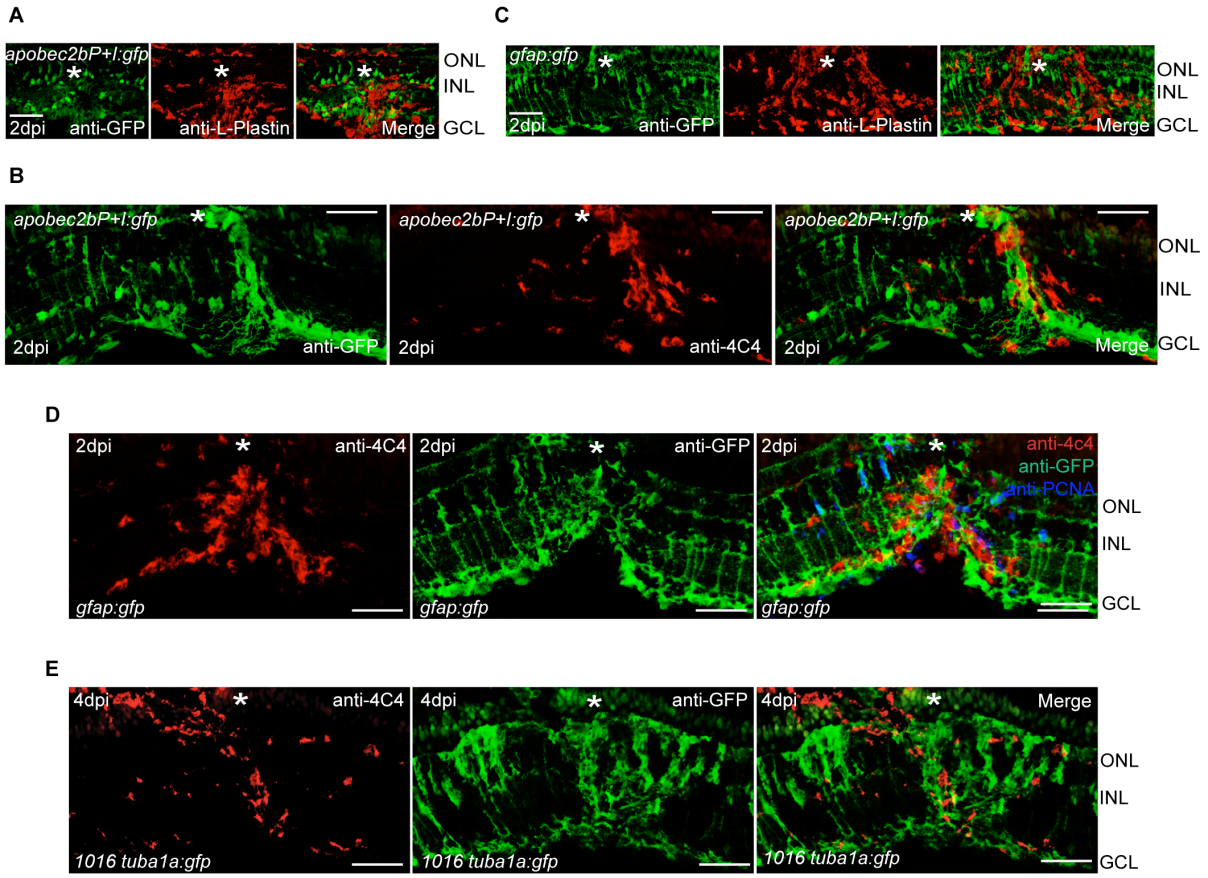

Figure 5.4 Immunocompetent cells reside in proximity to MGPCs and activated RGCs following injury

(A and B) Immunostaining of sections prepared from injured *apobec2bP+I* transgenic fish indicates that immunocompetent cells identified by (A) L-Plastin and (B) 4C4 staining do not express *apobec2b*, but suggests that these immunocompetent cells are in close proximity to GFP+ Müller glia derived progenitors (MGPCs) and activated retinal ganglion cells (RGCs). (C-E) Similar results were seen following staining of (C) Müller glia (MG) using *gfap:gfp* transgenic fish (GFP+ cells), (D) 2dpi MGPCs using *gfap:gfp* (GFP+, PCNA+ cells), and (E) 4dpi MGPCs using *1016 tuba1a:gfp* transgenic fish (GFP+ cells). Abbreviations as in Figure 5.2. The injury site is marked with an asterisk. Scale bars, 50 μm.

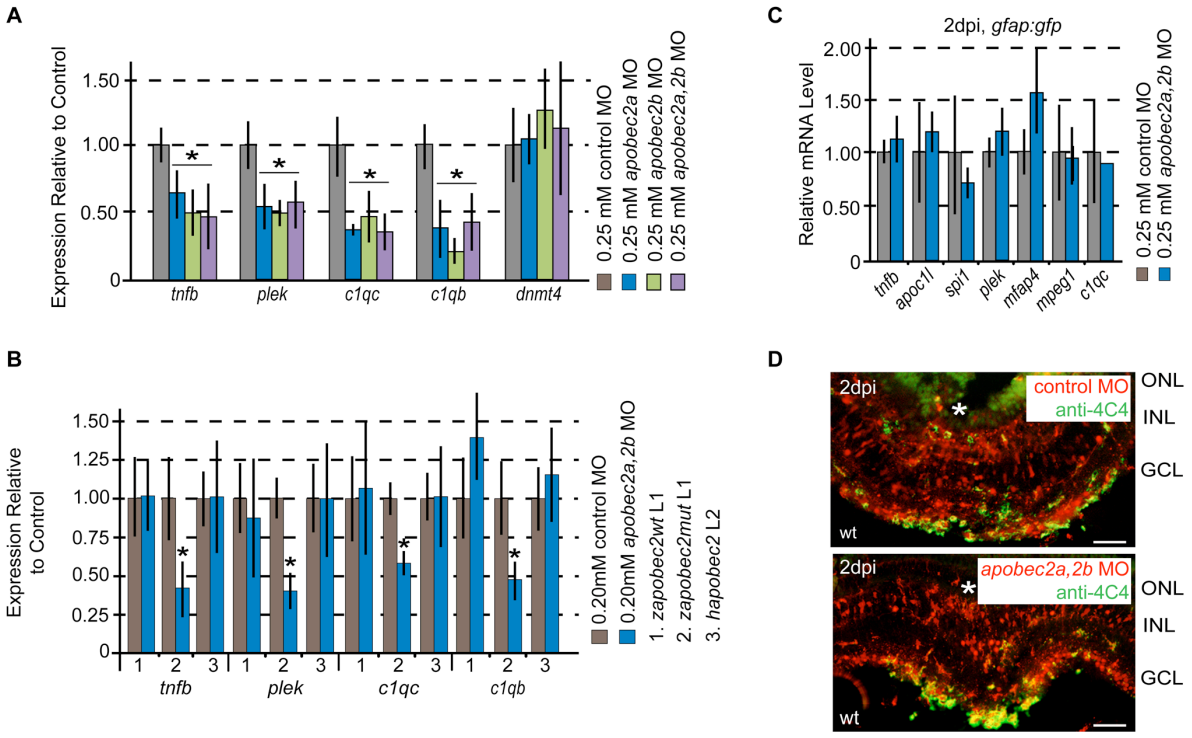

Figure 5.5 Apobec2a,2b regulate the injury-dependent activation of immune and complement gene expression programs in immunocompetent cells but not their localization to the injury site following mechanical injury

(A) Real-time PCR quantification of the indicated mRNAs isolated from retinas 2 days after injury and administration of 0.25 mM control, *apobec2a*, *apobec2b*, or *apobec2a,2b* MO demonstrates that injury-dependent activation of *tnfb*, *plek*, *c1qc*, and *c1qb* is regulated by Apobec2a,2b. (B) Real-time PCR quantification of the indicated mRNAs purified from FACS sorted GFP+, lissamine+ Müller glia derived progenitors (MGPCs) 2 days after injury and electroporation of 0.25 mM control or *apobec2a,2b* MO using *gfap:gfp* transgenic fish indicates that the expression of immune and complement genes is not regulated by Apobec2a,2b in MGPCs. (C) Real-time PCR quantification of the indicated mRNAs isolated from heat shocked *hsp70:zapobec2wt*, *hsp70:zapobec2mut*, or *hsp:70hAPOBEC2* transgenic fish retinas 2 days after injury and administration of 0.20 mM control or *apobec2a,2b* MO demonstrates that the *apobec2a,2b* MO knockdown phenotype can be rescued by inducing the expression of the *zapobec2wt* and *hAPOBEC2* transgenes, but not the *zapobec2mut* transgene. (D) Immunostaining of immunocompetent cells after the knockdown of Apobec2a,2b indicates that Apobec2a,2b do not regulate the localization of immunocompetent cells to the injury site. For real-time PCR analyses, the expression of *gapdh* served as the internal control. mRNA levels were normalized to levels of the control MO samples, which were given a value of 1. Data represents means ± s.d. (n=3 individual cDNA sets; compared with control, time points marked with an asterisk have a $P < 0.03862$). Abbreviation as in Figure 5.1 and 5.2. Scale bars, 50 μm.

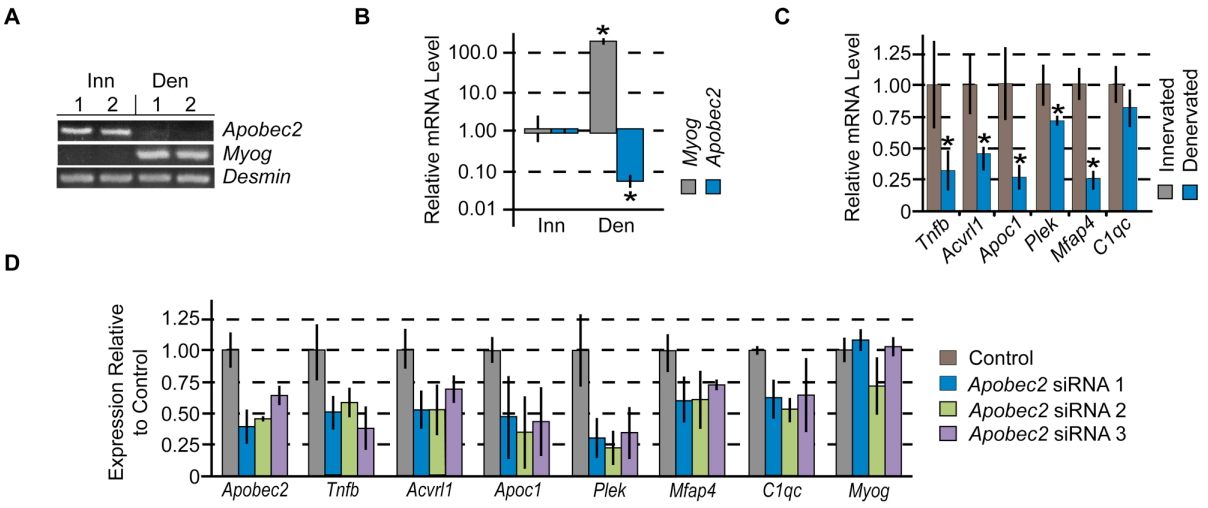

Figure 5.6 Apobec2 regulates the expression of immune and complement programs in muscle

(A) RT-PCR analysis and (B and C) real-time PCR quantification of the indicated mRNAs isolated from innervated or denervated (3 days post denervation) mouse TA muscle demonstrates that *Apobec2*, *Tnfb*, *Acvrl1*, *Apoc1*, *Plek*, and *Mfap4* expression levels decrease following denervation. (D) Real-time PCR quantification of the indicated mRNAs isolated from innervated mouse TA muscle 10 days after injection and electroporation of control (no siRNA) or *Apobec2* siRNA solutions suggests that the expression of *Tnfb*, *Acvrl1*, *Apoc1*, *Plek*, *Mfap4*, and *C1qc* is dependent on Apobec2. For RT-PCR and real-time PCR analyses, the expression of *Desmin* served as the internal control. For real-time PCR analyses, mRNA levels were normalized to levels of (B and C) denervated muscle or (D) control electroporation, which were given a value of 1. (B and C) Data represents means ± s.d. (n=3 individual cDNA sets; compared with control, time points marked with an asterisk have a $P <$ 0.04248. (D) Because the control and *Apobec2* siRNA3 samples are an n=2 (not n=3 as the other samples), no analyses of significance was performed. TA, tibialis anterior; Inn, innervated; Den, denervated.

5.8 Tables

Primer Set	Application	Sequence 5'->3'
mfap4 probe	Cloning and In Situ Probe Generation	F, TTCGAATTCAGTGACTGTACATCCATGCCCTTCG
		R, TTCGCGGCCGCTCATACTGACAGTGTGAGTGCCTTTCC
tnfb probe	Cloning and In Situ Probe Generation	F, TTCGAATTCGGAGAACTAGCAGCATGGTGAGATACG
		R, TTCGCGGCCGCGTAGTGCCCTTGTTATAGTGCTCTTGACTG
plek probe	Cloning and In Situ Probe Generation	F, TTCGAATTCGTGTGGGTTGTGTTAAAAGACGATGCT
		R, TTCGCGGCCGCAACAGGAGAATGCTGGACACTGAAGA
c1qc probe	Cloning and In Situ Probe Generation	F, GCAGGATCCGCGATGGAAGGCAAGGAATGAAG
		R, TTCGCGGCCGCCAACAATCAGTGTGCATGAATCAGGA
spi1 probe	Cloning and In Situ Probe Generation	F, TTCGAATTCGTAGAGAGAGGGTAACCTGGACTGGCT
		R, TTCGCGGCCGCGACTTCTCCCGTCTTTCCGTAGTTTCT
mpeg1 probe	Cloning and In Situ Probe Generation	F, TTCGAATTCCCACCGGTGGTTATTCTTGTCCTC
		R, TTCGCGGCCGCGGGTTTTCATTTGCAGCTTCATTCTG
apoc1l probe	Cloning and In Situ Probe Generation	F, TACCACATCGCAAAGCTGTAAGGAGA
		R, CTCATTTTTTCTTATTTTACAGCATCCCAC
gapdh	SQ RT-PCR and Real-Time PCR	F, ATGACCCCTCCAGCATGA
		R, GGCGGTGTAGGCATGAAC
apobec2a	SQ RT-PCR and Real-Time PCR	F, CTGCTGCAGACGGAGAAAAACCA
		R, CCAGCGTGCTCGTCCTCAATGTA
apobec2b	SQ RT-PCR and Real-Time PCR	F, ATGAGGAGTTTGAGCTAGAGCCGATG
		R, ATCCTCCAGGTAACCACGAACGC
tnfb	SQ RT-PCR and Real-Time PCR	F, GAGCACAAAGGCTGCCATTCACT
		R, GACCATCTCCTTCAACATCTTCAACG
plek	SQ RT-PCR and Real-Time PCR	F, AAGAGAGCGCTGGTTTTCAAGGTG
		R, TCATGCACACGTACAGTTCACTCAGG
c1qc	SQ RT-PCR and Real-Time PCR	F, GTCTGGCCTCTGCTGACACCTGT
		R, GGATCTCCATGGGGACCTCTCTTT
c1qb	SQ RT-PCR and Real-Time PCR	F, TTAAGGCCACCATCTGTTTTCCAAC
		R, TCTCCTTTAGCACCATCCTTCCCAT
tuba1a	SQ RT-PCR and Real-Time PCR	F, GGCTGCCCTGGAGAAAGATTATGA
		R, AGGATTGACCTTTTAGCCAGTTGACA
mfap4	SQ RT-PCR and Real-Time PCR	F, CCTGCAACAATAAGAAGGTGTGAGTGAA
		R, CCCGGCTGGATAGATGGTGTAAAC
spi1	SQ RT-PCR and Real-Time PCR	F, TTATAACACGCATCACATTCATCCAGTG
		R, TGTCCGGGGCAAGTATGTCATCT
spi1l	SQ RT-PCR and Real-Time PCR	F, GCAAGTGGGAAACCAGAGACAGAGAC
		R, TCAGTGCTGAGATACGGGTAGAAGTCG
pparg	SQ RT-PCR and Real-Time PCR	F, GCTTCTTCCACAGCTACCAGTCCAGA
		R, GAGATCAGGGTCCCGTCTTTATTCAT
ptpn6	SQ RT-PCR and Real-Time PCR	F, AGAAGCCGTTTTGAAGAGCCGAG
		R, CCTGTAGGGTTCCATGATCTCCAGTG

apoc1l	SQ RT-PCR and Real-Time PCR	F, AGCCCAATTCTTTCGAGGACTGC
		R, ACCAAGCTCGCTCTGTTCAATGTTC
dnmt4	SQ RT-PCR and Real-Time PCR	F, CAGAGCAGAGACGGCCAATCAGAG
		R, CATTACAGGGACTTCCACCAATCACC
mmapobec2	SQ RT-PCR and Real-Time PCR	F, CTTCCGCCCTTCGAGATTGTCAC
		R, TCGAAAGCTGGCAGGATGGTGT
mmmyog	SQ RT-PCR and Real-Time PCR	F, GAGAAGCACCCTGCTCAAC
		R, GGTGACAGACATATCCTCC
mmdesmin	SQ RT-PCR and Real-Time PCR	F, AATGACATCCCGCGTGTACC
		R, AAGAAGCGCACCTTCTCGAT
mmacvrl1	SQ RT-PCR and Real-Time PCR	F, CTTCTTGGTGCAGAGGACGGTAGC
		R, GGCGATGAAGCCTAGGATGTTGTC
mmmfap4	SQ RT-PCR and Real-Time PCR	F, TGCCACTGATGCTGATGCTGCT
		R, ACTTGCCGCCCTCAGTTGTCAT
mmtnfb	SQ RT-PCR and Real-Time PCR	F, AAACCTGCTGCTCACCTTGTTGG
		R, AGGTAGATGGGAGTGGGAATGGC
mmc1qc	SQ RT-PCR and Real-Time PCR	F, GTGGAGGGCCGATACAAACAGAAG
		R, TTGGCCGTATGCGATGTGTAGTAGAC
mmplek	SQ RT-PCR and Real-Time PCR	F, CATGATCTCCGCTTCCCTGCTC
		R, CCTGCTTGATGATAACCCCTCTGAAT
mmapoc1	SQ RT-PCR and Real-Time PCR	F, GCTCTTCATCGCTCTTCCTGTCCT
		R, GGGTCTTGGTCAAAATTTCCTTCTGTT

Table 5.1 List of primers used in this study and their applications

Chapter 6:
Conclusions and Future Directions

I began this dissertation by introducing three topics that I felt would be useful in providing context for my thought processes and the design of my experiments: retina and optic nerve regeneration, DNA methylation, and the Apobec protein family. I believe that the research presented in this dissertation has contributed to the current understanding of each one of these fields. Examples of these contributions, as well as potential future directions stemming from this work, are discussed below.

6.1 Conclusions

6.1.1 Retina and Optic Nerve Regeneration

As stressed at multiple locations throughout this dissertation, the key to stimulating a mammalian regenerative response following retina or optic nerve damage likely resides in our ability to awaken the innate regenerative potential of Müller glia (MG) or retinal ganglion cells (RGCs), respectively. Our capacity to perform this task is aided by understanding the mechanisms required for the endogenous regenerative events that occur in an organism such as zebrafish.

In our studies of zebrafish retina regeneration described in Chapter 2, we showed that the expression of *apobec2a* and *apobec2b* (*apobec2a,2b)* is highly induced in MG activated by injury and in proliferating Müller glia progenitor cells (MGPCs). We show that the injury-dependent expression of *apobec2b* is stimulated by the basic helix-loop-helix transcription factor Ascl1a (Fausett et al., 2008). Importantly, knockdown of Apobec2a and/or Apobec2b impedes MG activation and the proliferation of MGPCs, demonstrating their necessity for these events. Moreover, we show that Apobec2a,2b are required for the maximal injury-dependent expression of *ascl1a* and Ascl1a target genes such as *tuba1a* and

lin28 (Fausett et al., 2008; Ramachandran et al., 2010a). In our studies of optic nerve regeneration, we showed that the expression of *apobec2b* and *ascl1a* is induced in RGCs following optic nerve damage and that Apobec2a, Apobec2b, and Ascl1a are required for the stimulation of RGCs to a growth-permissive state. In Chapters 3 and 4, the biochemical function of Apobec2a,2b was explored (discussed in more detail below) and a model was proposed whereby Apobec2a,2b function by binding to the DNA binding domain of the transcription factor Pou6F2, perturbing its ability to interact with DNA and to regulate gene transcription. The developmental expression of Pou6F2 has been correlated with the differentiation of retinal neurons (Zhou et al., 1996) and suggests that it may act as an inhibitor of retina and optic nerve regeneration. Additional work is needed to test and validate this model.

In Chapter 3, I describe research that, to the best of my knowledge, represents the first in-depth, site-specific, genomic DNA methylation analysis of a cell functioning in an endogenous regenerative event or of a cell isolated directly from a complex tissue. While the reprogramming events of early development (Mayer et al., 2000; Oswald et al., 2000; Saitou et al., 2012), induced pluripotent stem cell (iPSC) generation (Meissner et al., 2008; Mikkelsen et al., 2008; Polo et al., 2012; Hackett et al., 2013; Kumar et al., 2013b), heterokaryon formation (Bhutani et al., 2009), and nuclear transfer (Simonsson and Gurdon, 2004; Jullien et al., 2011) are marked with large-scale changes in the DNA methylation landscape, particularly in pluripotency factor promoter regions, we presented evidence that zebrafish MG are basally programmed (at least at the level of DNA methylation) for a regenerative response. This basal methylation landscape may contribute to the high efficiency and speed by which MG reprogram following zebrafish retina damage when compared to other reprogramming events such as iPSC generation (Mikkelsen et al., 2008). Interestingly, we showed that aspects of this basal programming are shared with mammalian MG, suggesting that if provided the correct signal, they too may respond with a regenerative response.

While we did not find changes in DNA methylation occurring in the promoters of pluripotency factor and early-induced regeneration associated genes, we did identify a changing DNA methylation landscape as MG reprogram to MGPCs, and we demonstrated that the expression of genes which encode modulators of DNA methylation is regulated

during retina regeneration. We showed evidence that the early events (0-2dpi) and later events (2-4dpi) of retina regeneration are marked by a preponderance of DNA demethylation and methylation, respectively, and we correlated these changes in methylation with changes in gene expression. Although the exact purpose for these methylation changes remains unknown, we hypothesize that the early events of DNA demethylation are needed for transcriptional activation during MG reprogramming and that the later increase in DNA methylation is needed for the initiation of MGPC differentiation. Importantly, we showed that the perturbation of the basal and changing MG DNA methylation landscape during zebrafish retina regeneration (via inhibition of DNA methyltransferases) blocks the regenerative ability of MG, stressing the importance of DNA methylation in this process. We did not address the regulation of DNA methylation within RGCs during optic nerve regeneration, though it would make for an interesting comparison. Furthermore, the role of other epigenetic marks, such as histone modifications, in the process of retina and optic nerve regeneration remains to be explored.

In our studies outlined in Chapter 4, we demonstrated that C-to-U RNA editing is regulated as MG are activated following injury and generate MGPCs. This represents, to my knowledge, the first in-depth analysis of RNA editing during an endogenous regenerative event. Interestingly, the majority of these editing changes are synonymous, occurring in translated regions of the transcript that do not result in any change in the protein primary sequence. While less abundant, C-to-U RNA editing that results in non-synonymous changes was also noted, as well as editing in the 5' and 3' untranslated regions. It would be interesting to know if similar editing is seen in RGCs during optic nerve regeneration. How these editing events occur, as well as their function, remains to be determined.

Finally, in Chapter 5 we add to the current body of evidence that indicates that an immune response is stimulated following injury to the zebrafish retina (Craig et al., 2010) or optic nerve. We characterized inflammatory gene expression programs, localizing changes in inflammatory gene expression to immunocompetent cells localized at the site of injury. We monitored the localization of immunocompetent cells in the retina before and at multiple time points following injury. Interestingly, our research indicates that Apobec2a,2b regulate the expression of inflammatory and complement genes via a communication event between MG/MGPCs/RGCs and immunocompetent cells. Additional work is needed to establish this

possibility and to ascertain if this inflammatory response is necessary for retina and optic nerve regeneration.

6.1.2 DNA Methylation

Epigenetic marks, such as DNA methylation, play a critical role in the establishment of cellular identity. Much has been learned about the regulation of DNA methylation since I began my dissertation research, particularly concerning the mechanism of DNA demethylation. In fact, when I was first designing my experiments, it was still uncertain as to whether or not DNA demethylation in eukaryotes occurred passively (replication-dependent), actively (replication-independent), or both.

Evidence for both passive and active mechanisms of DNA methylation has been provided by many studies since the onset of my dissertation research (Kohli and Zhang, 2013), and our methylation analyses described in Chapter 3 have added to this body of evidence. Our results support a role for active DNA demethylation during MG activation, as we noted demethylation that occurred prior to MGPC proliferation. Furthermore we characterized the expression of genes that encode proteins thought to regulate DNA demethylation during retina regeneration and found that many of them are induced within MGPCs following injury (Chapters 2 and 3). We showed that site-specific active DNA demethylation during MG activation likely occurs through a cytosine deaminase-independent mechanism, as the knockdown of Apobec2a,2b proteins did not impact this demethylation. Furthermore, our expression analyses measuring zebrafish *aid* (the only other Apobec protein in zebrafish) suggested that it is not expressed in the retina before or after injury (Chapter 1). While the exact mechanism whereby these changes occur remains unclear, it is possible that an oxidative pathway involving Tet and TDG enzymes is employed. In support for this hypothesis, expression analyses of MG and MGPC suggest that MG basally express these genes and that the expression of *tet3* and *tdg* is induced in MGPCs (Chapter 3).

6.1.3 Apobec2 Proteins

Although Apobec2 was identified over 13 years ago (Liao et al., 1999; Anant et al., 2001a), very little was known about the biochemical function of Apobec2 proteins when I began my thesis work. Because the expression of *Apobec2* is highest in muscle tissue (Liao

et al., 1999; Anant et al., 2001a; Mikl et al., 2005), much of the early work regarding Apobec2 was focused on studies of the muscle. *Apobec2* knockout mice, which were originally characterized as lacking any notable phenotype (Mikl et al., 2005), were later shown to have altered muscle fiber type ratios, diminished body mass, and myopathy (Sato et al., 2009). In support of this report, and soon after I began my dissertation, a research article was published that demonstrated that the knockdown of Apobec2a or Apobec2b during zebrafish development results in a dystrophic muscle phenotype (Etard et al., 2010). Others have reported a role for these proteins in developmental left-right axis specification (Vonica et al., 2011) and tumorigenesis (Okuyama et al., 2011). Prominent hypotheses for these correlations between Apobec expression and the resulting phenotype have included roles for Apobec2 proteins in DNA demethylation (Rai et al., 2008) and RNA editing (Etard et al., 2010; Okuyama et al., 2011; Vonica et al., 2011). Surprising, there has been no follow up research of any of these correlations to directly test these possibilities. In contrast to these hypotheses, which all rely on the deaminase activity of Apobec2 proteins, biochemical data has questioned the ability of these proteins to act as cytosine deaminases (Harris et al., 2002a; Mikl et al., 2005; Lada et al., 2011) or to bind polynucleotides (Anant et al., 2001a; Sato et al., 2009).

Chapter 2 of this dissertation is similar to the other studies of Apobec2 proteins mentioned above in that no mechanistic insights were gained. We correlated the expression of Apobec2 proteins with a phenotype; Apobec2a,2b are required for retina and optic nerve regeneration. The results of this early study were aided by our development of the *apobec2bP+I:gfp* transgenic fish, which labels *apobec2b* expressing cells with GFP. This transgenic fish may be useful in future studies of zebrafish Apobec2b. Unlike other studies, which have only correlated the expression of Apobec2 with a phenotype, this thesis represents the only body of work that took the next step: using these correlations in an attempt to decipher the biochemical function of Apobec2 proteins. We carefully designed our experiments to test the function of these proteins in the cells in which they are functioning endogenously: MG (and possibly RGCs in the future). In Chapters 2 and 3 we provide compelling evidence against the role of Apobec2 proteins in the regulation of site-specific DNA demethylation and RNA editing. Mutagenesis assays using zebrafish Apobec2a,2b demonstrated that they, like other previously characterized Apobec2 proteins,

fail to induce cytosine deaminase-dependent mutations in bacterial mutagenesis assays. Cumulatively, our data, in combination with biochemical data gathered by others, places doubt in the possibility that Apobec2 proteins function as cytosine deaminases.

To gain additional insights into the role of Apobec2 proteins during zebrafish regeneration, we designed Apobec2a,2b knockdown rescue experiments using transgenic fish that allow the conditional expression of transgenes via heat shock. We demonstrate that the conditional expression of exogenously introduced Apobec2a,2b using *hsp70:zapobec2wt* transgenic fish can rescue the phenotype resultant from the knockdown of endogenous Apobec2a,2b. This represents the first report of a morpholino knockdown rescue experiment during zebrafish retina regeneration. In addition, other transgenic fish that we developed revealed that the biochemical function of Apobec2 proteins during retina regeneration is conserved between fish and mammals (*hsp70:hAPOBEC2* transgenic fish) and that this function requires the proper coordination of zinc by Apobec2s (*hsp70:zapobec2mut* transgenic fish). Work is still needed to determine if the same is true of Apobec2a,2b during optic nerve regeneration.

To identify Apobec2 interacting proteins that may help reveal its functioning during regeneration, we designed a novel full-length, normalized cDNA yeast two-hybrid library using RNA isolated from MGPCs. With this library, we identified Ubc9, Toporsa, and Pou6F2 as Apobec2a,2b interacting proteins and demonstrate that these interactions are conserved with human APOBEC2. Moreover, characterization of these interactions revealed that Ubc9 and Toporsa regulate the N-terminal sumoylation of Apobec2 proteins and that this sumoylation can influence their nuclear exclusion. Characterization of the interaction between Apobec2 proteins and Pou6F2 revealed that Apobec2 proteins interact with the DNA binding domain of Pou6F2, possibly precluding its ability to bind DNA. Interestingly, our analyses, which are the only characterization performed within living cells, suggest that zebrafish Apobec2a and Apobec2b proteins do not oligomerize, at least in yeast.

Finally, as described above, our research suggests that Apobec2a,2b may control aspects of an inflammatory response which parallels, or participates in, the regenerative response following damage to the retina or optic nerve (Chapter 5). Research by others supports a connection between Apobec2 proteins and inflammation (Matsumoto et al., 2006; Iio et al., 2010). Interestingly, our work suggests that Apobec2 proteins may perform a

similar function in muscle as their knockdown in mouse muscle decreases the expression of many inflammatory genes (Chapter 5). Cumulatively, the work described in this dissertation has greatly contributed to the current understanding of Apobec2 proteins and their biochemical function.

6.2 Future Directions

While much has been learned through this work, it seems like we have uncovered more questions than we have answered. Many of these lapses in understanding have been mentioned above or have been described in previous chapters. A few directions that I feel would be the most logical next steps are discussed below.

6.2.1 Additional Rescue Experiments

The morpholino knockdown rescue experiments, which we designed for retina regeneration in Chapter 4, can be used as a powerful tool for asking a wide range of questions. A few that stem from my work include:

1) Do Apobec2a,2b function redundantly? Our work indicates that the functions of Apobec2a and Apobec2b are highly similar. Their knockdown impacts similar gene expression programs (Chapter 2), and they interact with the same proteins (Chapter 4); moreover, these protein interactions appear to perform similar functions (Chapter 4). Yet, we showed that the knockdown of either one of these proteins blocks retina and optic nerve regeneration (Chapter 1). Similarly, the knockdown of either Apobec2a or Apobec2b during zebrafish development results in a dystrophic phenotype (Etard et al., 2010). This may suggest that Apobec2a and Apobec2b do not function redundantly, but that they each have a unique, and currently unknown function (though some aspects of their function may be shared). This is commonly seen with gene duplications. Alternatively, it may suggest that the absolute level of Apobec2 protein (Apobec2a and Apobec2b) is critical. What is evident from our work in Chapter 5 is that the function of Apobec2a,2b during retina regeneration is conserved with human APOBEC2, as exogenously introduced hAPOBEC2 can rescue Apobec2a,2b knockdown during retina regeneration. Because of this, I hypothesize that the function of zebrafish Apobec2a,2b during retina and optic nerve regeneration is largely redundant and that the absolute levels of these proteins is what matters. To test this

hypothesis, transgenic fish that allow the conditional expression of Apobec2a or Apobec2b, independently, can be developed and assayed for their ability to rescue the knockdown of Apobec2b or Apobec2a, respectively.

2) Does the N-terminal sumoylation of Apobec2a,2b or their interaction with Ubc9 or Toporsa play an important role during regeneration? As mentioned in Chapter 4, Apobec2 proteins interact with Ubc9 and Toporsa at their N-termini. Furthermore, we demonstrated that at least one of the purposes of these interactions is to facilitate the N-terminal sumoylation of Apobec2 proteins and that this sumoylation can stimulate their nuclear exclusion. But, these interactions and this sumoylation could have multiple roles. In addition, while we analyzed the sumoylation of Apobec2 proteins by SUMO1, it is likely that they can be modified by other SUMO proteins. While addressing each one of these possibilities would add to our current understanding of Apobec2 proteins, arguably the most important question, in terms of regeneration, is whether or not these interactions, and the outcome of these interactions, are necessary for retina and optic nerve regeneration. To test this possibility, transgenic fish that allow the conditional expression of N-terminally truncated Apobec2 proteins (precluding their interaction with Ubec9 and Toporsa) can be generated and tested for their ability to rescue the knockdown of Apobec2a,2b. Alternatively, to address sumoylation specifically, the sumoylation sites of Apobec2a,2b can be mapped and mutated to prevent their sumoylation. Transgenic fish can then be made that produce these mutated Apobec proteins.

3) Is the interaction between Apobec2a,2b and Pou6f2 necessary for regeneration? In Chapter 4 we hypothesize that the interaction between Apobec2a,2b and the DNA binding domain of Pou6F2 precludes the ability of Pou6F2 to bind DNA. Our current work in the lab is directed at testing this possibility. Furthermore, I hypothesize that this is the main function of Apobec2 proteins; that they interact with and modulate the activity of select transcription factors, functioning independent of cytosine deamination. If the main function of Apobec2a,2b during retina regeneration is to bind Pou6F2 and modulate its activity, one would expect that by preventing this interaction, MG activation and MGPC proliferation would be diminished, as this is the phenotype seen after Apobec2a,2b knockdown (Chapter 1). Currently we know that the interaction between Pou6F2 and Apobec2a,2b occurs in a region of Apobec2a,2b other than their N-termini. These studies could be extended to

generate mutant Apobec2a,2b proteins that are unable to interact with Pou6F2. Then transgenic fish that allow the conditional expression of these mutated Apobec2 proteins can be generated and examined for their ability to rescue the knockdown of Apobec2a,2b.

4) Is Pou6F2 an inhibitor of the regenerative response? In our model of Apobec2a,2b function proposed in Chapter 4, we suggest that Pou6F2, whose expression is associated with retinal differentiation during development (Zhou et al., 1996), acts as an inhibitor of retina and optic nerve regeneration. Interestingly, one of the major obstacles in stimulating a regenerative response in mammals is the ability to overcome intrinsic inhibitory signals, so the identification of inhibitors of these regenerative events could be very useful. To test this theory, transgenic fish can be generated that allow the conditional expression of Pou6F2 and tested for their ability to inhibit retina or optic nerve regeneration.

6.2.2 The Role of Apobec2a,2b in the Inflammatory Response

As mentioned previously, our research suggests that Apobec2a,2b may regulate an inflammatory response via a communication event occurring between MG/MGPCs/RGCs and immunocompetent cells after damage to the retina or optic nerve (Chapter 5). While we present a considerable amount of data in support for this hypothesis during retina regeneration, this work needs to be extended to incorporate optic nerve regeneration. Questions that remain to be answered include:

1) Do Apobec2a,2b modulate the immune response during optic nerve regeneration? Like retina regeneration, we see a striking correlation between the time course of injury-dependent expression of *apobec2b* and those of the immune response following optic nerve cut. To determine if the regulation of gene expression in immunocompetent cells depends on the function of Apobec2a,2b in RGCs, expression analyses can be performed following Apobec2a,2b knockdown during optic nerve regeneration. This knockdown is arguably better and more informative than the knockdown performed during retina regeneration as it can be performed selectively in RGCs (see Chapter 2). The ability of *hsp70:zapobec2wt, hsp:70zapobec2mut,* and *hsp70:hAPOBEC2* transgenic fish to rescue this potential phenotype can also be assessed.

2) Is an immune response necessary for retina or optic nerve regeneration? While we (Chapter 5), and others (Craig et al., 2010; Nelson and Hyde, 2012), have reported that an

immune response is activated following damage to the zebrafish retina or optic nerve, it is unclear whether or not this response contributes to zebrafish retina or optic nerve regeneration. The correlation between immune and regenerative responses has also been noted in other regenerative model systems (Eming et al., 2009). Interestingly, the activity of macrophages has been shown to be important for adult salamander limb regeneration (Godwin et al., 2013) and muscle regeneration (Tidball and Wehling-Henricks, 2007; Deng et al., 2012; Kharraz et al., 2013). Likewise, I hypothesize that immunocompetent cells perform an essential function during retina and optic nerve regeneration. To test this hypothesis, immunocompetent cells can be depleted from the retina using clondronate liposomes (Godwin et al., 2013). Following the ablation of these cells, the activation of MG and the proliferation of MGPCs can be assessed during retina regeneration and RGC axonal outgrowth can be assessed following optic nerve injury.

6.2.3 The Role of Apobec2 in Muscle Regeneration

Muscle is a highly regenerative tissue, even in mammals (Ciciliot and Schiaffino, 2010). While it is easy to image that a regenerative event would follow injury or a period of intense exertion, one could also imagine that the mechanical motion of every day use would cause wear-and-tear in muscle that would require continuous regeneration. Since their identification, it has been known that the expression of Apobec2 proteins is highest in muscle tissue (Liao et al., 1999; Anant et al., 2001a). I hypothesize that, similar to zebrafish retina and optic nerve regeneration, Apobec2 proteins play an important role in muscle regeneration. Furthermore, I hypothesize that they perform this function by modulating the activity of transcription factors in an injury/activity-dependent fashion. While Apobec2 null mice have been generated (Mikl et al., 2005; Sato et al., 2009), there have been no reports of studies analyzing the role that Apobec2 proteins may perform during muscle regeneration. Questions that merit analysis include:

1) Is *Apobec2* mRNA or Apobec2 protein regulated in muscle fibers in an injury/activity-dependent manner? If Apobec2 plays an important role during muscle regeneration, one might expect changes in its abundance after injury, similar to what we see during zebrafish retina and optic nerve regeneration. But, because the expression of *Apobec2* is already high in muscle (possible due to a continual need to regenerate), one could image

that Apobec2 proteins are regulated in an activity/injury-dependent fashion. This regulation may include stability, sumoylation, or subcellular localization. It would be worthwhile to test these possibilities following muscle damage. In addition, correlations could be tested between changes found in the regulation of Apobec2 with changes in the immune response, such as the presence of immunocompetent cells and their expression changes (discussed below).

2) Is the expression of Apobec2 necessary for muscle regeneration? While this question would be facilitated through the use of Apobec2 null mice, these experiments can also be performed in mice using siRNAs or in zebrafish using anti-sense morpholinos. The ability of the animal to respond to muscle injury (for example, after an injection of cardiotoxin) following Apobec2 knockdown/out could be assessed relative to a control. Metrics could include gene expression and the proliferation of myogenic precursor cells.

3) Does Apobec2 control an immune response during muscle regeneration? Interestingly, as mentioned above, macrophages have been shown to play an important role during muscle regeneration (Tidball and Wehling-Henricks, 2007; Deng et al., 2012; Lesault et al., 2012; Kharraz et al., 2013). Similar to zebrafish retina regeneration, our preliminary expression analyses suggest that Apobec2 proteins control an inflammatory immune response following damage to mouse muscle via electroporation (Chapter 5). It would be worth developing these expression analyses, possibly including additional, earlier time points (1 to 4dpi) when macrophages have been shown to function most robustly following muscle injury (Deng et al., 2012).

6.2.4 Ascl1a/Lin28 Heat Shock Transgenic Fish

The ultimate goal in using zebrafish as a model system for studying retina and optic nerve regeneration is to be able to apply what we learn to mammalian systems. Ideally, one could identify the minimal components necessary to stimulate MG and RGC activation in zebrafish and attempt to stimulate a similar regenerative response in mammals. For this purpose, we designed the transgenic fish described in Appendix A, which allow the conditional expression of Ascl1a and/or Lin28, two master regulators controlling MG activation and MGPC proliferation. In the simplest sense, these fish were designed to answer one question: does the conditional expression of Ascl1a, Lin28, or both in combination

stimulate a regenerative response in the absence of injury? While this seems relatively straightforward, additional work may be necessary to show that the transgenes are functional (as the tags may preclude some aspect of their function) and that they induce to sufficient levels within MG. If the transgenes are unable to induce MG to generate MGPCs without injury, attempts at stimulating a regenerative response after injury can also be explored.

6.3 Final Conclusions

Our understanding of retina and optic nerve regeneration is expanding rapidly and has a very promising future. Applying what we have learned and will learn through studying zebrafish retina and optic nerve regeneration to mammalian systems will be an interesting next step. Understanding the biochemical function that Apobec2 proteins perform will likely prove useful in this and other endeavors.

It is my hope that after reviewing this thesis, you can better understand why I designed and performed these experiments and that you can appreciate the contributions that they provide. This dissertation, which represents years of my life, has been a personal journey. The knowledge and experience that I have gained extends far beyond any field of science. Perhaps most importantly, I have learned a lot about myself, for which I am especially grateful.

APPENDIX

Appendix A

Generation of transgenic fish that allow the conditional expression of Ascl1a and/or Lin28 via heat shock

A.1 Abstract

During zebrafish retina regeneration, Müller glia (MG) become activated and generate a population of Müller glia derived progenitors (MGPCs) capable of replacing lost neurons and glia. The ultimate goal of studying retina regeneration in zebrafish is to gain the knowledge necessary to stimulate the endogenous regenerative potential of mammalian MG. Key to this objective is the ability to stimulate MG activation and the generation of MGPCs. During zebrafish retina regeneration, the expression of *ascl1a* and *lin28* is rapidly induced following retinal injury, but their expression remains unchanged following damage to the mammalian retina. Ascl1a (a basic helix-loop-helix transcription factor) controls a large component of the expression program in activated MG and MGPCs during zebrafish retina regeneration, and Lin28 (an RNA binding protein) inhibits the maturation of, and stimulates the degradation of, miRNAs that maintain the MG in a differentiated state. Because these proteins play critical roles during zebrafish retina regeneration, yet are absent following mammalian retina damage, we sought to determine if the conditional expression of Ascl1a, Lin28, or both is sufficient to stimulate MG activation and the generation of MGPCs in zebrafish. Here we describe the generation of transgenic fish that will be used in our attempt to address this question.

A.2 Introduction

Unlike mammals, zebrafish respond to retinal damage with a robust regenerative response. Multiple injury models have been employed in the study of this regenerative event including light-mediated photoablation (Vihtelic and Hyde, 2000; Bernardos et al., 2007),

intraocular injection of cytotoxic chemicals (Fimbel et al., 2007), cell type-specific expression of toxic genes (Montgomery et al., 2010), and mechanical damage (Senut et al., 2004; Fausett and Goldman, 2006). Each of these models results in a unique injury signature; photoablation results in the death of rods and cones, intraocular injection of cytotoxic chemicals (depending on the dose) results in the death of retinal ganglion cells and inner nuclear layer neurons, cell-type specific cell ablation results in the death of a targeted cell type, and mechanical damage results in the death of all retinal cell types. This suggests that MG respond to stimuli from a variety of sources. The exact identities of these stimuli remain unknown, but may include: the loss of contact between MG and neurons as a result of neuronal cell death, the phagocytosis of cellular debris by MG, or the secretion of molecules from dying cells or from microglia recruited to the injury. Recent work has indicated that these secreted molecules may include factors such as Wnts (Ramachandran et al., 2011), Hbegf (Wan et al., 2012), and TNFα (Nelson et al., 2013).

Interestingly, regardless of the source of stimuli, expression analyses of the early regenerative response (including MG activation and the generation of MGPCs) indicate that there is a high degree of commonality in the downstream effects of these stimuli (Thummel et al., 2008b; Qin et al., 2009; Morris et al., 2011; Ramachandran et al., 2012). This suggests that no matter the initial stimulus, each converges on a common signaling cascade necessary for MG activation and the generation of MGPCs. While aspects of the regenerative response resemble developmental processes, it is evident that certain components are unique, as MG do not serve as progenitors during retinal development (Weissman et al., 2003). Although many factors have been shown to be necessary for MG activation and the generation of MGPCs, it is likely that some of these are downstream of a common signaling molecule. Two proteins that have emerged as major players in the establishment of the regenerative state are the basic helix-loop-helix transcription factor Ascl1a and the pluripotency factor Lin28.

Ascl1a was one of the first molecules identified as being necessary for zebrafish retina regeneration (Fausett et al., 2008). Since that time, Ascl1a has been shown to control the expression of a number of other genes, each shown to play important roles during regeneration, including *tuba1a* (Fausett et al., 2008), *lin28* (Ramachandran et al., 2010a), *dkk* (Ramachandran et al., 2011), *apobec2b* (Powell et al., 2012), and *insm1a* (Ramachandran et

al., 2012). *Ascl1* is expressed by retinal progenitors cells during development (Brzezinski et al., 2011) and is a key factor involved in neuronal fate conversion (Vierbuchen et al., 2010). Unlike during zebrafish retina regeneration, the expression of *Ascl1* is not induced in the mouse retina after injury (Karl et al., 2008), likely contributing to its inability to regenerate. Interestingly, the viral induction of *Ascl1* in mouse MG in culture is sufficient to reprogram them into progenitors (Pollak et al., 2013). Whether or not this holds true for MG residing within the intact retina remains to be determined.

Lin28 is a pluripotency factor whose expression is associated with embryonic stem cells and cancer (Nimmo and Slack, 2009). Its expression, in combination with *SOX2, OCT4,* and *NANOG,* is sufficient to convert human somatic cells into induced pluripotent stem cells (Yu et al., 2007). Unlike other pluripotency factors, Lin28 is not a transcription factor, but is an RNA binding protein (Moss et al., 1997) that binds to miRNAs, such as *let-7* miRNAs, inhibiting their maturation and stimulating their degradation (Rybak et al., 2008; Viswanathan et al., 2008; Heo et al., 2009). In contrast to *Lin28*, the expression of *let-7* miRNAs is associated with differentiation (Rybak et al., 2008; Nimmo and Slack, 2009; Melton et al., 2010). In zebrafish, *let-7* miRNA levels are high in differentiated MG and target the mRNAs of pluripotency genes and *ascl1a* for degradation. After injury, the expression of *lin28* is rapidly induced. This induction is important for the activation of MG and the generation of MGPCs, as Lin28 suppresses the activity of *let-7* miRNAs, thus relieving its degradation of pluripotency and *ascl1a* mRNAs (Ramachandran et al., 2010a). Unlike *ascl1a*, *lin28* is not expressed in the developing retina (Ramachandran et al., 2010a), suggesting that this component of the regenerative response is specific to retina regeneration. Interestingly, the decreased regenerative potential of *C. elegans* with age has been associated with increases in *let-7* miRNAs (Zou et al., 2013). Furthermore, the reactivation of *Lin28* expression in mice stimulates the regeneration of multiple tissues including hair follicles, cartilage, bone, and mesenchyme (Shyh-Chang et al., 2013). Whether or not an increased regenerative response occurs following damage to the retina remains to be seen.

These results summarized above support the hypothesis that the induction of Ascl1a, Lin28, or both in the absence of injury may be sufficient to stimulate the activation of MG and the generation of MGPCs. Previously, we generated a transgenic fish that allowed the conditional expression of Apobec2a,2b and found that they were unable to induce a

regenerative response in the absence of injury (Chapter 4). Here we build upon that study and describe the creation of transgenic fish that allow the conditional expression of Ascl1a, Lin28, or both.

A.3 Results

A.3.1 Generation of heat shock inducible fish

hsp70:ascl1a and *hsp70:lin28* transgenic fish were generated as outlined in the materials and methods (Figure 5.7). Two lines were generated for each transgene, and experimental size populations have been generated and are being maintained. Preliminary expression analyses of these transgenic fish have demonstrated functionality of the transgenes (data not shown). Homozygous populations were generated of *hsp70:ascl1a* and *hsp70:lin28* transgenic fish have been prepared and crossed to produced *hsp70:ascl1a, hsp70:lin28* double transgenic fish. The ability of these transgenic fish (individual and in combination) to stimulate a regenerative response in the absence of injury has yet to be determined.

A.4 Discussion

The discussion of this topic is included in Chapter 6 as a future directions.

A.5 Material and Methods

A.5.1 Animals

Zebrafish were kept at 26-28 °C on a 14/10 hr light/dark cycle. Fish were handled in accordance with the University of Michigan Committee on Use and Care of Animals. Construction of *hsp70* transgenic fish was carried out as outlined in Chapter 4. Briefly, the *1016 tuba1a:gfp SV40* cassette (Fausett and Goldman, 2006) was cloned followed by a second expression cassette encoding 1523 bp of the *hsp70* promoter (Halloran et al., 2000) driving the expression of: 1) *flag-myc-ascl1a* (*hsp70:ascl1a*) or 2) *myc-lin28* (*hsp70:lin28*) followed by an *SV40* sequence into the *pT2AL200R150G* Tol2 vector (Urasaki et al., 2006). *flag-myc-ascl1a* and *myc-lin28* were amplified from pCS2 clones described previously (Ramachandran et al., 2010a) using the primers listed in Table 5.2. Cloning into *hsp70*

construct was carried out with the restriction enzymes SmaI and KpnI. Tol2 transposase-mediated integration of the transgene was performed by injection into single-cell zebrafish embryos, which were raised to adulthood and screened for transgenic progeny (Powell et al., 2012). Multiple independent lines were selected and grown to adulthood. Homozygous lines of *hsp70:ascl1a* and *hsp70:lin28* were generated and crossed to produce *hsp70:ascl1a, hsp70:lin28* double transgenic fish. Insertion of both transgenes was validated by genotyping (gDNA isolated from tail clip) using the primers listed in Table 5.2. One genotyping primer is specific to sequence within *ascl1a* or *lin28* and the other is specific to pTal construct, thus specifically amplifying the transgene.

A.6 Acknowledgements

This work was supported by NEI Grants RO1 EY018132, 1R21 EY022707 (D. Goldman), the University of Michigan Vision Research Training Grant 5T32EY13934-10 (C. Powell), and the University of Michigan Predoctoral Fellowship (C. Powell). I thank R. Gangji for help genotyping the transgenic fish. R. Karr and J. Kirk for fish care; Members of the Goldman lab for helpful comments.

A.7 Figures

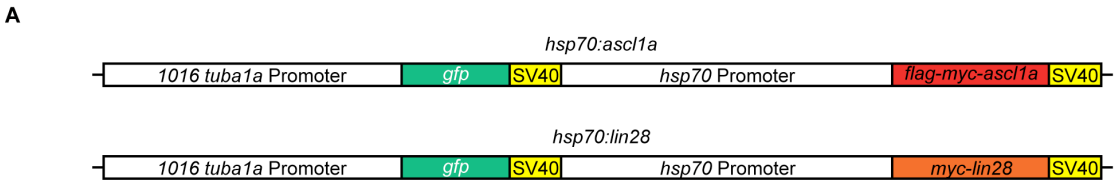

Figure A.1 Graphic depicting the composition of the *hsp70:ascl1a* and *hsp70:lin28* transgenes

A.8 Tables

Primer Set	Application	Sequence 5'->3'
pCS2-Spe1F	pTal Ascl1a and pTal Lin28 Cloning	GCTTAACTAGTTTGCAGGATCCCTTCGATTTAAAGCTA
pCS2-SV40R	pTal Ascl1a and pTal Lin28 Cloning	CTCACTAAAGGGAACAAAAGCTGGGTACCG
ptal insert F	pTal hsp70:Ascl1a and pTal hsp70;Lin28 Cloning	GCACCCGGGCTAGTGGATCAACAAGCTACTTGTTCT
ptal R	pTal hsp70:Ascl1a and pTal hsp70;Lin28 Cloning	AGCTGGCGAAAGGGGGATGTGCTGCAAGG
ascl1ascreen-F	Genotyping	ATGGACTACAAGGACGACGATGACAAG
ascl1ascreen-R	Genotyping	AGTTTTGGGAGATGGTGGGTGACA
lin28screen-F	Genotyping	ACCCGGTGCTACTTGTTCTTTTTGC
Lin28screen-R	Genotyping	TCGATCTCCTTTTGACCGCCTCTT

Table A.1 List of primers used in this study and their applications

References

Abdouni H, King JJ, Suliman M, Quinlan M, Fifield H, Larijani M (2013) Zebrafish AID is capable of deaminating methylated deoxycytidines. Nucleic Acids Res 41:5457-5468.

Achour M, Jacq X, Ronde P, Alhosin M, Charlot C, Chataigneau T, Jeanblanc M, Macaluso M, Giordano A, Hughes AD, Schini-Kerth VB, Bronner C (2008) The interaction of the SRA domain of ICBP90 with a novel domain of DNMT1 is involved in the regulation of VEGF gene expression. Oncogene 27:2187-2197.

Aguiar RS, Peterlin BM (2008) APOBEC3 proteins and reverse transcription. Virus Res 134:74-85.

Akalin A, Kormaksson M, Li S, Garrett-Bakelman FE, Figueroa ME, Melnick A, Mason CE (2012) methylKit: a comprehensive R package for the analysis of genome-wide DNA methylation profiles. Genome Biol 13:R87.

Anant S, Davidson NO (2000) An AU-rich sequence element (UUUN[A/U]U) downstream of the edited C in apolipoprotein B mRNA is a high-affinity binding site for Apobec-1: binding of Apobec-1 to this motif in the 3' untranslated region of c-myc increases mRNA stability. Mol Cell Biol 20:1982-1992.

Anant S, Mukhopadhyay D, Sankaranand V, Kennedy S, Henderson JO, Davidson NO (2001a) ARCD-1, an apobec-1-related cytidine deaminase, exerts a dominant negative effect on C to U RNA editing. Am J Physiol Cell Physiol 281:C1904-1916.

Anant S, Henderson JO, Mukhopadhyay D, Navaratnam N, Kennedy S, Min J, Davidson NO (2001b) Novel role for RNA-binding protein CUGBP2 in mammalian RNA editing. CUGBP2 modulates C to U editing of apolipoprotein B mRNA by interacting with apobec-1 and ACF, the apobec-1 complementation factor. J Biol Chem 276:47338-47351.

Arakawa H, Hauschild J, Buerstedde JM (2002) Requirement of the activation-induced deaminase (AID) gene for immunoglobulin gene conversion. Science 295:1301-1306.

Arand J, Spieler D, Karius T, Branco MR, Meilinger D, Meissner A, Jenuwein T, Xu G, Leonhardt H, Wolf V, Walter J (2012) In vivo control of CpG and non-CpG DNA methylation by DNA methyltransferases. PLoS Genet 8:e1002750.

Arita K, Ariyoshi M, Tochio H, Nakamura Y, Shirakawa M (2008) Recognition of hemi-methylated DNA by the SRA protein UHRF1 by a base-flipping mechanism. Nature 455:818-821.

Arnold L, Henry A, Poron F, Baba-Amer Y, van Rooijen N, Plonquet A, Gherardi RK, Chazaud B (2007) Inflammatory monocytes recruited after skeletal muscle injury switch into antiinflammatory macrophages to support myogenesis. J Exp Med 204:1057-1069.

Avery OT, Macleod CM, McCarty M (1944) Studies on the Chemical Nature of the Substance Inducing Transformation of Pneumococcal Types : Induction of Transformation by a Desoxyribonucleic Acid Fraction Isolated from Pneumococcus Type Iii. J Exp Med 79:137-158.

Avvakumov GV, Walker JR, Xue S, Li Y, Duan S, Bronner C, Arrowsmith CH, Dhe-Paganon S (2008) Structural basis for recognition of hemi-methylated DNA by the SRA domain of human UHRF1. Nature 455:822-825.

Bailey TJ, Fossum SL, Fimbel SM, Montgomery JE, Hyde DR (2010) The inhibitor of phagocytosis, O-phospho-L-serine, suppresses Muller glia proliferation and cone cell regeneration in the light-damaged zebrafish retina. Exp Eye Res 91:601-612.

Barakat TS, Gribnau J (2012) X chromosome inactivation in the cycle of life. Development 139:2085-2089.

Barreto G, Schafer A, Marhold J, Stach D, Swaminathan SK, Handa V, Doderlein G, Maltry N, Wu W, Lyko F, Niehrs C (2007) Gadd45a promotes epigenetic gene activation by repair-mediated DNA demethylation. Nature 445:671-675.

Barreto VM, Pan-Hammarstrom Q, Zhao Y, Hammarstrom L, Misulovin Z, Nussenzweig MC (2005) AID from bony fish catalyzes class switch recombination. J Exp Med 202:733-738.

Bartel PL, Fields S (1997) The yeast two-hybrid system: New York:Oxford University Press.

Becker T, Bernhardt RR, Reinhard E, Wullimann MF, Tongiorgi E, Schachner M (1998) Readiness of zebrafish brain neurons to regenerate a spinal axon correlates with differential expression of specific cell recognition molecules. J Neurosci 18:5789-5803.

Benjamini Y, Hochberg Y (1995) Controlling the False Discovery Rate: a Practical and Powerful Approach to Multiple Testing. Journal of the Royla Statistical Society 57:289-300.

Bernardos RL, Barthel LK, Meyers JR, Raymond PA (2007) Late-stage neuronal progenitors in the retina are radial Muller glia that function as retinal stem cells. J Neurosci 27:7028-7040.

Bhutani N, Brady JJ, Damian M, Sacco A, Corbel SY, Blau HM (2009) Reprogramming towards pluripotency requires AID-dependent DNA demethylation. Nature.

Blanc V, Davidson NO (2010) APOBEC-1-mediated RNA editing. Wiley Interdiscip Rev Syst Biol Med 2:594-602.

Blanc V, Henderson JO, Newberry RD, Xie Y, Cho SJ, Newberry EP, Kennedy S, Rubin DC, Wang HL, Luo J, Davidson NO (2007) Deletion of the AU-rich RNA binding protein Apobec-1 reduces intestinal tumor burden in Apc(min) mice. Cancer Res 67:8565-8573.

Bogerd HP, Wiegand HL, Doehle BP, Cullen BR (2007) The intrinsic antiretroviral factor APOBEC3B contains two enzymatically active cytidine deaminase domains. Virology 364:486-493.

Bohn MF, Shandilya SM, Albin JS, Kouno T, Anderson BD, McDougle RM, Carpenter MA, Rathore A, Evans L, Davis AN, Zhang J, Lu Y, Somasundaran M, Matsuo H, Harris RS, Schiffer CA (2013) Crystal structure of the DNA cytosine deaminase APOBEC3F: the catalytically active and HIV-1 Vif-binding domain. Structure 21:1042-1050.

Bourc'his D, Bestor TH (2004) Meiotic catastrophe and retrotransposon reactivation in male germ cells lacking Dnmt3L. Nature 431:96-99.

Boyer H (1964) Genetic Control of Restriction and Modification in Escherichia Coli. J Bacteriol 88:1652-1660.

Braisted JE, Raymond PA (1992) Regeneration of dopaminergic neurons in goldfish retina. Development 114:913-919.

Bransteitter R, Prochnow C, Chen XS (2009) The current structural and functional understanding of APOBEC deaminases. Cell Mol Life Sci 66:3137-3147.

Brar SS, Sacho EJ, Tessmer I, Croteau DL, Erie DA, Diaz M (2008) Activation-induced deaminase, AID, is catalytically active as a monomer on single-stranded DNA. DNA Repair (Amst) 7:77-87.

Bringmann A, Reichenbach A (2001) Role of Muller cells in retinal degenerations. Front Biosci 6:E72-92.

Bringmann A, Pannicke T, Grosche J, Francke M, Wiedemann P, Skatchkov SN, Osborne NN, Reichenbach A (2006) Muller cells in the healthy and diseased retina. Prog Retin Eye Res 25:397-424.

Bringmann A, Pannicke T, Biedermann B, Francke M, Iandiev I, Grosche J, Wiedemann P, Albrecht J, Reichenbach A (2009) Role of retinal glial cells in neurotransmitter uptake and metabolism. Neurochem Int 54:143-160.

Brzezinski JAt, Kim EJ, Johnson JE, Reh TA (2011) Ascl1 expression defines a subpopulation of lineage-restricted progenitors in the mammalian retina. Development 138:3519-3531.

Burnett A, Spearman P (2007) APOBEC3G multimers are recruited to the plasma membrane for packaging into human immunodeficiency virus type 1 virus-like particles in an RNA-dependent process requiring the NC basic linker. J Virol 81:5000-5013.

Cao W, Wen R, Li F, Lavail MM, Steinberg RH (1997) Mechanical injury increases bFGF and CNTF mRNA expression in the mouse retina. Exp Eye Res 65:241-248.

Casadesus J, Low D (2006) Epigenetic gene regulation in the bacterial world. Microbiol Mol Biol Rev 70:830-856.

Chakarova CF et al. (2007) Mutations in TOPORS cause autosomal dominant retinitis pigmentosa with perivascular retinal pigment epithelium atrophy. Am J Hum Genet 81:1098-1103.

Chang ML, Wu CH, Chien HF, Jiang-Shieh YF, Shieh JY, Wen CY (2006) Microglia/macrophages responses to kainate-induced injury in the rat retina. Neurosci Res 54:202-212.

Chaurasiya KR, McCauley MJ, Wang W, Qualley DF, Wu T, Kitamura S, Geertsema H, Chan DS, Hertz A, Iwatani Y, Levin JG, Musier-Forsyth K, Rouzina I, Williams MC (2014) Oligomerization transforms human APOBEC3G from an efficient enzyme to a slowly dissociating nucleic acid-binding protein. Nat Chem 6:28-33.

Chedin F, Lieber MR, Hsieh CL (2002) The DNA methyltransferase-like protein DNMT3L stimulates de novo methylation by Dnmt3a. Proc Natl Acad Sci U S A 99:16916-16921.

Chen KM, Harjes E, Gross PJ, Fahmy A, Lu Y, Shindo K, Harris RS, Matsuo H (2008) Structure of the DNA deaminase domain of the HIV-1 restriction factor APOBEC3G. Nature 452:116-119.

Chen T, Hevi S, Gay F, Tsujimoto N, He T, Zhang B, Ueda Y, Li E (2007) Complete inactivation of DNMT1 leads to mitotic catastrophe in human cancer cells. Nat Genet 39:391-396.

Ciciliot S, Schiaffino S (2010) Regeneration of mammalian skeletal muscle. Basic mechanisms and clinical implications. Curr Pharm Des 16:906-914.

Conticello SG (2008) The AID/APOBEC family of nucleic acid mutators. Genome Biol 9:229.

Conticello SG, Langlois MA, Neuberger MS (2007) Insights into DNA deaminases. Nat Struct Mol Biol 14:7-9.

Conticello SG, Thomas CJ, Petersen-Mahrt SK, Neuberger MS (2005) Evolution of the AID/APOBEC family of polynucleotide (deoxy)cytidine deaminases. Mol Biol Evol 22:367-377.

Cook AL, Sturm RA (2008) POU domain transcription factors: BRN2 as a regulator of melanocytic growth and tumourigenesis. Pigment Cell Melanoma Res 21:611-626.

Cortellino S et al. (2011) Thymine DNA glycosylase is essential for active DNA demethylation by linked deamination-base excision repair. Cell 146:67-79.

Costanzi S, Vincenzetti S, Cristalli G, Vita A (2006) Human cytidine deaminase: a three-dimensional homology model of a tetrameric metallo-enzyme inferred from the crystal structure of a distantly related dimeric homologue. J Mol Graph Model 25:10-16.

Craig SE, Calinescu AA, Hitchcock PF (2008) Identification of the molecular signatures integral to regenerating photoreceptors in the retina of the zebra fish. J Ocul Biol Dis Infor 1:73-84.

Craig SE, Thummel R, Ahmed H, Vasta GR, Hyde DR, Hitchcock PF (2010) The zebrafish galectin Drgal1-l2 is expressed by proliferating Muller glia and photoreceptor progenitors and regulates the regeneration of rod photoreceptors. Invest Ophthalmol Vis Sci 51:3244-3252.

Dancyger AM, King JJ, Quinlan MJ, Fifield H, Tucker S, Saunders HL, Berru M, Magor BG, Martin A, Larijani M (2011) Differences in the enzymatic efficiency of human and bony fish AID are mediated by a single residue in the C terminus modulating single-stranded DNA binding. FASEB J 26:1517-1525.

Daroczi B, Kari G, Ren Q, Dicker AP, Rodeck U (2009) Nuclear factor kappaB inhibitors alleviate and the proteasome inhibitor PS-341 exacerbates radiation toxicity in zebrafish embryos. Mol Cancer Ther 8:2625-2634.

Das AV, Mallya KB, Zhao X, Ahmad F, Bhattacharya S, Thoreson WB, Hegde GV, Ahmad I (2006) Neural stem cell properties of Muller glia in the mammalian retina: regulation by Notch and Wnt signaling. Dev Biol 299:283-302.

de Lima S, Habboub G, Benowitz LI (2012) Combinatorial therapy stimulates long-distance regeneration, target reinnervation, and partial recovery of vision after optic nerve injury in mice. Int Rev Neurobiol 106:153-172.

Deaton AM, Bird A (2011) CpG islands and the regulation of transcription. Genes Dev 25:1010-1022.

Deng B, Wehling-Henricks M, Villalta SA, Wang Y, Tidball JG (2012) IL-10 triggers changes in macrophage phenotype that promote muscle growth and regeneration. J Immunol 189:3669-3680.

Ehrlich M (2009) DNA hypomethylation in cancer cells. Epigenomics 1:239-259.

Ehrlich M, Lacey M (2013) DNA hypomethylation and hemimethylation in cancer. Adv Exp Med Biol 754:31-56.

Ellett F, Pase L, Hayman JW, Andrianopoulos A, Lieschke GJ (2011) mpeg1 promoter transgenes direct macrophage-lineage expression in zebrafish. Blood 117:e49-56.

Eming SA, Hammerschmidt M, Krieg T, Roers A (2009) Interrelation of immunity and tissue repair or regeneration. Semin Cell Dev Biol 20:517-527.

Etard C, Roostalu U, Strahle U (2010) Lack of Apobec2-related proteins causes a dystrophic muscle phenotype in zebrafish embryos. J Cell Biol 189:527-539.

Farthing CR, Ficz G, Ng RK, Chan CF, Andrews S, Dean W, Hemberger M, Reik W (2008) Global mapping of DNA methylation in mouse promoters reveals epigenetic reprogramming of pluripotency genes. PLoS Genet 4:e1000116.

Faude F, Francke M, Makarov F, Schuck J, Gartner U, Reichelt W, Wiedemann P, Wolburg H, Reichenbach A (2001) Experimental retinal detachment causes widespread and multilayered degeneration in rabbit retina. J Neurocytol 30:379-390.

Fausett BV, Goldman D (2006) A role for alpha1 tubulin-expressing Muller glia in regeneration of the injured zebrafish retina. J Neurosci 26:6303-6313.

Fausett BV, Gumerson JD, Goldman D (2008) The proneural basic helix-loop-helix gene ascl1a is required for retina regeneration. J Neurosci 28:1109-1117.

Feng S, Jacobsen SE, Reik W (2010) Epigenetic reprogramming in plant and animal development. Science 330:622-627.

Fimbel SM, Montgomery JE, Burket CT, Hyde DR (2007) Regeneration of inner retinal neurons after intravitreal injection of ouabain in zebrafish. J Neurosci 27:1712-1724.

Fischer D (2012) Stimulating axonal regeneration of mature retinal ganglion cells and overcoming inhibitory signaling. Cell Tissue Res 349:79-85.

Fischer D, Leibinger M (2012) Promoting optic nerve regeneration. Prog Retin Eye Res 31:688-701.

Fisher SK, Lewis GP (2003) Muller cell and neuronal remodeling in retinal detachment and reattachment and their potential consequences for visual recovery: a review and reconsideration of recent data. Vision Res 43:887-897.

Flotho A, Melchior F (2013) Sumoylation: a regulatory protein modification in health and disease. Annu Rev Biochem 82:357-385.

Francke M, Faude F, Pannicke T, Uckermann O, Weick M, Wolburg H, Wiedemann P, Reichenbach A, Uhlmann S, Bringmann A (2005) Glial cell-mediated spread of retinal degeneration during detachment: a hypothesis based upon studies in rabbits. Vision Res 45:2256-2267.

Franze K, Grosche J, Skatchkov SN, Schinkinger S, Foja C, Schild D, Uckermann O, Travis K, Reichenbach A, Guck J (2007) Muller cells are living optical fibers in the vertebrate retina. Proc Natl Acad Sci U S A 104:8287-8292.

Fu QL, Wu W, Wang H, Li X, Lee VW, So KF (2008) Up-regulated endogenous erythropoietin/erythropoietin receptor system and exogenous erythropoietin rescue retinal ganglion cells after chronic ocular hypertension. Cell Mol Neurobiol 28:317-329.

Gaspar-Maia A, Alajem A, Meshorer E, Ramalho-Santos M (2011) Open chromatin in pluripotency and reprogramming. Nat Rev Mol Cell Biol 12:36-47.

Gee P, Ando Y, Kitayama H, Yamamoto SP, Kanemura Y, Ebina H, Kawaguchi Y, Koyanagi Y (2011) APOBEC1-mediated editing and attenuation of herpes simplex virus 1 DNA indicate that neurons have an antiviral role during herpes simplex encephalitis. J Virol 85:9726-9736.

Godwin JW, Pinto AR, Rosenthal NA (2013) Macrophages are required for adult salamander limb regeneration. Proc Natl Acad Sci U S A 110:9415-9420.

Goldberg JL, Barres BA (2000) The relationship between neuronal survival and regeneration. Annu Rev Neurosci 23:579-612.

Goldberg JL, Klassen MP, Hua Y, Barres BA (2002) Amacrine-signaled loss of intrinsic axon growth ability by retinal ganglion cells. Science 296:1860-1864.

Goll MG, Kirpekar F, Maggert KA, Yoder JA, Hsieh CL, Zhang X, Golic KG, Jacobsen SE, Bestor TH (2006) Methylation of tRNAAsp by the DNA methyltransferase homolog Dnmt2. Science 311:395-398.

Gowher H, Liebert K, Hermann A, Xu G, Jeltsch A (2005) Mechanism of stimulation of catalytic activity of Dnmt3A and Dnmt3B DNA-(cytosine-C5)-methyltransferases by Dnmt3L. J Biol Chem 280:13341-13348.

Gratchev A, Kzhyshkowska J, Kannookadan S, Ochsenreiter M, Popova A, Yu X, Mamidi S, Stonehouse-Usselmann E, Muller-Molinet I, Gooi L, Goerdt S (2008) Activation of a TGF-beta-specific multistep gene expression program in mature macrophages requires glucocorticoid-mediated surface expression of TGF-beta receptor II. J Immunol 180:6553-6565.

Gu H, Smith ZD, Bock C, Boyle P, Gnirke A, Meissner A (2011) Preparation of reduced representation bisulfite sequencing libraries for genome-scale DNA methylation profiling. Nat Protoc 6:468-481.

Guo JU, Su Y, Zhong C, Ming GL, Song H (2011) Hydroxylation of 5-methylcytosine by TET1 promotes active DNA demethylation in the adult brain. Cell 145:423-434.

Hackett JA, Dietmann S, Murakami K, Down TA, Leitch HG, Surani MA (2013) Synergistic Mechanisms of DNA Demethylation during Transition to Ground-State Pluripotency. Stem Cell Reports 1:518-531.

Hajkova P, Erhardt S, Lane N, Haaf T, El-Maarri O, Reik W, Walter J, Surani MA (2002) Epigenetic reprogramming in mouse primordial germ cells. Mech Dev 117:15-23.

Hakata Y, Landau NR (2006) Reversed functional organization of mouse and human APOBEC3 cytidine deaminase domains. J Biol Chem 281:36624-36631.

Halloran MC, Sato-Maeda M, Warren JT, Su F, Lele Z, Krone PH, Kuwada JY, Shoji W (2000) Laser-induced gene expression in specific cells of transgenic zebrafish. Development 127:1953-1960.

Han H, Cortez CC, Yang X, Nichols PW, Jones PA, Liang G (2011) DNA methylation directly silences genes with non-CpG island promoters and establishes a nucleosome occupied promoter. Hum Mol Genet 20:4299-4310.

Harada C, Harada T, Slusher BS, Yoshida K, Matsuda H, Wada K (2000) N-acetylated-alpha-linked-acidic dipeptidase inhibitor has a neuroprotective effect on mouse retinal ganglion cells after pressure-induced ischemia. Neurosci Lett 292:134-136.

Harris RS, Petersen-Mahrt SK, Neuberger MS (2002a) RNA editing enzyme APOBEC1 and some of its homologs can act as DNA mutators. Mol Cell 10:1247-1253.

Harris RS, Sale JE, Petersen-Mahrt SK, Neuberger MS (2002b) AID is essential for immunoglobulin V gene conversion in a cultured B cell line. Curr Biol 12:435-438.

Harris RS, Bishop KN, Sheehy AM, Craig HM, Petersen-Mahrt SK, Watt IN, Neuberger MS, Malim MH (2003) DNA deamination mediates innate immunity to retroviral infection. Cell 113:803-809.

Hata K, Okano M, Lei H, Li E (2002) Dnmt3L cooperates with the Dnmt3 family of de novo DNA methyltransferases to establish maternal imprints in mice. Development 129:1983-1993.

Haynes T, Luz-Madrigal A, Reis ES, Echeverri Ruiz NP, Grajales-Esquivel E, Tzekou A, Tsonis PA, Lambris JD, Del Rio-Tsonis K (2013) Complement anaphylatoxin C3a is a potent inducer of embryonic chick retina regeneration. Nat Commun 4:2312.

He YF, Li BZ, Li Z, Liu P, Wang Y, Tang Q, Ding J, Jia Y, Chen Z, Li L, Sun Y, Li X, Dai Q, Song CX, Zhang K, He C, Xu GL (2011) Tet-Mediated Formation of 5-Carboxylcytosine and Its Excision by TDG in Mammalian DNA. Science.

Hemberger M, Dean W, Reik W (2009) Epigenetic dynamics of stem cells and cell lineage commitment: digging Waddington's canal. Nat Rev Mol Cell Biol 10:526-537.

Heo I, Joo C, Kim YK, Ha M, Yoon MJ, Cho J, Yeom KH, Han J, Kim VN (2009) TUT4 in concert with Lin28 suppresses microRNA biogenesis through pre-microRNA uridylation. Cell 138:696-708.

Herman JG, Baylin SB (2003) Gene silencing in cancer in association with promoter hypermethylation. N Engl J Med 349:2042-2054.

Hitchcock PF, Lindsey Myhr KJ, Easter SS, Jr., Mangione-Smith R, Jones DD (1992) Local regeneration in the retina of the goldfish. J Neurobiol 23:187-203.

Holden LG, Prochnow C, Chang YP, Bransteitter R, Chelico L, Sen U, Stevens RC, Goodman MF, Chen XS (2008) Crystal structure of the anti-viral APOBEC3G catalytic domain and functional implications. Nature 456:121-124.

Huang T, Cui J, Li L, Hitchcock PF, Li Y (2012) The role of microglia in the neurogenesis of zebrafish retina. Biochem Biophys Res Commun 421:214-220.

Ihara M, Stein P, Schultz RM (2008) UBE2I (UBC9), a SUMO-conjugating enzyme, localizes to nuclear speckles and stimulates transcription in mouse oocytes. Biol Reprod 79:906-913.

Iio K, Nagasawa Y, Iwatani H, Yamamoto R, Horii A, Okuzaki D, Furumatsu Y, Inohara H, Nojima H, Imai E, Isaka Y, Rakugi H (2010) Microarray analysis of tonsils in immunoglobulin A nephropathy patients. Biochem Biophys Res Commun 393:565-570.

Ito S, D'Alessio AC, Taranova OV, Hong K, Sowers LC, Zhang Y (2010) Role of Tet proteins in 5mC to 5hmC conversion, ES-cell self-renewal and inner cell mass specification. Nature 466:1129-1133.

Iwatani Y, Chan DS, Wang F, Maynard KS, Sugiura W, Gronenborn AM, Rouzina I, Williams MC, Musier-Forsyth K, Levin JG (2007) Deaminase-independent inhibition of HIV-1 reverse transcription by APOBEC3G. Nucleic Acids Res 35:7096-7108.

Jackson-Grusby L, Beard C, Possemato R, Tudor M, Fambrough D, Csankovszki G, Dausman J, Lee P, Wilson C, Lander E, Jaenisch R (2001) Loss of genomic methylation causes p53-dependent apoptosis and epigenetic deregulation. Nat Genet 27:31-39.

Jadhav AP, Roesch K, Cepko CL (2009) Development and neurogenic potential of Muller glial cells in the vertebrate retina. Prog Retin Eye Res 28:249-262.

Jarmuz A, Chester A, Bayliss J, Gisbourne J, Dunham I, Scott J, Navaratnam N (2002) An anthropoid-specific locus of orphan C to U RNA-editing enzymes on chromosome 22. Genomics 79:285-296.

Jia D, Jurkowska RZ, Zhang X, Jeltsch A, Cheng X (2007) Structure of Dnmt3a bound to Dnmt3L suggests a model for de novo DNA methylation. Nature 449:248-251.

Johansson E, Mejlhede N, Neuhard J, Larsen S (2002) Crystal structure of the tetrameric cytidine deaminase from Bacillus subtilis at 2.0 A resolution. Biochemistry 41:2563-2570.

Johns PR (1977) Growth of the adult goldfish eye. III. Source of the new retinal cells. J Comp Neurol 176:343-357.

Johns PR, Fernald RD (1981) Genesis of rods in teleost fish retina. Nature 293:141-142.

Jones PA (2012) Functions of DNA methylation: islands, start sites, gene bodies and beyond. Nat Rev Genet 13:484-492.

Jones PA, Liang G (2009) Rethinking how DNA methylation patterns are maintained. Nat Rev Genet 10:805-811.

Jullien J, Pasque V, Halley-Stott RP, Miyamoto K, Gurdon JB (2011) Mechanisms of nuclear reprogramming by eggs and oocytes: a deterministic process? Nat Rev Mol Cell Biol 12:453-459.

Jungblut M, Tiveron MC, Barral S, Abrahamsen B, Knobel S, Pennartz S, Schmitz J, Perraut M, Pfrieger FW, Stoffel W, Cremer H, Bosio A (2012) Isolation and characterization of living primary astroglial cells using the new GLAST-specific monoclonal antibody ACSA-1. Glia 60:894-907.

Kaneda M, Okano M, Hata K, Sado T, Tsujimoto N, Li E, Sasaki H (2004) Essential role for de novo DNA methyltransferase Dnmt3a in paternal and maternal imprinting. Nature 429:900-903.

Karl MO, Hayes S, Nelson BR, Tan K, Buckingham B, Reh TA (2008) Stimulation of neural regeneration in the mouse retina. Proc Natl Acad Sci U S A 105:19508-19513.

Kassen SC, Ramanan V, Montgomery JE, C TB, Liu CG, Vihtelic TS, Hyde DR (2007) Time course analysis of gene expression during light-induced photoreceptor cell death and regeneration in albino zebrafish. Dev Neurobiol 67:1009-1031.

Kato Y, Kaneda M, Hata K, Kumaki K, Hisano M, Kohara Y, Okano M, Li E, Nozaki M, Sasaki H (2007) Role of the Dnmt3 family in de novo methylation of imprinted and repetitive sequences during male germ cell development in the mouse. Hum Mol Genet 16:2272-2280.

Kaur C, Sivakumar V, Yong Z, Lu J, Foulds WS, Ling EA (2007) Blood-retinal barrier disruption and ultrastructural changes in the hypoxic retina in adult rats: the beneficial effect of melatonin administration. J Pathol 212:429-439.

Kharraz Y, Guerra J, Mann CJ, Serrano AL, Munoz-Canoves P (2013) Macrophage plasticity and the role of inflammation in skeletal muscle repair. Mediators Inflamm 2013:491497.

Kim D, Pertea G, Trapnell C, Pimentel H, Kelley R, Salzberg SL (2013) TopHat2: accurate alignment of transcriptomes in the presence of insertions, deletions and gene fusions. Genome Biol 14:R36.

Kitamura S, Ode H, Nakashima M, Imahashi M, Naganawa Y, Kurosawa T, Yokomaku Y, Yamane T, Watanabe N, Suzuki A, Sugiura W, Iwatani Y (2012) The APOBEC3C crystal structure and the interface for HIV-1 Vif binding. Nat Struct Mol Biol 19:1005-1010.

Kizil C, Dudczig S, Kyritsis N, Machate A, Blaesche J, Kroehne V, Brand M (2012) The chemokine receptor cxcr5 regulates the regenerative neurogenesis response in the adult zebrafish brain. Neural Dev 7:27.

Kohli RM, Zhang Y (2013) TET enzymes, TDG and the dynamics of DNA demethylation. Nature 502:472-479.

Koito A, Ikeda T (2012) Apolipoprotein B mRNA-editing, catalytic polypeptide cytidine deaminases and retroviral restriction. Wiley Interdiscip Rev RNA 3:529-541.

Kostic C, Shaw PH (2000) Isolation and characterization of sixteen novel p53 response genes. Oncogene 19:3978-3987.

Kreutzberg GW (1996) Microglia: a sensor for pathological events in the CNS. Trends Neurosci 19:312-318.

Kristensen DG, Nielsen JE, Jorgensen A, Skakkebaek NE, Rajpert-De Meyts E, Almstrup K (2013) Evidence that active demethylation mechanisms maintain the genome of carcinoma in situ cells hypomethylated in the adult testis. Br J Cancer.

Kroehne V, Freudenreich D, Hans S, Kaslin J, Brand M (2011) Regeneration of the adult zebrafish brain from neurogenic radial glia-type progenitors. Development 138:4831-4841.

Krueger F, Andrews SR (2011) Bismark: a flexible aligner and methylation caller for Bisulfite-Seq applications. Bioinformatics 27:1571-1572.

Krueger F, Kreck B, Franke A, Andrews SR (2012) DNA methylome analysis using short bisulfite sequencing data. Nat Methods 9:145-151.

Krzysiak TC, Jung J, Thompson J, Baker D, Gronenborn AM (2012) APOBEC2 is a monomer in solution: implications for APOBEC3G models. Biochemistry 51:2008-2017.

Kumar A, Shamsuddin N (2012) Retinal Muller glia initiate innate response to infectious stimuli via toll-like receptor signaling. PLoS One 7:e29830.

Kumar A, Pandey RK, Miller LJ, Singh PK, Kanwar M (2013a) Muller glia in retinal innate immunity: a perspective on their roles in endophthalmitis. Crit Rev Immunol 33:119-135.

Kumar R, DiMenna L, Schrode N, Liu TC, Franck P, Munoz-Descalzo S, Hadjantonakis AK, Zarrin AA, Chaudhuri J, Elemento O, Evans T (2013b) AID stabilizes stem-cell phenotype by removing epigenetic memory of pluripotency genes. Nature 500:89-92.

Lada AG, Krick CF, Kozmin SG, Mayorov VI, Karpova TS, Rogozin IB, Pavlov YI (2011) Mutator effects and mutation signatures of editing deaminases produced in bacteria and yeast. Biochemistry (Mosc) 76:131-146.

Lamba D, Karl M, Reh T (2008) Neural regeneration and cell replacement: a view from the eye. Cell Stem Cell 2:538-549.

Landreth GE, Agranoff BW (1979) Explant culture of adult goldfish retina: a model for the study of CNS regeneration. Brain Res 161:39-55.

Langmann T (2007) Microglia activation in retinal degeneration. J Leukoc Biol 81:1345-1351.

Langmead B, Trapnell C, Pop M, Salzberg SL (2009) Ultrafast and memory-efficient alignment of short DNA sequences to the human genome. Genome Biol 10:R25.

Lau PP, Zhu HJ, Nakamuta M, Chan L (1997) Cloning of an Apobec-1-binding protein that also interacts with apolipoprotein B mRNA and evidence for its involvement in RNA editing. J Biol Chem 272:1452-1455.

Lawrence JM, Singhal S, Bhatia B, Keegan DJ, Reh TA, Luthert PJ, Khaw PT, Limb GA (2007) MIO-M1 cells and similar muller glial cell lines derived from adult human retina exhibit neural stem cell characteristics. Stem Cells 25:2033-2043.

Lecossier D, Bouchonnet F, Clavel F, Hance AJ (2003) Hypermutation of HIV-1 DNA in the absence of the Vif protein. Science 300:1112.

Lederberg S (1965) Host-controlled restriction and modification of deoxyribonucleic acid in Escherichia coli. Virology 27:378-387.

Lenkowski JR, Raymond PA (2014) Muller glia: Stem cells for generation and regeneration of retinal neurons in teleost fish. Prog Retin Eye Res.

Lenkowski JR, Qin Z, Sifuentes CJ, Thummel R, Soto CM, Moens CB, Raymond PA (2013) Retinal regeneration in adult zebrafish requires regulation of TGFbeta signaling. Glia 61:1687-1697.

Lesault PF, Theret M, Magnan M, Cuvellier S, Niu Y, Gherardi RK, Tremblay JP, Hittinger L, Chazaud B (2012) Macrophages improve survival, proliferation and migration of engrafted myogenic precursor cells into MDX skeletal muscle. PLoS One 7:e46698.

Lewis GP, Fisher SK (2000) Muller cell outgrowth after retinal detachment: association with cone photoreceptors. Invest Ophthalmol Vis Sci 41:1542-1545.

Li H, Durbin R (2009) Fast and accurate short read alignment with Burrows-Wheeler transform. Bioinformatics 25:1754-1760.

Li H, Handsaker B, Wysoker A, Fennell T, Ruan J, Homer N, Marth G, Abecasis G, Durbin R (2009) The Sequence Alignment/Map format and SAMtools. Bioinformatics 25:2078-2079.

Li J, Zhao XL, Gilbert ER, Li DY, Liu YP, Wang Y, Zhu Q, Wang YG, Chen Y, Tian K (2014) APOBEC2 mRNA and protein is predominantly expressed in skeletal and cardiac muscles of chickens. Gene.

Liao W, Hong SH, Chan BH, Rudolph FB, Clark SC, Chan L (1999) APOBEC-2, a cardiac- and skeletal muscle-specific member of the cytidine deaminase supergene family. Biochem Biophys Res Commun 260:398-404.

Lister R, Pelizzola M, Dowen RH, Hawkins RD, Hon G, Tonti-Filippini J, Nery JR, Lee L, Ye Z, Ngo QM, Edsall L, Antosiewicz-Bourget J, Stewart R, Ruotti V, Millar AH, Thomson JA, Ren B, Ecker JR (2009) Human DNA methylomes at base resolution show widespread epigenomic differences. Nature 462:315-322.

Long KO, Fisher SK, Fariss RN, Anderson DH (1986) Disc shedding and autophagy in the cone-dominant ground squirrel retina. Exp Eye Res 43:193-205.

Ma DK, Guo JU, Ming GL, Song H (2009a) DNA excision repair proteins and Gadd45 as molecular players for active DNA demethylation. Cell Cycle 8.

Ma DK, Jang MH, Guo JU, Kitabatake Y, Chang ML, Pow-Anpongkul N, Flavell RA, Lu B, Ming GL, Song H (2009b) Neuronal activity-induced Gadd45b promotes epigenetic DNA demethylation and adult neurogenesis. Science 323:1074-1077.

Magalhaes MM, Coimbra A (1972) The rabbit retina Muller cell. A fine structural and cytochemical study. J Ultrastruct Res 39:310-326.

Mangeat B, Turelli P, Caron G, Friedli M, Perrin L, Trono D (2003) Broad antiretroviral defence by human APOBEC3G through lethal editing of nascent reverse transcripts. Nature 424:99-103.

Mariani R, Chen D, Schrofelbauer B, Navarro F, Konig R, Bollman B, Munk C, Nymark-McMahon H, Landau NR (2003) Species-specific exclusion of APOBEC3G from HIV-1 virions by Vif. Cell 114:21-31.

Martin CC, Laforest L, Akimenko MA, Ekker M (1999) A role for DNA methylation in gastrulation and somite patterning. Dev Biol 206:189-205.

Marz M, Schmidt R, Rastegar S, Strahle U (2011) Regenerative response following stab injury in the adult zebrafish telencephalon. Dev Dyn 240:2221-2231.

Matsumoto T, Marusawa H, Endo Y, Ueda Y, Matsumoto Y, Chiba T (2006) Expression of APOBEC2 is transcriptionally regulated by NF-kappaB in human hepatocytes. FEBS Lett 580:731-735.

Maul RW, Gearhart PJ (2010) AID and somatic hypermutation. Adv Immunol 105:159-191.

Mayer W, Niveleau A, Walter J, Fundele R, Haaf T (2000) Demethylation of the zygotic paternal genome. Nature 403:501-502.

McCarty M, Avery OT (1946) Studies on the Chemical Nature of the Substance Inducing Transformation of Pneumococcal Types : Ii. Effect of Desoxyribonuclease on the Biological Activity of the Transforming Substance. J Exp Med 83:89-96.

Mehta A, Banerjee S, Driscoll DM (1996) Apobec-1 interacts with a 65-kDa complementing protein to edit apolipoprotein-B mRNA in vitro. J Biol Chem 271:28294-28299.

Meissner A, Mikkelsen TS, Gu H, Wernig M, Hanna J, Sivachenko A, Zhang X, Bernstein BE, Nusbaum C, Jaffe DB, Gnirke A, Jaenisch R, Lander ES (2008) Genome-scale DNA methylation maps of pluripotent and differentiated cells. Nature 454:766-770.

Melton C, Judson RL, Blelloch R (2010) Opposing microRNA families regulate self-renewal in mouse embryonic stem cells. Nature 463:621-626.

Mensinger AF, Powers MK (1999) Visual function in regenerating teleost retina following cytotoxic lesioning. Vis Neurosci 16:241-251.

Meyers JR, Hu L, Moses A, Kaboli K, Papandrea A, Raymond PA (2012) beta-catenin/Wnt signaling controls progenitor fate in the developing and regenerating zebrafish retina. Neural Dev 7:30.

Mikkelsen TS, Hanna J, Zhang X, Ku M, Wernig M, Schorderet P, Bernstein BE, Jaenisch R, Lander ES, Meissner A (2008) Dissecting direct reprogramming through integrative genomic analysis. Nature 454:49-55.

Mikl MC, Watt IN, Lu M, Reik W, Davies SL, Neuberger MS, Rada C (2005) Mice deficient in APOBEC2 and APOBEC3. Mol Cell Biol 25:7270-7277.

Mohn F, Weber M, Rebhan M, Roloff TC, Richter J, Stadler MB, Bibel M, Schubeler D (2008) Lineage-specific polycomb targets and de novo DNA methylation define restriction and potential of neuronal progenitors. Mol Cell 30:755-766.

Mohr F, Dohner K, Buske C, Rawat VP (2011) TET genes: new players in DNA demethylation and important determinants for stemness. Exp Hematol 39:272-281.

Monk M, Boubelik M, Lehnert S (1987) Temporal and regional changes in DNA methylation in the embryonic, extraembryonic and germ cell lineages during mouse embryo development. Development 99:371-382.

Montgomery JE, Parsons MJ, Hyde DR (2010) A novel model of retinal ablation demonstrates that the extent of rod cell death regulates the origin of the regenerated zebrafish rod photoreceptors. J Comp Neurol 518:800-814.

Morgan HD, Dean W, Coker HA, Reik W, Petersen-Mahrt SK (2004) Activation-induced cytidine deaminase deaminates 5-methylcytosine in DNA and is expressed in pluripotent tissues: implications for epigenetic reprogramming. J Biol Chem 279:52353-52360.

Morris AC, Forbes-Osborne MA, Pillai LS, Fadool JM (2011) Microarray analysis of XOPS-mCFP zebrafish retina identifies genes associated with rod photoreceptor degeneration and regeneration. Invest Ophthalmol Vis Sci 52:2255-2266.

Moss EG, Lee RC, Ambros V (1997) The cold shock domain protein LIN-28 controls developmental timing in C. elegans and is regulated by the lin-4 RNA. Cell 88:637-646.

Mukhopadhyay D, Anant S, Lee RM, Kennedy S, Viskochil D, Davidson NO (2002) C-->U editing of neurofibromatosis 1 mRNA occurs in tumors that express both the type II transcript and apobec-1, the catalytic subunit of the apolipoprotein B mRNA-editing enzyme. Am J Hum Genet 70:38-50.

Muramatsu M, Kinoshita K, Fagarasan S, Yamada S, Shinkai Y, Honjo T (2000) Class switch recombination and hypermutation require activation-induced cytidine deaminase (AID), a potential RNA editing enzyme. Cell 102:553-563.

Muramatsu M, Sankaranand VS, Anant S, Sugai M, Kinoshita K, Davidson NO, Honjo T (1999) Specific expression of activation-induced cytidine deaminase (AID), a novel member of the RNA-editing deaminase family in germinal center B cells. J Biol Chem 274:18470-18476.

Nagashima M, Barthel LK, Raymond PA (2013) A self-renewing division of zebrafish Muller glial cells generates neuronal progenitors that require N-cadherin to regenerate retinal neurons. Development.

Nagelhus EA, Horio Y, Inanobe A, Fujita A, Haug FM, Nielsen S, Kurachi Y, Ottersen OP (1999) Immunogold evidence suggests that coupling of K+ siphoning and water transport in rat retinal Muller cells is mediated by a coenrichment of Kir4.1 and AQP4 in specific membrane domains. Glia 26:47-54.

Narvaiza I, Linfesty DC, Greener BN, Hakata Y, Pintel DJ, Logue E, Landau NR, Weitzman MD (2009) Deaminase-independent inhibition of parvoviruses by the APOBEC3A cytidine deaminase. PLoS Pathog 5:e1000439.

Navaratnam N, Shah R, Patel D, Fay V, Scott J (1993) Apolipoprotein B mRNA editing is associated with UV crosslinking of proteins to the editing site. Proc Natl Acad Sci U S A 90:222-226.

Nelson CM, Hyde DR (2012) Muller glia as a source of neuronal progenitor cells to regenerate the damaged zebrafish retina. Adv Exp Med Biol 723:425-430.

Nelson CM, Gorsuch RA, Bailey TJ, Ackerman KM, Kassen SC, Hyde DR (2012) Stat3 defines three populations of Muller glia and is required for initiating maximal muller glia proliferation in the regenerating zebrafish retina. J Comp Neurol 520:4294-4311.

Nelson CM, Ackerman KM, O'Hayer P, Bailey TJ, Gorsuch RA, Hyde DR (2013) Tumor necrosis factor-alpha is produced by dying retinal neurons and is required for Muller glia proliferation during zebrafish retinal regeneration. J Neurosci 33:6524-6539.

Nimmo RA, Slack FJ (2009) An elegant miRror: microRNAs in stem cells, developmental timing and cancer. Chromosoma 118:405-418.

Okano M, Bell DW, Haber DA, Li E (1999) DNA methyltransferases Dnmt3a and Dnmt3b are essential for de novo methylation and mammalian development. Cell 99:247-257.

Okuyama S, Marusawa H, Matsumoto T, Ueda Y, Matsumoto Y, Endo Y, Takai A, Chiba T (2011) Excessive activity of apolipoprotein B mRNA editing enzyme catalytic polypeptide 2 (APOBEC2) contributes to liver and lung tumorigenesis. Int J Cancer 130:1294-1301.

Oswald J, Engemann S, Lane N, Mayer W, Olek A, Fundele R, Dean W, Reik W, Walter J (2000) Active demethylation of the paternal genome in the mouse zygote. Curr Biol 10:475-478.

Otteson DC, D'Costa AR, Hitchcock PF (2001) Putative stem cells and the lineage of rod photoreceptors in the mature retina of the goldfish. Dev Biol 232:62-76.

Park E, Williams B, Wold BJ, Mortazavi A (2012) RNA editing in the human ENCODE RNA-seq data. Genome Res 22:1626-1633.

Pastor WA, Aravind L, Rao A (2013) TETonic shift: biological roles of TET proteins in DNA demethylation and transcription. Nat Rev Mol Cell Biol 14:341-356.

Pennings JL, van Dartel DA, Pronk TE, Hendriksen PJ, Piersma AH (2011) Identification by gene coregulation mapping of novel genes involved in embryonic stem cell differentiation. Stem Cells Dev 20:115-126.

Petersen-Mahrt SK, Neuberger MS (2003) In vitro deamination of cytosine to uracil in single-stranded DNA by apolipoprotein B editing complex catalytic subunit 1 (APOBEC1). J Biol Chem 278:19583-19586.

Petersen-Mahrt SK, Harris RS, Neuberger MS (2002) AID mutates E. coli suggesting a DNA deamination mechanism for antibody diversification. Nature 418:99-103.

Piec I, Listrat A, Alliot J, Chambon C, Taylor RG, Bechet D (2005) Differential proteome analysis of aging in rat skeletal muscle. FASEB J 19:1143-1145.

Pollak J, Wilken MS, Ueki Y, Cox KE, Sullivan JM, Taylor RJ, Levine EM, Reh TA (2013) Ascl1 reprograms mouse Muller glia into neurogenic retinal progenitors. Development.

Polo JM, Anderssen E, Walsh RM, Schwarz BA, Nefzger CM, Lim SM, Borkent M, Apostolou E, Alaei S, Cloutier J, Bar-Nur O, Cheloufi S, Stadtfeld M, Figueroa ME, Robinton D, Natesan S, Melnick A, Zhu J, Ramaswamy S, Hochedlinger K (2012) A molecular roadmap of reprogramming somatic cells into iPS cells. Cell 151:1617-1632.

Popp C, Dean W, Feng S, Cokus SJ, Andrews S, Pellegrini M, Jacobsen SE, Reik W (2010) Genome-wide erasure of DNA methylation in mouse primordial germ cells is affected by AID deficiency. Nature 463:1101-1105.

Potok ME, Nix DA, Parnell TJ, Cairns BR (2013) Reprogramming the maternal zebrafish genome after fertilization to match the paternal methylation pattern. Cell 153:759-772.

Pow DV, Crook DK (1996) Direct immunocytochemical evidence for the transfer of glutamine from glial cells to neurons: use of specific antibodies directed against the d-stereoisomers of glutamate and glutamine. Neuroscience 70:295-302.

Powell C, Elsaeidi F, Goldman D (2012) Injury-dependent Muller glia and ganglion cell reprogramming during tissue regeneration requires Apobec2a and Apobec2b. J Neurosci 32:1096-1109.

Powell C, Grant AR, Cornblath E, Goldman D (2013) Analysis of DNA methylation reveals a partial reprogramming of the Muller glia genome during retina regeneration. Proc Natl Acad Sci U S A 110:19814-19819.

Prochnow C, Bransteitter R, Chen XS (2009) APOBEC deaminases-mutases with defensive roles for immunity. Sci China C Life Sci 52:893-902.

Prochnow C, Bransteitter R, Klein MG, Goodman MF, Chen XS (2007) The APOBEC-2 crystal structure and functional implications for the deaminase AID. Nature 445:447-451.

Provost E, Rhee J, Leach SD (2007) Viral 2A peptides allow expression of multiple proteins from a single ORF in transgenic zebrafish embryos. Genesis 45:625-629.

Qin Z, Barthel LK, Raymond PA (2009) Genetic evidence for shared mechanisms of epimorphic regeneration in zebrafish. Proc Natl Acad Sci U S A 106:9310-9315.

Rai K, Huggins IJ, James SR, Karpf AR, Jones DA, Cairns BR (2008) DNA demethylation in zebrafish involves the coupling of a deaminase, a glycosylase, and gadd45. Cell 135:1201-1212.

Rai K, Sarkar S, Broadbent TJ, Voas M, Grossmann KF, Nadauld LD, Dehghanizadeh S, Hagos FT, Li Y, Toth RK, Chidester S, Bahr TM, Johnson WE, Sklow B, Burt R, Cairns BR, Jones DA (2010) DNA demethylase activity maintains intestinal cells in an undifferentiated state following loss of APC. Cell 142:930-942.

Ramachandran R, Fausett BV, Goldman D (2010a) Ascl1a regulates Muller glia dedifferentiation and retinal regeneration through a Lin-28-dependent, let-7 microRNA signalling pathway. Nat Cell Biol 12:1101-1107.

Ramachandran R, Zhao XF, Goldman D (2011) Ascl1a/Dkk/beta-catenin signaling pathway is necessary and glycogen synthase kinase-3beta inhibition is sufficient for zebrafish retina regeneration. Proc Natl Acad Sci U S A 108:15858-15863.

Ramachandran R, Zhao XF, Goldman D (2012) Insm1a-mediated gene repression is essential for the formation and differentiation of Muller glia-derived progenitors in the injured retina. Nat Cell Biol 14:1013-1023.

Ramachandran R, Reifler A, Parent J, Goldman D (2010b) Conditional Expression and Lineage Tracing of Tuba1a Expressing Cells during Zebrafish Development and Retina Regeneration. Journal of Comparative Neurology Accepted with Revisions.

Raymond PA, Barthel LK, Bernardos RL, Perkowski JJ (2006) Molecular characterization of retinal stem cells and their niches in adult zebrafish. BMC Dev Biol 6:36.

Redd MJ, Kelly G, Dunn G, Way M, Martin P (2006) Imaging macrophage chemotaxis in vivo: studies of microtubule function in zebrafish wound inflammation. Cell Motil Cytoskeleton 63:415-422.

Reddington JP, Pennings S, Meehan RR (2013) Non-canonical functions of the DNA methylome in gene regulation. Biochem J 451:13-23.

Reichenbach A, Reichelt W (1986) Postnatal development of radial glial (Muller) cells of the rabbit retina. Neurosci Lett 71:125-130.

Roesch K, Jadhav AP, Trimarchi JM, Stadler MB, Roska B, Sun BB, Cepko CL (2008) The transcriptome of retinal Muller glial cells. J Comp Neurol 509:225-238.

Rosenzweig HL, Galster KT, Planck SR, Rosenbaum JT (2009) NOD1 expression in the eye and functional contribution to IL-1beta-dependent ocular inflammation in mice. Invest Ophthalmol Vis Sci 50:1746-1753.

Rybak A, Fuchs H, Smirnova L, Brandt C, Pohl EE, Nitsch R, Wulczyn FG (2008) A feedback loop comprising lin-28 and let-7 controls pre-let-7 maturation during neural stem-cell commitment. Nat Cell Biol 10:987-993.

Saclier M, Cuvellier S, Magnan M, Mounier R, Chazaud B (2013) Monocyte/macrophage interactions with myogenic precursor cells during skeletal muscle regeneration. FEBS J 280:4118-4130.

Saitou M, Kagiwada S, Kurimoto K (2012) Epigenetic reprogramming in mouse pre-implantation development and primordial germ cells. Development 139:15-31.

Santos F, Hendrich B, Reik W, Dean W (2002) Dynamic reprogramming of DNA methylation in the early mouse embryo. Dev Biol 241:172-182.

Santos F, Peat J, Burgess H, Rada C, Reik W, Dean W (2013) Active demethylation in mouse zygotes involves cytosine deamination and base excision repair. Epigenetics Chromatin 6:39.

Sato Y, Probst HC, Tatsumi R, Ikeuchi Y, Neuberger MS, Rada C (2009) Deficiency in APOBEC2 leads to a shift in muscle fiber-type, diminished body mass and myopathy. J Biol Chem.

Sawyer SL, Emerman M, Malik HS (2004) Ancient adaptive evolution of the primate antiviral DNA-editing enzyme APOBEC3G. PLoS Biol 2:E275.

Schmitz KM, Schmitt N, Hoffmann-Rohrer U, Schafer A, Grummt I, Mayer C (2009) TAF12 recruits Gadd45a and the nucleotide excision repair complex to the promoter of rRNA genes leading to active DNA demethylation. Mol Cell 33:344-353.

Schutte M, Werner P (1998) Redistribution of glutathione in the ischemic rat retina. Neurosci Lett 246:53-56.

Schwab ME (2004) Nogo and axon regeneration. Curr Opin Neurobiol 14:118-124.

Seki M, Nawa H, Fukuchi T, Abe H, Takei N (2003) BDNF is upregulated by postnatal development and visual experience: quantitative and immunohistochemical analyses of BDNF in the rat retina. Invest Ophthalmol Vis Sci 44:3211-3218.

Senut MC, Gulati-Leekha A, Goldman D (2004) An element in the alpha1-tubulin promoter is necessary for retinal expression during optic nerve regeneration but not after eye injury in the adult zebrafish. J Neurosci 24:7663-7673.

Seong KM, Nam SY, Kim JY, Yang KH, An S, Jin YW, Kim CS (2012) TOPORS modulates H2AX discriminating genotoxic stresses. J Biochem Mol Toxicol 26:429-438.

Sethi CS, Lewis GP, Fisher SK, Leitner WP, Mann DL, Luthert PJ, Charteris DG (2005) Glial remodeling and neural plasticity in human retinal detachment with proliferative vitreoretinopathy. Invest Ophthalmol Vis Sci 46:329-342.

Severi F, Chicca A, Conticello SG (2011) Analysis of reptilian APOBEC1 suggests that RNA editing may not be its ancestral function. Mol Biol Evol 28:1125-1129.

Shamsuddin N, Kumar A (2011) TLR2 mediates the innate response of retinal Muller glia to Staphylococcus aureus. J Immunol 186:7089-7097.

Shandilya SM, Nalam MN, Nalivaika EA, Gross PJ, Valesano JC, Shindo K, Li M, Munson M, Royer WE, Harjes E, Kono T, Matsuo H, Harris RS, Somasundaran M, Schiffer CA (2010) Crystal structure of the APOBEC3G catalytic domain reveals potential oligomerization interfaces. Structure 18:28-38.

Sheehy AM, Gaddis NC, Choi JD, Malim MH (2002) Isolation of a human gene that inhibits HIV-1 infection and is suppressed by the viral Vif protein. Nature 418:646-650.

Shen L, Kondo Y, Guo Y, Zhang J, Zhang L, Ahmed S, Shu J, Chen X, Waterland RA, Issa JP (2007) Genome-wide profiling of DNA methylation reveals a class of normally methylated CpG island promoters. PLoS Genet 3:2023-2036.

Shen W, Fruttiger M, Zhu L, Chung SH, Barnett NL, Kirk JK, Lee S, Coorey NJ, Killingsworth M, Sherman LS, Gillies MC (2012) Conditional Mullercell ablation causes independent neuronal and vascular pathologies in a novel transgenic model. J Neurosci 32:15715-15727.

Sherpa T, Fimbel SM, Mallory DE, Maaswinkel H, Spritzer SD, Sand JA, Li L, Hyde DR, Stenkamp DL (2008) Ganglion cell regeneration following whole-retina destruction in zebrafish. Dev Neurobiol 68:166-181.

Shyh-Chang N, Zhu H, Yvanka de Soysa T, Shinoda G, Seligson MT, Tsanov KM, Nguyen L, Asara JM, Cantley LC, Daley GQ (2013) Lin28 enhances tissue repair by reprogramming cellular metabolism. Cell 155:778-792.

Silver J, Miller JH (2004) Regeneration beyond the glial scar. Nat Rev Neurosci 5:146-156.

Simonsson S, Gurdon J (2004) DNA demethylation is necessary for the epigenetic reprogramming of somatic cell nuclei. Nat Cell Biol 6:984-990.

Skuse GR, Cappione AJ, Sowden M, Metheny LJ, Smith HC (1996) The neurofibromatosis type I messenger RNA undergoes base-modification RNA editing. Nucleic Acids Res 24:478-485.

Smith HC, Bennett RP, Kizilyer A, McDougall WM, Prohaska KM (2012) Functions and regulation of the APOBEC family of proteins. Semin Cell Dev Biol 23:258-268.

Smyth GK (2004) Linear models and empirical bayes methods for assessing differential expression in microarray experiments. Stat Appl Genet Mol Biol 3:Article3.

Stadtfeld M, Hochedlinger K (2010) Induced pluripotency: history, mechanisms, and applications. Genes Dev 24:2239-2263.

Stickney HL, Schmutz J, Woods IG, Holtzer CC, Dickson MC, Kelly PD, Myers RM, Talbot WS (2002) Rapid mapping of zebrafish mutations with SNPs and oligonucleotide microarrays. Genome Res 12:1929-1934.

Suva ML, Riggi N, Bernstein BE (2013) Epigenetic reprogramming in cancer. Science 339:1567-1570.

Takahashi K, Yamanaka S (2006) Induction of pluripotent stem cells from mouse embryonic and adult fibroblast cultures by defined factors. Cell 126:663-676.

Tang H, Macpherson P, Marvin M, Meadows E, Klein WH, Yang XJ, Goldman D (2009) A histone deacetylase 4/myogenin positive feedback loop coordinates denervation-dependent gene induction and suppression. Mol Biol Cell 20:1120-1131.

Teng B, Burant CF, Davidson NO (1993) Molecular cloning of an apolipoprotein B messenger RNA editing protein. Science 260:1816-1819.

Teng BB, Ochsner S, Zhang Q, Soman KV, Lau PP, Chan L (1999) Mutational analysis of apolipoprotein B mRNA editing enzyme (APOBEC1). structure-function relationships of RNA editing and dimerization. J Lipid Res 40:623-635.

Terada K, Furukawa T (2010) Sumoylation controls retinal progenitor proliferation by repressing cell cycle exit in Xenopus laevis. Dev Biol 347:180-194.

Tezel G, Wax MB (2000) Increased production of tumor necrosis factor-alpha by glial cells exposed to simulated ischemia or elevated hydrostatic pressure induces apoptosis in cocultured retinal ganglion cells. J Neurosci 20:8693-8700.

Thomas JL, Nelson CM, Luo X, Hyde DR, Thummel R (2012) Characterization of multiple light damage paradigms reveals regional differences in photoreceptor loss. Exp Eye Res 97:105-116.

Thummel R, Kassen SC, Montgomery JE, Enright JM, Hyde DR (2008a) Inhibition of Muller glial cell division blocks regeneration of the light-damaged zebrafish retina. Dev Neurobiol 68:392-408.

Thummel R, Kassen SC, Enright JM, Nelson CM, Montgomery JE, Hyde DR (2008b) Characterization of Muller glia and neuronal progenitors during adult zebrafish retinal regeneration. Exp Eye Res 87:433-444.

Thummel R, Enright JM, Kassen SC, Montgomery JE, Bailey TJ, Hyde DR (2010) Pax6a and Pax6b are required at different points in neuronal progenitor cell proliferation during zebrafish photoreceptor regeneration. Exp Eye Res 90:572-582.

Tidball JG, Wehling-Henricks M (2007) Macrophages promote muscle membrane repair and muscle fibre growth and regeneration during modified muscle loading in mice in vivo. J Physiol 578:327-336.

Tokuda N, Mano T, Levy RB (1992) Phagocytosis by the murine testicular TM4 Sertoli cell line in culture. J Urol 147:278-282.

Tout S, Chan-Ling T, Hollander H, Stone J (1993) The role of Muller cells in the formation of the blood-retinal barrier. Neuroscience 55:291-301.

Trapnell C, Williams BA, Pertea G, Mortazavi A, Kwan G, van Baren MJ, Salzberg SL, Wold BJ, Pachter L (2010) Transcript assembly and quantification by RNA-Seq reveals unannotated transcripts and isoform switching during cell differentiation. Nat Biotechnol 28:511-515.

Uchimura Y, Nakao M, Saitoh H (2004a) Generation of SUMO-1 modified proteins in E. coli: towards understanding the biochemistry/structural biology of the SUMO-1 pathway. FEBS Lett 564:85-90.

Uchimura Y, Nakamura M, Sugasawa K, Nakao M, Saitoh H (2004b) Overproduction of eukaryotic SUMO-1- and SUMO-2-conjugated proteins in Escherichia coli. Anal Biochem 331:204-206.

Uetake H, Toyama S, Hagiwara S (1964) On the Mechanism of Host-Induced Modification. Multiplicity Activation and Thermolabile Factor Responsible for Phage Growth Restriction. Virology 22:202-213.

Urasaki A, Morvan G, Kawakami K (2006) Functional dissection of the Tol2 transposable element identified the minimal cis-sequence and a highly repetitive sequence in the subterminal region essential for transposition. Genetics 174:639-649.

Veldman MB, Bemben MA, Goldman D (2010) Tuba1a gene expression is regulated by KLF6/7 and is necessary for CNS development and regeneration in zebrafish. Mol Cell Neurosci 43:370-383.

Veldman MB, Bemben MA, Thompson RC, Goldman D (2007) Gene expression analysis of zebrafish retinal ganglion cells during optic nerve regeneration identifies KLF6a and KLF7a as important regulators of axon regeneration. Dev Biol 312:596-612.

Vierbuchen T, Ostermeier A, Pang ZP, Kokubu Y, Sudhof TC, Wernig M (2010) Direct conversion of fibroblasts to functional neurons by defined factors. Nature 463:1035-1041.

Vihtelic TS, Hyde DR (2000) Light-induced rod and cone cell death and regeneration in the adult albino zebrafish (Danio rerio) retina. J Neurobiol 44:289-307.

Viswanathan SR, Daley GQ, Gregory RI (2008) Selective blockade of microRNA processing by Lin28. Science 320:97-100.

Vonica A, Rosa A, Arduini BL, Brivanlou AH (2011) APOBEC2, a selective inhibitor of TGFbeta signaling, regulates left-right axis specification during early embryogenesis. Dev Biol 350:13-23.

Walsh CP, Chaillet JR, Bestor TH (1998) Transcription of IAP endogenous retroviruses is constrained by cytosine methylation. Nat Genet 20:116-117.

Wan J, Ramachandran R, Goldman D (2012) HB-EGF is necessary and sufficient for Muller glia dedifferentiation and retina regeneration. Dev Cell 22:334-347.

Wang J, Shinkura R, Muramatsu M, Nagaoka H, Kinoshita K, Honjo T (2006) Identification of a specific domain required for dimerization of activation-induced cytidine deaminase. J Biol Chem 281:19115-19123.

Wang JS, Kefalov VJ (2011) The cone-specific visual cycle. Prog Retin Eye Res 30:115-128.

Wang X, Iannaccone A, Jablonski MM (2005) Contribution of Muller cells toward the regulation of photoreceptor outer segment assembly. Neuron Glia Biol 1:1-6.

Weber M, Hellmann I, Stadler MB, Ramos L, Paabo S, Rebhan M, Schubeler D (2007) Distribution, silencing potential and evolutionary impact of promoter DNA methylation in the human genome. Nat Genet 39:457-466.

Wei F, Scholer HR, Atchison ML (2007) Sumoylation of Oct4 enhances its stability, DNA binding, and transactivation. J Biol Chem 282:21551-21560.

Weissman T, Noctor SC, Clinton BK, Honig LS, Kriegstein AR (2003) Neurogenic radial glial cells in reptile, rodent and human: from mitosis to migration. Cereb Cortex 13:550-559.

Wen R, Song Y, Cheng T, Matthes MT, Yasumura D, LaVail MM, Steinberg RH (1995) Injury-induced upregulation of bFGF and CNTF mRNAS in the rat retina. J Neurosci 15:7377-7385.

Wu H, Zhang Y (2014) Reversing DNA methylation: mechanisms, genomics, and biological functions. Cell 156:45-68.

Wu SC, Zhang Y (2010) Active DNA demethylation: many roads lead to Rome. Nat Rev Mol Cell Biol 11:607-620.

Xue Y, Zhou F, Fu C, Xu Y, Yao X (2006) SUMOsp: a web server for sumoylation site prediction. Nucleic Acids Res 34:W254-257.

Yasuhara T, Shingo T, Date I (2004a) The potential role of vascular endothelial growth factor in the central nervous system. Rev Neurosci 15:293-307.

Yasuhara T, Shingo T, Kobayashi K, Takeuchi A, Yano A, Muraoka K, Matsui T, Miyoshi Y, Hamada H, Date I (2004b) Neuroprotective effects of vascular endothelial growth factor (VEGF) upon dopaminergic neurons in a rat model of Parkinson's disease. Eur J Neurosci 19:1494-1504.

Yiu G, He Z (2006) Glial inhibition of CNS axon regeneration. Nat Rev Neurosci 7:617-627.

Yu J, Vodyanik MA, Smuga-Otto K, Antosiewicz-Bourget J, Frane JL, Tian S, Nie J, Jonsdottir GA, Ruotti V, Stewart R, Slukvin, II, Thomson JA (2007) Induced pluripotent stem cell lines derived from human somatic cells. Science 318:1917-1920.

Yuan L, Neufeld AH (2000) Tumor necrosis factor-alpha: a potentially neurodestructive cytokine produced by glia in the human glaucomatous optic nerve head. Glia 32:42-50.

Zakrzewska A, Cui C, Stockhammer OW, Benard EL, Spaink HP, Meijer AH (2010) Macrophage-specific gene functions in Spi1-directed innate immunity. Blood 116:e1-11.

Zhang H, Yang B, Pomerantz RJ, Zhang C, Arunachalam SC, Gao L (2003) The cytidine deaminase CEM15 induces hypermutation in newly synthesized HIV-1 DNA. Nature 424:94-98.

Zhang J, Webb DM (2004) Rapid evolution of primate antiviral enzyme APOBEC3G. Hum Mol Genet 13:1785-1791.

Zhang S, Cui P (2014) Complement system in zebrafish. Dev Comp Immunol.

Zhou H, Yoshioka T, Nathans J (1996) Retina-derived POU-domain factor-1: a complex POU-domain gene implicated in the development of retinal ganglion and amacrine cells. J Neurosci 16:2261-2274.

Zhu B, Zheng Y, Angliker H, Schwarz S, Thiry S, Siegmann M, Jost JP (2000) 5-Methylcytosine DNA glycosylase activity is also present in the human MBD4 (G/T mismatch glycosylase) and in a related avian sequence. Nucleic Acids Res 28:4157-4165.

Zhu JK (2009) Active DNA demethylation mediated by DNA glycosylases. Annu Rev Genet 43:143-166.

Zhu RL, Cho KS, Guo CY, Chew J, Chen DF, Yang L (2013) Intrinsic determinants of optic nerve regeneration. Chin Med J (Engl) 126:2543-2547.

Zordan P, Rigamonti E, Freudenberg K, Conti V, Azzoni E, Rovere-Querini P, Brunelli S (2014) Macrophages commit postnatal endothelium-derived progenitors to angiogenesis and restrict endothelial to mesenchymal transition during muscle regeneration. Cell Death Dis 5:e1031.

Zou Y, Chiu H, Zinovyeva A, Ambros V, Chuang CF, Chang C (2013) Developmental decline in neuronal regeneration by the progressive change of two intrinsic timers. Science 340:372-376.